Slope Stability

Course No: G04-001
Credit: 4 PDH

Gilbert Gedeon, P.E.

This course was adapted from the United States Army Corps of Engineers (USACE), Publication No. EM 1110-2-1902, "Slope Stability", which is in the public domain.

TABLE OF CONTENTS

Chapter 1
Introduction

1-1. Purpose and Scope

This engineer manual (EM) provides guidance for analyzing the static stability of slopes of earth and rock-fill dams, slopes of other types of embankments, excavated slopes, and natural slopes in soil and soft rock. Methods for analysis of slope stability are described and are illustrated by examples in the appendixes. Criteria are presented for strength tests, analysis conditions, and factors of safety. The criteria in this EM are to be used with methods of stability analysis that satisfy all conditions of equilibrium. Methods that do not satisfy all conditions of equilibrium may involve significant inaccuracies and should be used only under the restricted conditions described herein. This manual is intended to guide design and construction engineers, rather than to specify rigid procedures to be followed in connection with a particular project.

1-2. Applicability

This EM is applicable to all USACE elements and field operating activities having responsibility for analyzing stability of slopes.

1-3. References

Appendix A contains a list of Government and non-Government references pertaining to this manual. Each reference is identified in the text by either the designated publication number or by author and date.

1-4. Notation and Glossary

Symbols used in this manual are listed and defined in Appendix B. The notation in this manual corresponds whenever possible to that recommended by the American Society of Civil Engineers.

1-5. Basic Design Considerations

   a. General overview. Successful design requires consistency in the design process. What are considered to be appropriate values of factor of safety are inseparable from the procedures used to measure shear strengths and analyze stability. Where procedures for sampling, testing, or analysis are different from the procedures described in this manual, it is imperative to evaluate the effects of those differences.

   b. Site characterization. The stability of dams and slopes must be evaluated utilizing pertinent geologic information and information regarding in situ engineering properties of soil and rock materials. The geologic information and site characteristics that should be considered include:

   (1)   Groundwater and seepage conditions.

   (2)   Lithology, stratigraphy, and geologic details disclosed by borings and geologic interpretations.

   (3)   Maximum past overburden at the site as deduced from geological evidence.

   (4)   Structure, including bedding, folding, and faulting.

   (5)   Alteration of materials by faulting.

(6)   Joints and joint systems.

(7)   Weathering.

(8)   Cementation.

(9)   Slickensides.

(10) Field evidence relating to slides, earthquake activity, movement along existing faults, and tension jointing.

c.   Material characterization. In evaluating engineering properties of soil and rock materials for use in design, consideration must be given to: (1) possible variation in natural deposits or borrow materials, (2) natural water contents of the materials, (3) climatic conditions, (4) possible variations in rate and methods of fill placement, and (5) variations in placement water contents and compacted densities that must be expected with normal control of fill construction. Other factors that must be considered in selecting values of design parameters, which can be evaluated only through exercise of engineering judgment, include: (1) the effect of differential settlements where embankments are located on compressible foundations or in narrow, deep valleys, and (2) stress-strain compatibility of zones of different materials within an embankment, or of the embankment and its foundation. The stability analyses presented in this manual assume that design strengths can be mobilized simultaneously in all materials along assumed sliding surfaces.

d.   Conventional analysis procedures (limit equilibrium). The conventional limit equilibrium methods of slope stability analysis used in geotechnical practice investigate the equilibrium of a soil mass tending to move downslope under the influence of gravity. A comparison is made between forces, moments, or stresses tending to cause instability of the mass, and those that resist instability. Two-dimensional (2-D) sections are analyzed and plane strain conditions are assumed. These methods assume that the shear strengths of the materials along the potential failure surface are governed by linear (Mohr-Coulomb) or nonlinear relationships between shear strength and the normal stress on the failure surface.

(1) A free body of the soil mass bounded below by an assumed or known surface of sliding (potential slip surface), and above by the surface of the slope, is considered in these analyses. The requirements for static equilibrium of the soil mass are used to compute a factor of safety with respect to shear strength. The factor of safety is defined as the ratio of the available shear resistance (the capacity) to that required for equilibrium (the demand). Limit equilibrium analyses assume the factor of safety is the same along the entire slip surface. A value of factor of safety greater than 1.0 indicates that capacity exceeds demand and that the slope will be stable with respect to sliding along the assumed particular slip surface analyzed. A value of factor of safety less than 1.0 indicates that the slope will be unstable.

(2) The most common methods for limit equilibrium analyses are methods of slices. In these methods, the soil mass above the assumed slip surface is divided into vertical slices for purposes of convenience in analysis. Several different methods of slices have been developed. These methods may result in different values of factor of safety because: (a) the various methods employ different assumptions to make the problem statically determinate, and (b) some of the methods do not satisfy all conditions of equilibrium. These issues are discussed in Appendix C.

e.   Special analysis procedures (finite element, three-dimensional (3-D), and probabilistic methods).

(1) The finite element method can be used to compute stresses and displacements in earth structures. The method is particularly useful for soil-structure interaction problems, in which structural members interact with a soil mass. The stability of a slope cannot be determined directly from finite element analyses, but the

computed stresses in a slope can be used to compute a factor of safety. Use of the finite element method for stability problems is a complex and time-consuming process. Finite element analyses are discussed briefly in Appendix C.

(2) Three-dimensional limit equilibrium analysis methods consider the 3-D shapes of slip surfaces. These methods, like 2-D methods, require assumptions to achieve a statically determinate definition of the problem. Most do not satisfy all conditions of static equilibrium in three dimensions and lack general methodologies for locating the most critical 3-D slip surface. The errors associated with these limitations may be of the same magnitude as the 3-D effects that are being modeled. These methods may be useful for estimating potential 3-D effects for a particular slip surface. However, 3-D methods are not recommended for general use in design because of their limitations. The factors of safety presented in this manual are based on 2-D analyses. Three-dimensional analysis methods are not included within the scope of this manual.

(3) Probabilistic approaches to analysis and design of slopes consider the magnitudes of uncertainties regarding shear strengths and the other parameters involved in computing factors of safety. In the traditional (deterministic) approach to slope stability analysis and design, the shear strength, slope geometry, external loads, and pore water pressures are assigned specific unvarying values. Appendix D discusses shear strength value selection. The value of the calculated factor of safety depends on the judgments made in selecting the values of the various design parameters. In probabilistic methods, the possibility that values of shear strength and other parameters may vary is considered, providing a means of evaluating the degree of uncertainty associated with the computed factor of safety. Although probabilistic techniques are not required for slope analysis or design, these methods allow the designer to address issues beyond those that can be addressed by deterministic methods, and their use is encouraged. Probabilistic methods can be utilized to supplement conventional deterministic analyses with little additional effort. Engineering Technical Letter (ETL) 1110-2-556 (1999) describes techniques for probabilistic analyses and their application to slope stability studies.

f.   Computer programs and design charts. Computer programs provide a means for detailed analysis of slope stability. Design charts provide a rapid method of analysis but usually require simplifying approximations for application to actual slope conditions. The choice to use computer programs or slope stability charts should be made based on the complexity of the conditions to be analyzed and the objective of the analysis. Even when computer programs are used for final analyses, charts are often useful for providing preliminary results quickly, and for providing an independent check on the results of the computer analyses. These issues are discussed in Appendix E.

g.   Use and value of results. Slope stability analyses provide a means of comparing relative merits of trial cross sections during design and for evaluating the effects of changes in assumed embankment and foundation properties. The value of stability analyses depends on the validity of assumed conditions, and the value of the results is increased where they can be compared with analyses for similar structures where construction and operating experiences are known.

h.   Strain softening and progressive failure. "Progressive failure" occurs under conditions where shearing resistance first increases and then decreases with increasing strain, and, as a result, the peak shear strengths of the materials at all points along a slip surface cannot be mobilized simultaneously. When progressive failure occurs, a critical assumption of limit equilibrium methods – that peak strength can be mobilized at all points along the shear surface -- is not valid. "Strain softening" is the term used to describe stress-strain response in which shear resistance falls from its peak value to a lower value with increasing shear strain. There are several fundamental causes and forms of strain softening behavior, including:

(1) Undrained strength loss caused by contraction-induced increase in pore water pressure. Liquefaction of cohesionless soils is an extreme example of undrained strength loss as the result of contraction-induced pore pressure, but cohesive soils are also subject to undrained strength loss from the same cause.

(2) Drained strength loss occurring as a result of dilatancy. As dense soil is sheared, it may expand, becoming less dense and therefore weaker.

(3) Under either drained or undrained conditions, platy clay particles may be reoriented by shear deformation into a parallel arrangement termed "slickensides," with greatly reduced shear resistance. If materials are subject to strain softening, it cannot be assumed that a factor of safety greater than one based on peak shear strength implies stability, because deformations can cause local loss of strength, requiring mobilization of additional strength at other points along the slip surface. This, in turn, can cause additional movement, leading to further strain softening. Thus, a slope in strain softening materials is at risk of progressive failure if the peak strength is mobilized anywhere along the failure surface. Possible remedies are to design so that the factor of safety is higher, or to use shear strengths that are less than peak strengths. In certain soils, it may even be necessary to use residual shear strengths.

i. Strain incompatibility. When an embankment and its foundation consist of dissimilar materials, it may not be possible to mobilize peak strengths simultaneously along the entire length of the slip surface. Where stiff embankments overly soft clay foundations, or where the foundation of an embankment consists of brittle clays, clay shales, or marine clays that have stress-strain characteristics different from those of the embankment, progressive failure may occur as a result of strain incompatibility.

j. Loss of strength resulting from tension cracks. Progressive failure may start when tension cracks develop as a result of differential settlements or shrinkage. The maximum depth of cracking can be estimated from Appendix C, Equation C-36. Shear resistance along tension cracks should be ignored, and in most cases it should be assumed that the crack will fill with water during rainfall.

k. Problem shales. Shales can be divided into two broad groups. Clay shales (compaction shales) lack significant strength from cementation. Cemented shales have substantial strength because of calcareous, siliceous, other types of chemical bonds, or heat, and pressure. Clay shales usually slake rapidly into unbonded clay when subjected to a few cycles of wetting and drying, whereas cemented shales are either unaffected by wetting and drying, or are reduced to sand-size aggregates of clay particles by wetting and drying. All types of shales may present foundation problems where they contain joints, shear bands, slickensides, faults, seams filled with soft material, or weak layers. Where such defects exist, they control the strength of the mass. Prediction of the field behavior of clay shales should not be based solely on results of conventional laboratory tests, since they may be misleading, but on detailed geologic investigations and/or large-scale field tests. Potential problem shales can be recognized by: (1) observation of landslides or faults through aerial or ground reconnaissance, (2) observation of soft zones, shear bands, or slickensides in recovered core or exploration trenches, and (3) clay mineralogical studies to detect the presence of bentonite layers.

1-6. Stability Analysis and Design Procedure

The process of evaluating slope stability involves the following chain of events:

a. Explore and sample foundation and borrow sources. EM 1110-1-1804 provides methods and procedures that address these issues.

b. Characterize the soil strength (see Appendix D). This usually involves testing representative samples as described in EM 1110-2-1906. The selection of representative samples for testing requires much care.

c. Establish the 2-D idealization of the cross section, including the surface geometry and the subsurface boundaries between the various materials.

d. Establish the seepage and groundwater conditions in the cross section as measured or as predicted for the design load conditions. EM 1110-2-1901 describes methods to establishing seepage conditions through analysis and field measurements.

e. Select loading conditions for analysis (see Chapter 2).

f. Select trial slip surfaces and compute factors of safety using Spencer's method. In some cases it may be adequate to compute factors of safety using the Simplified Bishop Method or the force equilibrium method (including the Modified Swedish Method) with a constant side force (Appendix C). Appendix F provides example problems and calculations for the simplified Bishop and Modified Swedish Procedures.

g. Repeat step f above until the "critical" slip surface has been located. The critical slip surface is the one that has the lowest factor of safety and which, therefore, represents the most likely failure mechanism.

Steps *f* and *g* are automated in most slope stability computer programs, but several different starting points and search criteria should be used to ensure that the critical slip surface has been located accurately.

h. Compare the computed factor of safety with experienced-based criteria (see Chapter 3).

Return to any of the items above, and repeat the process through step *h*, until a satisfactory design has been achieved. When the analysis has been completed, the following steps (not part of this manual) complete the design process:

i. The specifications should be written consistent with the design assumptions.

j. The design assumptions should be verified during construction. This may require repeating steps *b, c, d, f, g,* and *h* and modifying the design if conditions are found that do not match the design assumptions.

k. Following construction, the performance of the completed structure should be monitored. Actual piezometric surfaces based on pore water pressure measurements should be compared with those assumed during design (part *d* above) to determine if the embankment meets safe stability standards.

1-7. Unsatisfactory Slope Performance

a. Shear failure. A shear failure involves sliding of a portion of an embankment, or an embankment and its foundation, relative to the adjacent mass. A shear failure is conventionally considered to occur along a discrete surface and is so assumed in stability analyses, although the shear movements may in fact occur across a zone of appreciable thickness. Failure surfaces are frequently approximately circular in shape. Where zoned embankments or thin foundation layers overlying bedrock are involved, or where weak strata exist within a deposit, the failure surface may consist of interconnected arcs and planes.

b. Surface sloughing. A shear failure in which a surficial portion of the embankment moves downslope is termed a surface slough. Surface sloughing is considered a maintenance problem, because it usually does not affect the structural capability of the embankment. However, repair of surficial failures can entail considerable cost. If such failures are not repaired, they can become progressively larger, and may then represent a threat to embankment safety.

c. Excessive deformation. Some cohesive soils require large strains to develop peak shear resistance. As a consequence, these soils may deform excessively when loaded. To avoid excessive deformations, particular attention should be given to the stress-strain response of cohesive embankment and foundation soils during design. When strains larger than 15 percent are required to mobilize peak strengths, deformations in

the embankment or foundation may be excessive. It may be necessary in such cases to use the shearing resistance mobilized at 10 or 15 percent strain, rather than peak strengths, or to limit placement water contents to the dry side of optimum to reduce the magnitudes of failure strains. However, if cohesive soils are compacted too dry, and they later become wetter while under load, excessive settlement may occur. Also, compaction of cohesive soils dry of optimum water content may result in brittle stress-strain behavior and cracking of the embankment. Cracks can have adverse effects on stability and seepage. When large strains are required to develop shear strengths, surface movement measurement points and piezometers should be installed to monitor movements and pore water pressures during construction, in case it becomes necessary to modify the cross section or the rate of fill placement.

   d. Liquefaction. The phenomenon of soil liquefaction, or significant reduction in soil strength and stiffness as a result of shear-induced increase in pore water pressure, is a major cause of earthquake damage to embankments and slopes. Most instances of liquefaction have been associated with saturated loose sandy or silty soils. Loose gravelly soil deposits are also vulnerable to liquefaction (e.g., Coulter and Migliaccio 1966; Chang 1978; Youd et al. 1984; and Harder 1988). Cohesive soils with more than 20 percent of particles finer than 0.005 mm, or with liquid limit (LL) of 34 or greater, or with the plasticity index (PI) of 14 or greater are generally considered not susceptible to liquefaction. The methodology to evaluate liquefaction susceptibility will be presented in an Engineer Circular, "Dynamic Analysis of Embankment Dams," which is still in draft form.

   e. Piping. Erosion and piping can occur when hydraulic gradients at the downstream end of a hydraulic structure are large enough to move soil particles. Analyses to compute hydraulic gradients and procedures to control piping are contained in EM 1110-2-1901.

   f. Other types of slope movements. Several types of slope movements, including rockfalls, topples, lateral spreading, flows, and combinations of these, are not controlled by shear strength (Huang 1983). These types of mass movements are not discussed in this manual, but the possibility of their occurrence should not be ignored.

Chapter 2
Design Considerations

2-1. Introduction

Evaluation of slope stability requires:

    a. Establishing the conditions, called "design conditions" or "loading conditions," to which the slope may be subjected during its life, and

    b. Performing analyses of stability for each of these conditions. There are four design conditions that must be considered for dams: (1) during and at the end of construction, (2) steady state seepage, (3) sudden drawdown, and (4) earthquake loading. The first three conditions are static; the fourth involves dynamic loading.

Details concerning the analysis of slope stability for the three static loading conditions are discussed in this chapter. Criteria regarding which static design conditions should be applied and values of factor of safety are discussed in Chapter 3. Procedures for analysis of earthquake loading conditions can be found in an Engineer Circular, "Dynamic Analysis of Embankment Dams," which is still in draft form..

2-2. Aspects Applicable to All Load Conditions

    a. General. Some aspects of slope stability computations are generally applicable, independent of the design condition analyzed. These are discussed in the following paragraphs.

    b. Shear strength. Correct evaluation of shear strength is essential for meaningful analysis of slope stability. Shear strengths used in slope stability analyses should be selected with due consideration of factors such as sample disturbance, variability in borrow materials, possible variations in compaction water content and density of fill materials, anisotropy, loading rate, creep effects, and possibly partial drainage. The responsibility for selecting design strengths lies with the designer, not with the laboratory.

    (1) Drained and undrained conditions. A prime consideration in characterizing shear strengths is determining whether the soil will be drained or undrained for each design condition. For drained conditions, analyses are performed using drained strengths related to effective stresses. For undrained conditions, analyses are performed using undrained strengths related to total stresses. Table 2-1 summarizes appropriate shear strengths for use in analyses of static loading conditions.

    (2) Laboratory strength tests. Laboratory strength tests can be used to evaluate the shear strengths of some types of soils. Laboratory strength tests and their interpretation are discussed in Appendix D.

    (3) Linear and nonlinear strength envelopes. Strength envelopes used to characterize the variation of shear strength with normal stress can be linear or nonlinear, as shown in Figure 2-1.

    (a) Linear strength envelopes correspond to the Mohr-Coulomb failure criterion. For total stresses, this is expressed as:

$$s = c + \sigma \tan \varphi \tag{2-1}$$

Table 2-1
Shear Strengths and Pore Pressures for Static Design Conditions

Design Condition	Shear Strength	Pore Water Pressure
During Construction and End-of-Construction	Free draining soils – use drained shear strengths related to effective stresses[1]	Free draining soils – Pore water pressures can be estimated using analytical techniques such as hydrostatic pressure computations if there is no flow, or using steady seepage analysis techniques (flow nets or finite element analyses).
	Low-permeability soils – use undrained strengths related to total stresses[2]	Low-permeability soils – Total stresses are used; pore water pressures are set to zero in the slope stability computations.
Steady-State Seepage Conditions	Use drained shear strengths related to effective stresses.	Pore water pressures from field measurements, hydrostatic pressure computations for no-flow conditions, or steady seepage analysis techniques (flow nets, finite element analyses, or finite difference analyses).
Sudden Drawdown Conditions	Free draining soils – use drained shear strengths related to effective stresses.	Free draining soils – First-stage computations (before drawdown) – steady seepage pore pressures as for steady seepage condition. Second- and third-stage computations (after drawdown) – pore water pressures estimated using same techniques as for steady seepage, except with lowered water level.
	Low-permeability soils – Three-stage computations: First stage--use drained shear strength related to effective stresses; second stage--use undrained shear strengths related to consolidation pressures from the first stage; third stage--use drained strengths related to effective stresses, or undrained strengths related to consolidation pressures from the first stage, depending on which strength is lower – this will vary along the assumed shear surface.	Low-permeability soils – First-stage computations--steady-state seepage pore pressures as described for steady seepage condition. Second-stage computations – total stresses are used; pore water pressures are set to zero. Third-stage computations -- same pore pressures as free draining soils if drained strengths are used; pore water pressures are set to zero where undrained strengths are used.

[1] Effective stress shear strength parameters can be obtained from consolidated-drained (CD, S) tests (direct shear or triaxial) or consolidated-undrained (CU, $\overline{R}$) triaxial tests on saturated specimens with pore water pressure measurements. Repeated direct shear or Bromhead ring shear tests should be used to measure residual strengths. Undrained strengths can be obtained from unconsolidated-undrained (UU, Q) tests. Undrained shear strengths can also be estimated using consolidated-undrained (CU, R) tests on specimens consolidated to appropriate stress conditions representative of field conditions; however, the "R" or "total stress" envelope and associated c and ϕ, from CU, R tests should not be used.

[2] For saturated soils use $\phi = 0$. Total stress envelopes with $\phi > 0$ are only applicable to partially saturated soils.

where

 s = maximum possible value of shear stress = shear strength

 c = cohesion intercept

 σ = normal stress

 ϕ = total stress friction angle.

(b) For effective stresses, the Mohr-Coulomb failure criterion is expressed as

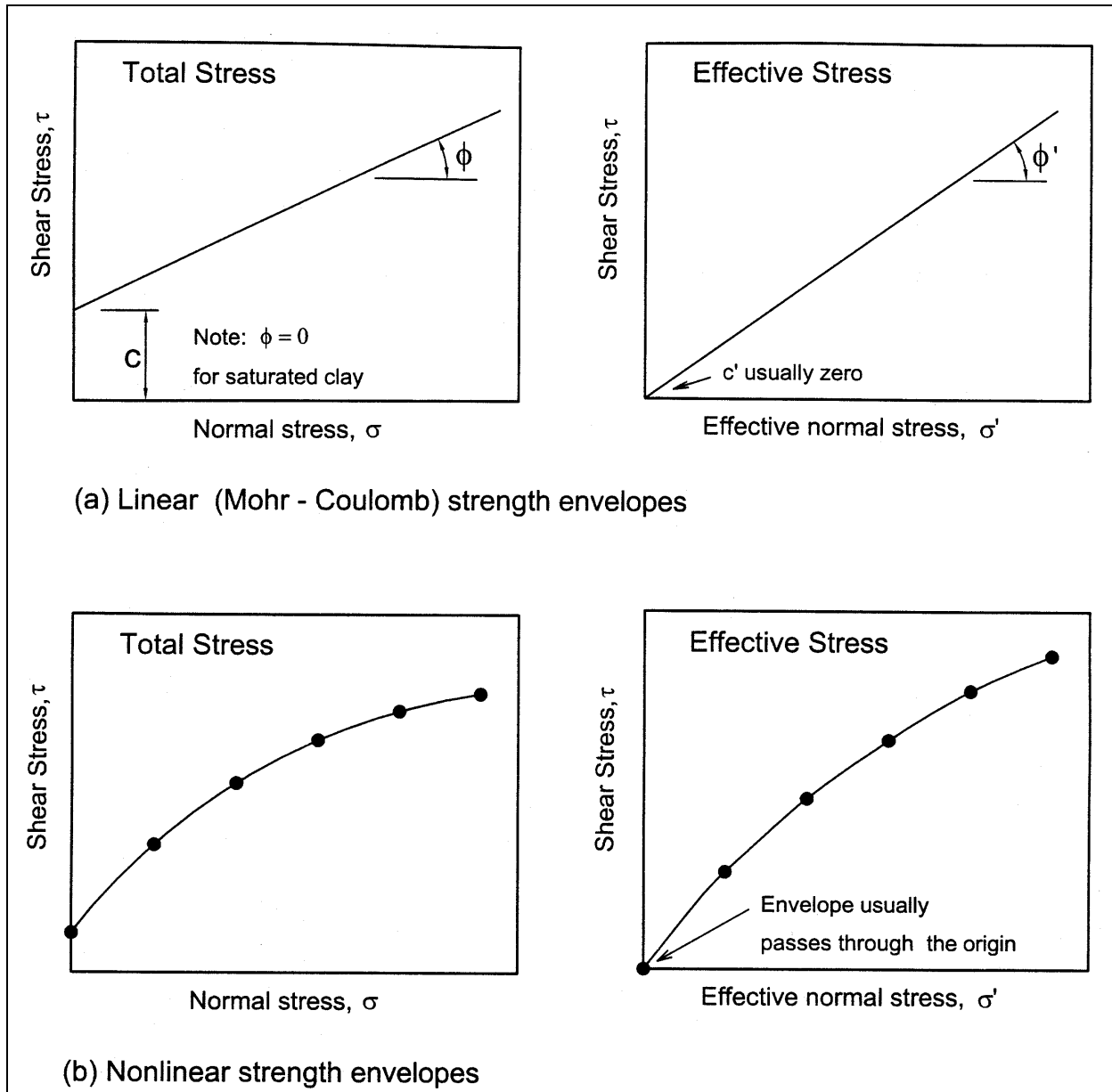$$s = c' + \sigma' \tan \varphi' \qquad (2\text{-}2)$$

Figure 2-1. Strength envelopes for soils

where

  s = maximum possible value of shear stress = shear strength

  c' = effective stress cohesion intercept

  σ' = effective normal stress

  ϕ' = effective stress friction angle.

 (c) Nonlinear strength envelopes are represented by pairs of values of s and σ, or s and σ'.

(4) Ductile and brittle stress-strain behavior. For soils with ductile stress-strain behavior (shear resistance does not decrease significantly as strain increases beyond the peak), the peak shear strength can be used in evaluating slope stability. Ductile stress-strain behavior is characteristic of most soft clays, loose sands, and clays compacted at water contents higher than optimum. For soils with brittle stress-strain behavior (shear resistance decreases significantly as strain increases beyond the peak), the peak shear resistance should not be used in evaluating slope stability, because of the possibility of progressive failure. A shear resistance lower than the peak, possibly as low as the residual shear strength, should be used, based on the judgment of the designer. Brittle stress-strain behavior is characteristic of stiff clays and shales, dense sands, and clays compacted at optimum water content or below.

(5) Peak, fully softened, and residual shear strengths. Stiff-fissured clays and shales pose particularly difficult problems with regard to strength evaluation. Experience has shown that the peak strengths of these materials measured in laboratory tests should not be used in evaluating long-term slope stability. For slopes without previous slides, the "fully softened" strength should be used. This is the same as the drained strength of remolded, normally consolidated test specimens. For slopes with previous slides, the "residual" strength should be used. This is the strength reached at very large shear displacements, when clay particles along the shear plane have become aligned in a "slickensided" parallel orientation. Back analysis of slope failures is an effective means of determining residual strengths of stiff clays and shales. Residual shear strengths can be measured in repeated direct shear tests on undisturbed specimens with field slickensided shear surfaces appropriately aligned in the shear box, repeated direct shear tests on undisturbed or remolded specimens with precut shear planes, or Bromhead ring shear tests on remolded material.

(6) Strength anisotropy. The shear strengths of soils may vary with orientation of the failure plane. An example is shown in Figure 2-2. In this case the undrained shear strength on horizontal planes ($\alpha = 0$) was low because the clay shale deposit had closely spaced horizontal fissures. Shear planes that crossed the fissures, even at a small angle, are characterized by higher strength.

(7) Strain compatibility. As noted in Appendix D, Section D-9, different soils reach their full strength at different values of strain. In a slope consisting of several soil types, it may be necessary to consider strain compatibility among the various soils. Where there is a disparity among strains at failure, the shear resistances should be selected using the same strain failure criterion for all of the soils.

c. Pore water pressures. For effective stress analyses, pore water pressures must be known and their values must be specified. For total stress analyses using computer software, hand computations, or slope stability charts, pore water pressures are specified as zero although, in fact, the pore pressures are not zero. This is necessary because all computer software programs for slope stability analyses subtract pore pressure from the total normal stress at the base of the slice:

normal stress on base of slice $= \sigma - u$ (2-3)

The quantity σ in this equation is the total normal stress, and u is pore water pressure.

(1) For total stress analyses, the normal stress should be the total normal stress. To achieve this, the pore water pressure should be set to zero. Setting the pore water pressure to zero ensures that the total normal stress is used in the calculations, as is appropriate.

(2) For effective stress analyses, appropriate values of pore water pressure should be used. In this case, using the actual pore pressure ensures that the effective normal stress ($\sigma' = \sigma - u$) on the base of the slice is calculated correctly.
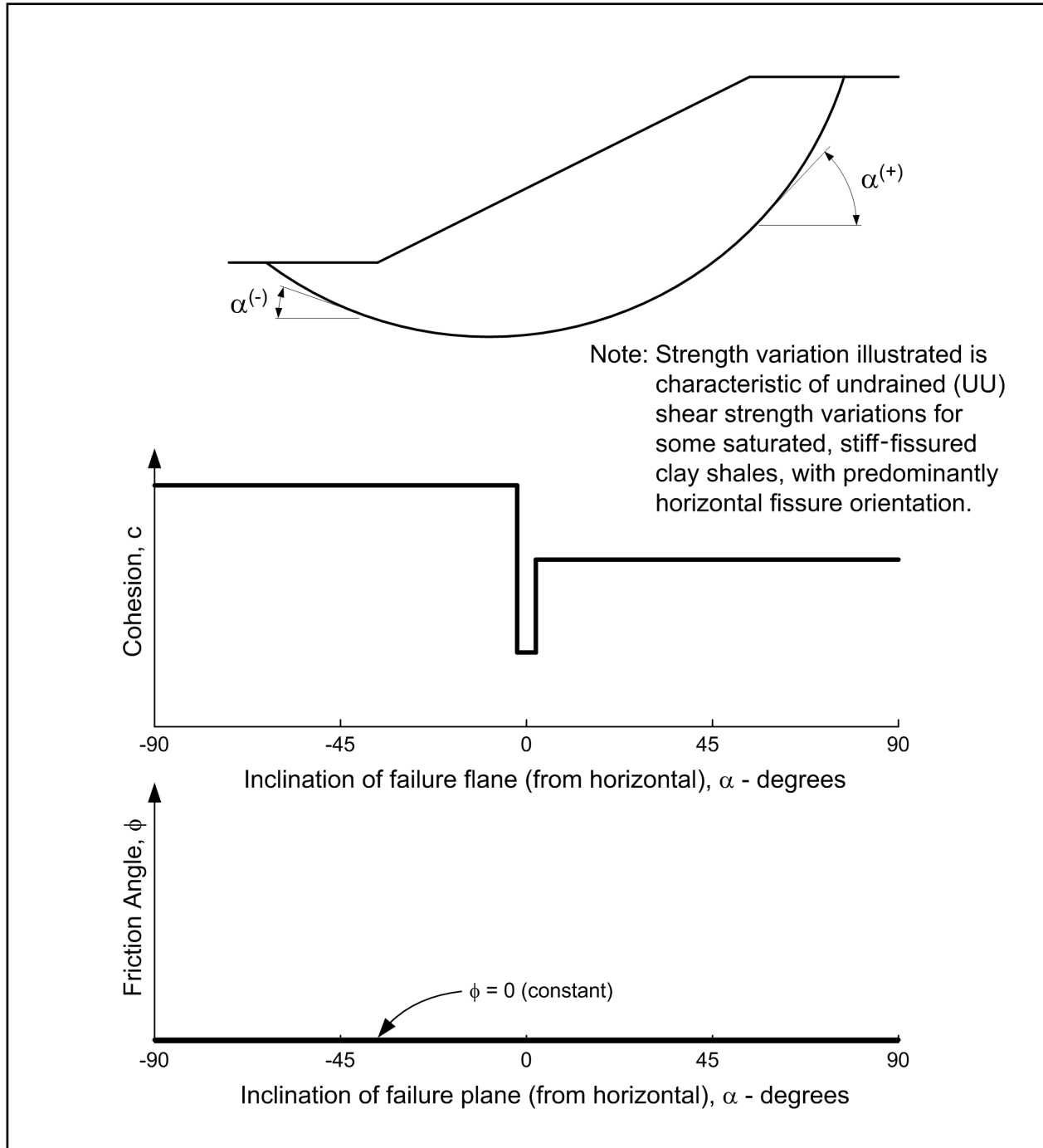
Figure 2-2. Representation of shear strength parameters for anisotropic soil

d. Unit weights. The methods of analysis described in this manual use total unit weights for both total stress analyses and effective stress analyses. This applies for soils regardless of whether they are above or below water. Use of buoyant unit weights is not recommended, because experience has shown that confusion often arises as to when buoyant unit weights can be used and when they cannot. When computations are performed with computer software, there is no computational advantage in the use of buoyant unit weights. Therefore, to avoid possible confusion and computational errors, total unit weights should be used for all soils in all conditions. Total unit weights are used for all formulations and examples presented in this manual.

e. External loads. All external loads imposed on the slope or ground surface should be represented in slope stability analyses, including loads imposed by water pressures, structures, surcharge loads, anchor forces, hawser forces, or other causes. Slope stability analyses must satisfy equilibrium in terms of total stresses and forces, regardless of whether total or effective stresses are used to specify the shear strength.

f. Tensile stresses and vertical cracks. Use of Mohr-Coulomb failure envelopes with an intercept, c or c', implies that the soil has some tensile strength (Figure 2-3). Although a cohesion intercept is convenient for representing the best-fit linear failure envelope over a range of positive normal stresses, the implied tensile strength is usually not reasonable. Unless tension tests are actually performed, which is rarely done, the implied tensile strength should be neglected. In most cases actual tensile strengths are very small and contribute little to slope stability.

(1) One exception, where the tensile strengths should be considered, is in back-analyses of slope failures to estimate the shear strength of natural deposits. In many cases, the existence of steep natural slopes can only be explained by tensile strength of the natural deposits. The near vertical slopes found in loess deposits are an example. It may be necessary to include significant tensile strength in back-analyses of such slopes to obtain realistic strength parameters. If strengths are back-calculated assuming no tensile strength, the shear strength parameters may be significantly overestimated.

(2) Significant tensile strengths in uncemented soils can often be attributed to partially saturated conditions. Later saturation of the soil mass can lead to loss of strength and slope failure. Thus, it may be most appropriate to assume significant tensile strength in back-analyses and then ignore the tensile strength (cohesion) in subsequent forward analysis of the slope. Guidelines to estimate shear strength in partially saturated soils are given in Appendix D, Section D-11.

(3) When a strength envelope with a significant cohesion intercept is used in slope stability computations, tensile stresses appear in the form of negative forces on the sides of slices and sometimes on the bases of slices. Such tensile stresses are almost always located along the upper portion of the shear surface, near the crest of the slope, and should be eliminated unless the soil possesses significant tensile strength because of cementing which will not diminish over time. The tensile stresses are easily eliminated by introducing a vertical crack of an appropriate depth (Figure 2-4). The soil upslope from the crack (to the right of the crack in Figure 2-4) is then ignored in the stability computations. This is accomplished in the analyses by terminating the slices near the crest of the slope with a slice having a vertical boundary, rather than the usual triangular shape, at the upper end of the shear surface. If the vertical crack is likely to become filled with water, an appropriate force resulting from water in the crack should be computed and applied to the boundary of the slice adjacent to the crack.

(4) The depth of the crack should be selected to eliminate tensile stresses, but not compressive stresses. As the crack depth is gradually increased, the factor of safety will decrease at first (as tensile stresses are eliminated), and then increase (as compressive stresses are eliminated) (Figure 2-5). The appropriate depth for a crack is the one producing the minimum factor of safety, which corresponds to the depth where tensile, but not compressive, stresses are eliminated.

(5) The depth of a vertical crack often can be estimated with suitable accuracy from the Rankine earth pressure theory for active earth pressures beneath a horizontal ground surface. The stresses in the tensile stress zone of the slope can be approximated by active Rankine earth pressures as shown in Figure 2-6. In the case where shear strengths are expressed using total stresses, the depth of tensile stress zone, z_t, is given by:

$$z_t = \frac{2c_D}{\gamma} \tan\left(45° + \frac{\phi_D}{2}\right) \tag{2-4}$$
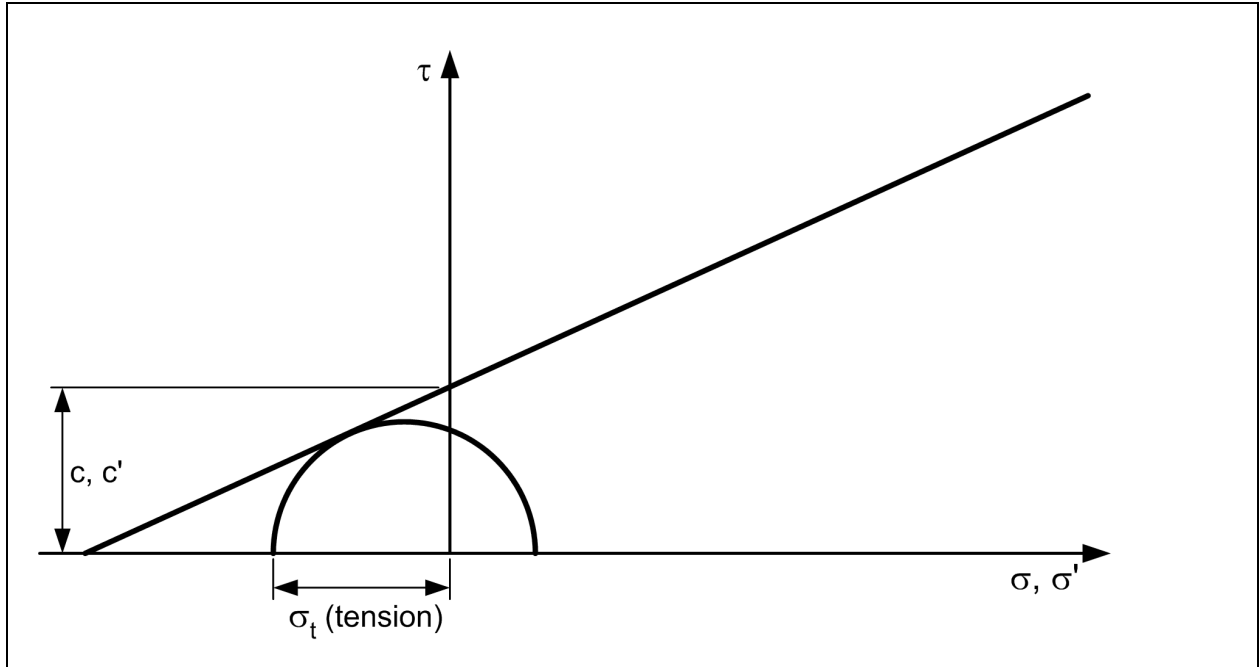
Figure 2-3.   Tensile stresses resulting from a Mohr-Coulomb failure envelope with a cohesion intercept
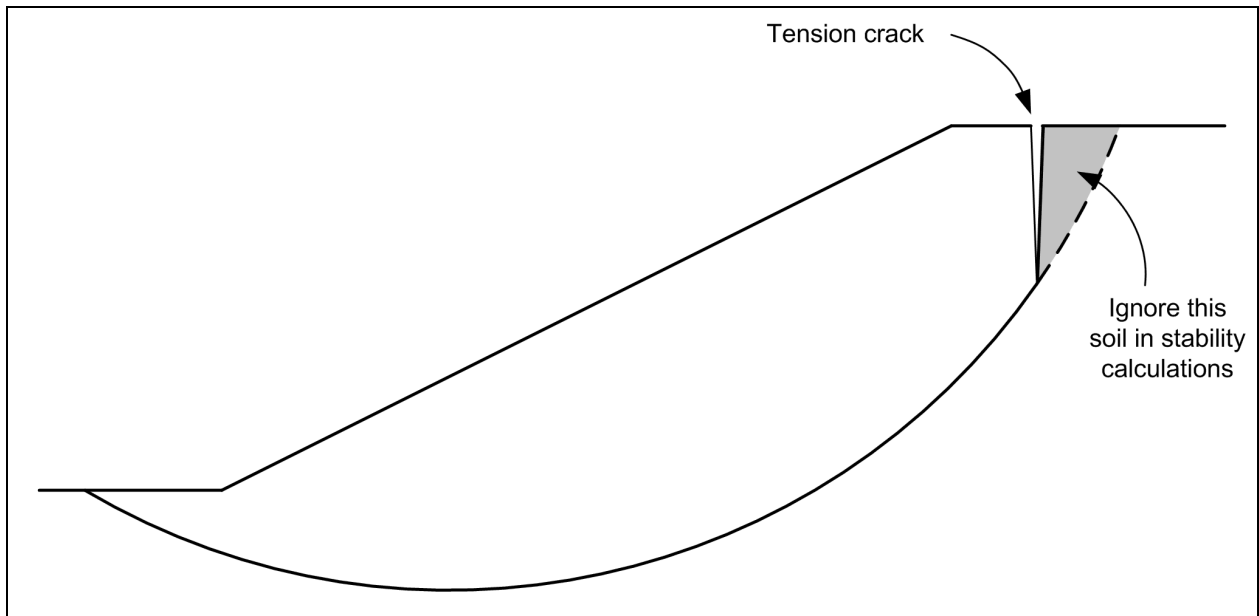
Figure 2-4.   Vertical tension crack introduced to avoid tensile stresses in cohesive soils
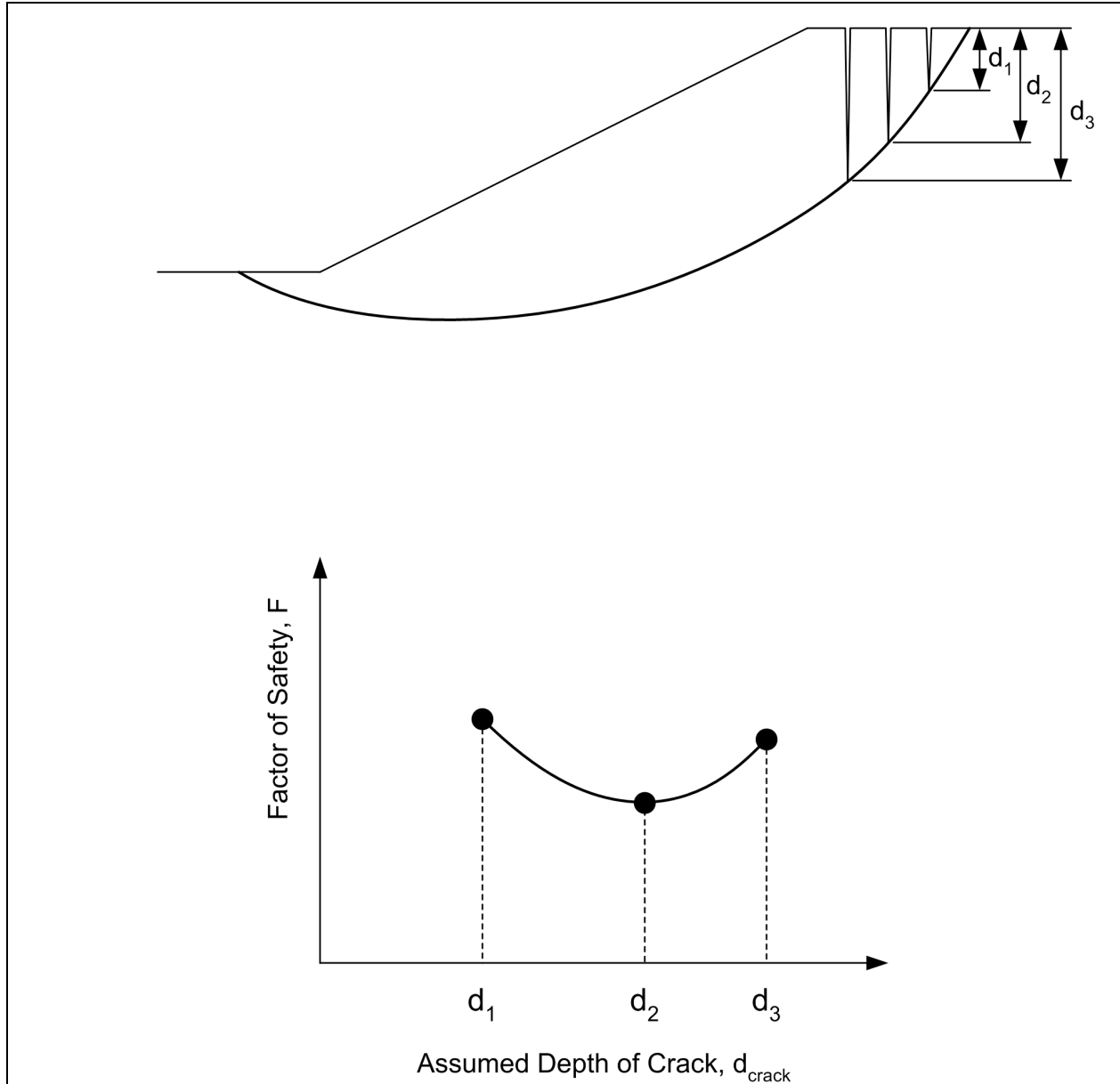
Figure 2-5.   Variation in the factor of safety with the assumed depth of vertical crack

where c_D and ϕ_D represent the "developed" cohesion value and friction angle, respectively.

The developed shear strength parameters are expressed by:

$$c_D = \frac{c}{F}$$

(2-5)

and

$$\phi_D = \arctan\left(\frac{\tan\phi}{F}\right)$$

(2-6)
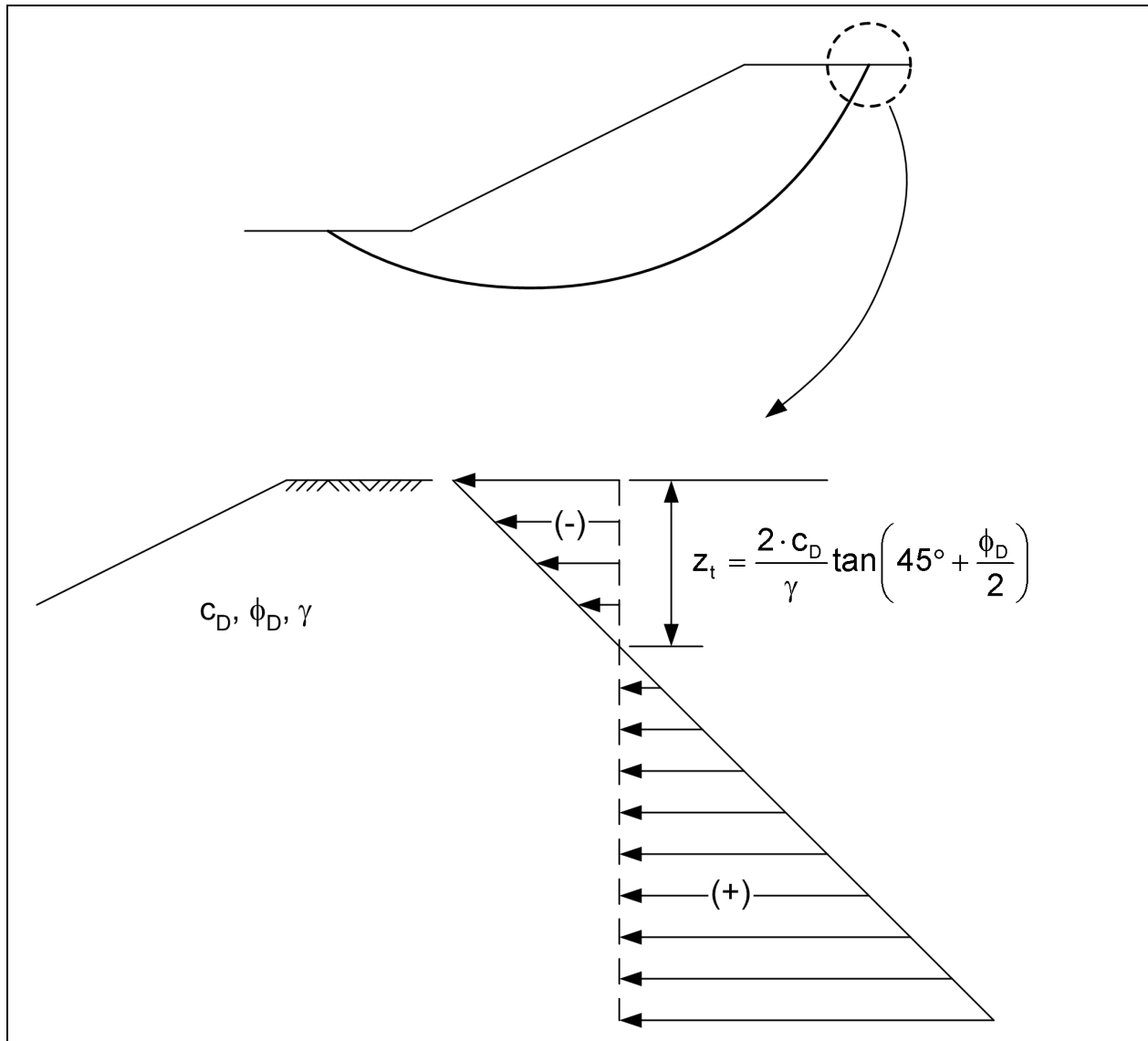
Figure 2-6. Horizontal stresses near the crest of the slope according to Rankine active earth pressure theory

$$z_t = \frac{2 \cdot c_D}{\gamma} \tan\left(45° + \frac{\phi_D}{2}\right)$$

where c, ϕ, and F are cohesion, angle of internal friction, and factor of safety.

In most practical problems, the factor of safety can be estimated with sufficient accuracy to estimate the developed shear strength parameters (c_D and ϕ_D) and the appropriate depth of the tension crack.

(6) For effective stress analyses the depth of the tension crack can also be estimated from Rankine active earth pressure theory. In this case effective stress shear strength parameters, c' and ϕ' are used, with appropriate pore water pressure conditions.

2-3. Analyses of Stability during Construction and at the End of Construction

a. General. Computations of stability during construction and at the end of construction are performed using drained strengths in free-draining materials and undrained strengths in materials that drain slowly. Consolidation analyses can be used to determine what degree of drainage may develop during the

construction period. As a rough guideline, materials with values of permeability greater than 10^{-4} cm/sec usually will be fully drained throughout construction. Materials with values of permeability less than 10^{-7} cm/sec usually will be essentially undrained at the end of construction. In cases where appreciable but incomplete drainage is expected during construction, stability should be analyzed assuming fully drained and completely undrained conditions, and the less stable of these conditions should be used as the basis for design. For undrained conditions, pore pressures are governed by several factors, most importantly the degree of saturation of the soil, the density of the soil, and the loads imposed on it. It is conceivable that pore pressures for undrained conditions could be estimated using results of laboratory tests or various empirical rules, but in most cases pore pressures for undrained conditions cannot be estimated accurately. For this reason, undrained conditions are usually analyzed using total stress procedures rather than effective stress procedures.

b.   Shear strength properties. During construction and at end of construction, stability is analyzed using drained strengths expressed in terms of effective stresses for free-draining materials and undrained strengths expressed in terms of total stresses for materials that drain slowly.

(1) Staged construction may be necessary for embankments built on soft clay foundations. Consolidated-undrained triaxial tests can be used to determine strengths for partial consolidation during staged construction (Appendix D, Section D-10.)

(2) Strength test specimens should be representative of the soil in the field: for naturally occurring soils, undisturbed samples should be obtained and tested at their natural water contents; for compacted soils, strength test specimens should be compacted to the lowest density, at the highest water content permitted by the specifications, to measure the lowest undrained strength of the material that is consistent with the specifications.

(3) The potential for errors in strengths caused by sampling disturbance should always be considered, particularly when using Q tests in low plasticity soils. Methods to account for disturbances are discussed in Appendix D, Section D-3.

c.   Pool levels. In most cases the critical pool level for end of construction stability of the upstream slope is the minimum pool level possible. In some cases, it may be appropriate to consider a higher pool for end-of-construction stability of the downstream slope. (Section 2-4).

d.   Pore water pressures. For free-draining materials with strengths expressed in terms of effective stresses, pore water pressures must be determined for analysis of stability during and at the end of construction. These pore water pressures are determined by the water levels within and adjacent to the slope. Pore pressures can be estimated using the following analytical techniques:

(1) Hydrostatic pressure computations for conditions of no flow.

(2) Steady-state seepage analysis techniques such as flow nets or finite element analyses for nonhydrostatic conditions.

For low-permeability soils with strengths expressed in of total stresses, pore water pressures are set to zero for purposes of analysis, as explained in Section 2-2.

2-4. Analyses of Steady-State Seepage Conditions

a.   General. Long-term stability computations are performed for conditions that will exist a sufficient length of time after construction for steady-state seepage or hydrostatic conditions to develop. (Hydrostatic conditions are a special case of steady-state seepage, in which there is no flow.) Stability computations are

performed using shear strengths expressed in terms of effective stresses, with pore pressures appropriate for the long-term condition.

b. Shear strength properties. By definition, all soils are fully drained in the long-term condition, regardless of their permeability. Long-term conditions are analyzed using drained strengths expressed in terms of effective stress parameters (c' and ϕ').

c. Pool levels. The maximum storage pool (usually the spillway crest elevation) is the maximum water level that can be maintained long enough to produce a steady-state seepage condition. Intermediate pool levels considered in stability analyses should range from none to the maximum storage pool level. Intermediate pool levels are assumed to exist over a period long enough to develop steady-state seepage.

d. Surcharge pool. The surcharge pool is considered a temporary pool, higher than the storage pool, that adds a load to the driving force but often does not persist long enough to establish a steady seepage condition. The stability of the downstream slope should be analyzed at maximum surcharge pool. Analyses of this surcharge pool condition should be performed using drained strengths in the embankment, assuming the extreme possibility of steady-state seepage at the surcharge pool level.

(1) In some cases it may also be appropriate to consider the surcharge pool condition for end of construction (as discussed in Section 2-3), in which case low-permeability materials in the embankment would be assigned undrained strengths.

(2) For all analyses, the tailwater levels should be appropriate for the various pool levels.

e. Pore water pressures. The pore pressures used in the analyses should represent the field conditions of water pressure and steady-state seepage in the long-term condition. Pore pressures for use in the analyses can be estimated from:

(1) Field measurements of pore pressures in existing slopes.

(2) Past experience and judgement.

(3) Hydrostatic pressure computations for conditions of no flow.

(4) Steady-state seepage analyses using such techniques as flow nets or finite element analyses.

2-5. Analyses of Sudden Drawdown Stability

a. General. Sudden drawdown stability computations are performed for conditions occurring when the water level adjacent to the slope is lowered rapidly. For analysis purposes, it is assumed that drawdown is very fast, and no drainage occurs in materials with low permeability; thus the term "sudden" drawdown. Materials with values of permeability greater than 10^{-4} cm/sec can be assumed to drain during drawdown, and drained strengths are used for these materials. Two procedures are presented in Appendix G for computing slope stability for sudden drawdown.

(1) The first is the procedure recommended by Wright and Duncan (1987) and later modified by Duncan, Wright, and Wong (1990). This is the preferred procedure.

(2) The second is the procedure originally presented in the 1970 version of the USACE slope stability manual (EM 1110-2-1902). This procedure is referred to as the USACE 1970 procedure and is described in further detail in Appendix G. Both procedures are believed to be somewhat conservative in that they utilize

the lower of the drained or undrained strength to compute the stability for sudden drawdown. However, the 1970 procedure employs assumptions that may make it excessively conservative, especially for soils that dilate or tend to dilate when sheared. Further details and examples of the procedures for sudden drawdown are presented in Appendix G.

b. Analysis stages. The recommended procedure involves three stages of analysis. The purpose of the first set of computations is to compute the effective stresses along the shear surface (on the base of each slice) to which the soil is consolidated prior to drawdown. These consolidation stresses are used to estimate undrained shear strengths for the second-stage computations, with the reservoir lowered. The third set of computations also analyzes stability after drawdown, using the lower of the drained or undrained strength, to ensure that a conservative value of factor of safety is computed.

c. Partial drainage. Partial drainage during drawdown may result in reduced pore water pressures and improved stability. Theoretically such improvement in stability could be computed and taken into account by effective stress stability analyses. The computations would be performed as for long-term stability, except that pore water pressures representing partial drainage would be used. Although such an approach seems logical, it is beyond the current state of the art. The principal difficulty lies in predicting the pore water pressures induced by drawdown. Approaches based on construction of flow nets and numerical solutions do not account for the pore pressures induced by shear deformations. Ignoring these shear-induced pore pressures results in errors that may be on the safe side if the shear-induced pore pressures are negative, or on the unsafe side if the shear-induced pore pressures are positive. For a more complete discussion of procedures for estimating pore water pressures resulting from sudden drawdown, consult Duncan, Wright, and Wong (1990) and Wright and Duncan (1987).

2-6. Analyses of Stability during Earthquakes

An Engineer Circular, "Dynamic Analysis of Embankment Dams," still in draft form, will provide guidance concerning types of analyses and design criteria for earthquake loading.

**Chapter 3
Design Criteria**

3-1. General

a. Applicability. This chapter provides guidance for analysis conditions and factors of safety for the design of slopes. Required factors of safety for embankment dams are based on design practice developed and successfully employed by the USACE over several decades. It is imperative that all phases of design be carried out in accord with established USACE methods and procedures to ensure results consistent with successful past practice.

(1) Because of the large number of existing USACE dams and the fact that somewhat different considerations must be applied to existing dams as opposed to new construction, appropriate stability conditions and factors of safety for the analysis of existing dam slopes are discussed as well.

(2) The analysis procedures recommended in this manual are also appropriate for analysis and design of slopes other than earth and rock-fill dams. Guidance is provided for appropriate factors of safety for slopes of other types of embankments, excavated slopes, and natural slopes.

b. Factor of safety guidance. Appropriate factors of safety are required to ensure adequate performance of slopes throughout their design lives. Two of the most important considerations that determine appropriate magnitudes for factor of safety are uncertainties in the conditions being analyzed, including shear strengths and consequences of failure or unacceptable performance.

(1) What is considered an acceptable factor of safety should reflect the differences between new slopes, where stability must be forecast, and existing slopes, where information regarding past slope performance is available. A history free of signs of slope movements provides firm evidence that a slope has been stable under the conditions it has experienced. Conversely, signs of significant movement indicate marginally stable or unstable conditions. In either case, the degree of uncertainty regarding shear strength and piezometric levels can be reduced through back analysis. Therefore, values of factors of safety that are lower than those required for new slopes can often be justified for existing slopes.

(2) Historically, geotechnical engineers have relied upon judgment, precedent, experience, and regulations to select suitable factors of safety for slopes. Reliability analyses can provide important insight into the effects of uncertainties on the results of stability analyses and appropriate factors of safety. However, for design and construction of earth and rock-fill dams, required factors of safety continue to be based on experience. Factors of safety for various types of slopes and analysis conditions are summarized in Table 3-1. These are minimum required factors of safety for new embankment dams. They are advisory for existing dams and other types of slopes.

c. Shear strengths. Shear strengths of fill materials for new construction should be based on tests performed on laboratory compacted specimens. The specimens should be compacted at the highest water content and the lowest density consistent with specifications. Shear strengths of existing fills should be based on the laboratory tests performed for the original design studies if they appear to be reliable, on laboratory tests performed on undisturbed specimens retrieved from the fill, and/or on the results of in situ tests performed in the fill. Shear strengths of natural materials should be based on the results of tests performed on undisturbed specimens, or on the results of in situ tests. Principles of shear strength characterization are summarized in Appendix D.

Table 3-1
Minimum Required Factors of Safety: New Earth and Rock-Fill Dams

Analysis Condition[1]	Required Minimum Factor of Safety	Slope
End-of-Construction (including staged construction)[2]	1.3	Upstream and Downstream
Long-term (Steady seepage, maximum storage pool, spillway crest or top of gates)	1.5	Downstream
Maximum surcharge pool[3]	1.4	Downstream
Rapid drawdown	1.1-1.3[4,5]	Upstream

[1] For earthquake loading, see ER 1110-2-1806 for guidance. An Engineer Circular, "Dynamic Analysis of Embankment Dams," is still in preparation.

[2] For embankments over 50 feet high on soft foundations and for embankments that will be subjected to pool loading during construction, a higher minimum end-of-construction factor of safety may be appropriate.

[3] Pool thrust from maximum surcharge level. Pore pressures are usually taken as those developed under steady-state seepage at maximum storage pool. However, for pervious foundations with no positive cutoff steady-state seepage may develop under maximum surcharge pool.

[4] Factor of safety (FS) to be used with improved method of analysis described in Appendix G.

[5] FS = 1.1 applies to drawdown from maximum surcharge pool; FS = 1.3 applies to drawdown from maximum storage pool.

For dams used in pump storage schemes or similar applications where rapid drawdown is a routine operating condition, higher factors of safety, e.g., 1.4-1.5, are appropriate. If consequences of an upstream failure are great, such as blockage of the outlet works resulting in a potential catastrophic failure, higher factors of safety should be considered.

(1) During construction of embankments, materials should be examined to ensure that they are consistent with the materials on which the design was based. Records of compaction, moisture, and density for fill materials should be compared with the compaction conditions on which the undrained shear strengths used in stability analyses were based.

(2) Particular attention should be given to determining if field compaction moisture contents of cohesive materials are significantly higher or dry unit weights are significantly lower than values on which design strengths were based. If so, undrained (UU, Q) shear strengths may be lower than the values used for design, and end-of-construction stability should be reevaluated. Undisturbed samples of cohesive materials should be taken during construction and unconsolidated-undrained (UU, Q) tests should be performed to verify end-of-construction stability.

d. Pore water pressure. Seepage analyses (flow nets or numerical analyses) should be performed to estimate pore water pressures for use in long-term stability computations. During operation of the reservoir, especially during initial filling and as each new record pool is experienced, an appropriate monitoring and evaluation program must be carried out. This is imperative to identify unexpected seepage conditions, abnormally high piezometric levels, and unexpected deformations or rates of deformations. As the reservoir is brought up and as higher pools are experienced, trends of piezometric levels versus reservoir stage can be used to project piezometric levels for maximum storage and maximum surcharge pool levels. This allows comparison of anticipated actual performance to the piezometric levels assumed during original design studies and analysis. These projections provide a firm basis to assess the stability of the downstream slope of the dam for future maximum loading conditions. If this process indicates that pore water pressures will be higher than those used in design stability analyses, additional analyses should be performed to verify long-term stability.

e. Loads on slopes. Loads imposed on slopes, such as those resulting from structures, vehicles, stored materials, etc. should be accounted for in stability analyses.

3-2. New Embankment Dams

a. Earth and rock-fill dams. Minimum required factors of safety for design of new earth and rock-fill dams are given in Table 3-1. Criteria and procedures for conducting each analysis condition are found in Chapter 2 and the appendices. The factors of safety in Table 3-1 are based on USACE practice, which includes established methodology with regard to subsurface investigations, drilling and sampling, laboratory testing, field testing, and data interpretation.

b. Embankment cofferdams. Cofferdams are usually temporary structures, but may also be incorporated into a final earth dam cross section. For temporary structures, stability computations only must be performed when the consequences of failure are serious. For cofferdams that become part of the final cross section of a new embankment dam, stability computations should be performed in the same manner as for new embankment dams.

3-3. Existing Embankment Dams

a. Need for reevaluation of stability. While the purpose of this manual is to provide guidance for correct use of analysis procedures, the use of slope stability analysis must be held in proper perspective. There is danger in relying too heavily on slope stability analyses for existing dams. Appropriate emphasis must be placed on the often difficult task of establishing the true nature of the behavior of the dam through field investigations and research into the historical design, construction records, and observed performance of the embankment. In many instances monitoring and evaluation of instrumentation are the keys to meaningful assessment of stability. Nevertheless, stability analyses do provide a useful tool for assessing the stability of existing dams. Stability analyses are essential for evaluating remedial measures that involve changes in dam cross sections.

(1) New stability analysis may be necessary for existing dams, particularly for older structures that did not have full advantage of modern state-of-the-art design methods. Where stability is in question, stability should be reevaluated using analysis procedures such as Spencer's method, which satisfy all conditions of equilibrium.

(2) With the force equilibrium procedures used for design analyses of many older dams, the calculated factor of safety is affected by the assumed side force inclination. The calculated factor of safety from these procedures may be in error, too high or too low, depending upon the assumptions made.

b. Analysis conditions. It is not necessary to analyze end-of-construction stability for existing dams unless the cross section is modified. Long-term stability under steady-state seepage conditions (maximum storage pool and maximum surcharge pool), and rapid drawdown should be evaluated if the analyses performed for design appear questionable. The potential for slides in the embankment or abutment slope that could block the outlet works should also be evaluated. Guidance for earthquake loading is provided in ER 1110-2-1806, and an Engineer Circular, "Dynamic Analysis of Embankment Dams," is in draft form.

c. Factors of safety. Acceptable values of factors of safety for existing dams may be less than those for design of new dams, considering the benefits of being able to observe the actual performance of the embankment over a period of time. In selecting appropriate factors of safety for existing dam slopes, the considerations discussed in Section 3-1 should be taken into account. The factor of safety required will have an effect on determining whether or not remediation of the dam slope is necessary. Reliability analysis techniques can be used to provide additional insight into appropriate factors of safety and the necessity for remediation.

3-4. Other Slopes

a. Factors of safety. Factors of safety for slopes other than the slopes of dams should be selected consistent with the uncertainty involved in the parameters such as shear strength and pore water pressures that affect the calculated value of factor of safety and the consequences of failure. When the uncertainty and the consequences of failure are both small, it is acceptable to use small factors of safety, on the order of 1.3 or even smaller in some circumstances. When the uncertainties or the consequences of failure increase, larger factors of safety are necessary. Large uncertainties coupled with large consequences of failure represent an unacceptable condition, no matter what the calculated value of the factor of safety. The values of factor of safety listed in Table 3-1 provide guidance but are not prescribed for slopes other than the slopes of new embankment dams. Typical minimum acceptable values of factor of safety are about 1.3 for end of construction and multistage loading, 1.5 for normal long-term loading conditions, and 1.1 to 1.3 for rapid drawdown in cases where rapid drawdown represents an infrequent loading condition. In cases where rapid drawdown represents a frequent loading condition, as in pumped storage projects, the factor of safety should be higher.

b. Levees. Design of levees is governed by EM 1110-2-1913. Stability analyses of levees and their foundations should be performed following the principles set forth in this manual. The factors of safety listed in Table 3-1 provide guidance for levee slope stability, but the values listed are not required.

c. Other embankment slopes. The analysis procedures described in this manual are applicable to other types of embankments, including highway embankments, railway embankments, retention dikes, stockpiles, fill slopes of navigation channels, river banks in fill, breakwaters, jetties, and sea walls.

(1) The factor of safety of an embankment slope generally decreases as the embankment is raised, the slopes become higher, and the load on the foundation increases. As a result, the end of construction usually represents the critical short-term (undrained) loading condition for embankments, unless the embankment is built in stages. For embankments built in stages, the end of any stage may represent the most critical short-term condition. With time following completion of the embankment, the factor of safety against undrained failure will increase because of the consolidation of foundation soils and dissipation of construction pore pressures in the embankment fill.

(2) Water ponded against a submerged or partially submerged slope provides a stabilizing load on the slope. The possibility of low water events and rapid drawdown should be considered.

d. Excavated slopes. The analysis procedures described in this manual are applicable to excavated slopes, including foundation excavations, excavated navigation and river channel slopes, and sea walls.

(1) In principle, the stability of excavation slopes should be evaluated for both the end-of-construction and the long-term conditions. The long-term condition is usually critical. The stability of an excavated slope decreases with time after construction as pore water pressures increase and the soils within the slope swell and become weaker. As a result, the critical condition for stability of excavated slopes is normally the long-term condition, when increase in pore water pressure and swelling and weakening of soils is complete. If the materials in which the excavation is made are so highly permeable that these changes occur completely as construction proceeds, the end-of-construction and the long-term conditions are the same. These considerations lead to the conclusion that an excavation that would be stable in the long-term condition would also be stable at the end of construction.

(2) In the case of soils with very low permeability and an excavation that will only be open temporarily, the long-term (fully drained) condition may never be established. In such cases, it may be possible to excavate a slope that would be stable temporarily but would not be stable in the long term. Design for such a

condition may be possible if sufficiently detailed studies are made for design, if construction delays are unlikely, and if the observational method is used to confirm the design in the field. Such a condition, where the long-term condition is unstable, is inherently dangerous and should only be allowed where careful studies are done, where the benefits justify the risk of instability, and where failures are not life-threatening.

(3) Instability of excavated slopes is often related to high internal water pressures associated with wet weather periods. It is appropriate to analyze such conditions as long-term steady-state seepage conditions, using drained strengths and the highest probable position of the piezometric surface within the slope. For submerged and partially submerged slopes, the possibility of low water events and rapid drawdown should be considered.

e. Natural slopes. The analysis procedures in this manual are applicable to natural slopes, including valley slopes and natural river banks. They are also applicable to back-analysis of landslides in soil and soft rock for the purpose of evaluating shear strengths and/or piezometric levels, and analysis of landslide stabilization measures.

(1) Instability of natural slopes is often related to high internal water pressures associated with wet weather periods. It is appropriate to analyze such conditions as long-term, steady-state seepage conditions, using drained strengths and the highest probable position of the piezometric surface within the slope. For submerged and partially submerged slopes, the possibility of low water events and rapid drawdown should be considered.

(2) Riverbanks are subject to fluctuations in water level, and consideration of rapid drawdown is therefore of prime importance. In many cases, river bank slopes are marginally stable as a result of bank seepage, drawdown, or river current erosion removing or undercutting the toe of the slope.

Chapter 4
Calculations and Presentations

4-1. Analysis Methods

a. Selection of suitable methods of analysis. The methods of analysis (computer program, charts, hand calculations) should be selected according to the complexity of the site or job and the data available to define the site conditions.

(1) Use of a reliable and verified slope stability analysis computer program is recommended for performing slope stability analyses where conditions are complex, where significant amounts of data are available, and where possible consequences of failure are significant. Computer programs provide a means for efficient and rapid detailed analysis of a wide variety of slope geometry and load conditions.

(2) Slope stability charts are relatively simple to use and are available for analysis of a variety of short-term and long-term conditions. Appendix E contains several different types of slope stability charts and guidance for their use.

(3) Spreadsheet analyses can be used to verify results of detailed computer analyses.

(4) Graphical (force polygon) analyses can also be used to verify results of computer analyses.

b. Verification of analysis method. Verification of the results of stability analyses by independent means is essential. Analyses should be performed using more than one method, or more than one computer program, in a manner that involves independent processing of the required information and data insofar as practical, to verify as many aspects of the analysis as possible. Many slope stability analyses are performed using computer programs. Selection and verification of suitable software for slope stability analysis is of prime importance. It is essential that the software used for analysis be tested and verified, and the verification process should be described in the applicable design and analysis memoranda (geotechnical report). Thorough verification of computer programs can be achieved by analyzing benchmark slope stability problems. Benchmark problems are discussed by Edris, Munger, and Brown (1992) and Edris and Wright (1992).

4-2. Verification of Computer Analyses and Results

a. General. All reports, except reconnaissance phase reports, that deal with critical embankments or slopes should include verification of the results of computer analyses. The verification should be commensurate with the level of risk associated with the structure and should include one or more of the following methods of analysis using:

(1) Graphical (force polygon) method.

(2) Spreadsheet calculations.

(3) Another slope stability computer program.

(4) Slope stability charts.

The historical U.S. Army Corps of Engineers' approach to verification of any computer analysis was to perform hand calculations (force polygon solution) of at least a simplified version of the problem. It was

acceptable to simplify the problem by using fewer slices, by averaging unit weights of soil layers, and by simplifying the piezometric conditions. While verification of stability analysis results is still required, it is no longer required that results be verified using graphical hand calculations. Stability analysis results can be verified using any of the methods listed above. Examples of verifications of analyses performed using Spencer's Method, the Simplified Bishop Method, and the Modified Swedish Method are shown in Figures 4-1, 4-2, 4-3, and 4-4.

   b.   Verification using a second computer program. For difficult and complex problems, a practical method of verifying or confirming computer results may be by the use of a second computer program. It is desirable that the verification analyses be performed by different personnel, to minimize the likelihood of repeating data entry errors.

   c.   Software versions.   Under most Microsoft Windows™ operating systems, the file properties, including version, size, date of creation, and date of modification can be reviewed to ensure that the correct version of the computer program is being used. Also, the size of the computer program file on disk can be compared with the size of the original file to ensure that the software has not been modified since it was verified. In addition, printed output may show version information and modification dates. These types of information can be useful to establish that the version of the software being used is the correct and most recent version available.

   d.   Essential requirements for appropriate use of computer programs. A thorough knowledge of the capabilities of the software and knowledge of the theory of limit equilibrium slope stability analysis methods will allow the user to determine if the software available is appropriate for the problem being analyzed.

   (1) To verify that data are input correctly, a cross section of the problem being analyzed should be drawn to scale and include all the required data. The input data should be checked against the drawing to ensure the data in the input file are correct. Examining graphical displays generated from input data is an effective method of checking data input.

   (2) The computed output should be checked to ensure that results are reasonable and consistent. Important items to check include the weights of slices, shear strength properties, and pore water pressures at the bottoms of slices. The user should be able to determine if the critical slip surface is going through the material it should. For automatic searches, the output should designate the most critical slip surface, as well as what other slip surfaces were analyzed during the search. Checking this information thoroughly will allow the user to determine that the problem being analyzed was properly entered into the computer and the software is correctly analyzing the problem.

   e.   Automatic search verification. Automatic searches can be performed for circular or noncircular slip surfaces. The automatic search procedures used in computer programs are designed to aid the user in locating the most critical slip surface corresponding to a minimum factor of safety. However, considerable judgment must be exercised to ensure that the most critical slip surface has actually been located. More than one local minimum may exist, and the user should use multiple searches to ensure that the global minimum factor of safety has been found.

   (1) Searches with circular slip surfaces. Various methods can used to locate the most critical circular slip surfaces in slopes. Regardless of the method used, the user should be aware of the assumptions and limitations in the search method.
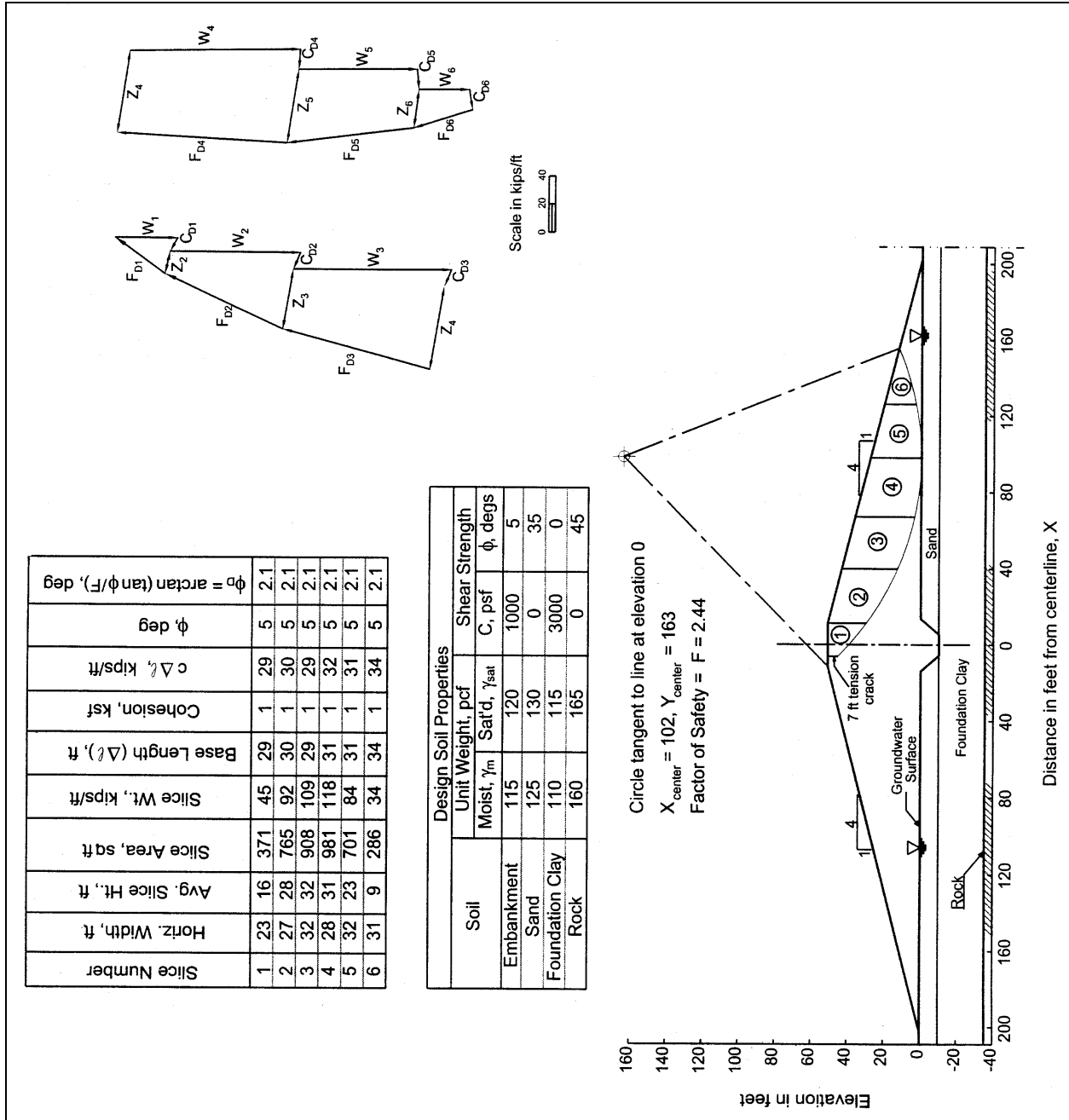
Figure 4-1. Hand verification using force equilibrium procedure to check stability computations performed via Spencer's Method – end-of-construction conditions

(a) During an automatic search, the program should not permit the search to jump from one face of the slope to another. If the initial trial slip surface is for the left face of the slope, slip surfaces on the right face of the slope should be rejected.

(b) In some cases, a slope may have several locally critical circles. The center of each such locally critical circle is surrounded by centers of circles that have higher values for the factor of safety. In such cases, when a search is performed, only one of the locally critical circles will be searched out, and the circle found may not be the one with the overall lowest factor of safety. To locate the overall critical

Center at
X = -102, Y = 163
Radius = 173
Factor of safety = 2.71

Soil	Unit Weight, pcf		Shear Strength	
	Moist, γ_m	Sat'd, γ_{sat}	c', psf	ϕ', degs
Embankment	115	120	100	25
Sand	125	130	0	35
Foundation Clay	110	115	0	28
Rock	160	165	0	45

Distance in feet from centerline, X

Slice Number	Horizontal Width (b), ft	Average Slice Height, ft	Slice Area, sq. ft	Total Unit Weight (γ), pcf	Partial Weights, kips	Total Weight (W), kips	Base Inclination (α), deg	W sin(α)	Ht. of Surface Water, ft	Avg. Surface Press., ksf	Base Inclination (α), deg	Surface Load (P), kips/ft	Horiz Moment Arm (d_h), ft	Vert Moment Arm (d_v), ft	Moment (MP), kip-ft	Piezometric Height, ft	Pore Water Pressure (u), ksf	Cohesion (c), ksf	Friction Angle (ϕ), deg	c'b + (W + Pcosβ- ub)tanϕ'	m_α (F=2.71)	[c'b+(W + Pcos β- ub)tan ϕ)] m_α
1	11	7	83	115	10	10	45	7	-	-	-	-	-	-	-	0	0.00	0.1	25	6	0.83	7
2	20	22	436	115	50	50	38	31	-	-	-	-	-	-	-	0	0.00	0.1	25	25	0.89	28
3 3'	10	30 3	311 34	115 120	36 4	40	32	21	-	-	-	-	-	-	-	3	0.20	0.1	25	19	0.94	20
4 4'	29	26 13	766 385	115 120	88 46	134	25	57	-	-	-	-	-	-	-	13	0.83	0.1	25	54	0.98	55
5 5' 5''	29	19 20 4	554 579 109	115 120 130	64 70 14	147	15	37	-	-	-	-	-	-	-	24	1.48	0	35	73	1.03	71
6 6' 6''	29	12 20 9	344 580 254	115 120 130	40 70 33	142	5	12	-	-	-	-	-	-	-	29	1.80	0	35	63	1.02	62
7 7' 7''	33	4 20 8	136 660 278	115 120 130	16 79 36	131	-6	-13	-	-	-	-	-	-	-	28	1.77	0	35	51	0.97	52
8 8'	25	17 3	421 85	120 130	51 11	62	-15	-16	3	0.19	14	5	45	146	399	23	1.46	0	35	21	0.90	23
9	20	7	139	120	17	17	-23	-7	9	0.55	14	11	68	152	1176	16	0.98	0.1	25	6	0.85	7
								129							1574							326

$$F = \frac{326}{129 - \frac{1574}{173}} = 2.71$$

Figure 4-2. Verification of computations using a spreadsheet for the Simplified Bishop Method – upstream slope, low pool

Center X = -135, y = 169
Factor of safety = 2.30

R = 169 ft.

¢

El. 50

El. 20

El. 0
El. -10

3 2 1

6 5 4

-240   -200   -160   -120   -80   -40   0   40   80   120   160   200   240

Distance in Feet from Centerline
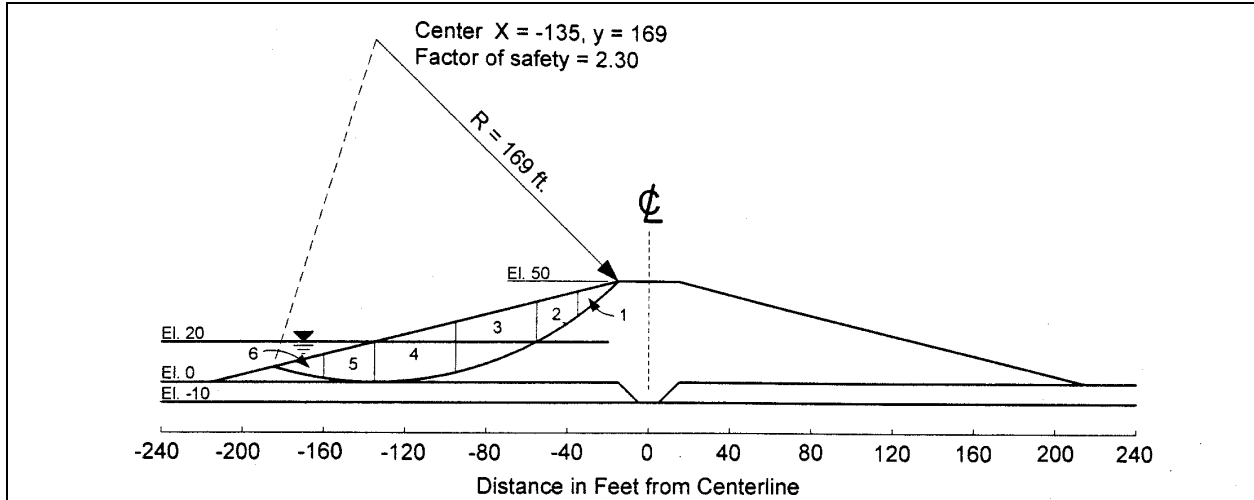
Material Properties

Soil	Cohesion	ϕ	Unit Weight
Embankment	200 psf	25 deg	115 pcf
Foundation Sand	0	35 deg	130 pcf
Foundation Clay	0	27 deg	115 pcf

Slice	Horizontal Width (b), ft	Avg. Slice Ht., ft	Slice Area, sq ft	Slice Weight (W), kips	Piezometric Ht.-Center, ft	Ht. of Surface Water, ft	Press. at top of Slice, ksf	Slope at Top of Slice, deg	Length of Top of Slice, deg	Surface Load (P), kips	Slice Base Length ($\Delta\ell$), ft	Pore Water Pressure (u), ksf	$U_b = u\Delta\ell$, kips	$c'\Delta\ell$, kips	$C_D = c'\Delta\ell/F$, kips	$\phi_D = \arctan(\tan(\phi')/F)$, deg
1	20	6	122	14	0	0	0	14	21	0	26	0.00	0	5.3	2.3	11.5
2	20	16	326	37	0	0	0	14	21	0	24	0.00	0	4.8	2.1	11.5
3	40	23	897	103	8	0	0	14	41	0	40	0.47	20	8.5	3.7	11.5
4	40	23	904	104	18	0	0	14	41	0	43	1.10	44	8.1	3.5	11.5
5	25	16	399	46	19	3	0.20	14	26	5	24	1.19	30	5.0	2.2	11.5
6	25	6	148	17	15	9	0.58	14	26	15	26	0.96	24	5.1	2.2	11.5

Figure 4-3.   Hand verification of computations using the Modified Swedish Method – upstream slope, low pool (Part 1 of 2, computed forces)

Interslice force inclination = arctan(1/4) = 14°

a. Resultant Force Diagrams

b. Force Equilibrium Polygons
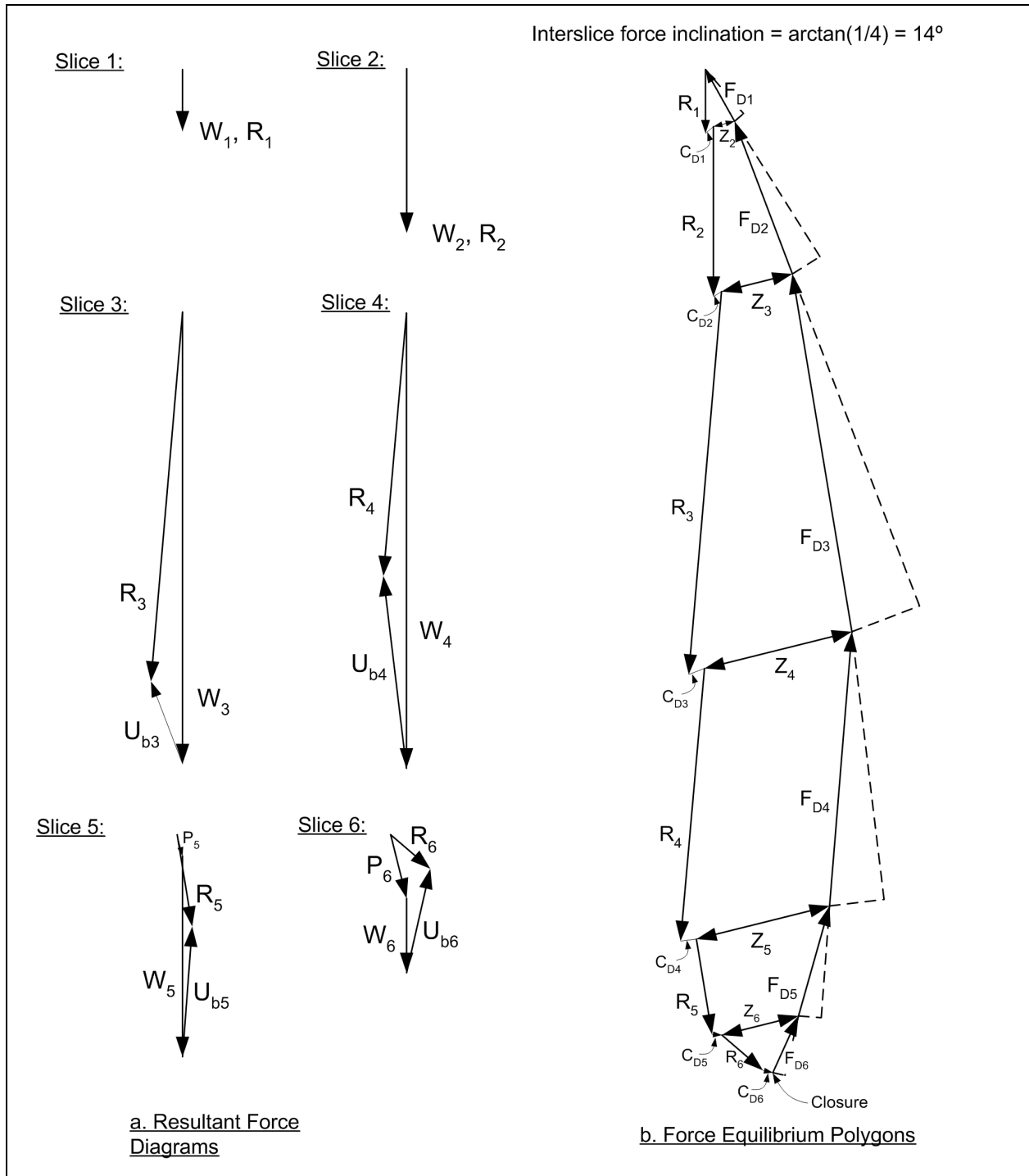
Figure 4-4. Hand verification of computations using the Modified Swedish Method (Part 2 of 2 – force polygons)

circle, several automatic searches should be performed using different starting points for the centers of the circles. The values of the factor of safety for each of the critical circles located by these independently started searches should then be compared by the user to determine the overall minimum factor of safety, and the location of the corresponding critical circle. This requires the user to perform several independently started searches for a given problem.

(c) An alternative approach is to perform analyses for a suite of circles with selected center points, and to vary the radii or depths of the circles for each center point. The computed factors of safety can be examined to determine the location of the most critical circle and the corresponding minimum factor of safety.

(2) Searches with noncircular slip surfaces. As with circular slip surfaces, various methods are used to search for critical noncircular slip surfaces. In all of these methods, the initial position of the slip surface is specified by the user and should correspond to the estimated position of the critical slip surface.

(a) In most methods of limit equilibrium slope stability analysis, the equilibrium equations used to compute the factor of safety may yield unrealistic values for the stresses near the toes of slip surfaces that are inclined upward at angles much steeper than those that would be logical based on considerations of passive earth pressure. Trial slip surfaces may become excessively steep in an automatic search unless some restriction is placed on their orientation.

(b) Because procedures for searching for critical noncircular slip surfaces have been developed more recently than those for circles, there is less experience with them. Thus, extra care and several trials may be required to select optimum values for the parameters that control the automatic search. The search parameters should be selected such that the search will result in an acceptably refined location for the most critical slip surface. The search parameters should be selected so that the final increments of distance used to shift the noncircular slip surface are no more than 10 to 25 percent of the thickness of the thinnest stratum through which the shear surface may pass.

4-3. Presentation of the Analysis and Results

a. Basic requirements. The description of the slope stability analysis should be concise, accurate, and self-supporting. The results and conclusions should be described clearly and should be supported by data.

b. Contents. It is recommended that the documentation of the stability analysis should include the items listed below. Some of the background information may be included by reference to other design documents. Essential content includes:

(1) Introduction.

(a) Scope. A brief description of the objectives of the analysis.

(b) Description of the project and any major issues or concerns that influence the analysis.

(c) References to engineering manuals, analysis procedures, and design guidance used in the analysis.

(2) Regional geology. Refer to the appropriate design memorandum, if published. If there is no previously published document on the regional geology, include a description of the regional geology to the extent that the regional geology is pertinent to the stability analysis.

(3) Site geology and subsurface explorations. Present detailed site geology including past and current exploration, drilling, and sampling activities. Present geologic maps and cross sections, in sufficient number and detail, to show clearly those features of the site that influence slope stability.

(4) Instrumentation and summary of data. Present and discuss any available instrumentation data for the site. Items of interest are piezometric data, subsurface movements observed with inclinometers, and surface movements.

(5) Field and laboratory test results.

(a) Show the location of samples on logs, plans, and cross sections.

(b) Present a summary of each laboratory test for each material, using approved forms as presented in EM 1110-2-1906, for laboratory soils testing.

(c) Show laboratory test reports for all materials. Examples are shown in Figures 4-5, 4-6, 4-7, 4-8, 4-9, and 4-10.

(d) Discuss any problems with sampling or testing of materials.

(e) Discuss the use of unique or special sampling or testing procedures.

(6) Design shear strengths. Present the design shear strength envelopes, accompanied by the shear strength envelopes developed from the individual test data for each material in the embankment, foundation, or slope, for each load condition analyzed. An example is shown in Figure 4-11.

(7) Material properties. Present the material properties for all the materials in the stability cross section, as shown in Figure 4-12. Explain how the assigned soil property values were obtained. In the case of an embankment, specify the location of the borrow area from which the embankment material is to be obtained. Discuss any factors regarding the borrow sites that would impact the material properties, especially the natural moisture content, and expected variations in the materials in the borrow area.

(8) Groundwater and seepage conditions. Present the pore water pressure information used in the stability analysis. Show the piezometric line(s) or discrete pore pressure points in the cross section used in the analysis, as shown in Figure 4-12. If the piezometric data are derived from a seepage analysis, include a summary of the seepage analysis in the report. Include all information used to determine the piezometric data, such as water surface levels in piezometers, artesian conditions at the site, excess pore water pressures measured, reservoir and river levels, and drawdown levels for rapid drawdown analysis.

(9) Stability analyses.

(a) State the method used to perform the slope stability analysis, e.g., Spencer's Method in a given computer program, Modified Swedish Method using hand calculations with the graphical (force polygon) method, or slope stability charts. Provide the required computer software verification information described in Section 4-1.

(b) For each load condition, present a tabulation of material property values, show the cross section analyzed on one or more figures, and show the locations and the factors of safety for the critical and other significant slip surfaces, as shown in Figure 4-12. For circular slip surfaces, show the center point, including the coordinates, and the value of radius.

(c) For the critical slip surface for each load condition, describe how the factor of safety results were verified and include details of the verification procedure, as discussed previously.
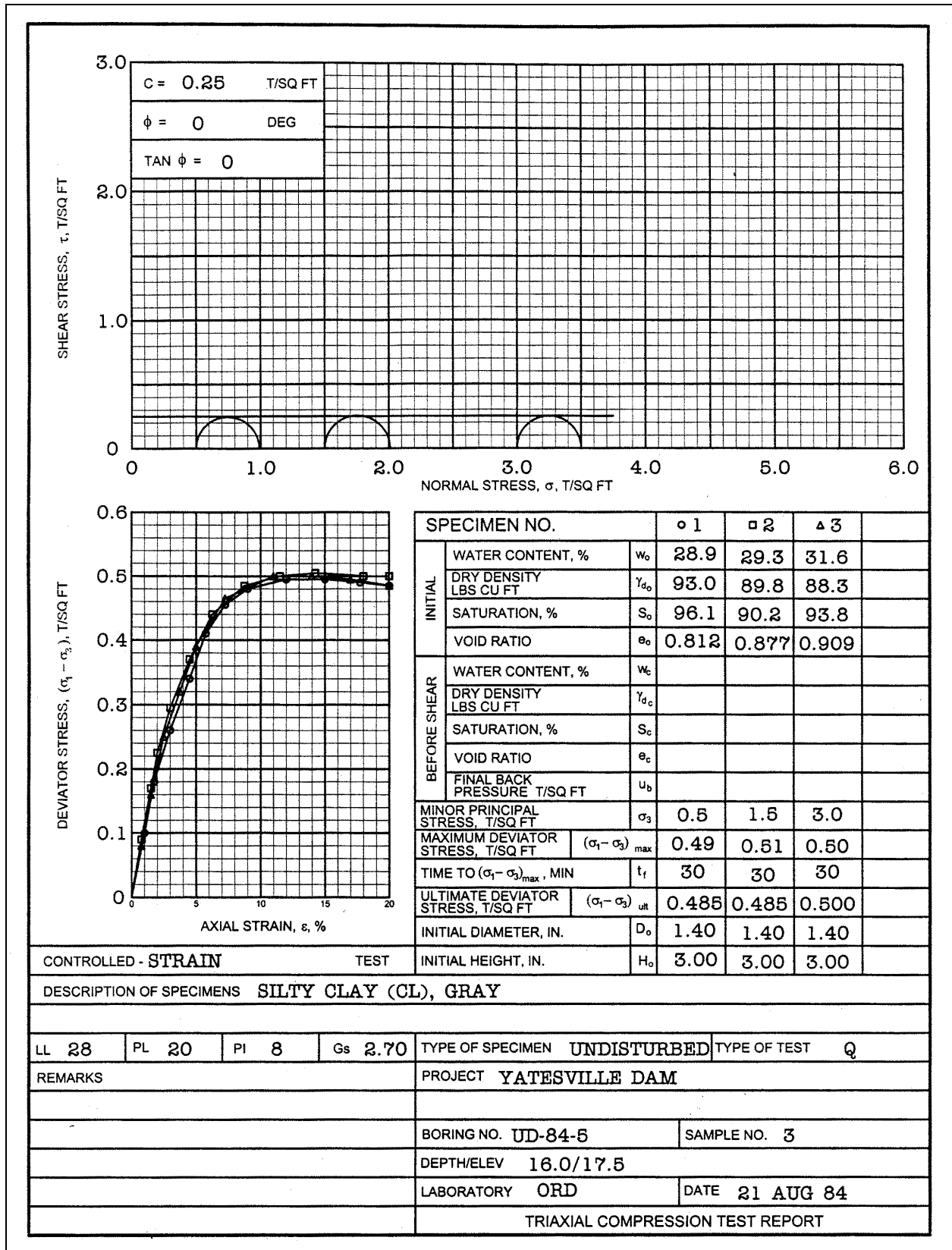
Figure 4-5.   Triaxial compression test report for Q (unconsolidated-undrained) tests

C_R = 0.4   T/SQ FT

ϕ_R = 13.5   DEG

TAN ϕ = 0.24

SHEAR STRESS, τ, T/SQ FT

NORMAL STRESS, σ, T/SQ FT

DEVIATOR STRESS, $(\sigma_1 - \sigma_3)$, T/SQ FT

AXIAL STRAIN, ε, %

SPECIMEN NO.			1	2	3	
INITIAL	WATER CONTENT, %	w_o	27.3	28.3	28.0	
	DRY DENSITY LBS CU FT	γ_{d_o}	98.2	94.6	95.9	
	SATURATION, %	S_o	100	97.8	99.7	
	VOID RATIO	e_o	0.717	0.782	0.758	
BEFORE SHEAR	WATER CONTENT, %	w_c	25.4	24.6	24.2	
	DRY DENSITY LBS CU FT	γ_{d_c}	103.9	103.4	105.0	
	SATURATION, %	S_c	100	100	100	
	VOID RATIO	e_c	0.622	0.630	0.605	
	FINAL BACK PRESSURE T/SQ FT	u_b	5.76	5.76	5.76	
MINOR PRINCIPAL STRESS, T/SQ FT		σ_3	2.0	4.0	6.0	
MAXIMUM DEVIATOR STRESS, T/SQ FT	$(\sigma_1 - \sigma_3)_{max}$		2.32	3.35	4.76	
TIME TO $(\sigma_1 - \sigma_3)_{max}$, MIN		t_f	793	913	920	
ULTIMATE DEVIATOR STRESS, T/SQ FT	$(\sigma_1 - \sigma_3)_{ult}$		2.18	3.28	4.50	
INITIAL DIAMETER, IN.		D_o	1.35	1.36	1.35	
INITIAL HEIGHT, IN.		H_o	3.00	3.00	3.00	

CONTROLLED - STRAIN TEST

DESCRIPTION OF SPECIMENS SILTY CLAY (CL), GRAY

LL 27	PL 17	PI 10	Gs 2.70	TYPE OF SPECIMEN UNDISTURBED	TYPE OF TEST R-BAR

REMARKS

PROJECT YATESVILLE DAM

BORING NO. UD-84-3   SAMPLE NO. 1

DEPTH/ELEV 18.0/19.8

LABORATORY USAEWES   DATE 31 JULY 1984

SHEET 1 OF 3   TRIAXIAL COMPRESSION TEST REPORT

Figure 4-6.   Triaxial compression test report for R-bar (consolidated-undrained) tests – total stress envelope

C = 0.175 T/SQ FT

φ = 28.1 DEG

TAN φ = 0.534

SHEAR STRESS, τ, T/SQ FT

EFFECTIVE NORMAL STRESS, σ, T/SQ FT

INDUCED PORE PRESSURE, T/SQ FT

AXIAL STRAIN, ε, %

SPECIMEN NO.			1	2	3	
INITIAL	WATER CONTENT, %	w_o	27.3	28.3	28.0	
	DRY DENSITY LBS CU FT	γ_{d_o}	98.2	94.6	95.9	
	SATURATION, %	S_o	100	97.8	99.7	
	VOID RATIO	e_o	0.717	0.782	0.758	
BEFORE SHEAR	WATER CONTENT, %	w_c	25.4	24.6	24.2	
	DRY DENSITY LBS CU FT	γ_{d_c}	103.9	103.4	105.0	
	SATURATION, %	S_c	100	100	100	
	VOID RATIO	e_c	0.622	0.630	0.605	
	FINAL BACK PRESSURE T/SQ FT	u_b	5.76	5.76	5.76	
MINOR PRINCIPAL STRESS, T/SQ FT		σ_3	0.82	1.40	2.14	
MAXIMUM DEVIATOR STRESS, T/SQ FT	$(\sigma_1 - \sigma_3)_{max}$		2.00	3.16	4.35	
TIME TO $(\sigma_1 - \sigma_3)_{max}$, MIN		t_f	793	913	920	
ULTIMATE DEVIATOR STRESS, T/SQ FT	$(\sigma_1 - \sigma_3)_{ult}$		2.18	3.28	4.50	
INITIAL DIAMETER, IN.		D_o	1.35	1.36	1.35	
INITIAL HEIGHT, IN.		H_o	3.00	3.00	3.00	

CONTROLLED - **STRAIN** TEST

DESCRIPTION OF SPECIMENS **SILTY CLAY (CL), GRAY**

LL **27**	PL **17**	PI **10**	Gs **2.70**	TYPE OF SPECIMEN **UNDISTURBED**	TYPE OF TEST **R-BAR**

REMARKS

PROJECT **YATESVILLE DAM**

BORING NO. **UD-84-3**   SAMPLE NO. **1**

DEPTH/ELEV **18.0/19.8**

LABORATORY **USAEWES**   DATE **31 JULY 1984**

SHEET 2 OF 3   TRIAXIAL COMPRESSION TEST REPORT

Figure 4-7. Triaxial compression test report for R-bar (consolidated-undrained) tests – effective stress envelope

Figure 4-8.   Variation of τ_{ff} with σ'_{fc} for R-bar test with isotropic consolidation

$\psi_{Kc = 1}$ = 15.0 degrees

$d_{kc = 1}$ = 0.45 tons per square ft

$\psi_{Kc = 1}$ = 15.0 degrees

$d_{kc = 1}$ = 0.45 tons per square ft

y-axis: $\tau_{ff} = (\sigma_1 - \sigma_3)_f / 2 \, (\cos \phi')$ tons per sqaure ft

x-axis: $\sigma'_{fc} = \sigma'_{3c}$ for K_c = 1 tons per square ft

Test	$\sigma'_{fc} = \sigma'_{3c}$ (tsf)	$(\sigma_1 - \sigma_3)$ (tsf)	τ_{ff} (tsf)
1	2.00	2.32	1.02
2	4.00	3.35	1.48
3	6.00	4.76	2.10

Note: ϕ' = 28.1 degrees, $\cos \phi'$ = 0.88

Sheet 3 of 3
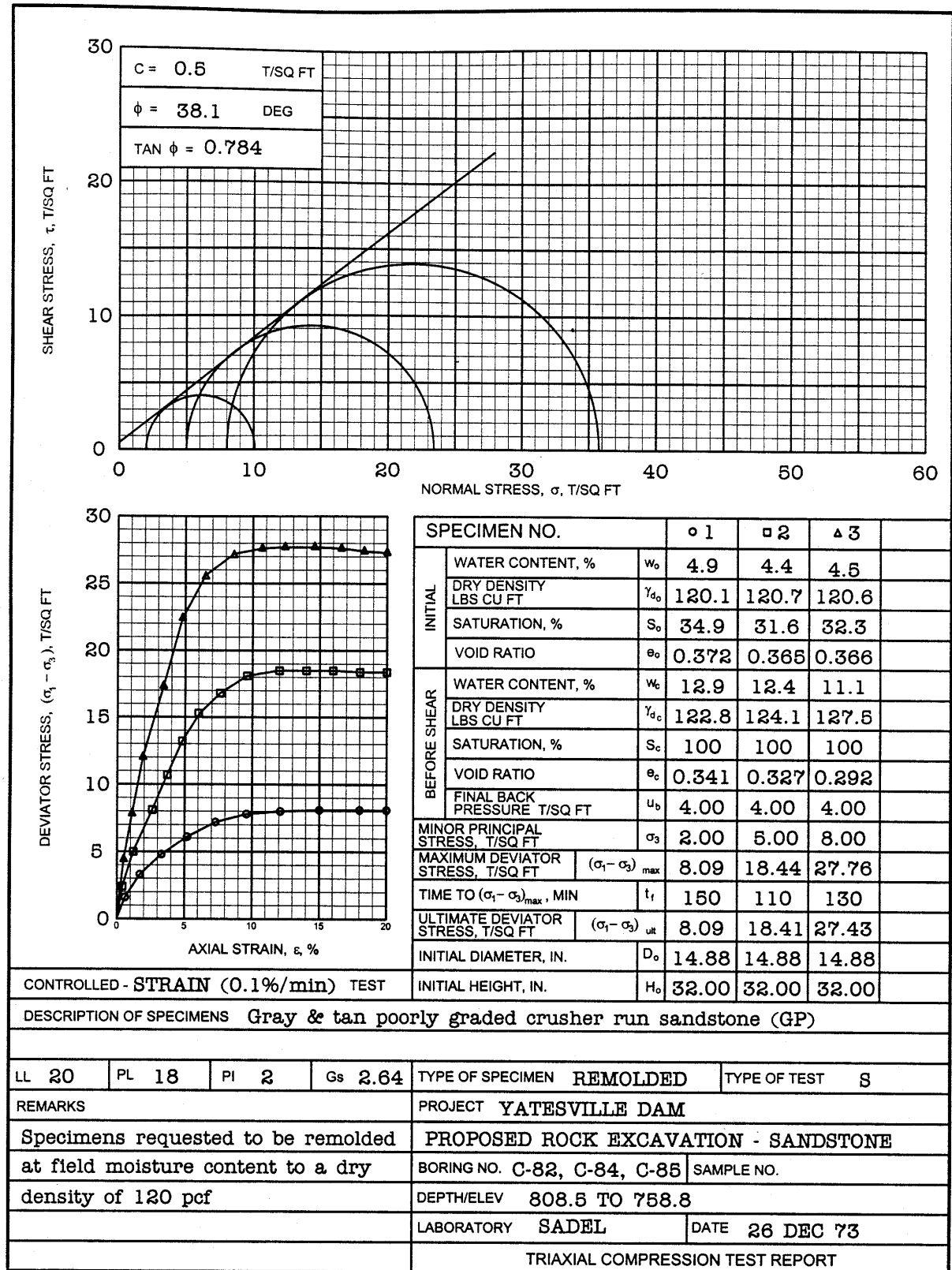
Figure 4-9. Triaxial compression test report for S (drained) tests – effective stress envelope

Shear Strength Parameters

$\phi' = $ ___27.0___ deg

$\tan\phi' = $ ___0.510___

$c' = $ ___0.0___ T/sq ft

☐ Controlled stress

☒ Controlled strain

			Test No.			
Initial	Water content	w_o	24.4%	24.4%	24.4%	
	Void ratio	e_o	0.769	0.709	0.779	
	Saturation	S_o	87%	95%	86%	
	Dry density lb/cu ft	γ_d	97.2	100.4	96.5	
	Void ratio after consolidation	e_c	0.694	0.615	0.610	
	Time for 50 percent consolidation, min	t_{50}	16	24	23	
Final	Water content	w_f	23.3%	26.1%	26.4	
	Void ratio	e_f	0.555	0.464	0.424	
	Saturation	S_f	100	100	100	
	Normal stress T/sq ft	σ	3.0	6.0	9.0	
	Maximum shear stress, T/sq ft	τ_{max}	1.60	3.16	4.47	
	Actual time to failure, min	t_f	500	600	600	
	Rate of displ., in/min			0.0003	0.0003	0.0003	
	Ultimate shear stress, T/sq ft	τ_{ult}	1.58	3.00	4.08	

Type of specimen Undisturbed	3.25 in. square	0.50 in. thick

Classification Brown and Gray Lean CLAY (CL)

LL 34.1	PL 20.9	PI 13.2		G_s 2.75

Remarks	Project Yatesville Dam
-	
	Area
	Boring No. UD-1A Sample No. 4
	Depth/Elev 579.5-577.0 Date DEC 1973
	DIRECT SHEAR TEST REPORT

Figure 4-10.   Direct shear test report – effective stress envelope

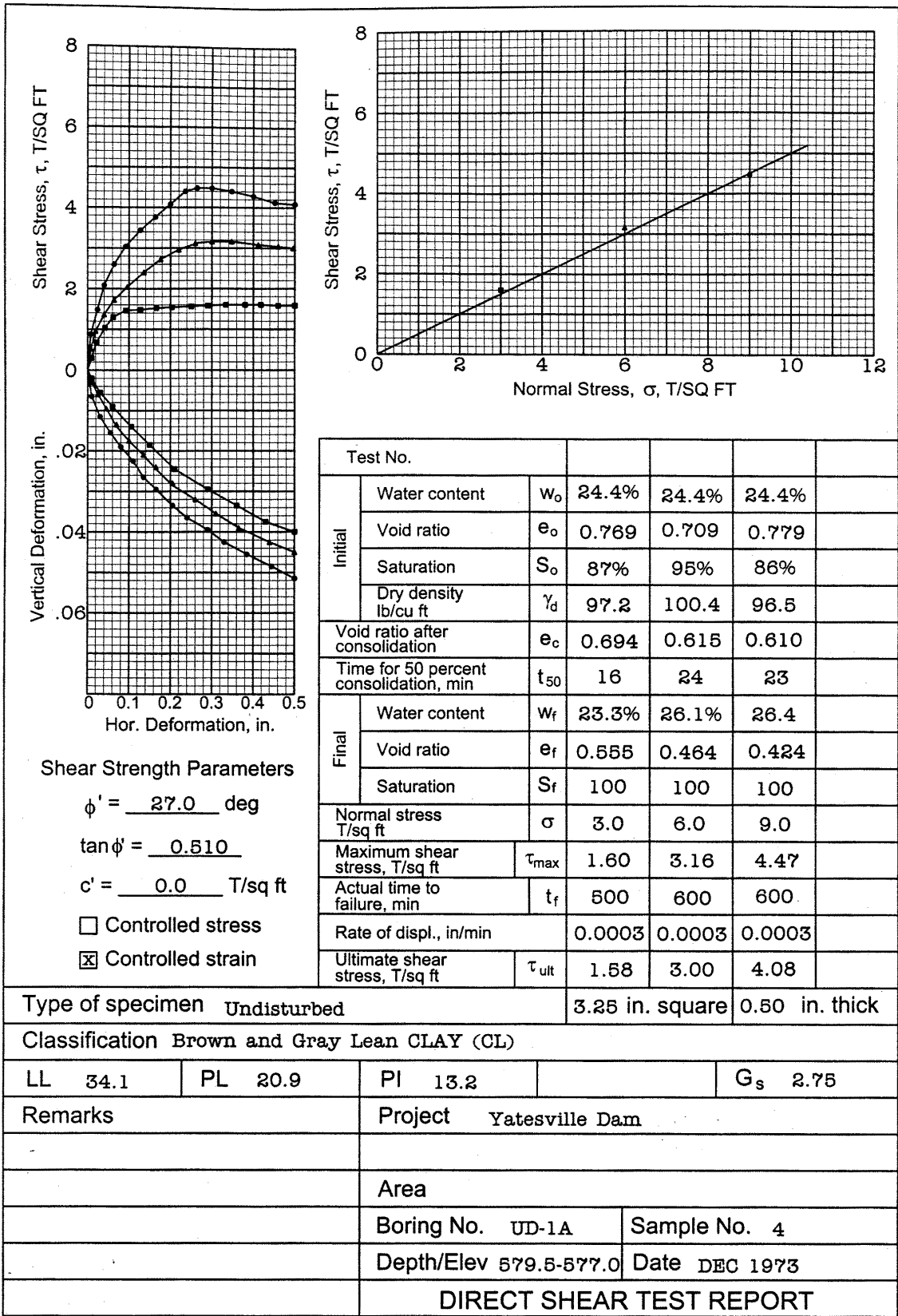| Boring	Sample	Depth - ft	Specimen	Moist density	Saturated density	C' tsf	φ' degrees
UD-2	1	42.0 - 44.0	1	126.0	129.9		
UD-2	1	42.0 - 44.0	2	125.4	127.0	0.0	27.7
UD-2	1	42.0 - 44.0	3	124.0	126.5		
UD-2	2	108 - 109.5	1	129.8	134.9		
UD-2	2	108 - 109.5	2	133.5	135.9	0.0	34.6
UD-2	2	108 - 109.5	3	128.6	134.0		
UD-4	3	58.0 - 59.5	1	122.3	124.4		
UD-4	3	58.0 - 59.5	2	121.6	123.9	0.0	25.7
UD-5	1	42.0 - 44.1	1	131.5	132.5		
UD-5	1	42.0 - 44.1	2	129.5	131.4	0.0	38.9
			Average	126.7	129.5	0.0	31.7
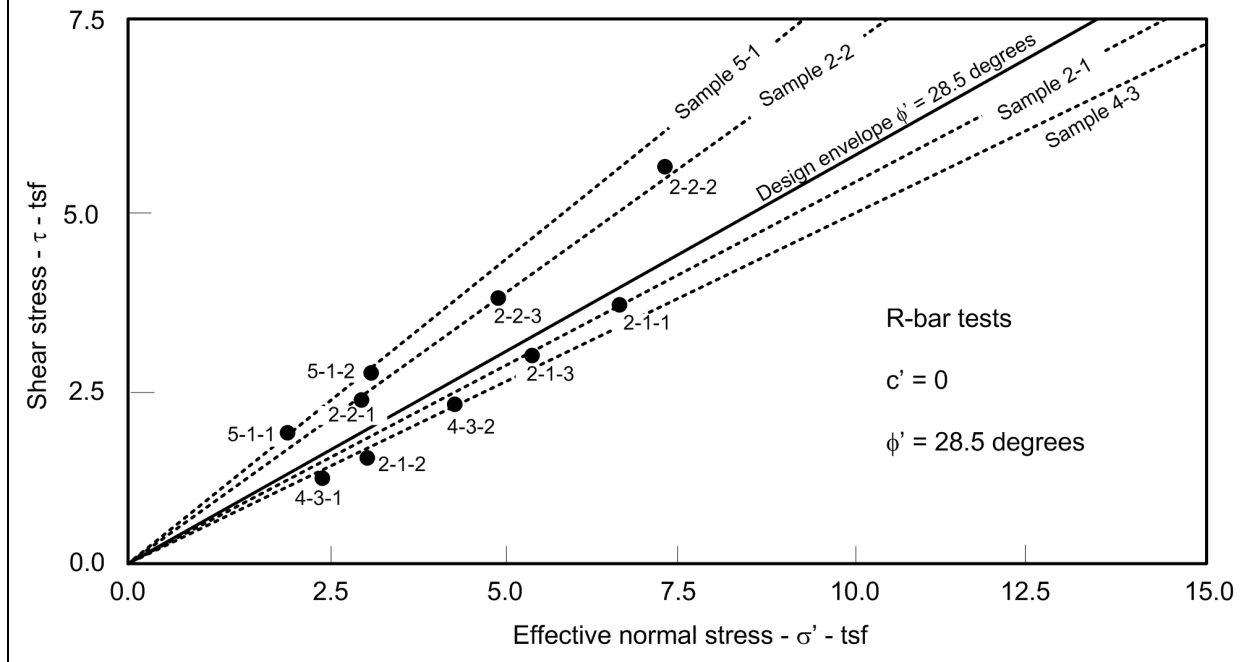
Figure 4-11. Presentation of design strength values

Critical circles

Tangent elevation	X	Y	Factor of safety
815 ft.	182	1086	2.18 before drawdown 1.87 after drawdown
790 ft.	244	1074	2.15 before drawdown 1.64 after drawdown
775 ft.	280	1110	2.53 before drawdown 2.16 after drawdown

Soil Properties

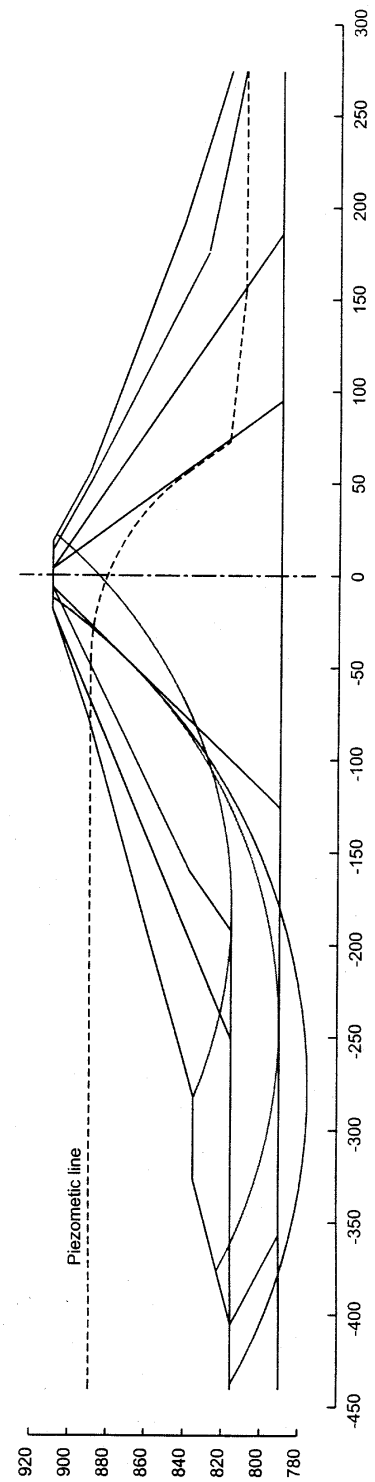| Mat'l	γ_{moist} pcf	γ_{sat} pcf	c' psi	ϕ degs	$d_{K_c=1}$ psf	$\psi_{K_c=1}$ degs	Description
1	127	130	800	21	1700	13	Impervious core
2	132	136	400	18	1600	12	Random impervious
3	140	143	0	36	-	-	Pervious shell
4	114	127	0	28	-	-	Weathered rockfill
5	100	125	0	35	-	-	Proposed rockfill
6	135	140	0	33	-	-	Foundation outwash
7	-	130	0	27	-	-	Silty aluvium

Figure 4-12.   Presentation of slope stability analysis results

Appendix A
References

EM 1110-1-1804
EM 1110-1-1804. "Geotechnical Investigations," U.S. Army Engineer Waterways Experiment Station, Vicksburg, MS.

EM 1110-2-1601
EM 1110-2-1601. "Hydraulic Design of Flood Control Channels," U.S. Army Engineer Waterways Experiment Station, Vicksburg, MS.

EM 1110-2-1806
EM 1110-2-1806. **"**Earthquake Design and Evaluation for Civil Works Projects," Washington, DC.

EM 1110-2-1901
EM 1110-2-1901. "Seepage Analysis and Control for Dams," U.S. Army Engineers Waterways Experiment Station, Vicksburg, MS.

EM 1110-2-1902
EM 1110-2-1902. 1970. "Stability of Earth and Rock-Fill Dams," U.S. Army Engineer Waterways Experiment Station, Vicksburg, MS.

EM 1110-2-1906
EM 1110-2-1906. "Laboratory Testing of Soils," U.S. Army Engineer Waterways Experiment Station, Vicksburg, MS.

EM 1110-2-1912
EM 1110-2-1912. "Stability of Excavated and Natural Slopes in Soils and Clay Shales," U.S. Army Engineer Waterways Experiment Station, Vicksburg, MS.

EM 1110-2-1913
EM 1110-2-1913. "Design and Construction of Levees," U.S. Army Engineer Waterways Experiment Station, Vicksburg, MS.

EM 1110-2-2300
EM 1110-2-2300. "Earth and Rockfill Dams, General Design and Construction Considerations," U.S. Army Engineer Waterways Experiment Station, Vicksburg, MS.

ETL 1110-2-556
ETL 1110-2-556. "Risk Based Analysis in Geotechnical Engineering for Support of Planning Studies," Washington, DC.

American Society for Testing and Materials 1999
American Society for Testing and Materials. 1999. "D 2850: Standard Test Method for Unconsolidated-Undrained Triaxial Compression Test on Cohesive Soils," West Conshohocken, PA.

Bishop and Morgenstern 1960
Bishop, A. W., and Morgenstern, N. 1960. "Stability Coefficients for Earth Slopes," *Geotechnique*, Vol 10, No. 4, pp 129-150.

Bishop 1955
Bishop, A. W. 1955. "The Use of the Slip Circle in the Stability Analysis of Slopes," *Geotechnique*, Vol 5, No. 1, pp 7-17.

Bjerrum 1973
Bjerrum, L. 1973. "Problems of Soil Mechanics and Construction on Soft Clays and Structurally Unstable Soils (Collapsible, Expansive and Others)." *Proceedings of the Eighth International Conference on Soil Mechanics and Foundation Engineering*, Moscow, Vol 3, pp 111-159.

Bolton 1979
Bolton, M. 1979. *A Guide to Soil Mechanics.* A Halstead Press Book, John Wiley and Sons, New York, 439 pp.

Budhu 2000
Budhu, M. 2000. *Soil Mechanics and Foundations.* John Wiley and Sons, 586 pp.

Casagrande 1936
Casagrande, A. 1936. "Characteristics of Cohesionless Soils Affecting the Stability of Slopes and Earth Fills," Originally published in *Journal of the Boston Society of Civil Engineers*, reprinted in *Contributions to Soil Mechanics 1925-1940*, Boston Society of Civil Engineers, pp 257-276.

Celestino and Duncan 1981
Celestino, T. B., and Duncan, J. M. 1981. "Simplified Search for Non-Circular Slip Surfaces," *Proceedings, Tenth International Conference on Soil Mechanics and Foundation Engineering*, International Society for Soil Mechanics and Foundation Engineering, Stockholm, A.A. Balkema, Rotterdam, Holland, Vol 3, pp 391-394.

Chang 1978
Chang, K. T. 1978. "An Analysis of Damage of Slope Sliding by Earthquake on the Paiho Main Dam and its Earthquake Strengthening," Tseng-hua Design Section, Department of Earthquake-Resistant Design and Flood Control Command of Miyna Reservoir, Peoples Republic of China.

Ching and Fredlund 1983
Ching, R. K. H., and Fredlund, D. G. 1983. "Some Difficulties Associated with the Limit Equilibrium Method of Slices," *Canadian Geotechnical Journal*, Vol 20, No. 4, pp 661- 672.

Chirapunta and Duncan 1975
Chirapuntu, S., and Duncan, J. M. 1975. "The Role of Fill Strength in the Stability of Embankments on Soft Clay Foundations," Geotechnical Engineering Research Report, Department of Civil Engineering, University of California, Berkeley.

Coulter and Migliaccio 1966
Coulter, H.W., and Migliaccio, R. R. 1966. "Effects of the Earthquake of March 27, 1964 at Valdez, Alaska," *Geological Survey Professional Paper No. 542-C*, U.S. Department of the Interior, Washington, DC.

Duncan 1996
Duncan, J. M. 1996. "State of the Art: Limit Equilibrium and Finite-Element Analysis of Slopes," *Journal of Geotechnical Engineering*, Vol 122, No. 7, July, pp 557-596.

Duncan and Buchignani 1975
Duncan, J. M., and Buchignani, A. L. 1975. "An Engineering Manual for Stability Studies," Civil Engineering 270B, University of California, Berkeley, CA.

Duncan, Buchignani, and DeWet 1987
Duncan, J. M., Buchignani, A. L., and DeWet, M. 1987. "An Engineering Manual for Slope Stability Studies," Department of Civil Engineering, Geotechnical Engineering, Virginia Polytechnic Institute and State University, Blacksburg, VA.

Duncan, Horz, and Yang 1989
Duncan, J. M., Horz, R. C., and Yang, T. L. 1989. "Shear Strength Correlations for Geotechnical Engineering," Virginia Tech, Department of Civil Engineering, August, 100 pp.

Duncan, Navin, and Patterson 1999
Duncan, J. M, Navin, M., and Patterson, K. 1999. "Manual for Geotechnical Engineering Reliability Calculations," Department of Civil and Environmental Engineering, Virginia Polytechnic Institute and State University, Blacksburg, VA.

Duncan and Wright 1980
Duncan, J. M., and Wright, S. G. 1980. "The Accuracy of Equilibrium Methods of Slope Stability Analysis," *Engineering Geology*, Vol 16, No. 1/2, pp 5-17.

Duncan, Wright, and Wong 1990
Duncan, J. M., Wright, S. G., and Wong, K. S. 1990. "Slope Stability During Rapid Drawdown," H. Bolton Seed Symposium, Vol. 2, University of California at Berkeley, pp 253-272.

Edris, Munger, and Brown 1992
Edris, E. V., Jr., Munger, D., and Brown, R. 1992. "User's Guide: UTEXAS3 Slope Stability Package: Volume III Example Problems," Instruction Report GL-87-1, U.S. Army Engineer Waterways Experiment Station, Vicksburg, MS.

Edris and Wright 1992
Edris, E. V., Jr. and Wright, S. G. 1992. "User's Guide: UTEXAS3 Slope Stability Package: Volume IV User's Manual," Instruction Report GL-87-1, U.S. Army Engineer Waterways Experiment Station, Vicksburg, MS.

Fellenius 1936
Fellenius, W. 1936. "Calculation of the Stability of Earth Dams," *Transactions*, *2nd International Congress on Large Darns*, International Commission on Large Dams, Washington, DC, pp 445-459.

Fredlund 1989
Fredlund, D. G. 1989. "Negative Pore Water Pressures in Slope Stability," *Proceedings*, *Symposio Suramericano de Deslizamientos*, Paipa, Columbia, pp 429-439.

Fredlund 1995
Fredlund, D. G. 1995. "The Stability of Slopes with Negative Pore-Water Pressures." *Proceedings*, *Ian Boyd Donald Symposium on Modern Developments in Geomechanics*, Monash University, Melbourne, Australia, pp 99-116.

Fredlund 2000
Fredlund, D. G. 2000. "The 1999 R. M. Hardy Lecture: The Implementation of Unsaturated Soil Mechanics into Geotechnical Engineering," *Canadian Geotechnical Journal*, Vol 37, No. 5, October, pp 963-986.

Fredlund and Krahn 1977
Fredlund, D. G., and Krahn, J. 1977. "Comparison of Slope Stability Methods of Analysis," *Canadian GeotechnicaI Journal*, Vol 14, No. 3, pp 429-439.

Fredlund and Rahardjo 1993
Fredlund, D. G., and Rahardjo, H. 1993. *Soil Mechanics for Unsaturated Soils.* John Wiley and Sons, New York, 517 pp.

Harder 1988
Harder, L. F. 1988. "Use of Penetration Tests to Determine the Cyclic Loading Resistance of Gravelly Soils During Earthquake Shaking," PhD dissertation, University of California, Berkeley.

Head 1986
Head, K. H. 1986. *Manual of Soil Laboratory Testing.* Volume 3 – Effective Stress Tests, A Halstead Press Book, John Wiley and Sons, 1238 pp.

Huang 1983
Huang, Y. H. 1983. *Stability Analysis of Earth Slopes*, Van Nostrand Reinhold Co. Inc., New York, 305 pp.

Hunter 1968
Hunter, J. H. 1968. "Stability of Simple Cuts in Normally Consolidated Clays," PhD dissertation, University of Colorado, Boulder.

Hunter and Schuster 1968
Hunter, J. H., and Schuster, R. L. 1968. "Stability of Simple Cuts in Normally Consolidated Clays," *Geotechnique*, Vol. 18, No. 3, pp 372-378.

Janbu 1954
Janbu, N. 1954. "Application of Composite Slip Surface for Stability Analysis," European Conference on Stability Analysis, Stockholm, Sweden.

Janbu 1968
Janbu, N. 1968. "Slope Stability Computations," Institutt for Geotknikk og Fundamenteringslære, Norges Tekniske Høgskole, Soils Mechanics and Foundation Engineering, the Technical University of Norway.

Janbu 1973
Janbu, N. 1973. "Slope Stability Computations," *Embankment Dam Engineering - Casagrande Volume*, R.C. Hirschfeld and S.J. Poulos, eds., John Wiley and Sons, New York, pp 47-86.

Jewell 1985
Jewell, R. A. 1985. "Limit Equilibrium Analysis of Reinforced Soil Walls." *Proceedings of the Eleventh International Conference on Soil Mechanics and Foundation Engineering.* International Society for Soil Mechanics and Foundation Engineering, A.A. Balkema, Rotterdam and Boston, pp 1705-1708.

Jumikis 1962
Jumikis, A. R. 1962. "Active and Passive Earth Pressure Coefficient Tables," *Engineering Research Publication No. 43*, Rutgers University, New Brunswick, NY.

Koutsoftas and Ladd 1985
Koutsoftas, D. C., and Ladd, C. C. 1985. "Design Strengths for an Offshore Clay," *Journal of Geotechnical Engineering*, Vol 111, No. 3, Mar., pp 337-355.

Ladd 1991
Ladd, C. C. 1991. "Stability Evaluation During Staged Construction," Twenty-Second Karl Terzaghi Lecture, *Journal of Geotechnical Engineering*, American Society of Civil Engineers, Vol 117, No. 4, April, pp 540-615.

Ladd and Foott 1974
Ladd, C. C., and Foott, R. 1974. "New Design Procedure for Stability of Soft Clays," *Journal of the Geotechnical Engineering Division*, ASCE, Vol 100, No. GT7, July, pp 763-786.

Leavell and Peters 1987
Leavell, D. A., and Peters, J. F. 1987. "Uniaxial Tensile Test for Soils," *Technical Report GL-87-10*, U.S. Army Engineer Waterways Experiment Station, Vicksburg, MS.

Lowe and Karafiath 1960
Lowe, J., and Karafiath, L. 1960. "Stability of Earth Dams upon Drawdown." *Proceedings of the First PanAmencan Conference on Soil Mechanics and Foundation Engineering.* Mexican Society of Soil Mechanics, Mexico D.F., pp 537-552.

Marachi et al. 1969
Marachi, N. D., et al. 1969. "Strength and Deformation Characteristics of Rockfill Material," Report No. TE-60-5, University of California, Berkeley.

Marcuson, Hynes, and Franklin 1990
Marcuson, W. F. III, Hynes, M. E., and Franklin, A. G. 1990. "Evaluation and Use of Residual Strength in Seismic Safety Analysis of Embankments," *Earthquake Spectra*, Vol 6, No. 3, pp 529-572.

Morgenstern 1963
Morgenstern, N. 1963. "Stability Charts for Earth Slopes During Rapid Drawdown," *Geotechnique*, Vol 13, No. 2, pp 121-131.

Morgenstern and Price 1965
Morgenstern, N. R., and Price, V. E. 1965. "The Analysis of the Stability of General Slip Surfaces," *Geotechnique*, Vol 15, No. 1, pp 79-93.

Peck 1988
Peck, R. B. 1988. "The Place of Stability Calculations in Evaluating the Safety of Existing Embankment Dams," *Civil Engineering Practice*, Vol 3, No. 2, pp 67-80.

Peterson 1987
Peterson, R. W. 1987. "Interpretation of Triaxial Compression Tests on Partially Saturated Soils," *Advanced Triaxial Testing of Soil and Rock*, *STP 977*, R.T. Donaghe, R.C. Chaney, and M.L. Silver, eds., American Society of Testing and Materials, Philadelphia, pp 512-538.

Roscoe, Schofield, and Wroth 1958
Roscoe, K. H., Schofield, A. N., and Wroth, C. P. 1958. "On the Yielding of Soils," *Geotechnique*, Institution of Civil Engineers, Great Britain, Vol 8, No. 1, pp 22-53.

Scott 1963
Scott, R. F. 1963. *Principles of Soil Mechanics*, Addison-Wesley, Reading, MA.

Seed 1979
Seed, H. B. 1979. "19th Rankine Lecture: Considerations in the Earthquake Resistant Design of Earth and Rockfill Dams," *Geotechnique*, Vol 29, No. 3, pp 215-263.

Skempton 1977
Skempton, A. W. 1977. "Slope Stability of Cuttings in Brown London Clay." *Proceedings*, *Ninth International Conference on Soil Mechanics and Foundation Engineering.* Tokyo, Vol 3, pp 261-270.

Spencer 1967
Spencer, E. 1967. "A Method of Analysis of the Stability of Embankments Assuming Parallel Inter-Slice Forces," *Geotechnique*, Vol 17, No. 1, pp 11-26.

Stark and Eid 1993
Stark, T. D., and Eid, H. T. 1993. "Modified Bromhead Ring Shear Apparatus," *Geotechnical Testing Journal*, American Society for Testing and Materials, Vol 16, No. 1, Mar., pp 100-107.

Stark and Eid 1994
Stark, T. D., and Eid, H. T. 1994. "Drained Residual Strength of Cohesive Soils," *Journal of Geotechnical Engineering*, ASCE, Vol 120, No. 5, May, pp 856-871.

Stark and Eid 1997
Stark, T. D., and Eid, H. T. 1997. "Slope Stability Analyses in Stiff Fissured Clays," *Journal of Geotechnical and Geoenvironmental Engineering*," ASCE, Vol 123, No. 4, Apr., pp 335-343.

Taylor 1937
Taylor, D. W. 1937. "Stability of Earth Slopes," *Journal of the Boston Society of Civil Engineers*, Vol 24, No. 3, July, pp 197-247, reprinted in *Contributions to Soil Mechanics 1925-1940*, Boston Society of Civil Engineers, 1940, pp 337-386.

Whitman and Bailey 1967
Whitman, R. V., and Bailey, W. A. 1967. "Use of Computers for Slope Stability Analysis," *Journal of the Soil Mechanics and Foundations Division*, ASCE, Vol 93, No. SM4, pp 475-498.

Wright 1969
Wright, S. G. 1969. "A Study of Slope Stability and the Undrained Shear Strength of Clay Shales," thesis presented to the University of California at Berkeley, California, in partial fulfillment of requirements for degree of Doctor of Philosophy.

Wright 1982
Wright S. G. 1982. "Review of Limit Equilibrium Slope Analysis Procedures," *Technology Update Lecture*, U. S. Bureau of Reclamation, Denver, CO, pp 1-36.

Wright 1991
Wright, S. G. 1991. "Limit Equilibrium Slope Stability Equations Used in the Computer Program UTEXAS3," *Geotechnical Engineering Software GS 91-2*, Geotechnical Engineering Center, The University of Texas, Austin.

Wright, Kulhawy, and Duncan 1973
Wright, S. G., Kulhawy, F. H., and Duncan, J. M. 1973. "Accuracy of Equilibrium Slope Stability Analysis," *Journal of the Soil Mechanics and Foundations Division*, American Society of Civil Engineers, Vol 99, No. 10, October, pp 783-791.

Wright and Duncan 1987
Wright, S. G., and Duncan, J. M. 1987. "An Examination of Slope Stability Computation Procedures for Sudden Drawdown," *Miscellaneous Paper GL-87-25*, U. S. Army Engineer Waterways Experiment Station, Vicksburg, MS.

Youd et al. 1984
Youd, T. L., Harp, E. L., Keefer, D. K., and Wilson, R. C. 1984. "Liquefaction Generated by the 1983 Borah Peak, Idaho Earthquake," *Proceedings of Workshop XXVIII On the Borah Peak, Idaho Earthquake*, Volume A, Open-File Report 85-290-A, U.S. Geological Survey, Menlo Park, CA, pp 625-634.

Appendix B
Notation

Dimensions: F indicates force, L indicates length

A	=	cross-sectional area of slice (L^2)
b	=	width of slice (L)
b	=	slope ratio = $\cot \beta$ (dimensionless)
c	=	cohesion intercept for Mohr-Coulomb diagram plotted in terms of total normal stress, σ (F/L^2)
c'	=	cohesion intercept for Mohr-Coulomb diagram plotted in terms of total effective stress, σ' (F/L^2)
c_R	=	cohesion intercept as determined from the R envelope (F/L^2)
c_b	=	cohesion at the base of an embankment (F/L^2)
c_{avg}	=	average cohesion over length of slip surface (F/L^2)
c_D	=	'developed' or 'mobilized' cohesion (F/L^2)
c'_D	=	'developed' or 'mobilized' cohesion (F/L^2)
C_D	=	force because of the 'developed' or 'mobilized' cohesion on base of slice (F)
C_1	=	term used to calculate side forces on a slice (F)
C_2	=	term used to calculate side forces on a slice (F)
C_3	=	term used to calculate side forces on a slice (F)
C_4	=	term used to calculate side forces on a slice (F)
d	=	depth factor = D/H (dimensionless)
d	=	intercept value of failure envelope on 'p-q' diagram (F/L^2)
d_h	=	horizontal moment arm (L)
d_V	=	vertical moment arm (L)
d'	=	intercept value of failure envelope on (σ_1-σ_3) vs. σ_3 'modified' Mohr-Coulomb diagram (F/L^2)
d_R	=	intercept value of R failure envelope on 'p-q' diagram (F/L^2)
d_{crack}	=	depth of vertical 'tension' crack (L)
$d_{Kc=1}$	=	intercept value for τ_{ff} vs. σ'_{fc} shear strength envelope for isotropic consolidation (F/L^2)
D	=	depth from toe of slope to lowest point on the slip circle (L)
e	=	void ratio (dimensionless)
E	=	horizontal component of the interslice force (F)
E_A	=	active force acting on a wedge (F)
E_P	=	passive force acting on a wedge (F)
F	=	factor of safety (defined with respect to shear strength) (dimensionless)

FS	=	factor of safety (defined with respect to shear strength) (dimensionless)
F_D	=	resultant force because of total normal force, N, and developed frictional resistance, N tan ϕ_D, on the bottom of a slice (F)
h_{avg}	=	average height of slice (L)
h_i	=	piezometric height above the bottom of the slice (pressure head) at the upslope side of the slice (L)
h_{i+1}	=	piezometric height above the bottom of the slice (pressure head) at the downslope side of the slice (L)
h_p	=	piezometric height above the bottom of the slice (pressure head) at the midpoint of the slice (L)
h_s	=	average height of water above top of slice (L)
H	=	height of the slope (L)
H_0	=	height above slope where soil strength vs. depth intersects zero (L)
H_w	=	depth of water outside slope (L)
H'_w	=	height of water within slope (L)
K_o	=	at-rest pressure coefficient (dimensionless)
K_A	=	active earth pressure coefficient (dimensionless)
K_P	=	passive earth pressure coefficient (dimensionless)
K_c	=	effective principal stress ratio, $\sigma'_{1c}/\sigma'_{3c}$, for consolidation (dimensionless)
K_f	=	effective principal stress ratio, $\sigma'_{1f}/\sigma'_{3f}$ at failure (dimensionless)
ℓ_{top}	=	length of the top of the slice (L)
m_α	=	term used in the Simplified Bishop method (dimensionless)
M	=	term to relate height above slope where soil strength is zero to height of slope
M_P	=	moment produced by the force P about the center of the circle (FL)
n_α	=	term used to calculate side forces on a slice (dimensionless)
N	=	total normal force on the bottom of the slice (F)
N	=	stability number for an embankment with an uniform increase in cohesion with depth (dimensionless)
N'	=	effective normal force on the bottom of the slice (F)
N_0	=	stability number for a homogeneous embankment and foundation overlying a rigid boundary with $\phi_u=0$ (dimensionless)
N_{cf}	=	stability number for a homogeneous embankment and foundation overlying a rigid boundary with $\phi>0$ (dimensionless)
p	=	total stress state variable used to plot 'modified' Mohr-Coulomb diagrams, usually $\frac{1}{2}(\sigma_1+\sigma_3)$ but sometimes used to represent $\frac{1}{3}(\sigma_1+\sigma_2+\sigma_3)$ (F/L^2)
p'	=	effective stress state variable used to plot 'modified' Mohr-Coulomb diagrams, usually $\frac{1}{2}(\sigma_1+\sigma_3)$ but sometimes used to represent $\frac{1}{3}(\sigma_1+\sigma_2+\sigma_3)$ (F/L^2)
p_{avg}	=	average water pressure on top of slice (F/L^2)

P $\quad$ = $\quad$ water force on top of slice, acting perpendicular to top of slice (F)

P_d $\quad$ = $\quad$ term to account for weight of slope and surcharge loading, submergence, and tension crack corrections (F/L^2)

P_e $\quad$ = $\quad$ term to account for the effects of water within the slope (F/L^2)

q $\quad$ = $\quad$ surcharge load (F/L^2)

q $\quad$ = $\quad$ stress state variable used to plot 'modified' Mohr-Coulomb diagrams, usually $\frac{1}{2}(\sigma_1-\sigma_3)$ but sometimes used to represent $(\sigma_1-\sigma_3)$ (F/L^2)

q_{ult} $\quad$ = $\quad$ ultimate bearing capacity (F/L^2)

R $\quad$ = $\quad$ radius of the circle (L)

R $\quad$ = $\quad$ resultant force because of weight of slice and water pressures on top, sides and bottom of slice (F)

s $\quad$ = $\quad$ shear strength (F/L^2)

s_d $\quad$ = $\quad$ drained shear strength (F/L^2)

$s_{passive}$ $\quad$ = $\quad$ shear strength based on active Rankine stress state (F/L^2)

s_2 $\quad$ = $\quad$ shear strength used for second stage of computations for rapid drawdown (F/L^2)

S $\quad$ = $\quad$ shear force on the bottom of the slice (F)

u $\quad$ = $\quad$ pore water pressure (F/L^2)

u_{bp} $\quad$ = $\quad$ back pressure – pore water pressure for consolidation and drained shear in the triaxial test (F/L^2)

u_c $\quad$ = $\quad$ pore water pressure at consolidation (F/L^2)

u_f $\quad$ = $\quad$ pore water pressure at failure (F/L^2)

U_b $\quad$ = $\quad$ force resulting from pore water pressure on the bottom of the slice (F)

U_i $\quad$ = $\quad$ force resulting from water pressures on the upslope side of the slice (F)

U_{i+1} $\quad$ = $\quad$ force resulting from water pressures on the downslope side of the slice (F)

U_L $\quad$ = $\quad$ water force on left of slice (F)

U_R $\quad$ = $\quad$ water force on right of slice (F)

W $\quad$ = $\quad$ weight of slice (F)

W' $\quad$ = $\quad$ effective weight of slice (F)

X $\quad$ = $\quad$ shear component of the interslice force (F)

y_t $\quad$ = $\quad$ location of side forces (L)

z $\quad$ = $\quad$ vertical depth to a plane parallel to slope (L)

Z_i $\quad$ = $\quad$ interslice force on the upslope side of the slice (F)

Z_{i+1} $\quad$ = $\quad$ interslice force on the downslope side of the slice (F)

z_t $\quad$ = $\quad$ depth of tensile stresses (L)

α $\quad$ = $\quad$ inclination from horizontal of the bottom of the slice (degrees)

α_s $\quad$ = $\quad$ angle between flow lines and embankment face (degrees)

β = inclination from horizontal of the top of the slice (degrees)

δ = inclination of the earth pressure force (degrees)

$\Delta \ell$ = length of bottom of slice (L)

Δu = change in pore water pressure, usually during shear (F/L^2)

Δx = width of slice (F)

$\Delta \phi$ = change in friction angle (degrees)

γ = total unit weight of soil (F/L^3)

γ' = submerged unit weight of soil (F/L^3)

γ_m = moist unit weight of soil (F/L^3)

γ_w = unit weight of water (F/L^3)

γ_{sat} = saturated unit weight of soil (F/L^3)

$\lambda_{c\phi}$ = term to relate P_e with shear strength parameters (dimensionless)

μ_q = surcharge correction factor (dimensionless)

μ_w = submergence correction factor (dimensionless)

μ_t = tension crack correction factor (dimensionless)

μ'_w = seepage correction factor (dimensionless)

Ω = term used to calculate the inclination of the critical slip surface (dimensionless)

ϕ = angle of internal friction for Mohr-Coulomb diagram plotted in terms of total normal stress, σ (degrees)

ϕ' = angle of internal friction for Mohr-Coulomb diagram plotted in terms of effective normal stress, σ' (degrees)

ϕ_D = 'developed' or 'mobilized' total stress angle of internal friction (degrees)

ϕ'_D = 'developed' or 'mobilized' effective stress angle of internal friction (degrees)

ϕ_R = angle of internal friction as determined from the R envelope (degrees)

ϕ_u = undrained friction angle (degrees)

ϕ_{secant} = secant value of friction angle (tan $\phi_{secant} = \tau_f/\sigma_f$) (degrees)

σ = total normal stress (F/L^2)

σ' = effective normal stress (F/L^2)

σ'_v = effective vertical stress (F/L^2)

σ'_{vc} = effective vertical stress for consolidation (F/L^2)

σ_{1f} = major principal total stress at failure (F/L^2)

σ'_{1f} = major principal effective stress at failure (F/L^2)

σ'_{1c} = effective major principal stress for consolidation (F/L^2)

σ_{3f} = minor principal total stress at failure (F/L^2)

σ'_{3f} = minor principal effective stress at failure (F/L^2)

σ'_{3c} = minor principal effective stress for consolidation (F/L^2)

$\sigma'_{3\text{-critical}}$ = 'critical' effective confining pressure for critical state (F/L^2)

σ'_c = effective normal stress on the slip surface at consolidation, before rapid drawdown (F/L^2)

σ'_d = effective normal stress on the slip surface after drainage following rapid drawdown (F/L^2)

σ'_{fc} = effective normal stress on the failure plane at consolidation (F/L^2)

σ_i = normal stress where R and S envelopes intersect (F/L^2)

σ'_1/σ'_3 = principal stress ratio (dimensionless)

$(\sigma_1-\sigma_3)$ = principal stress difference (F/L^2)

$(\sigma_1-\sigma_3)_f$ = principal stress difference at failure (F/L^2)

τ = shear stress (F/L^2)

τ_c = shear stress on the slip surface at consolidation, before rapid drawdown (F/L^2)

τ_{fc} = shear stress on the failure plane at consolidation (F/L^2)

τ_{ff} = shear stress on the failure plane at failure (F/L^2)

$\tau_{ff\text{-Kc}=1}$ = shear stress (strength) from envelope of τ_{ff} vs. σ'_{fc} for isotropic consolidation (F/L^2)

$\tau_{ff\text{-Kc}=Kf}$ = shear stress (strength) from envelope of τ_{ff} vs. σ'_{fc} for maximum degree of anisotropic consolidation, $K_c = K_f$ (F/L^2)

θ = inclination of the interslice force (degrees)

Ψ = angle of inclination of failure envelope on 'p-q' diagram (degrees)

Ψ' = angle of inclination of failure envelope on $(\sigma_1-\sigma_3)$ vs. σ_3 'modified' Mohr-Coulomb diagram (degrees)

Ψ_R = angle of inclination of the R failure envelope on 'p-q' diagram (degrees)

$\Psi_{Kc=1}$ = slope angle for τ_{ff} vs. σ'_{fc} shear strength envelope for isotropic consolidation (degrees)

Appendix C
Stability Analysis Procedures - Theory and Limitations

C-1. Fundamentals of Slope Stability Analysis

   a.   Conventional approach. Conventional slope stability analyses investigate the equilibrium of a mass of soil bounded below by an assumed potential slip surface and above by the surface of the slope. Forces and moments tending to cause instability of the mass are compared to those tending to resist instability. Most procedures assume a two-dimensional (2-D) cross section and plane strain conditions for analysis. Successive assumptions are made regarding the potential slip surface until the most critical surface (lowest factor of safety) is found. Figure C-1 shows a potential slide mass defined by a candidate slip surface. If the shear resistance of the soil along the slip surface exceeds that necessary to provide equilibrium, the mass is stable. If the shear resistance is insufficient, the mass is unstable. The stability or instability of the mass depends on its weight, the external forces acting on it (such as surcharges or accelerations caused by dynamic loads), the shear strengths and porewater pressures along the slip surface, and the strength of any internal reinforcement crossing potential slip surfaces.
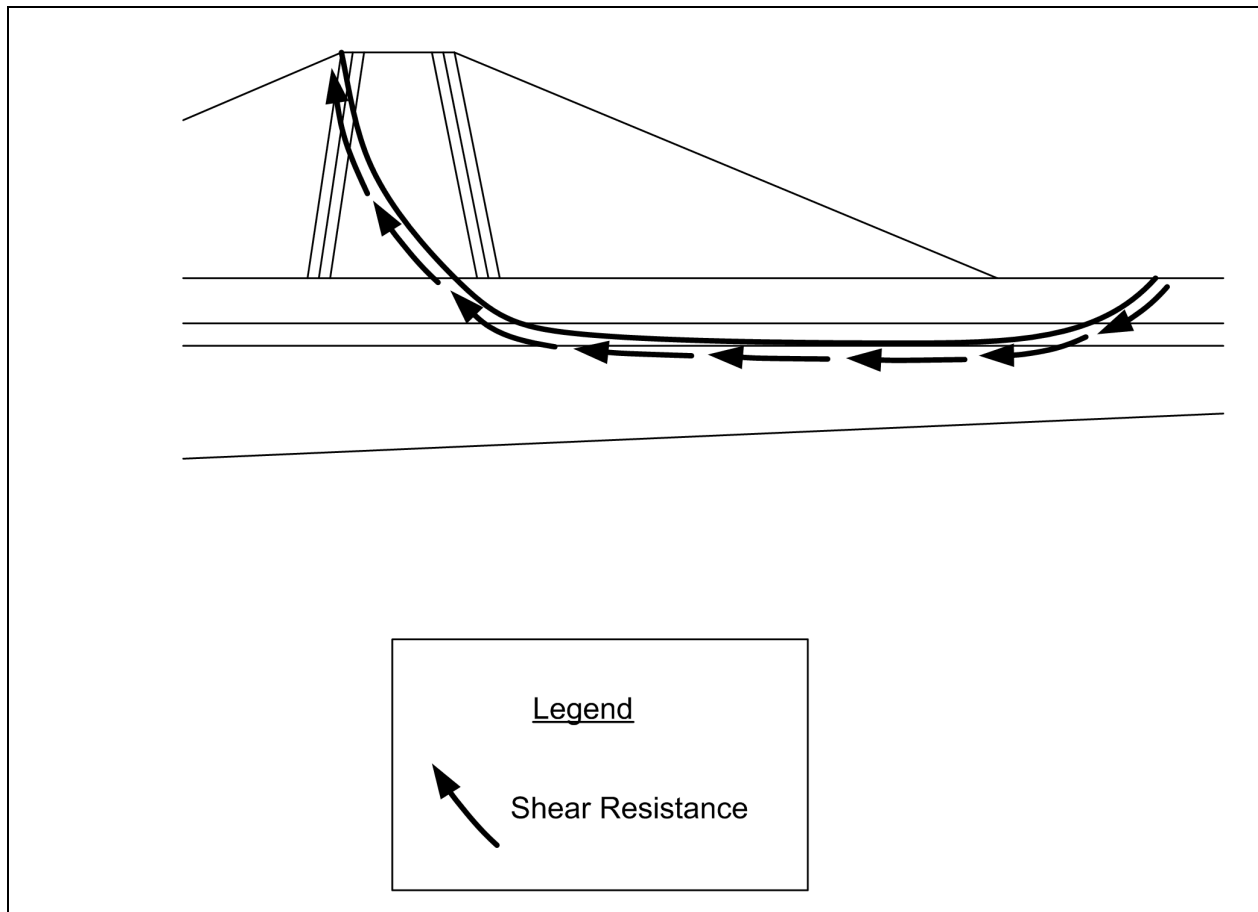

Figure C-1.   Slope and potential slip surface

   b.   The factor of safety. Conventional analysis procedures characterize the stability of a slope by calculating a factor of safety. The factor of safety is defined with respect to the shear strength of the soil as the ratio of the available shear strength (s) to the shear strength required for equilibrium (τ), that is:

$$F = \frac{\text{Available shear strength}}{\text{Equilibrium shear stress}} = \frac{s}{\tau} \tag{C-1}$$

(1) Shear strength is discussed further in Appendix D. If the shear strength is defined in terms of effective stresses, the factor of safety is expressed as:

$$F = \frac{c' + (\sigma - u)\tan\phi'}{\tau} \tag{C-2}$$

where

c' and ϕ' = Mohr-Coulomb cohesion and friction angle, respectively, expressed in terms of effective stresses

σ = total normal stress on the failure plane

u = pore water pressure; $(\sigma - u)$ is the effective normal stress on the failure plane

If the failure envelope is curved, the factor safety can be expressed as:

$$F = \frac{s\,(\sigma')}{\tau} \tag{C-3}$$

where s (σ') represents the shear strength determined from the effective stress failure envelope for the particular effective normal stress, σ'.

Equation C-2 can also still be used with a curved failure envelope by letting c' and ϕ' represent the intercept and slope of an equivalent linear Mohr-Coulomb envelope that is tangent to the curved failure envelope at the appropriate value of normal stress, σ'.

(2) For total stresses, the factor of safety is expressed using the shear strength parameters in terms of total stresses, i.e.:

$$F = \frac{c + \sigma\tan\phi}{\tau} \tag{C-4}$$

where c and ϕ are the Mohr-Coulomb cohesion and friction angle, respectively, expressed in terms of total stresses. Curved failure envelopes are handled for total stresses in much the same way they are handled for effective stresses: The strength is determined from the curved failure envelope using the particular value of total normal stress, σ. In the remaining sections of this Appendix, the effective stress form of the equation for the factor of safety (Equation C-2) will be used. Any of the equations presented in terms of effective stress can be converted to their equivalent total stress form by using c and ϕ, rather than c' and ϕ', and by setting pore water pressure, u, equal to zero.

c. Limit equilibrium methods – General assumptions. All of the methods presented in this manual for computing slope stability are termed "limit equilibrium" methods. In these methods, the factor of safety is calculated using one or more of the equations of static equilibrium applied to the soil mass bounded by an assumed, potential slip surface and the surface of the slope. In some methods, such as the Infinite Slope

method, the shear and normal stresses (σ and τ) can be calculated directly from the equations of static equilibrium and then used with Equation C-2 or C-4 to compute the factor of safety. In most other cases, including the Simplified Bishop, the Corps of Engineers' Modified Swedish Method, and Spencer's Method, a more complex procedure is required to calculate the factor of safety. First, the shear stress along the shear surface is related to the shear strength and the factor of safety using Equation C-2 or C-4. In the case of effective stresses, the shear stress according to Equation C-2 is expressed as:

$$\tau = \frac{c' + (\sigma - u)\tan\phi'}{F} \tag{C-5}$$

The factor of safety is computed by repeatedly assuming values for F and calculating the corresponding shear stress from Equation C-5 until equilibrium is achieved. In effect, the strength is reduced by the factor of safety, F, until a just-stable, or limiting, equilibrium condition is achieved. Equation C-5 can be expanded and written as:

$$\tau = \frac{c'}{F} + \frac{(\sigma - u)\tan\phi'}{F} \tag{C-6}$$

The first term represents the contribution of "cohesion" to shear resistance; the second term represents the contribution of "friction." The "developed" cohesion and friction are defined as follows:

$$c'_D = \frac{c'}{F} \tag{C-7}$$

and

$$\tan\phi'_D = \frac{\tan\phi'}{F} \tag{C-8}$$

where

c'_D = developed cohesion

ϕ'_D = developed friction angle

d. Assumptions in methods of slices. Many of the limit equilibrium methods (Ordinary Method of Slices (OMS), Simplified Bishop, Corps of Engineers' Modified Swedish, Spencer) address static equilibrium by dividing the soil mass above the assumed slip surface into a finite number of vertical slices. The forces acting on an individual slice are illustrated in Figure C-2. The forces include:

W - slice weight

E - horizontal (normal) forces on the sides of the slice

X - vertical (shear) forces between slices

N - normal force on the bottom of the slice

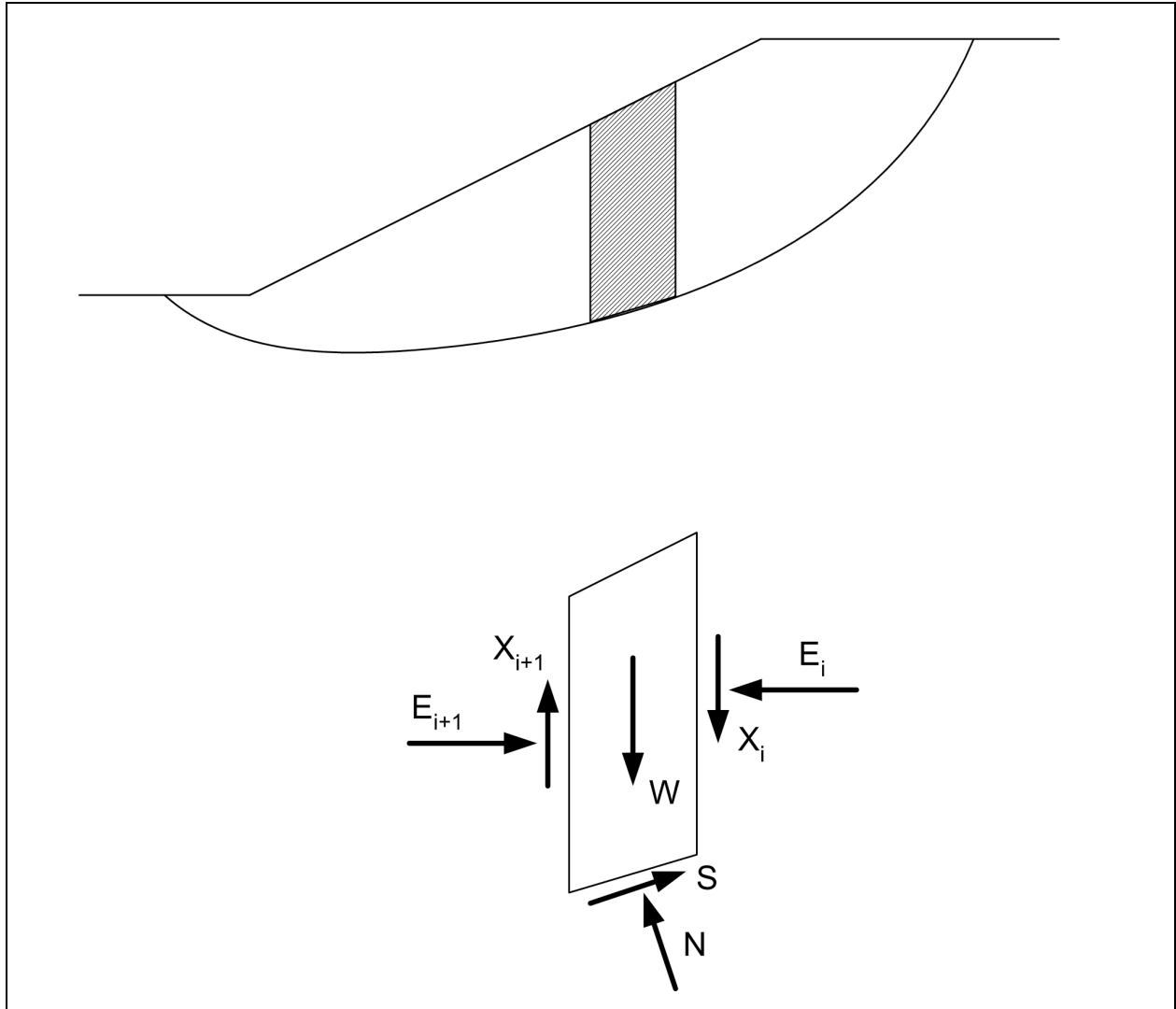S - shear force on the bottom of the slice

Figure C-2. Typical slice and forces for method of slices

Except for the weight of the slice, all of these forces are unknown and must be calculated in a way that satisfies static equilibrium.

  (1) For the current discussion, the shear force (S) on the bottom of the slice is not considered directly as an unknown in the equilibrium equations that are solved. Instead, the shear force is expressed in terms of other known and unknown quantities, as follows: S on the base of a slice is equal to the shear stress, τ, multiplied by the length of the base of the slice, $\Delta\ell$, i.e.,

$$S = \tau\Delta\ell \tag{C-9}$$

or, by introducing Equation C-5, which is based on the definition of the factor of safety,

$$S = \frac{c'\Delta\ell}{F} + \frac{(\sigma - u)\Delta\ell \tan\phi'}{F} \tag{C-10}$$

Finally, noting that the normal force N is equal to the product of the normal stress (σ) and the length of the bottom of the slice (Δℓ), i.e., N = σ Δℓ, Equation C-9 can be written as:

$$S = \frac{c'\Delta\ell}{F} + \frac{(N - u\Delta\ell)\tan\phi'}{F}$$ (C-11)

(2) Equation C-11 relates the shear force, S, to the normal force on the bottom of the slice and the factor of safety. Thus, if the normal force and factor of safety can be calculated from the equations of static equilibrium, the shear force can be calculated (is known) from Equation C-11. Equation C-11 is derived from the Mohr-Coulomb equation and the definition of the factor of safety, independently of the conditions of static equilibrium. The forces and other unknowns that must be calculated from the equilibrium equations are summarized in Table C-1. As discussed above, the shear force, S, is not included in Table C-1, because it can be calculated from the unknowns listed and the Mohr-Coulomb equation (C-11), independently of static equilibrium equations.

Table C-1
Unknowns and Equations for Limit Equilibrium Methods

Unknowns	Number of Unknowns for n Slices
Factor of safety (F)	1
Normal forces on bottom of slices (N)	N
Interslice normal forces, E	n – 1
Interslice shear forces, X	n – 1
Location of normal forces on base of slice	N
Location of interslice normal forces	n – 1
TOTAL NUMBER OF UNKNOWNS	5n – 2
Equations	**Number of Equations for n Slices**
Equilibrium of forces in the horizontal direction, $\Sigma F_x = 0$	n
Equilibrium of forces in the vertical direction, $\Sigma F_y = 0$	n
Equilibrium of moments	n
TOTAL NUMBER OF EQUILIBRIUM EQUATIONS	3n

(3) In order to achieve a statically determinate solution, there must be a balance between the number of unknowns and the number of equilibrium equations. The number of equilibrium equations is shown in the lower part of Table C-1. The number of unknowns (5n – 2) exceeds the number of equilibrium equations (3n) if n is greater than one. Therefore, some assumptions must be made to achieve a statically determinate solution.

(4) The various limit equilibrium methods use different assumptions to make the number of equations equal to the number of unknowns. They also differ with regard to which equilibrium equations are satisfied. For example, the Ordinary Method of Slices, the Simplified Bishop Method, and the U.S. Army Corps of Engineers' Modified Swedish Methods do not satisfy all the conditions of static equilibrium. Methods such as the Morgenstern and Price's and Spencer's do satisfy all static equilibrium conditions. Methods that satisfy static equilibrium fully are referred to as "complete" equilibrium methods. Details of various limit equilibrium procedures and their differences are presented in Sections C-2 through C-7. Detailed comparison of limit equilibrium slope stability analysis methods have been reported by Whitman and Bailey (1967), Wright (1969), Duncan and Wright (1980) and Fredlund and Krahn (1977).[1]

e. Limitations of limit equilibrium methods. Complete equilibrium methods have generally been more accurate than those procedures which do not satisfy complete static equilibrium and are therefore preferable to

---

[1] References information is presented in Appendix A.

"incomplete" methods. However, the "incomplete" methods are often sufficiently accurate and useful for many practical applications, including hand checks and preliminary analyses. In all of the procedures described in this manual, the factor of safety is applied to both cohesion and friction, as shown by Equation C-6.

(1) The factor of safety is also assumed to be constant along the shear surface. Although the factor of safety may not in fact be the same at all points on the slip surface, the average value computed by assuming that F is constant provides a valid measure of stability for slopes in ductile (nonbrittle) soils. For slopes in brittle soils, the factor of safety computed assuming F is the same at all points on the slip surface may be higher than the actual factor of safety.

(2) If the strength is fully mobilized at any point on the slip surface, the soil fails locally. If the soil has brittle stress-strain characteristics so that the strength drops once the peak strength is mobilized, the stress at that point of failure is reduced and stresses are transferred to adjacent points, which in turn may then fail. In extreme cases this may lead to progressive failure and collapse of the slope. If soils possess brittle stress-strain characteristics with relatively low residual shear strengths compared to the peak strengths, reduced strengths and/or higher factors of safety may be required for stability. Limitations of limit equilibrium procedures are summarized in Table C-2.

Table C-2
Limitations of Limit-Equilibrium Methods

1. The factor of safety is assumed to be constant along the potential slip surface.
2. Load-deformation (stress-strain) characteristics are not explicitly accounted for.
3. The initial stress distribution within the slope is not explicitly accounted for.
4. Unreasonably large and or negative normal forces may be calculated along the base of slices under certain conditions (SectionC-l0.b and C-10.c).
5. Iterative, trial and error, solutions may not converge in certain cases (Section C-10d).

f. Shape of the slip surface. All of the limit equilibrium methods require that a potential slip surface be assumed in order to calculate the factor of safety. Calculations are repeated for a sufficient number of trial slip surfaces to ensure that the minimum factor of safety has been calculated. For computational simplicity the candidate slip surface is often assumed to be circular or composed of a few straight lines (Figure C-3). However, the slip surface will need to have a more complicated shape in complex stratigraphy. The assumed shape is dependent on the problem geometry and stratigraphy, material characteristics (especially anisotropy), and the capabilities of the analysis procedure used. Commonly assumed shapes are discussed below.

(1) Circular. Observed failures in relatively homogeneous materials often occur along curved failure surfaces. A circular slip surface, like that shown in Figure C-3a, is often used because it is convenient to sum moments about the center of the circle, and because using a circle simplifies the calculations. A circular slip surface must be used in the Ordinary Method of Slices and Simplified Bishop Method. Circular slip surfaces are almost always useful for starting an analysis. Also, circular slip surfaces are generally sufficient for analyzing relatively homogeneous embankments or slopes and embankments on foundations with relatively thick soil layers.

(2) Wedge. "Wedge" failure mechanisms are defined by three straight line segments defining an active wedge, central block, and passive wedge (Figure C-3b). This type of slip surface may be appropriate for slopes where the critical potential slip surface includes a relatively long linear segment through a weak material bounded by stronger material. A common example is a relatively strong levee embankment founded on weaker, stratified alluvial soils. Wedge methods, including methods for defining or calculating the inclination of the base of the wedges, are discussed in Section C-1g.

a. Circular

b. Wedge

c. General noncircular
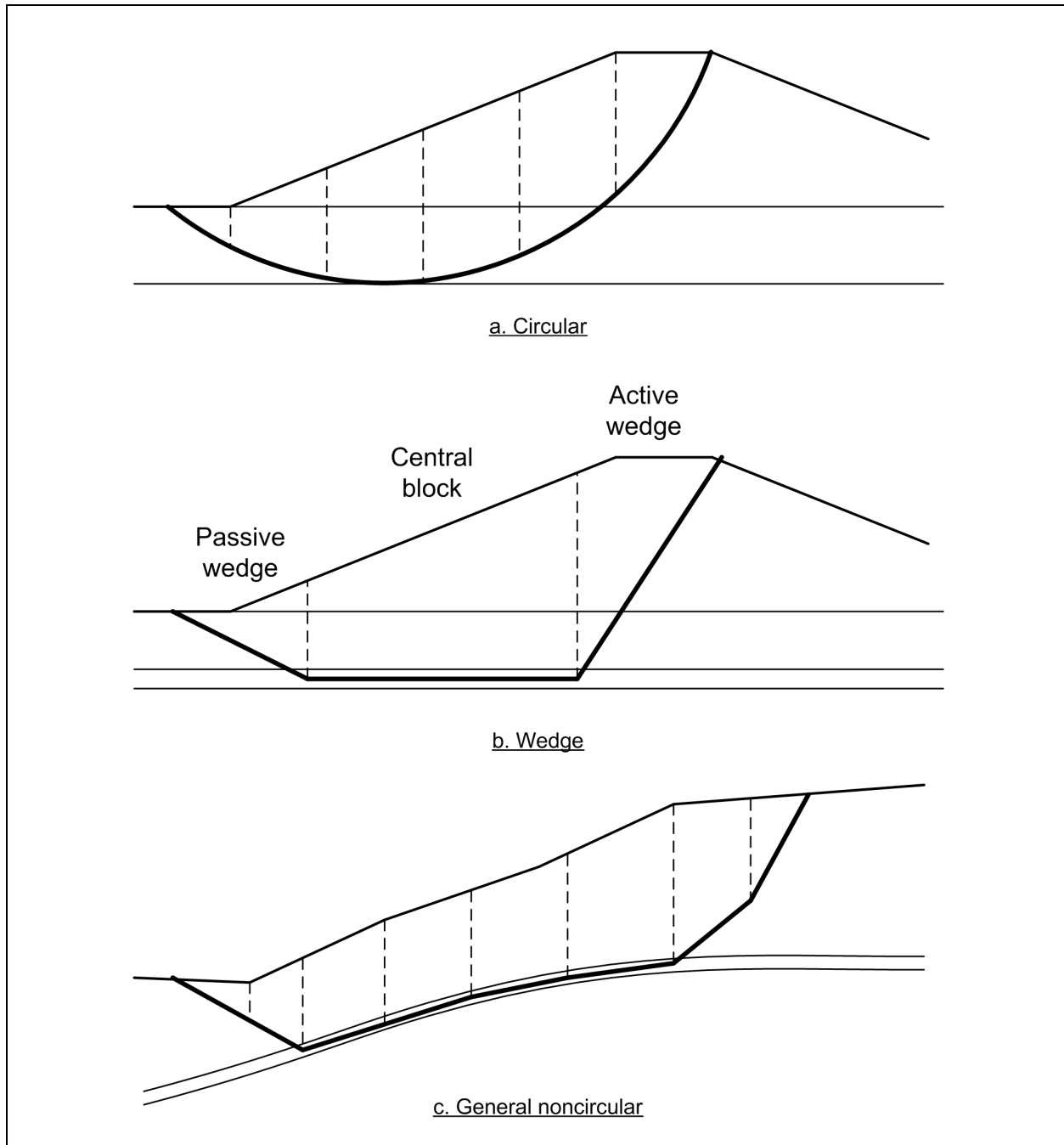
Figure C-3.   Shapes for potential slip surfaces

(3) Two circular segments with a linear midsection. This is a combination of the two shapes (circular and wedge) discussed above that is used by some computer programs.

(4) General, noncircular shape. Slope failure may occur by sliding along surfaces that do not correspond to either the wedge or circular shapes. The term general slip surface refers to a slip surface composed of a number of linear segments which may each be of any length and inclined at any angle. The term "noncircular" is also used in reference to such general-shaped slip surfaces. Prior to about 1990, slip surfaces of a general shape, other than simple wedges, were seldom analyzed, largely because of the difficulty in

systematically searching for the critical slip surface. However, in recent years improved search techniques and computer software have increased the capability to analyze such slip surfaces. Stability analyses based on general slip surfaces are now much more common and are useful as a design check of critical slip surfaces of traditional shapes (circular, wedge) and where complicated geometry and material conditions exist. It is especially important to investigate stability with noncircular slip surfaces when soil shear strengths are anisotropic.

(a) Inappropriate selection of the shape for the slip surface can cause computational difficulties and erroneous solutions.

(b) A common problem occurs near the toe of the slope when the slip surface exits too steeply through materials with large values of ϕ or ϕ'.

(c) The problem of a steeply exiting slip surface is especially important and is covered in further detail in Section C-10.b.

g. Location of the critical slip surface. The critical slip surface is defined as the surface with the lowest factor of safety. Because different analysis procedures employ different assumptions, the location of the critical slip surface can vary somewhat among different methods of analysis. The critical slip surface for a given problem analyzed by a given method is found by a systematic procedure of generating trial slip surfaces until the one with the minimum factor of safety is found. Searching schemes vary with the assumed shape of the slip surface and the computer program used. Common schemes are discussed below.

(1) Circular slip surfaces. Search schemes for circular arc slip surfaces are illustrated in Figures C-4, C-5, and C-6. A circular surface is defined by the position of the circle center and either (a) the radius, (b) a point through which the circle must pass, or (c) a plane to which the slip surface must be tangent. In case (b), the toe of the slope is often specified as the point through which the circle must pass. Searches are usually accomplished by changing one of these variables and varying a second variable until a minimum factor of safety is found. For example, the location of the center point may be varied while the plane of tangency is fixed, or the radius may be varied while the center point is fixed. The first search variable is then fixed at a new value and the second variable is again varied. This process is repeated until the minimum factor of safety corresponding to both search variables is found. For a homogeneous slope in cohesionless soil (c = 0, c' = 0), a critical circle will degenerate to a plane parallel to the slope and the factor of safety will be identical to the one for an infinite slope. Theoretically, the critical "circle" will be one having a center point located an infinite distance away from the slope on a line perpendicular to the midpoint of the slope. The circle will have an infinite radius as well. When attempts are made to search for a critical circle in a homogeneous slope of cohesionless soil with most computer programs, the search will appear to "run-away" from the slope. The search will probably be stopped eventually as a result of either numerical errors and roundoff or some constraint imposed by the software being used. In such cases the Infinite Slope analysis procedure (Section C-7) should be used.

(2) Wedge-shaped slip surfaces. Wedge-shaped slip surfaces require searching for the critical location of the central block and for the critical inclination of the bases of the active and passive wedges. Searching for the critical location of the central block is illustrated in Figure C-7a and involves systematically varying the horizontal and vertical coordinates of the two ends of the base of the central block, until the central block corresponding to the minimum factor of safety is found. For each trial position of the central block, the base inclinations of the active and passive wedge segments must be set based on simple rules or by searching to locate critical inclinations. A simple and common assumption is to make the inclination of each active wedge segment (measured from the horizontal) $45 + \phi'_D/2$ degrees, and of each passive wedge segment $45 - \phi'_D/2$ degrees. The quantity ϕ'_D represents the developed friction angle (tan ϕ'_D = tan ϕ'/F) and should be
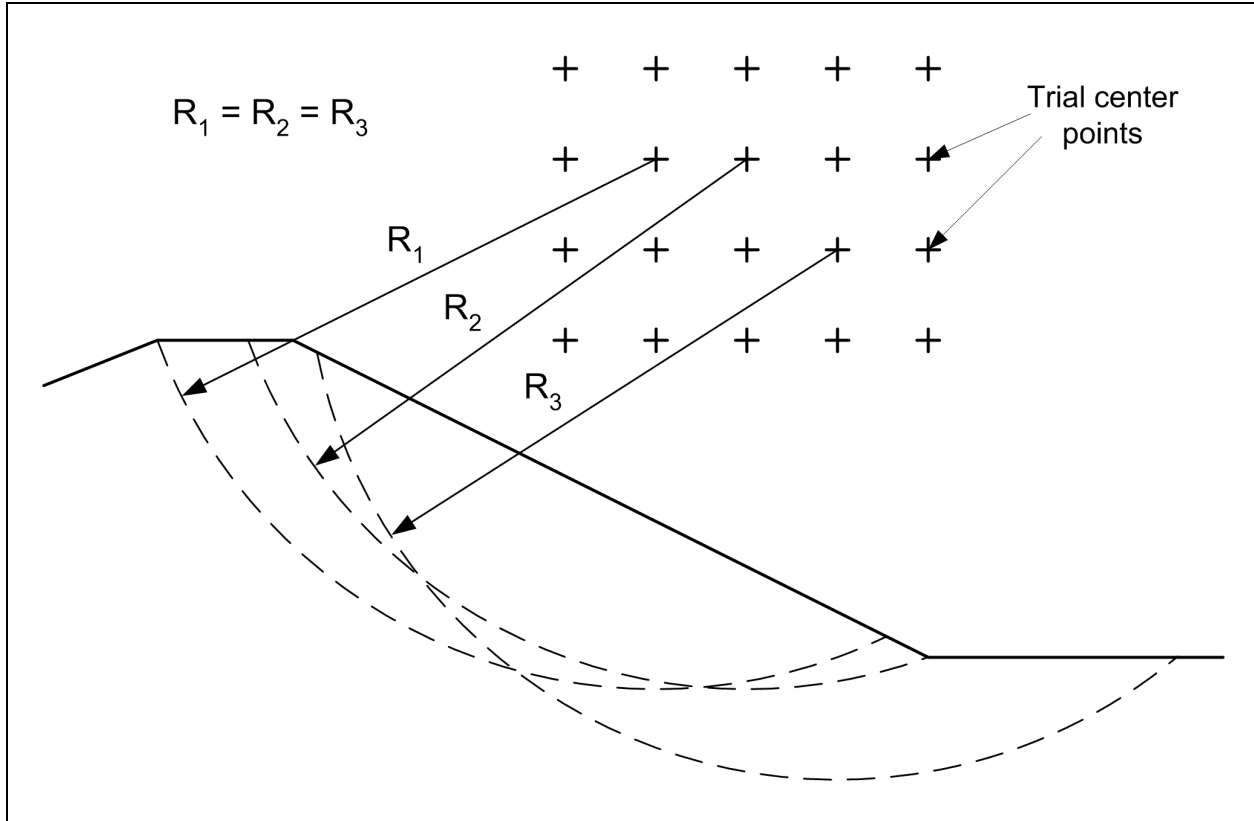
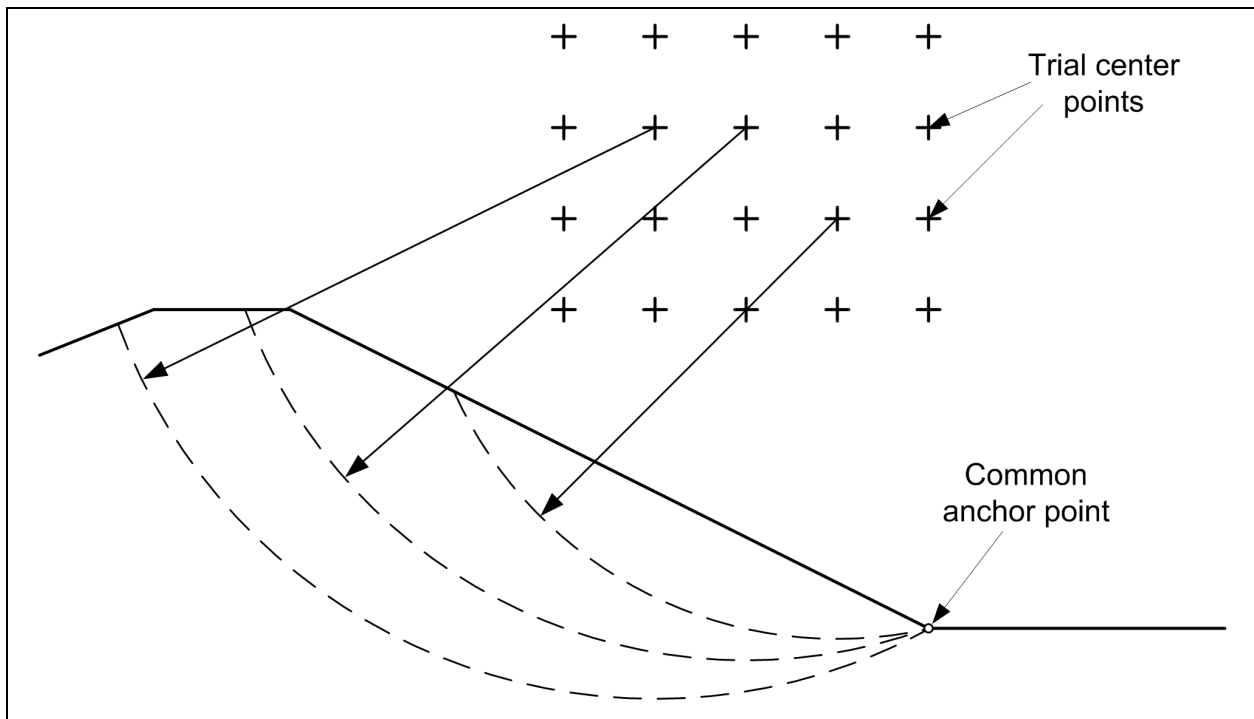**Figure C-4. Search with constant radius**

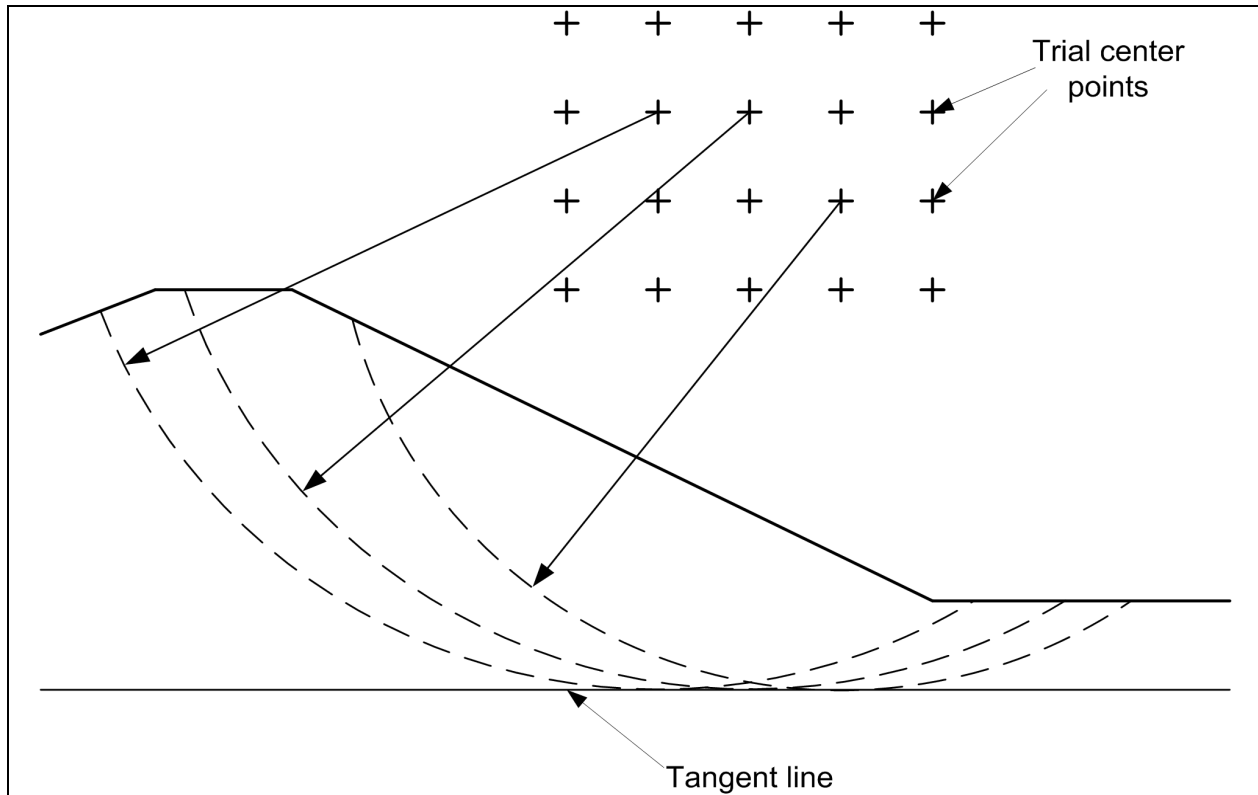**Figure C-5. Search with circles through a common point**

Figure C-6. Search with circles tangent to a prescribed tangent line

consistent with the computed factor of safety. This assumption for the inclination of the active and passive wedges is only appropriate where the top surfaces of the active and passive wedges are horizontal but provides reasonable results for gently inclined slopes. Common methods for searching for the inclination of the base of the wedges are shown in Figure C-7b. One technique, used where soil properties and inclinations of the base of each wedge vary in the zone of the active and passive wedges, is to assume that the bottoms of the wedges are inclined at $\alpha = \theta \pm \phi'_D/2$. The value of θ is then varied until the maximum interslice force is found for the active wedge and minimum interslice force is found for the passive wedge. A second search technique, where the bases of the active and passive wedges are considered to be single planes, is to vary the value of α until a maximum interslice force is obtained for the entire group of active wedge segments and the minimum is found for the entire group of passive wedge segments.

(3) General shapes. A number of techniques have been proposed and used to locate the most critical general-shaped slip surface. One of the most robust and useful procedures is the one developed by Celestino and Duncan (1981). The method is illustrated in Figure C-8. In this method, an initial slip surface is assumed and represented by a series of points that are connected by straight lines. The factor of safety is first calculated for the assumed slip surface. Next, all points except one are held fixed, and the "floating" point is shifted a small distance in two directions. The directions might be vertically up and down, horizontally left and right, or above and below the slip surface in some assumed direction. The factor of safety is calculated for the slip surface with each point shifted as described. This process is repeated for each point on the slip surface. As any one point is shifted, all other points are left at their original location. Once all points have been shifted in both directions and the factor of safety has been computed for each shift, a new location is estimated for the slip surface based on the computed factors of safety. The slip surface is then moved to the estimated location and the process of shifting points is repeated. This process is continued until no further reduction in factor of safety is noted and the distance that the shear surface is moved on successive approximations becomes minimal.

a. Search for critical central block

Vary θ_A to find maximum force on central block

$\alpha_A = \theta_A - \dfrac{\phi_D}{2}$

Vary θ_P to find minimum force on central block

$\alpha_P = \theta_P - \dfrac{\phi_D}{2}$

b. Search schemes for wedge inclinations
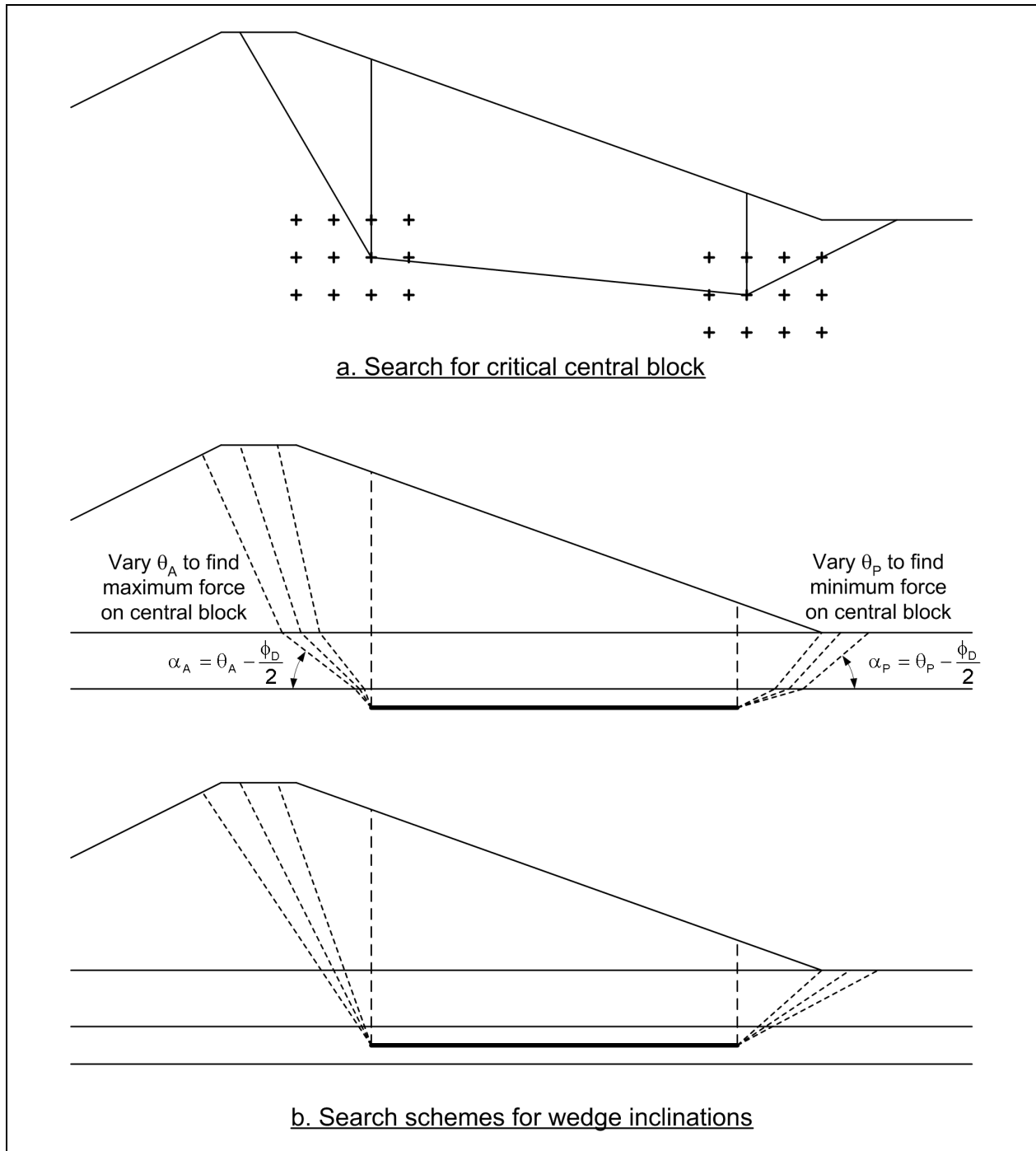
Figure C-7. Search schemes for wedges

(4) Limitations and precautions. Any search scheme employed in computer programs is restricted to investigating a finite number of slip surfaces. In addition, most of these schemes are designed to locate one slip surface with a minimum factor of safety. The schemes may not be able to locate more than one local minimum. The results of automatic searches are dependent on the starting location for the search and any constraints that are imposed on how the slip surface is moved. Automatic searches are controlled largely by the data that the user inputs into the software. Regardless of the software used, a number of separate searches should be conducted to confirm that the lowest factor of safety has been calculated.
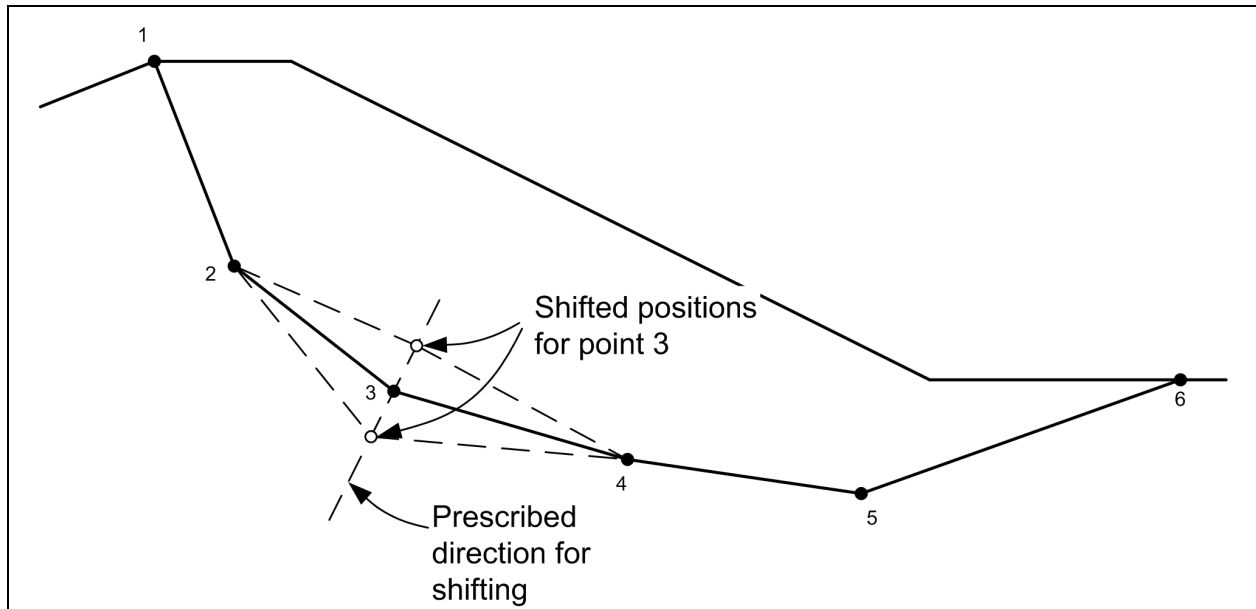
Figure C-8. Search scheme for noncircular slip surfaces (after Celistono and Duncan 1981)

(a) In some cases it is appropriate to calculate the factor of safety for selected potential slip surfaces that do not necessarily produce the minimum factor of safety but would be more significant in terms of the consequences of failure. For example, in slopes that contain cohesionless soil at the face of the slope, the lowest factor of safety may be found for very shallow (infinite slope) slip surfaces, yet shallow sloughing is usually much less important than deeper-seated sliding.

(b) Mine tailings, disposal dams, and cohesionless fill slopes on soft clay foundations provide examples where deeper slip surfaces than the one producing the minimum factor of safety are often more important. In such cases, deeper slip surfaces should be investigated in addition to the shallow slip surfaces having the lowest factors of safety.

h. Probabilistic methods. Conventional slope stability analyses are deterministic methods; meaning that all variables are assumed to have specific values. Probabilistic methods consider uncertainties in the values of the variables and evaluate the effects of these uncertainties on the computed values of factor of safety. Probabilistic approaches can be used in conjunction with any of the limit equilibrium stability methods. ETL 1110-2-556 (1999) describes techniques for probabilistic analyses and their application to slope stability studies.

C-2. The Ordinary Method of Slices

a. Assumptions. The Ordinary Method of Slices (OMS) was developed by Fellenius (1936) and is sometimes referred to as "Fellenius' Method." In this method, the forces on the sides of the slice are neglected (Figure C-9). The normal force on the base of the slice is calculated by summing forces in a direction perpendicular to the bottom of the slice. Once the normal force is calculated, moments are summed about the center of the circle to compute the factor of safety. For a slice and the forces shown in Figure C-9, the factor of safety is computed from the equation,

a. Slope and typical slice

b

W

N

α

$N = W \cos(\alpha)$

b. Slice for total stress analysis

b

W'

N'

α

$N' = W' \cos(\alpha)$

$W' = W - ub$

$N' = (W - ub) \cos(\alpha)$

c. Slice for effective stress analysis

Figure C-9.   Typical slice and forces for Ordinary Method of Slices

$$F = \frac{\sum\left[c'\Delta\ell + \left(W\cos\alpha - u\Delta\ell\cos^2\alpha\right)\tan\phi'\right]}{\sum W\sin\alpha} \qquad (C-12)$$
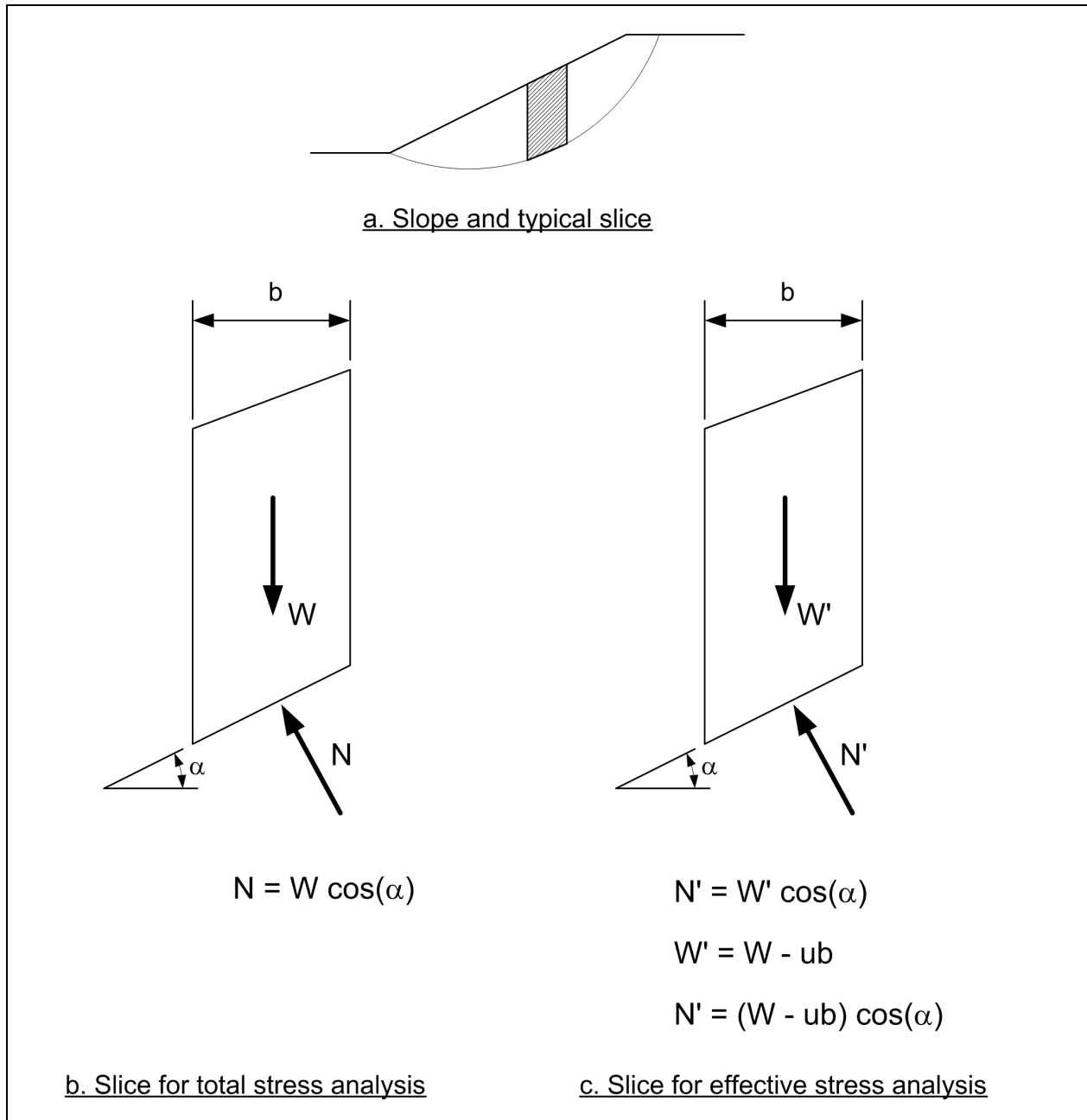
where

c' and ϕ' = shear strength parameters for the center of the base of the slice

W = weight of the slice

α = inclination of the bottom of the slice

u = pore water pressure at the center of the base of the slice

$\Delta\ell$ = length of the bottom of the slice

As shown in Table C-3, there is only one unknown in the Ordinary Method of Slices (F), and only one equilibrium equation is used (the equation of equilibrium of the entire soil mass around the center of the circle).

Table C-3
Unknowns and Equations for the Ordinary Method of Slices Procedure

Unknowns	Number of Unknowns for n Slices
Factor of safety (F)	1
TOTAL NUMBER OF UNKNOWNS	1
Equations	**Number of Equations for n Slices**
Equilibrium of moments of the entire soil mass	1
TOTAL NUMBER OF EQUILIBRIUM EQUATIONS	1

(1) Two different equations have been used to compute the factor of safety by the OMS with effective stresses and pore water pressures. The first equation is shown above as Equation C-12. Equation C-12 is derived by first calculating an "effective" slice weight, W', by subtracting the uplift force due to pore water pressure from the weight, and then resolving forces in a direction perpendicular to the base of the slice (Figure C-9). The other OMS equation for effective stress analyses is written as:

$$F = \frac{\sum\left[c'\Delta\ell + \left(W\cos\alpha - u\Delta\ell\right)\tan\phi'\right]}{\sum W\sin\alpha} \tag{C-13}$$

Equation C-13 is derived by first resolving the force because of the total slice weight (W) in a direction perpendicular to the base of the slice and then subtracting the force because of pore water pressures. Equation C-12 leads to more reasonable results when pore water pressures are used. Equation C-13 can lead to unrealistically low or negative stresses on the base of the slice because of pore water pressures and should not be used.

(2) External water on a slope can be treated in either of two ways: The water may simply be represented as soil with c = 0 and ϕ = 0. In this case, the trial slip surface is assumed to extend through the water and exit at the surface of the water. Some of the slices will then include water and the shear strength for any slices whose base lies in water will be assigned as zero. The second way that water can be treated in an analysis is to treat the water as an external, hydrostatic load on the top of the slices. In this case, the trial slip surface will only pass through soil, and each end will exit at the ground or slope surface (Figure C-10). For the equations presented in this appendix as well as the examples in Appendixes F and G, the water is treated as an external load. Treating the water as another "soil" involves simply modifying the geometry and properties of the slices.

(3) In the case where water loads act on the top of the slice, the expression for the factor of safety (Equation C-12) must be modified to the following:

$$F = \frac{\sum\left\{c'\Delta\ell + \left[W\cos\alpha + P\cos(\alpha-\beta) - u\Delta\ell\cos^2\alpha\right]\tan\phi'\right\}}{\sum W\sin\alpha - \dfrac{\sum M_P}{R}} \tag{C-14}$$

Moment, $M_P = P \times [d_v \sin(\beta) + d_h \cos(\beta)]$
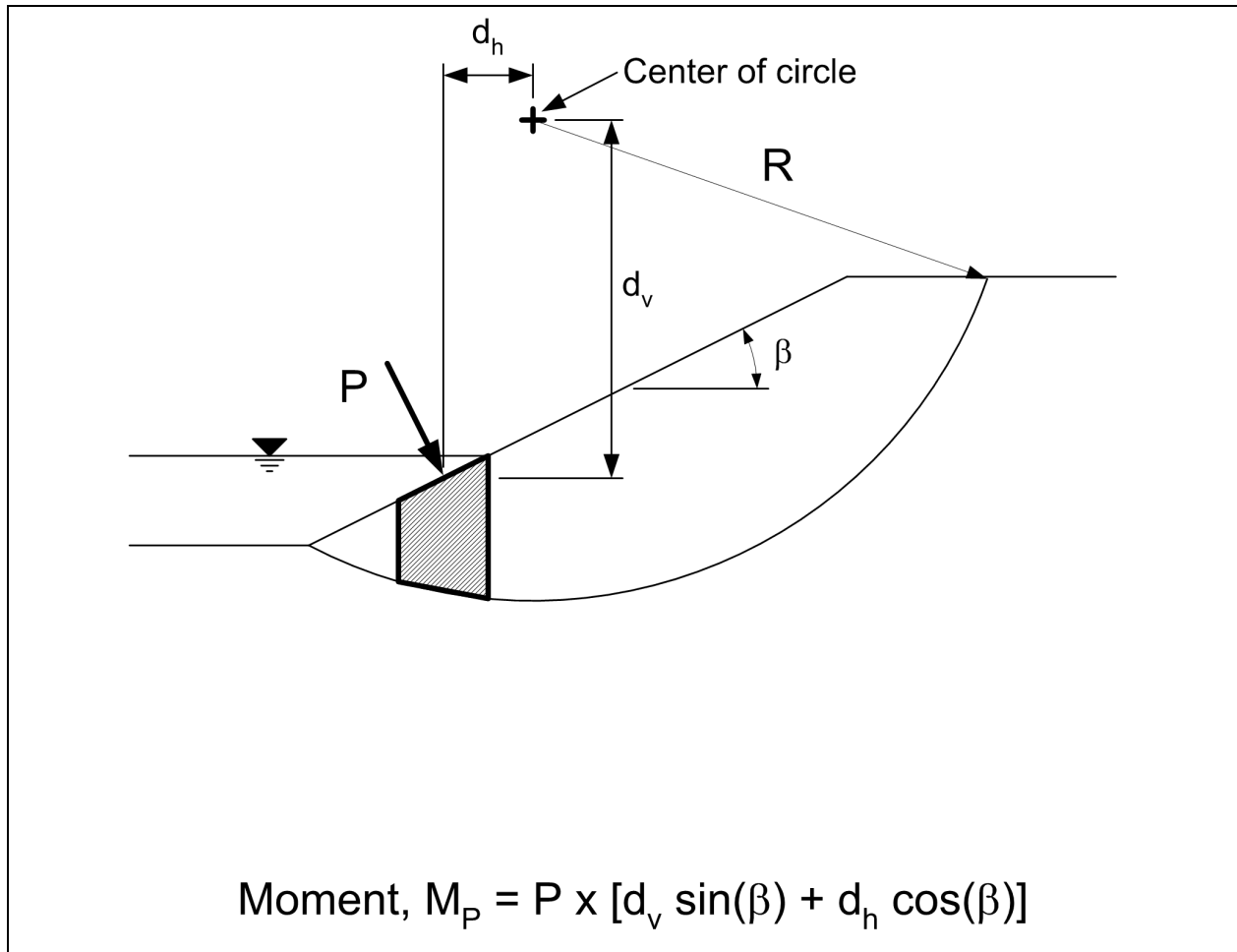
Figure C-10. Slice for Ordinary Method of Slices with external water loads

where

    P = resultant water force acting perpendicular to the top of the slice

    β = inclination of the top of the slice

    M_P = moment about the center of the circle produced by the water force acting on the top of the slice

    R = radius of the circle (Figure C-10).

The moment, M_P, is considered to be positive when it acts in the opposite direction to the moment produced by the weight of the sliding mass.

    b. Limitations. The principal limitation of the OMS comes from neglecting the forces on the sides of the slice. The method also does not satisfy equilibrium of forces in either the vertical or horizontal directions. Moment equilibrium is satisfied for the entire soil mass above the slip surface, but not for individual slices.

(1) Factors of safety calculated by the OMS may commonly differ as much as 20 percent from values calculated using rigorous methods (Whitman and Bailey 1967); in extreme cases (such as effective stress analysis with high pore water pressures), the differences may be even larger. The error is generally on the safe side (calculated factor of safety is too low), but the error may be so large as to yield uneconomical designs. Because of the tendency for errors to be on the "safe side," the OMS is sometimes mistakenly thought always to produce conservative values for the factor of safety. This is not correct. When $\phi = 0$, the OMS yields the same factor of safety as more rigorous procedures, which fully satisfy static equilibrium. Thus, the degree to which the OMS is conservative depends on the value of ϕ and whether the pore pressures are large or small.

(2) Although Equation C-12 does not specifically include the radius of the circle, the equation is based on the assumption that the slip surface is circular. The OMS can only be used with circular slip surfaces.

c. Recommendation for use. The OMS is included herein for reference purposes and completeness because numerous existing slopes have been designed using the method. As the method still finds occasional use in practice, occasions may arise where there is a need to review designs by others that were based on the method. Also, because the OMS is simple, it is useful where calculations must be done by hand using an electronic calculator. The method also may be used to overcome problems that may develop near the toe of steeply exiting shear surfaces as described in Section C-10.b.

C-3. The Simplified Bishop Method

a. Assumptions. The Simplified Bishop Method was developed by Bishop (1955). This procedure is based on the assumption that the interslice forces are horizontal, as shown in Figure C-11. A circular slip surface is also assumed in the Simplified Bishop Method. Forces are summed in the vertical direction. The resulting equilibrium equation is combined with the Mohr-Coulomb equation and the definition of the factor of safety to determine the forces on the base of the slice. Finally, moments are summed about the center of the circular slip surface to obtain the following expression for the factor of safety:

$$F = \frac{\sum \left[\dfrac{c'\Delta x + (W + P\cos\beta - u\Delta x \sec\alpha)\tan\phi'}{m_\alpha} \right]}{\sum W \sin\alpha - \dfrac{\sum M_P}{R}} \tag{C-15}$$

where Δx is the width of the slice, and m_α is defined by the following equation,

$$m_\alpha = \cos\alpha + \frac{\sin\alpha \tan\phi'}{F} \tag{C-16}$$

The terms W, c', ϕ', u, P, M_P, and R are as defined earlier for the OMS. Factors of safety calculated from Equation C-15 satisfy equilibrium of forces in the vertical direction and overall equilibrium of moments about the center of a circle. The unknowns and equations in the Simplified Bishop Method are summarized in Table C-4.

Because the value of the term m_α depends on the factor of safety, the factor of safety appears on both sides of Equation C-15. Equation C-15 cannot be manipulated such that an explicit expression is obtained for the factor of safety. Thus, an iterative, trial and error procedure is used to solve for the factor of safety.

a. Slope and typical slip surface
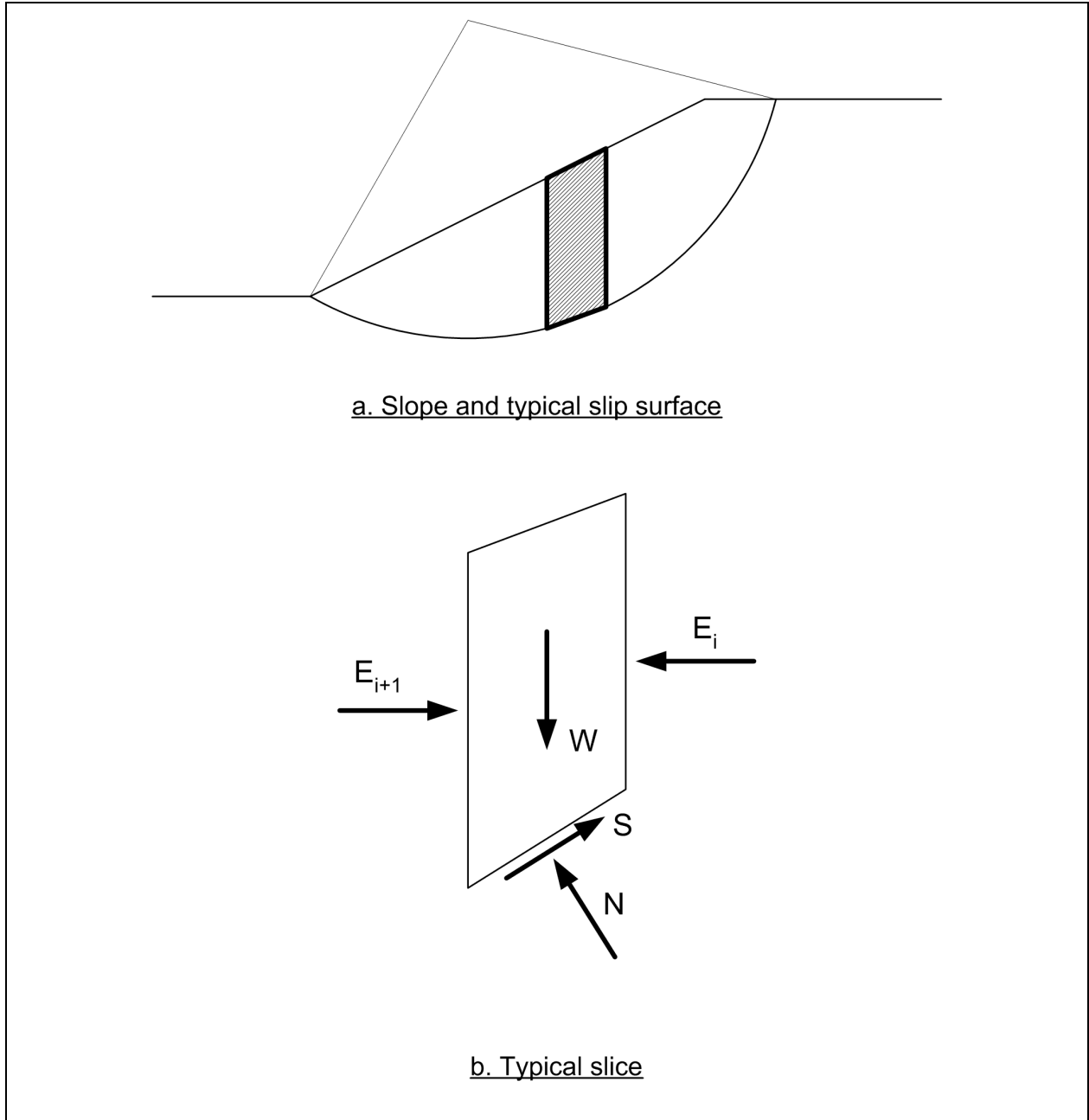
b. Typical slice

Figure C-11. Typical slice and forces for Simplified Bishop Method

Table C-4
Unknowns and Equations for the Simplified Bishop Method

Unknowns	Number of Unknowns for n Slices
Factor of safety (F)	1
Normal forces on bottom of slices (N)	n
TOTAL NUMBER OF UNKNOWNS	n + 1
Equations	**Number of Equations for n Slices**
Equilibrium of forces in the vertical direction, $\Sigma F_y = 0$	n
Equilibrium of moments of the entire soil mass	1
TOTAL NUMBER OF EQUILIBRIUM EQUATIONS	n + 1

b. Limitations. Horizontal equilibrium of forces is not satisfied by the Simplified Bishop Method. Because horizontal force equilibrium is not completely satisfied, the suitability of the Simplified Bishop Method for pseudo-static earthquake analyses where an additional horizontal force is applied is questionable. The method is also restricted to analyses with circular shear surfaces.

c. Recommendation for use. It has been shown by a number of investigators (Whitman and Bailey 1967; Fredlund and Krahn 1977) that the factors of safety calculated by the Simplified Bishop Method compare well with factors of safety calculated using rigorous methods, usually within 5 percent. Furthermore, the procedure is relatively simple compared to more rigorous solutions, computer solutions execute rapidly, and hand calculations are not very time-consuming. The method is widely used throughout the world, and thus, a strong record of experience with the method exists. The Simplified Bishop Method is an acceptable method of calculating factors of safety for circular slip surfaces. It is recommended that, where major structures are designed using the Simplified Bishop Method, the final design should be checked using Spencer's Method.

d. Verification procedures. When the Simplified Bishop Method is used for computer calculations, results can be verified by hand calculations using a calculator or a spreadsheet program, or using slope stability charts. An approximate check of calculations can also be performed using the Ordinary Method of Slices, although the OMS will usually give a lower value for the factor of safety, especially if ϕ is greater than zero and pore pressures are high.

C-4. Force Equilibrium Method, Including the Modified Swedish Method

a. Assumptions. Force equilibrium methods satisfy force equilibrium in both the horizontal and vertical directions, but they do not satisfy moment equilibrium. All force equilibrium methods are based on assuming the inclinations (θ) of the forces between slices (Figure C-12). The unknowns solved for and the equilibrium equations used are summarized in Table C-5.

The Modified Swedish Method is the name applied to force equilibrium procedures when they are used for analysis of circular slip surfaces. The Modified Swedish Method has been used extensively by the Corps of Engineers.

- Interslice forces have been represented in two ways in the Modified Swedish Method. In the first approach, the interslice forces are considered to represent the total forces between slices, the result of both effective stresses and pore water pressures. In the second approach, the side forces are considered to represent effective forces representing the effective stresses on the interslice boundaries. The forces resulting from water pressures are then considered as separate forces on the interslice boundaries. The computed value of the factor of safety will be different depending on the approach that is used.

- When total stresses are used to define the shear strengths in an analysis, e.g., for analyses with undrained strengths from UU (Q) tests, the interslice forces always represent total forces. In these cases, pore water pressures are not known, and thus, the forces from the water pressure on the sides of the slice cannot be calculated.
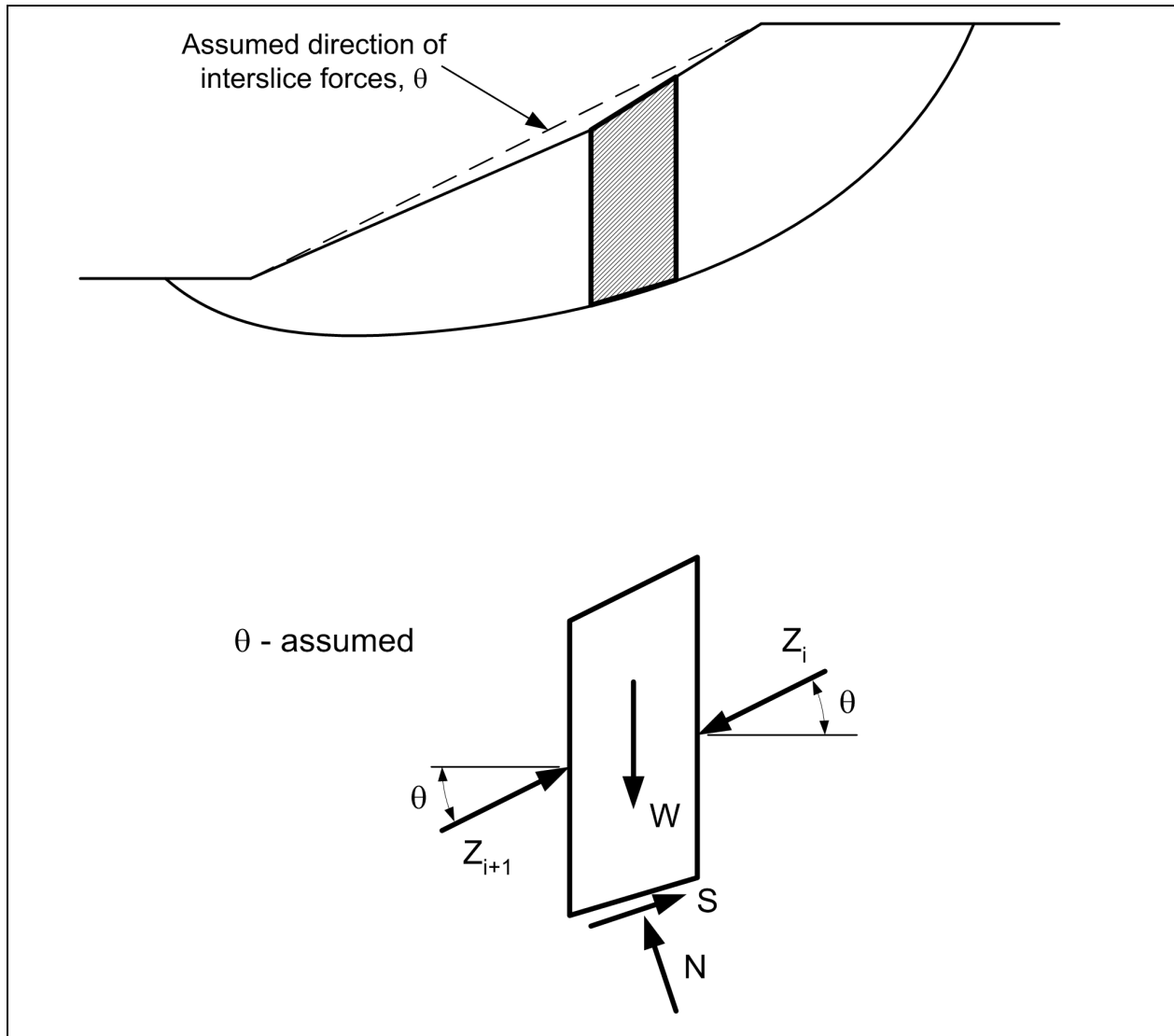
Figure C-12. Typical slice and forces for Modified Swedish Method

Table C-5
Unknowns and Equations for Force Equilibrium Methods

Unknowns	Number of Unknowns for n Slices
Factor of safety (F)	1
Normal forces on bottom of slices (N)	n
Resultant interslice forces, Z	n – 1
TOTAL NUMBER OF UNKNOWNS	2n

Equations	Number of Equations for n Slices
Equilibrium of forces in the horizontal direction, $\Sigma F_x = 0$	n
Equilibrium of forces in the vertical direction, $\Sigma F_y = 0$	n
TOTAL NUMBER OF EQUILIBRIUM EQUATIONS	2n

- When effective stresses are used to define the shear strengths, e.g., for analyses of steady-state seepage, a choice can be made between having the interslice forces (Z) represent either the total force or only the effective force. If the interslice forces are chosen to represent the effective force, the corresponding forces due to water pressures on the sides of the slice are calculated and included as additional forces in the analysis. In the equations presented in this appendix, the interslice forces for the Modified Swedish Method are represented as effective forces when effective stresses are used to characterize the shear strength. However, the equations and examples with effective interslice forces can easily be converted to represent interslice forces as total forces by setting the forces that represent water pressures on the sides of the slice to zero.

- The original version of the Modified Swedish Method represented interslice forces as effective forces whenever effective stress analyses were performed (USACE 1970). In contrast, many computer programs represent the interslice forces as total forces. Fundamentally, representation of interslice forces as effective forces is sound and feasible for effective stress analyses because the pore water pressures are known (defined) when effective stress analyses are performed. However, there are a number of reasons why it is appropriate to represent interslice forces as total forces, particularly in computer software:

(1) In complex stratigraphy, it is difficult to define and compute the resultant force from water pressures on the sides of each slice.

(2) In many analyses, total stresses are used in some soil zones, and effective stresses are used in others; the shear strengths of freely draining soils are represented using effective stresses; while the shear strengths of less permeable soils are represented using undrained shear strengths and total stresses. Interslice water pressures can only be calculated when effective stresses are used for all materials. Thus, interslice forces must be represented as total forces in the cases where mixed drained and undrained shear strengths are used.

(3) It makes almost no difference whether interslice forces are represented as effective or total forces when complete static equilibrium is satisfied, e.g., when Spencer's Method is used to calculate the factor of safety. Thus, in Spencer's Method total interslice forces are almost always used. The Modified Swedish Method is recommended for hand-checking calculations made with Spencer's Method. Accordingly, when the Modified Swedish Method is used to check calculations made using Spencer's Method, it is logical that the interslice forces should be total forces.

- Regardless of whether the interslice forces represent total or effective forces, their inclination must be assumed. The inclination that is assumed is the inclination of either the total force or the effective force, depending on how the interslice forces are represented. The Corps of Engineers' 1970 manual states that the side forces should be assumed to be parallel to the "average embankment slope". The "average embankment slope" is usually taken to be the slope of a straight line drawn between the crest and toe of the slope (Figure C-12). All side forces are assumed to have the same inclination. The assumption of side forces parallel to the average embankment slope has been shown to sometimes lead to unconservative results in many cases – the calculated factor of safety is too large - when compared to more rigorous procedures which satisfy both force and moment equilibrium such as Spencer's Method or the Morgenstern and Price procedure. The degree of inaccuracy is greater when total interslice forces are used. It is probably more realistic and safer to assume that the interslice forces are inclined at one-half the average embankment slope when total forces are used.

- To avoid possibly overestimating the factor of safety, some engineers in practice have assumed that the interslice forces are horizontal in the Modified Swedish Method. The assumption of horizontal interslice forces in procedures that only satisfy force equilibrium, and not moment equilibrium, is

sometimes referred to as the "Simplified Janbu" Method. This assumption, however, may significantly underestimate the value of the factor of safety. Accordingly, "correction" factors are sometimes applied to the value for the factor of safety calculated by the "Simplified Janbu" Method to account for the assumption of horizontal interslice forces (Janbu 1973). Some confusion exists in practice regarding whether the so-called "Simplified Janbu" Method should automatically include using the "correction" factors or not. Care should be exercised when reviewing results of slope stability calculations reported to have been made by the "Simplified Janbu" Method to determine whether a correction factor has been applied or not.

- Lowe and Karafiath (1960) suggested assuming that the interslice forces are inclined at an angle that is the average of the inclinations of the slope (ground surface) and shear surface at each vertical interslice boundary. Unlike the other assumptions described above, with Lowe and Karafiath's assumption the interslice force inclinations vary from slice to slice. This assumption appears to be better than any of the assumptions described earlier, especially when the side forces represent total, rather than effective, forces. Lowe and Karafiath's assumption produces factors of safety that are usually within 10 percent of the values calculated by procedures which satisfy complete static equilibrium (Duncan and Wright 1980).

(4) The force equilibrium equations for the Modified Swedish Method may be solved either graphically or numerically. Both the graphical and numerical solutions require an iterative, trial and error procedure to compute the factor of safety. A factor of safety is first assumed; force equilibrium is then checked. If force equilibrium is not satisfied, a new factor of safety is assumed and the process is repeated until force equilibrium is satisfied to an acceptable degree. The graphical and numerical procedures are each described separately in the sections that follow.

b. Graphical solution procedure. A solution for the factor of safety by any force equilibrium procedure (including the Modified Swedish Method) is obtained by repeatedly assuming a value for the factor of safety and then constructing the force vector polygon for each slice until force equilibrium is satisfied for all slices. A typical slice and the forces acting on it for a case where there is no surface or pore water pressure is shown in Figure C-12. The forces consist of the slice weight (W), the forces on the left and right sides of the slice (Z_i and Z_{i+1}), and the normal and shear forces on the base of the slice (N and S). The interslice force, Z_i, represents the force on the upslope side of the slice, while Z_{i+1} represents the force on the downslope side. Thus, Z_i acts on the right side of the slice for a left facing slope and on the left side of the slice for a right-facing slope. The shear force on the bottom of the slice is expressed as:

$$S = \frac{1}{F}\left(c\Delta\ell + N\tan\phi\right) \tag{C-17}$$

or

$$S = c_D\Delta\ell + N\tan\phi_D \tag{C-18}$$

where c_D and ϕ_D are the developed shear strength parameters.

In drawing the force polygons, the shear and normal forces are represented by a force resulting from cohesion, $c_D\Delta\ell$, and a force, F_D, representing the resultant force as a result of the normal force (N) and the frictional component of shear resistance ($N\tan\phi_D$). These forces are illustrated for a slice in Figure C-13b. The force $c_D\Delta\ell$ acts parallel to the base of the slice, while the force F_D acts at an angle ϕ_D from the normal to the base

a. Slope and trial slip surface

b. 1st Slice with forces

c. 2nd slice with forces

d. Force equilibrium polygons

e. Trial values

Figure C-13.   Forces and equilibrium force polygons for Modified Swedish Method

of the slice. A value must be assumed for the factor of safety to construct the force polygons because c_D and ϕ_D depend on the factor of safety. Once a factor of safety has been assumed and a suitable scale has been chosen, the force polygons are constructed for each slice as follows (Figure C-13d):

(1) A weight vector representing the weight (W) of the first slice is drawn vertically downward.

(2) A vector representing the force from the developed or developed or mobilized cohesion ($c_D \Delta \ell$) is drawn in a direction parallel to the base of the slice, starting at the tip of the weight vector.

(3) A line representing the direction of the resultant force, F_D, is drawn so that the tip of the vector meets the start (tail) of the weight vector. The vector is drawn so that it makes an angle, ϕ_D, with a line drawn perpendicular to the bottom of the slice and the shear component, $N \tan \phi_D$, is in the proper direction for the resisting force.

(4) A line representing the interslice force (Z) on the downslope side of the slice is drawn beginning at the end (tip) of the cohesion vector and extending in the direction assumed for the side forces. The intersection of this line with the line drawn in Step 3 defines the magnitude of the F_D and Z vectors.

(5) The process is continued for the next slice, except the weight vector begins at the tip of the vector representing the cohesion force (Figure C-13d). The construction for slice 2 is shown by dotted lines.

(6) Vectors are drawn slice-by-slice until the last slice is reached. Because there is no force on the left side of the last slice, the force polygon should close with the resultant vector, F_D, alone. However, unless the correct value was assumed for the factor of safety, the force polygon will not close and an artificial force Z_{i+1} is required to cause closure. This "error of closure" represents the force imbalance for the assumed factor of safety. Additional factors of safety must be assumed, and the error of closure is then plotted versus the trial factor of safety (Figure C-13e). Usually by plotting the results of three or four trials the factor of safety can be determined with acceptable accuracy. Further details of the equilibrium force polygons and solution are shown by the examples in Appendix F.

(7) A typical slice and the forces acting on it where the shear strength is expressed using effective stresses is shown in Figure C-14. The forces consist of the total weight of the slice (W), the water pressure forces on the left and right of the slice (U_L and U_R), the side forces resulting from effective stresses (Z_i and Z_{i+1}), the force resulting from developed or mobilized cohesion ($c'_D \Delta \ell$), the resultant force (F'_D) resulting from the effective normal force, N', and the frictional component of shear strength, $N' \tan \phi'$, and the force resulting from pore water pressures on the base of the slice (U_b). An additional force, P, will act on the top of the slice if the top of the slice is submerged. The forces W, U_L, U_R, U_b, and P are all known forces. To construct the force polygon these known forces are represented by a single resultant force R. The resultant force, R is represented graphically in Figure C-14c. The force will be vertical if there is no seepage (no flow); otherwise the force, R, will be inclined from vertical. Force polygons are constructed in a manner similar to that described above for no water pressures, except the vector, R, replaces the weight vector, W (Figure C-14d). Further details are shown by the examples in Appendix F.

c. Numerical solution method. In the numerical solution for any force equilibrium method (including the Modified Swedish Method), the side force on the downslope side of the slice is calculated using the following equation, derived from the equations of vertical and horizontal force equilibrium:

$$Z_{i+1} = Z_i + \frac{C_1 + C_2 + C_3 - C_4}{n_\alpha} \tag{C-19}$$

where

$$C_1 = W \left[\sin \alpha - \frac{\tan \phi' \cos \alpha}{F} \right] \tag{C-20a}$$

a. Slope and trial slip surface

c. Resultant force polygon

b. Slice with forces

d. Force equilibrium polygon for slice

Figure C-14. Forces for Modified Swedish Method with water

$$C_2 = \left(U_i - U_{i+1}\right)\left[\cos\alpha + \frac{\tan\phi'\sin\alpha}{F}\right]$$ (C-20b)

$$C_3 = P\left[\sin(\alpha-\beta) - \frac{\tan\phi'}{F}\cos(\alpha-\beta)\right]$$ (C-20c)

$$C_4 = (c' - u \tan \phi') \frac{\Delta \ell}{F} \tag{C-20d}$$

$$n_\alpha = \cos(\alpha - \theta) + \frac{\tan \phi' \sin(\alpha - \theta)}{F} \tag{C-21}$$

(1) The quantities Z_i and Z_{i+1} represent the forces on the upslope and downslope sides of the slice, respectively, U_i and U_{i+1} represent the water pressure forces on the upslope and downslope sides of the slice, and θ represents the inclination of the interslice forces. The remaining terms in Equation C-19 are the same as those defined earlier for the Ordinary Method of Slices and Simplified Bishop Methods. Equation C-19 is applied beginning with the first slice where $Z_i = 0$ and proceeding slice-by-slice until the last slice is reached. Here it is assumed that calculations are performed proceeding from the top of the slope to the bottom of the slope, regardless of the direction that the slope faces. The calculated interslice force Z_{i+1} for the downslope side of the last slice (toe of the slip surface) should be zero if a correct value has been assumed for the factor of safety. If the force on the downslope side of the last slice is not zero, a new value is assumed for the factor of safety and the process is repeated until the force on the downslope side of the last slice is zero. Example calculations for the Modified Swedish Method using both the numerical solution and the graphical procedure are presented in Appendix F.

(2) When the quantities, U_i and U_{i+1}, that represent water pressures on the sides of the slice are not zero, the interslice forces, Z_i and Z_{i+1}, represent forces in terms of effective stress. When total stresses are used, the quantities, U_i and U_{i+1}, are set to zero and the interslice forces then represent the total forces, including water pressures. The quantities, U_i and U_{i+1}, can also be set equal to zero for effective stress analyses and the side forces are then the total side forces. Total interslice forces are used in much of the computer software for slope stability analyses, but effective forces are recommended when the side forces are assumed to be parallel to the average embankment slope, as discussed in Section C-4a.

d. Limitations. The principal limitation of the Modified Swedish Method is that calculated factors of safety are sensitive to the assumed interslice force inclination. Depending on the inclination assumed for the interslice forces, the factor of safety may be either underestimated or overestimated compared to the value calculated by more rigorous methods that fully satisfy static equilibrium. The sensitivity of the method appears to be due in large part to the fact that moment equilibrium is not satisfied.

e. Recommendations for use. The force equilibrium procedure is the only method considered to this point that can be utilized for analyses with general shaped, noncircular slip surfaces. Although the force equilibrium method is not as accurate as Spencer's Method (described next) for analyses of general-shaped noncircular slip surfaces, the force equilibrium method is much simpler and is therefore suitable for hand calculations, whereas Spencer's Method is too lengthy for hand calculations. Accordingly, the force equilibrium method is recommended for use in hand calculations where noncircular slip surfaces are being analyzed. If the force equilibrium method is being used to check calculations that were performed using Spencer's Method, the side force inclination used for the hand calculations should be the one calculated by Spencer's Method (Section C-5). Spencer's Method and the force equilibrium procedure should produce identical results when the same side force inclination is used in both method. The Modified Swedish Method is useful where existing slopes have been designed using the method and are being analyzed for new conditions, such as updated pore pressure information, or where alterations are to be made. Using the same method will allow meaningful comparison of results to those from previous analyses. For all new designs, preference should be given to the Simplified Bishop (circular slip surfaces) and Spencer (noncircular slip surfaces) Methods.

f.   Verification procedures. As described above, either numerical or graphical procedures can be used in the Modified Swedish Method. Depending on which procedure was first used to compute the factor of safety (numerical or graphical), the other procedure can be used for verification. Thus, if the factor of safety was computed using the numerical procedure with Equation C-19, the force vector polygons can be drawn to confirm that force equilibrium has been satisfied. Likewise, if the graphical procedure was used to compute the factor of safety, the numerical solution (Equation C-19) can be used to compute the side forces and verify that equilibrium has been satisfied.

C-5. Spencer's Method

a.   Assumptions. <u>Spencer's Method</u> assumes that the side forces are parallel, i.e., all side forces are inclined at the same angle. However, unlike the Modified Swedish Method, the side force inclination is not assumed, but instead is calculated as part of the equilibrium solution. Spencer's Method also assumes that the normal forces on the bottom of the slice act at the center of the base – an assumption which has very little influence on the final solution. Spencer's Method fully satisfies the requirements for both force and moment equilibrium. The unknowns and equations involved in the method are listed in Table C-6.

Table C-6
Unknowns and Equations for Spencer's Methods

Unknowns	Number of Unknowns for n Slices
Factor of safety (F)	1
Inclination of interslice forces (θ)	1
Normal forces on bottom of slices (N)	n
Resultant interslice forces, Z	n – 1
Location of interslice normal forces	n – 1
TOTAL NUMBER OF UNKNOWNS	3n
Equilibrium Equations	
Equations	**Number of Equations for n Slices**
Equilibrium of forces in the horizontal direction, $\Sigma F_x = 0$	n
Equilibrium of forces in the vertical direction, $\Sigma F_y = 0$	n
Equilibrium of moments	n
TOTAL NUMBER OF EQUILIBRIUM EQUATIONS	3n

Although Spencer (1967) originally presented his method for circular slip surfaces, Wright (1969) showed that the method could readily be extended to analyses with noncircular slip surfaces. A solution by Spencer's Method first involves an iterative, trial and error procedure in which values for the factor of safety (F) and side force inclination (θ) are assumed repeatedly until all conditions of force and moment equilibrium are satisfied for each slice. Then the values of N, Z, and y_t are evaluated for each slice.

b.   Limitations. Spencer's Method requires computer software to perform the calculations. Because moment and force equilibrium must be satisfied for every slice and the calculations are repeated for a number of assumed trial factors of safety and interslice force inclinations, complete and independent hand-checking of a solution using Spencer's Method is impractical (Section C-5d).

c.   Recommendations for use. The use of Spencer's Method for routine analysis and design has become practical as computer resources improve. The method has been implemented in several commercial computer programs and is used by several government agencies. Spencer's Method should be used where a statically complete solution is desired. It should also be used as a check on final designs where the slope stability computations were performed by simpler methods.

d.   Verification procedures. Complete and independent hand-checking of a solution using Spencer's Methods is impractical because of the complexity of the method and the lengthy calculations involved. Instead the force equilibrium procedure is recommended, using either the graphical or numerical solution methods. When checking Spencer's Method using the force equilibrium procedure, the side force inclination

(θ) is assumed to be the same as the one found using Spencer's Method. In this case (same side force inclination), both the force equilibrium procedure and Spencer's Method should produce the same value for the factor of safety.

C-6. The Wedge Method

a. Assumptions. The Wedge Method is illustrated in Figure C-15. The method assumes that the sliding mass is composed of three regions: the active wedge, the central block, and the passive wedge. The inclination of the forces on the vertical boundaries between the zones are assumed. The Wedge Method is actually a special case of the force equilibrium procedure: the Wedge Method fully satisfies equilibrium of forces in the vertical and horizontal directions and ignores moment equilibrium. The only differences between the Wedge Method and the Modified Swedish Method are (1) the assumptions for the shape of the potential sliding surface, and (2) possibly, the inclinations of the "interslice" forces between wedges. In the Wedge Method, the interslice force inclination assumption is often made the same as for the Modified Swedish Method. However, the interslice force between the central block and the passive wedge is sometimes assumed to be horizontal.

b. Solution procedure. Solutions for the Wedge Method are the same as for any of the force equilibrium procedures (Section C-4).

c. Limitations. The Wedge Method has the same limitations as other force equilibrium procedures. In addition, the specific, "wedge" shape of the slip surface restricts use of the procedure to slopes where slip surfaces of this shape are likely to be critical.

d. Recommendations for use. Factors of safety calculated using the Wedge Method are sensitive to the assumed inclinations of the side forces. The Wedge Method may be used to check Spencer's solutions for three-part noncircular shear surfaces. The side force inclination is taken as the same side force inclination found in Spencer's. The Wedge Method also has use where existing slopes have been designed using the method and are being analyzed for new conditions, such as updated pore pressure information, or where alterations are to be made. Using the same method allows meaningful comparison of results to those from previous analyses. For all new designs, preference should be given to complete analysis procedures such as Spencer's Method, which can be used for noncircular and wedge-shaped shear surfaces.

e. Verification procedures. The same procedures, graphical or numerical, used to verify calculations performed by the Modified Swedish Method, may be used to verify calculations by the Wedge Method.

C-7. The Infinite Slope Method

a. Assumptions. The Infinite Slope Method assumes that the slope is of infinite lateral extent and that sliding occurs along a plane surface parallel to the face of the slope (Figure C-16). For slopes composed of uniform cohesionless soils (c' = 0), the critical slip surface will be parallel to the outer slope at small depth (z ≈ 0). In this situation, the instability mechanism involves individual soil particles rolling down the face of the slope. Analyses of this condition using circular slip surfaces will result in a critical circle that approximates the infinite slope failure mechanism with a circle that is very shallow and has a very large radius. The factor of safety will be the same as calculated using an infinite slope analysis. However, the infinite slope analysis is simpler and easier, and it should be used for slopes in cohesionless materials. The Infinite Slope Method is a special case of the force equilibrium procedure, with one slice. With only one slice, two equations are available (horizontal and vertical force equilibrium), and two unknowns must be evaluated (the factor of safety and the normal force on the base of the slice). Thus, the method is statically determinate.
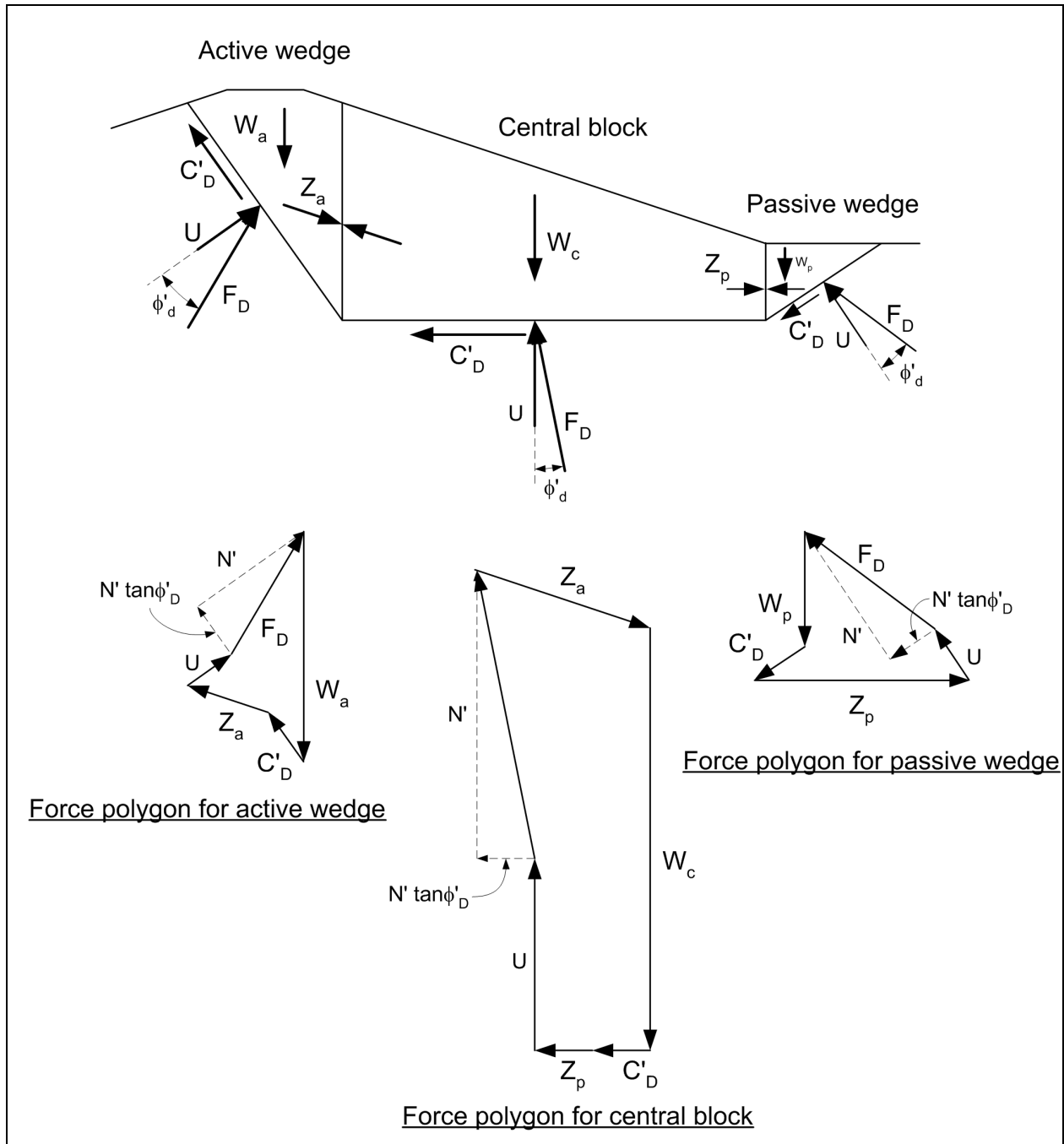
Figure C-15. Forces and equilibrium polygons for Wedge Method

b. Stability equations. For an infinite slope, the total normal and shear stresses on a plane parallel to the slope at a vertical depth, z, are given by:

$$\sigma = \gamma z \, \cos^2 \beta \qquad\qquad\qquad\qquad\text{(C-22)}$$

and

$$\tau = \gamma z \, \cos \beta \, \sin \beta \qquad\qquad\qquad\qquad\text{(C-23)}$$
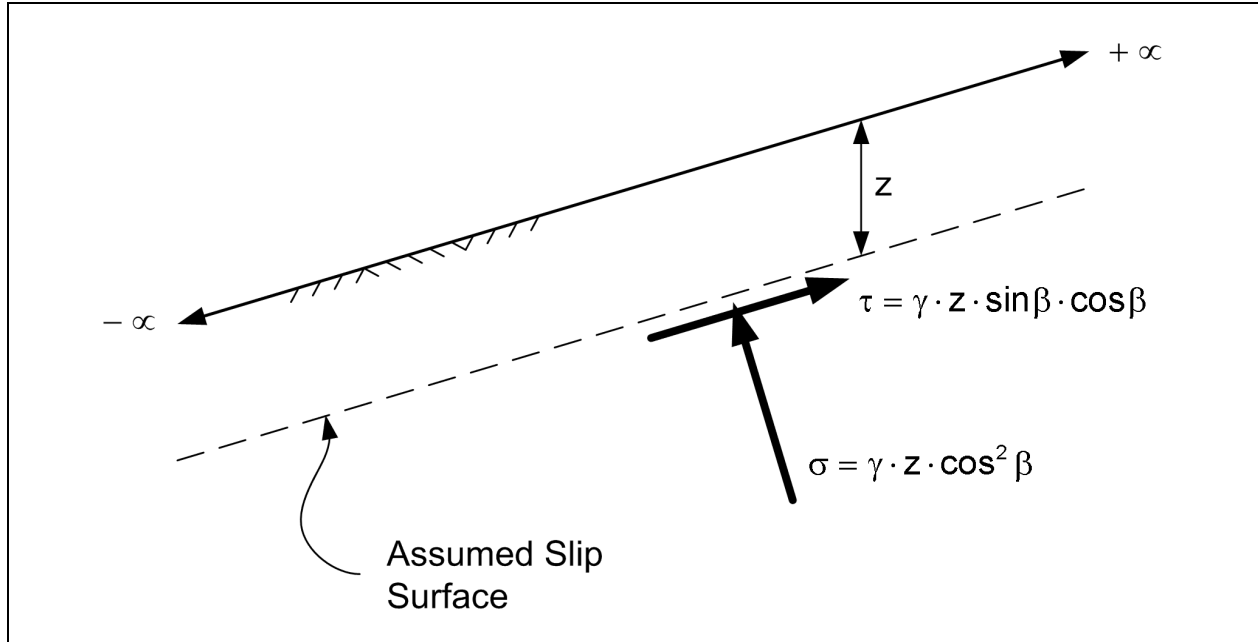
Figure C-16. Infinite slope

For shear strengths expressed in terms of effective stresses and zero cohesion (c' = 0), the factor of safety is given by:

$$F = \frac{s}{\tau} = \frac{(\sigma - u)\tan\phi'}{\tau} \tag{C-24}$$

where u is the pore water pressure at the depth of the shear plane.

Letting $r_u = u/\gamma z$ and substituting the expressions for σ and τ from Equations C-22 and C-23 into Equation C-24, gives:

$$F = \frac{s}{\tau} = \frac{(\cos^2\beta - r_u)\tan\phi'}{\cos\beta\sin\beta} \tag{C-25}$$

Equation C-25 can also be written as:

$$F = \frac{\tan\phi'}{\tan\beta}\left[1 - r_u\left(1 + \tan^2\beta\right)\right] \tag{C-26}$$

For the special case of no pore water pressure (u = 0; r_u = 0) Equation C-26 reduces to:

$$F = \frac{\tan\phi'}{\tan\beta} \tag{C-27}$$

(1) The stability equation for an infinite slope can also be written for conditions involving seepage through the slope, as shown in Figure C-17.
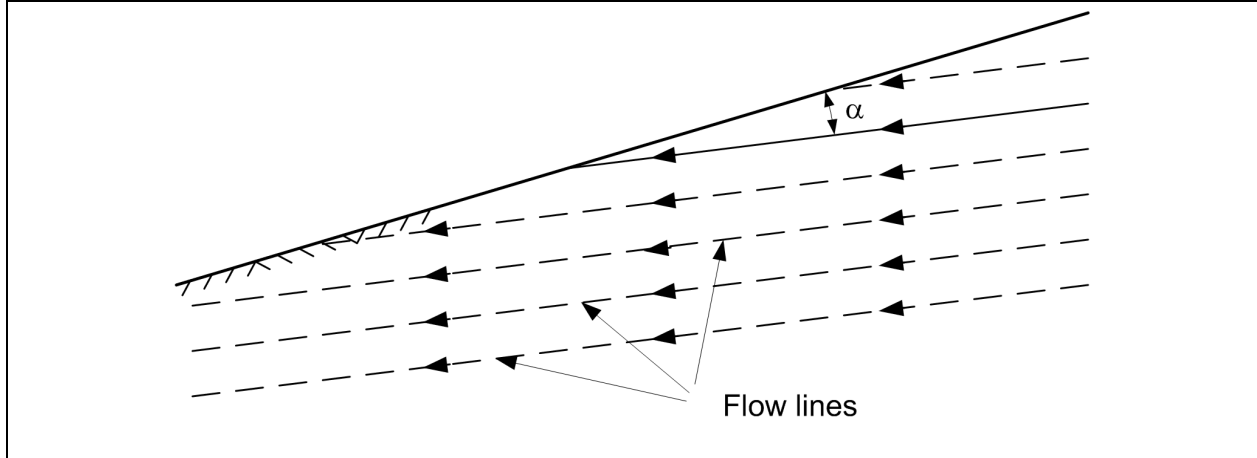
Figure C-17. Infinite slope with parallel flow lines

The factor of safety for an infinite slope with seepage can be expressed as follows (Bolton 1979):

$$F = \frac{\gamma' - \gamma_w \tan\alpha_s \tan\beta}{\gamma_{sat}} \frac{\tan\phi'}{\tan\beta} \tag{C-28}$$

where

$\gamma' = \gamma_{sat} - \gamma_w$ = submerged unit weight of soil

γ_w = unit weight of water

γ_{sat} = saturated unit weight of soil

α_s = angle between the flow lines and the embankment face (Figure C-17)

β = inclination of the slope measured from the horizontal

ϕ' = angle of internal friction expressed in terms of effective stresses

The cohesion, c', is assumed to be zero because the infinite slope analysis is primarily applicable to cohesionless soils.

(2) For the case where the direction of seepage is parallel to the slope ($\alpha_s = 0$), with the free surface of seepage at the ground surface, the factor of safety can be expressed as:

$$F = \frac{\gamma'}{\gamma_{sat}} \frac{\tan\phi'}{\tan\beta} \tag{C-29}$$

Similarly, for the case of horizontal seepage ($\alpha = \beta$)

$$F = \frac{\gamma' - \gamma_w \tan^2\beta}{\gamma_{sat}} \frac{\tan\phi'}{\tan\beta} \tag{C-30}$$

c.   Limitations. The equations for infinite slope factor of safety given by Equations C-24 through C-30 are applicable only to slopes in cohesionless materials. They apply to slopes in nonplastic silt, sand, gravel, and rock-fill where c' = 0. Charts for analysis of infinite slopes in materials with c' > 0 are given in Appendix E.

d.   Recommendations for use. The method is useful for evaluating the stability with respect to shallow sliding of slopes in cohesionless soils.

C-8. Simple Approximations

Simple approximations are sometimes useful for preliminary estimates of stability prior to more rigorous and complete calculations. Two such simplified approaches are discussed below.

a.   At-rest earth pressure method. The at-rest earth pressure method is used to estimate the potential for lateral spreading and horizontal sliding of an embankment, as shown in Figure C-18.

(1) Assumptions. The method compares the at-rest earth pressure on a vertical plane through the embankment to the shear resistance along the base of the embankment to one side of the plane. The method is only partly a limit-equilibrium method, because the at-rest earth pressures are calculated independently of any equilibrium conditions and, then, compared to the limiting shear resistance.

(2) Limitations. The method is not intended as a primary design method but only as a method to perform supplemental checks. It is applicable only to embankments.

(3) Recommendations for use. Ensuring that an embankment has an adequate factor of safety by this analysis will assist in limiting deformations where two or more materials with significantly different stress-strain behavior are present. A common example application is to zoned gravel or rock-fill dams with clay cores.

b.   Bearing capacity methods. Bearing capacity methods are useful for estimating the potential for weak, saturated, clay foundations to support embankments (Figure C-19).

(1) Assumptions. These methods compare the ultimate bearing capacity of the foundation beneath an embankment to the total vertical stress imposed by the embankment. The vertical stress is calculated by multiplying the full height of the embankment by the total unit weight of the fill material. The bearing capacity of the foundation is calculated from the classical bearing capacity equations for a strip footing resting on the surface of the ground. For a saturated clay and undrained loading ($\phi = 0$), the ultimate bearing capacity is computed as:

$$q_{ult} = 5.14c \qquad\qquad (C\text{-}31)$$

Although more sophisticated approximations can be made, bearing capacity analyses should not be considered to be a substitute for detailed slope stability analyses.

(2) Limitations. The bearing capacity methods are limited to homogeneous foundations where simple bearing capacity equations are applicable. These methods are also used primarily for evaluating short-term, undrained stability of embankments resting on soft, saturated clay foundations. These methods are intended only for preliminary analyses and for use as an approximate check of more rigorous and thorough analyses.

$$F = \frac{c' \cdot d + (W - \overline{u}d) \cdot \tan\phi'}{P_o}$$

P_o = total force due to at-rest pressures on vertical plane through center of embankment

c' and ϕ' = shear strength parameters along horizontal surface between embankment and foundation

$\overline{u}$ = average pore water pressure along embankment-foundation contact
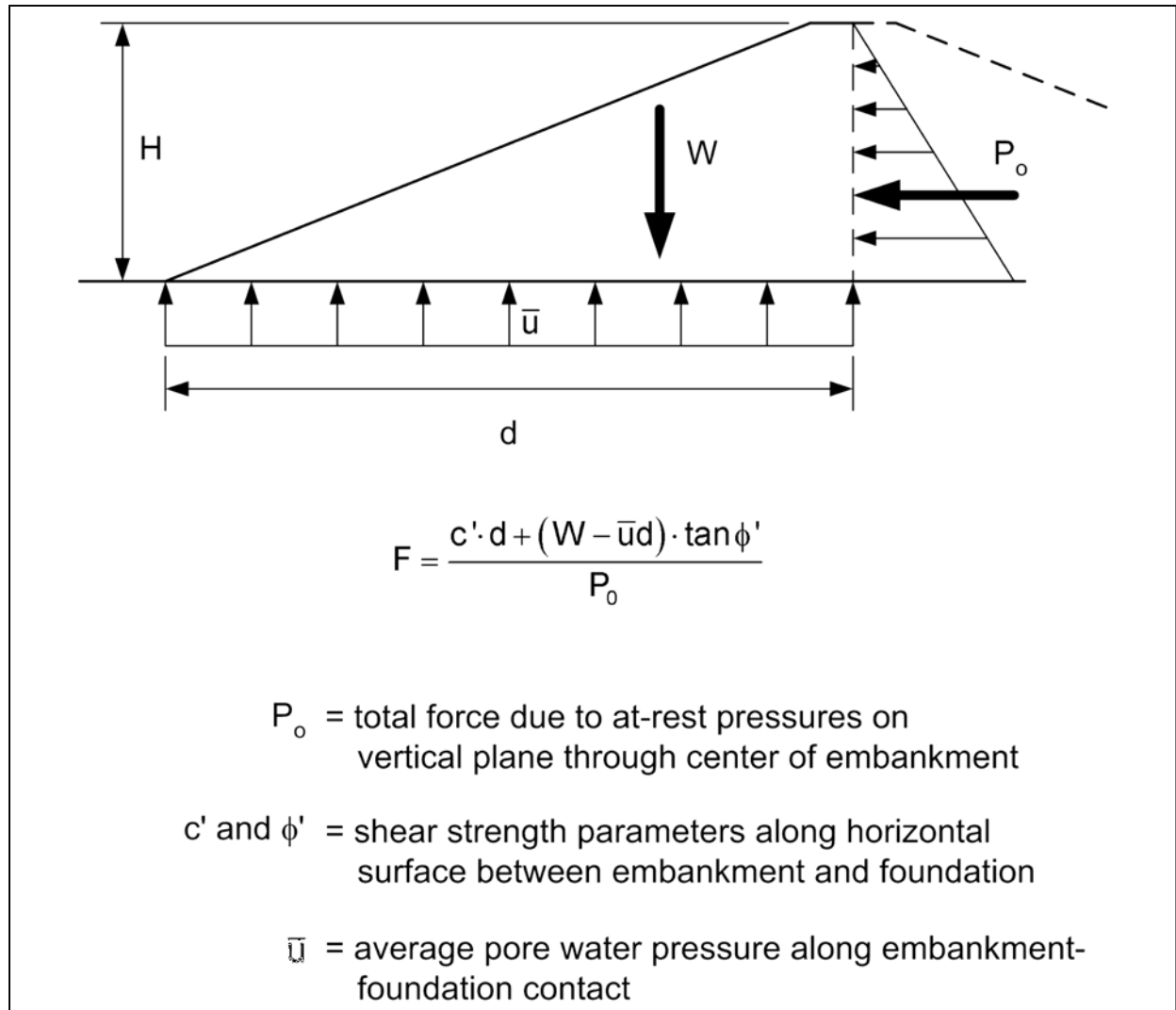
Figure C-18. At-rest earth pressure method

(3) Recommendations for use. This simple bearing capacity approach ignores the shear strength of the embankment fill and is conservative in this respect. Because the shear strength of the embankment material is ignored, questions about incompatibility between the stress-strain behavior of the embankment and the foundation do not arise.

C-9. Chart Solutions

a. Chart solutions are very useful for obtaining preliminary estimates of stability and for checking detailed analyses. For cases where the conditions represented by the stability charts match those of the actual slope, charts provide an accurate value of factor of safety. In such cases, factors of safety computed using charts are more accurate than those computed using procedures such as the Ordinary Method of Slices and the Modified Swedish Method.

Foundation: s = c (ϕ = 0)

a. Actual embankment and foundation

q = γH

$$F = \frac{q_{ult}}{q}$$

$$q_{ult} = N_c c = 5.14c$$

$$F = 5.14\frac{c}{\gamma H}$$

b. Bearing capacity approximation
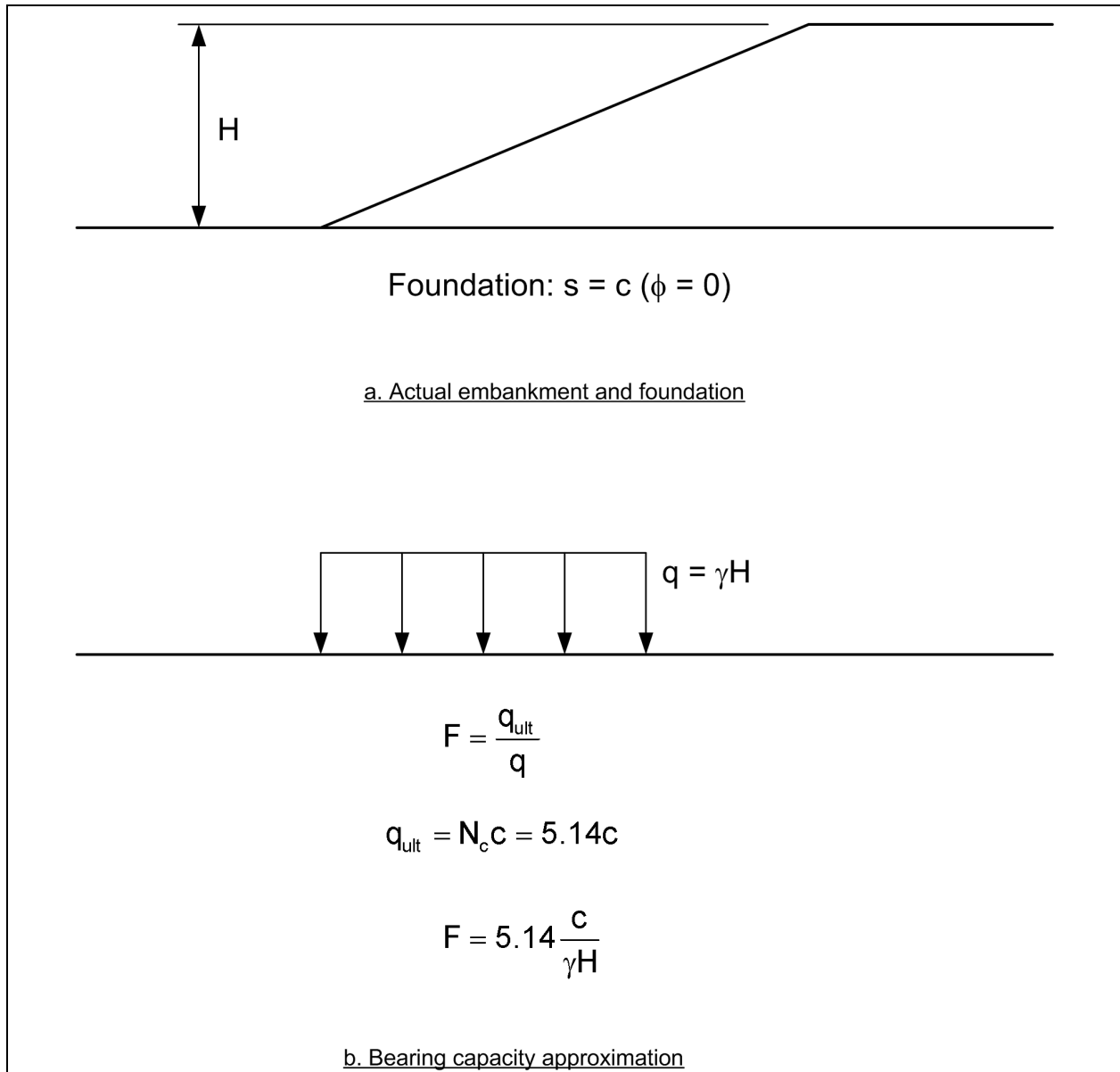
Figure C-19.   Use of bearing capacity methods to estimate stability of embankments on soft, saturated clay foundations

b.   In addition to charts derived from analyses using limit equilibrium procedures, like those described in the previous sections, charts based on field observations of slope performance have also been developed. This second type of chart includes effects of geologic and groundwater conditions, which is advantageous, but such charts are only useful for the area and the types of slopes for which they are developed.

c.   Charts developed using analytical methods are discussed in detail in Appendix E.

C-10. Acceptability of Solutions and Computational Problems

a.   General.   The assumptions introduced to render slope stability problems statically determinate sometimes lead to unrealistic solutions. Regardless of the method used, calculated results must be checked to

identify computational problems. Calculated values of normal forces (N) and interslice forces (Z) should be examined to be sure that their values are reasonable. Because most soils are not able to sustain significant tensile stresses, tensile forces should not exist on the sides or bottom of slices. Also the line of thrust (the locus of points describing the location of the interslice forces) should be within the sliding mass. Several specific computational problems are discussed below.

   b.   Very large forces or tensile forces due to slip surface geometry.   As shown in Figure C-20, the resultant force on the slip surface (F_D) can become parallel or nearly parallel to the interslice force (Z) if the slip surface exits too steeply at the toe. When this condition occurs, very large, infinite, or negative, values may be calculated for these forces (Ching and Fredlund 1983). If F_D and Z are parallel, division by zero occurs in the equilibrium equations, and the forces become infinite. If F_D and Z are close to parallel, division by a very small number occurs in the equilibrium equations, and the values of F_D and Z can be very large, either positive or negative. Factors of safety computed for such conditions are not meaningful. The condition of large positive or negative forces near the toe of the slope is usually caused by the slip surface exiting upward too steeply. The problem can be avoided by adjusting the inclination of the slip surface to conform more closely with the most critical slip surface that would be expected based on passive earth pressure theories. In the case where the ground surface and earth pressure (interslice) force are both horizontal, the inclination of the critical slip surface (shear plane) for passive earth pressure conditions is given by:

$$\alpha = -\left(45° - \frac{\phi'}{2}\right) \tag{C-32}$$

The negative sign arises from the sign convention used for the inclination of the shear surface in the slope stability equations. In the case of an inclined earth pressure (interslice) force, the inclination of the critical slip surface can be calculated from the following equation presented by Jumikis (1962):

$$\alpha = -\Omega + \phi \tag{C-33}$$

where

$$\Omega = \arctan\left[\frac{\tan\phi + \sqrt{\tan\phi(\tan\phi + \cot\phi)(1 + \tan\delta\cot\phi)}}{1 + \tan\delta(\tan\phi + \cot\phi)}\right] \tag{C-34}$$

where δ is the inclination of the earth pressure force, which corresponds to θ in Figure C-20.

The sign convention for α in Equation C-33 is such that α is negative for slip surfaces inclined upward at the toe of the slope. The existence of very large positive or negative values for the forces near the toe of the slope can lead to unreasonably large or unreasonably small values for the factor of safety. Depending on the procedure of slope stability analysis being used, the problem can be avoided in one of the following ways:

   (1)   The slip surface can be flattened near the toe as described above: This is probably the best approach, but the use of noncircular slip surfaces is required.

   (2)   The side force inclination can be changed: Of the procedures described in this manual, the Modified Swedish Method is the only one that allows the inclination of the side forces to be changed. It is also possible to change the assumed inclination for the side force with using the Morgenstern and Price method (Morgenstern and Price 1965). Changing the side force inclination to obtain a suitable solution with the Morgenstern and Price procedure can be time-consuming.
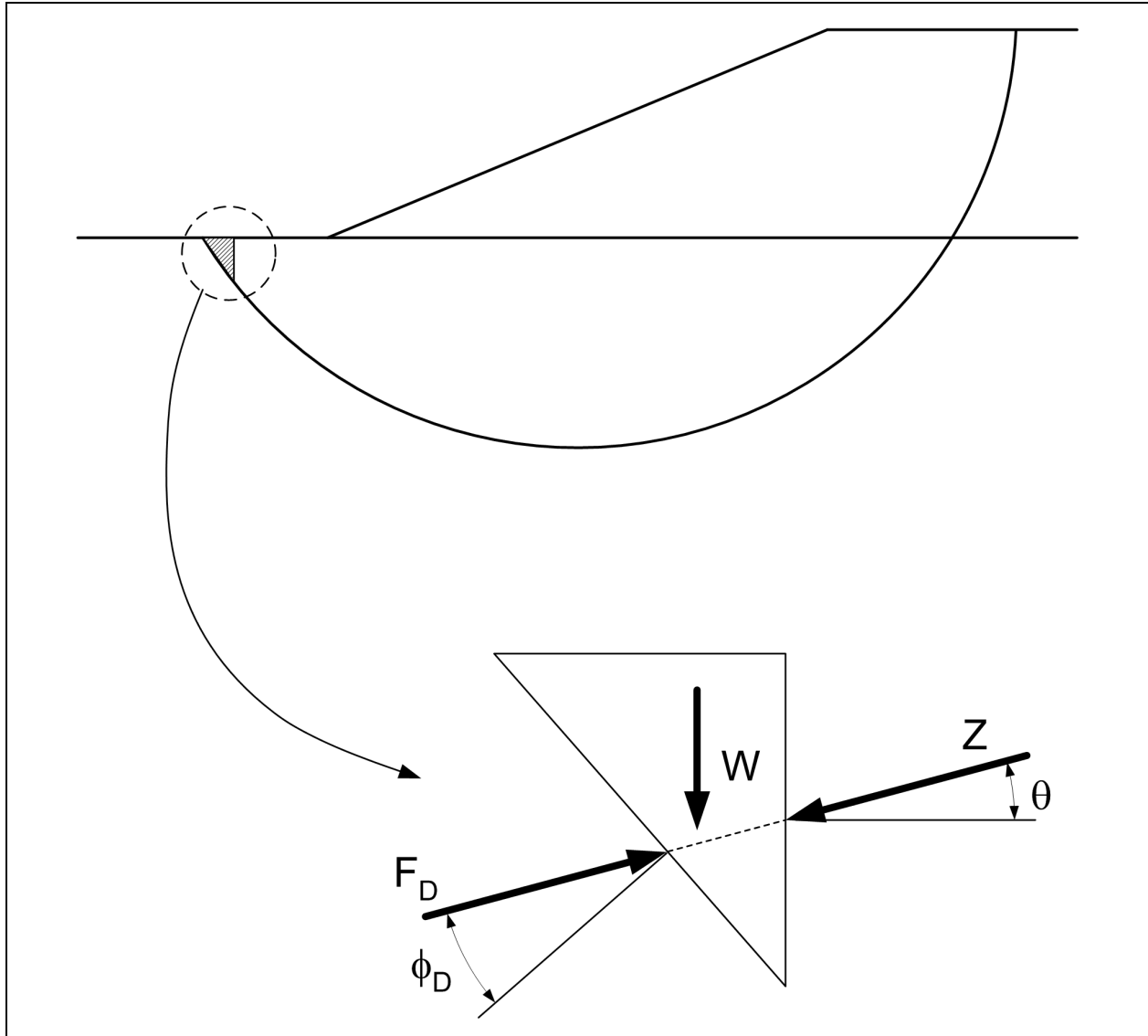
Figure C-20. Slice with parallel (co-linear) resultant force, *F_D*, and interslice force, *Z*, leading to infinite values of these forces

(3) The Ordinary Method of Slices can be used for the analysis. The problem described above does not occur with the OMS, because the OMS neglects side forces. However, the OMS is not accurate for effective stress analyses when pore pressures are high, and its use is undesirable for that reason.

(4) The shear strength in the zone where the slip surface exits can be estimated assuming a simple passive earth pressure state of stress. The shear strength is then assigned to this zone as a cohesion with $\phi = 0$. For cohesionless soil ($c = 0$), horizontal ground surface, and a horizontal earth pressure force, the shear strength $s_{passive}$ can be calculated from:

$$s_{passive} = \frac{1}{2}\left[\tan^2\left(45° + \frac{\phi'}{2}\right) - 1\right]\sigma'_v \cos\phi' \tag{C-35}$$

where σ'_v is the effective vertical stress.

In this case, the shear strength increases linearly with depth because the effective vertical stress also increases linearly with depth. Approach (4) is the only one that can be used to eliminate large positive or negative forces at the toe of the slope when the Simplified Bishop Method is used. Regardless of the procedure used to calculate the factor of safety, the details of the solution should be examined to determine if very large positive or negative forces are calculated for slices near the toe of the slope. If such conditions are found, one of the measures described above should be used to correct the problem.

    c. Tensile forces from cohesion. When soils at the crest of the slope have cohesion, the calculated values for the normal forces (N) and side forces (Z) in this area are often negative. Negative forces are consistent with what would be calculated by classical earth pressure theories for the active condition. The negative stresses result from the tensile strength that is implicit for any soil having a Mohr-Coulomb failure envelope with a cohesion intercept. This type of shear strength envelope implies that the soil has tensile strength, as shown in Figure C-21. Because few soils have tensile strength that can be relied on for slope stability, tensile stresses should be eliminated before an analysis is considered acceptable. Tensile stresses can be eliminated from an analysis by introducing a vertical tension crack near the upper end of the slip surface. The slip surface is terminated at the point where it reaches the bottom of crack elevation, as shown in Figure C-22. The appropriate crack depth can be determined in either of the following ways:

    (1) A range of crack depths can be assumed and the factor of safety calculated for each depth. The crack depth producing the minimum factor of safety is used for final analyses. The depth yielding the minimum factor of safety will correspond closely to the depth where tensile stresses are eliminated, but positive (driving) stresses are not.

    (2) The crack depth can be estimated as the depth over which the active Rankine earth pressures are negative. For total stresses and homogeneous soil the depth is given by:

$$d_{crack} = \frac{2c_D}{\gamma \tan\left(45° - \frac{\phi_D}{2}\right)} \tag{C-36}$$

where

    c_D and ϕ_D = developed shear strength parameters

        c_D = c/F

      $\tan \phi_D$ = tan ϕ/F

Similar expressions can be developed for the depth of tension for effective stresses and/or nonhomogeneous soil profiles. In some cases the depth of crack computed using Equation C-36 will be greater than the height of the slope. This is likely to be the case for low embankments of well-compacted clay. For embankments on weak foundations, where the crack depth computed using Equation C-36 is greater than the height of the embankment, the crack depth used in the stability analyses should be equal to the height of the embankment; the crack should not extend into the weak foundation.

$$\sigma_t = \sigma_3 = - 2\, c\, \tan(45^\circ - \phi/2)$$

$$\sigma_1 = 0$$

$$\phi$$

$$c$$

$$\sigma_t$$

σ_t = Uniaxial (unconfined) tensile strength
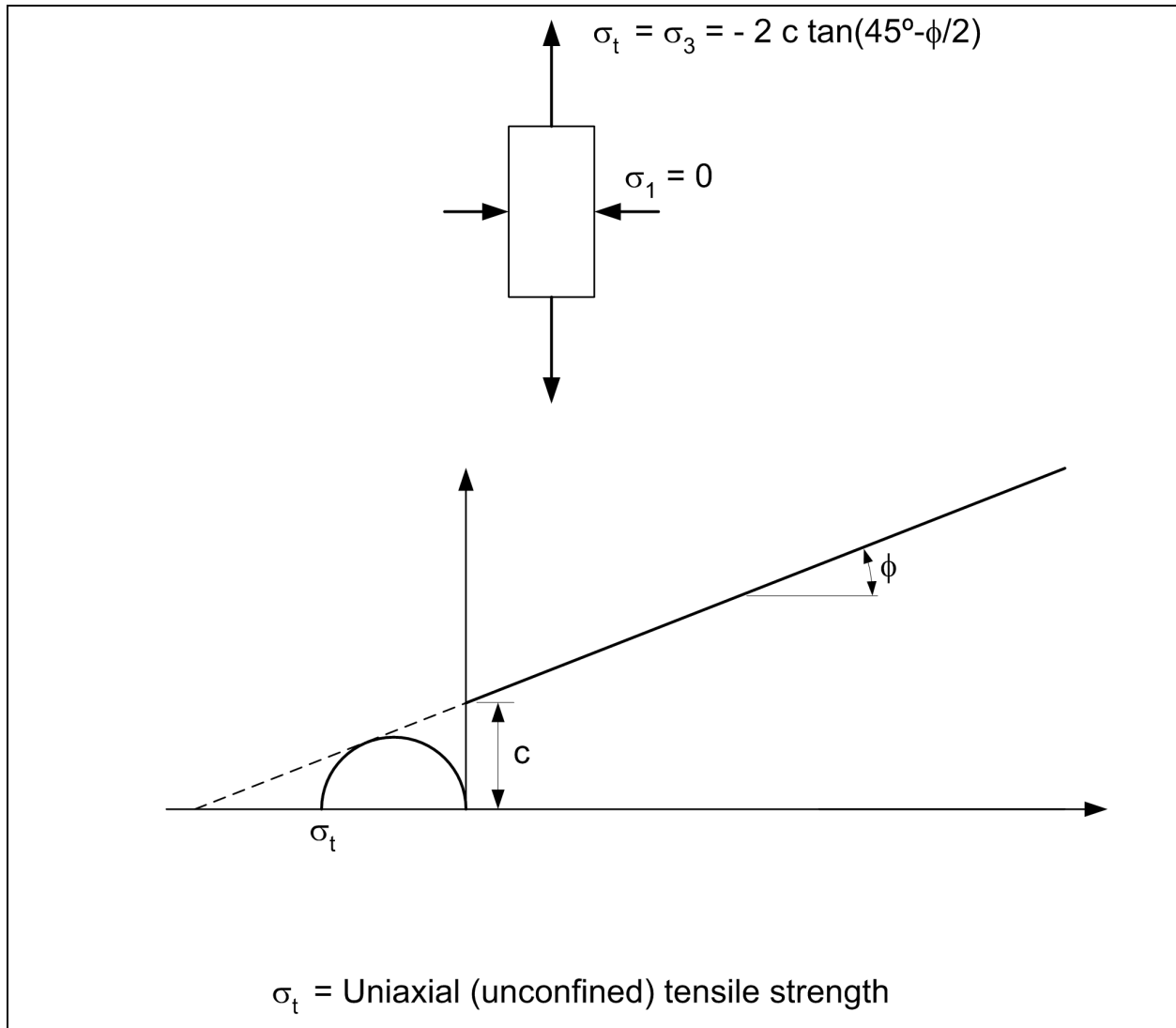
Figure C-21.   Tensile strength implied by a Mohr-Coulomb failure envelope with a cohesion intercept

d.   Nonconvergence. The Simplified Bishop, Modified Swedish, and Spencer's Methods all require iterative procedures to calculate the factor of safety. In certain cases, the trial and error solution may not converge. In very rare cases, the same data and slip surface can yield two different solutions for the factor of safety, depending on the initial value of factor of safety used in the iterative procedure. These difficulties can be avoided using one or more of the following measures:

(1) Use reasonable slip surface inclinations at the bottom of the slip surface, and use tension cracks at the top to eliminate tensile stresses. In essentially all cases where multiple solutions for the factor of safety are found for a given slip surface and data, one of the solutions is clearly unrealistic because of unusually large or negative stresses near the toe of the slope. Such inappropriate solutions can be easily identified and rejected.

(2) Avoid unrealistic initial estimates for the factor of safety. Iterative schemes implemented in computer programs usually limit the number of iterations and the amount by which the factor of safety can change from one iteration to the next. If the initial estimate of the factor of safety is far from the correct value, the solution may not be reached within the allowable number of iterations. In most cases this is not a problem because factors of safety will range from 0.5 to 3, and an estimate in this range is usually close enough.
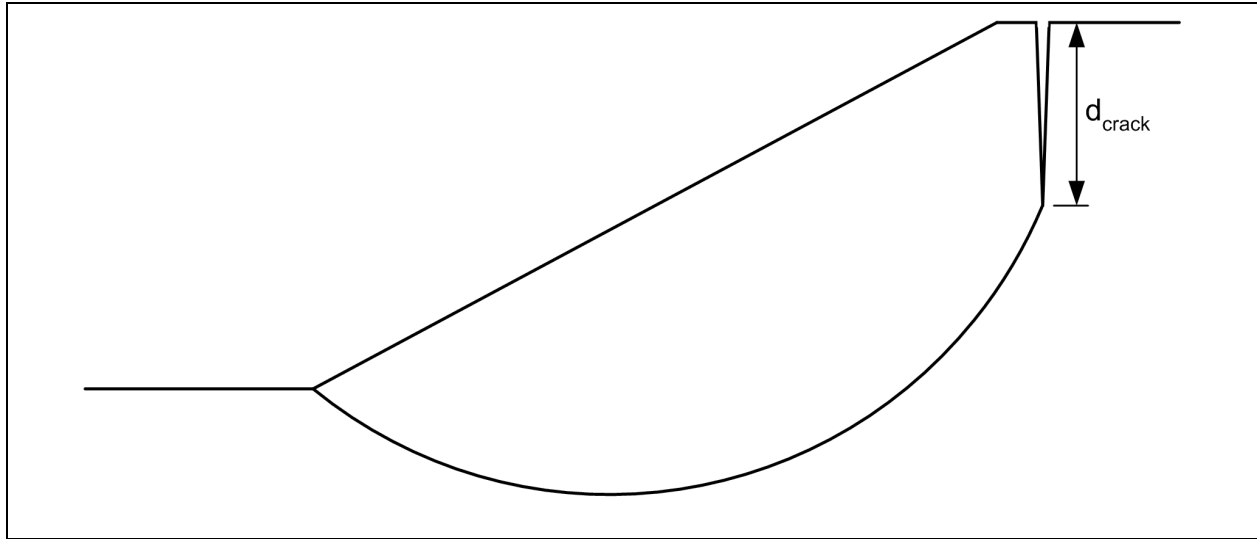
Figure C-22. Vertical crack introduced to eliminate tension near the crest of a slope

(3) It is often better to overestimate the initial value for the factor of safety, rather than underestimate the value. Experience with Spencer's Method in particular has revealed that the solution generally converges best when the initial trial value for the factor of safety is greater, rather than less, than the final value.

(4) Avoid unrealistic problems. For example, it is possible to prescribe either external loads or internal reinforcement forces that are large enough to make the slope stable with no shear strength mobilized. In fact, it is even possible to specify forces that are sufficiently large to cause the soil mass to fail in an upslope direction. In such cases, solutions usually fail to converge. To obtain a solution in these cases of upslope failure, either the factor of safety has to be treated as a negative quantity or the direction assumed for the shear force (S) has to be reversed. Most software cannot automatically recognize this, and the solution will not converge.

(5) Use realistic estimates for the position of the initial trial slip surface in an automatic search. If the initial estimate for the slip surface is not realistic, the computer software may be unable to compute the factor of safety and the automatic search may not be able to continue. Alternatively, the search may continue, but never reach a reasonable slip surface.

e. Other numerical problems. All computer software for slope stability computations requires extensive numerical computations related to the slope and soil profile geometry, and roundoff and truncation errors can occur in these calculations. Computed results should be examined to check for the possibility of such errors. The following measures will reduce problems with roundoff and truncation errors:

(1) Avoid placing the origin of the coordinate system very far from the slope, such that coordinates are very large with relatively little difference between them, e.g., 1000001 vs. 1000002.

(2) Avoid very nearly vertical, but not vertical boundaries between materials, slope faces, etc. Some computer programs do not allow vertical boundaries and/or slopes and require use of slightly inclined boundaries. Problems may occur if a boundary is only very slightly inclined.

(3) If possible, avoid potential slip surfaces that cross material boundaries at extremely flat angles. This may cause numerical problems in calculating intersections. The numerical differences in the slopes of two lines frequently appear in the denominator of an expression, and if the difference in slopes is small, but not

zero, this may cause errors. As a result of roundoff and computer word length, the calculated point of intersection can be a considerable distance from the actual point of intersection.

C-11. Selection of Method

Some methods of slope stability analysis (e.g., Spencer's) are more rigorous and should be favored for detailed evaluation of final designs. Some methods (e.g., Spencer's, Modified Swedish, and the Wedge) can be used to analyze noncircular slip surfaces. Some methods (e.g., the Ordinary Method of Slices, the Simplified Bishop, the Modified Swedish, and the Wedge) can be used without the aid of a computer and are therefore convenient for independently checking results obtained using computer programs. Also, when these latter methods are implemented in software, they execute extremely fast and are useful where very large numbers of trial slip surfaces are to be analyzed. The various methods covered in this appendix are summarized in Table C-7. This table can be helpful in selecting a suitable method for analysis.

Table C-7
Comparison of Features of Limit Equilibrium Methods

Feature	Ordinary Method of Slices	Simplified Bishop	Spencer	Modified Swedish	Wedge	Infinite Slope
Accuracy		X	X			X
Plane slip surfaces parallel to slope face						X
Circular slip surfaces	X	X	X	X		
Wedge failure mechanism			X	X	X	
Non-circular slip surfaces – any shape			X	X		
Suitable for hand calculations	X	X		X	X	X

C-12. Use of the Finite Element Method

a. General. The finite element method (FEM) can be used to compute displacements and stresses caused by applied loads. However, it does not provide a value for the overall factor of safety without additional processing of the computed stresses. The principal uses of the finite element method for design are as follows:

(1) Finite element analyses can provide estimates of displacements and construction pore water pressures. These may be useful for field control of construction, or when there is concern for damage to adjacent structures. If the displacements and pore water pressures measured in the field differ greatly from those computed, the reason for the difference should be investigated.

(2) Finite element analyses provide displacement pattern which may show potential and possibly complex failure mechanisms. The validity of the factor of safety obtained from limit equilibrium analyses depends on locating the most critical potential slip surfaces. In complex conditions, it is often difficult to anticipate failure modes, particularly if reinforcement or structural members such as geotextiles, concrete retaining walls, or sheet piles are included. Once a potential failure mechanism is recognized, the factor of safety against a shear failure developing by that mode can be computed using conventional limit equilibrium procedures.

(3) Finite element analyses provide estimates of mobilized stresses and forces. The finite element method may be particularly useful in judging what strengths should be used when materials have very dissimilar stress-strain and strength properties, i.e., where strain compatibility is an issue. The FEM can help

identify local regions where "overstress" may occur and cause cracking in brittle and strain softening materials. Also, the FEM is helpful in identifying how reinforcement will respond in embankments. Finite element analyses may be useful in areas where new types of reinforcement are being used or reinforcement is being used in ways different from the ways for which experience exists. An important input to the stability analyses for reinforced slopes is the force in the reinforcement. The FEM can provide useful guidance for establishing the force that will be used.

   b.   Use of finite element analyses to compute factors of safety. If desired, factors of safety equivalent to those computed using limit equilibrium analyses can be computed from results of finite element analyses. The procedure for using the FEM to compute factors of safety are as follows:

   (1) Perform an analysis using the FEM to determine the stresses for the slope.

   (2) Select a trial slip surface.

   (3) Subdivide the slip surface into segments.

   (4) Compute the normal stresses and shear stresses along an assumed slip surface. This requires interpolation of values of stress from the values calculated at Gauss points in the finite element mesh to obtain values at selected points on the slip surface. If an effective stress analysis is being performed, subtract pore pressures to determine the effective normal stresses on the slip surface. The pore pressures are determined from the same finite element analysis if a coupled analysis was performed to compute stresses and deformations. The pore pressures are determined from a separate steady seepage analysis if an uncoupled analysis was performed to compute stresses and deformations.

   (5) Use the normal stress and the shear strength parameters, c and ϕ, or c' and ϕ', to compute the available shear strength at points along the shear surface. Use total normal stresses and total stress shear strength parameters for total stress analysis and effective normal stresses and effective stress shear strength parameters for effective stress analyses.

   (6) Compute an overall factor of safety using the following equation:

$$F = \frac{\sum s_i \Delta\ell}{\sum \tau_i \Delta\ell}$$

   (C-37)

where

   s_i = available shear strength computed in step (4)

   τ_i = shear stress computed in step (3)

   $\Delta\ell$ = length of each individual segment into which the slip surface has been subdivided

The summations in Equation C-37 are performed over all the segments into which the slip surface has been subdivided.

   (a) Studies have shown that factors of safety determined using the procedure described are, for practical purposes, equal to factors of safety determined using accurate limit equilibrium methods.

(b) "Local" (point-by-point) factors of safety can also be calculated using the stresses and shear strength properties at selected points in a slope. Some of the local factors of safety will be lower than the overall minimum factor of safety computed from Equation C-37 or limit equilibrium analyses. Local factors of safety of one or less do not necessarily indicate that a slope is unstable. Stresses will be redistributed from points of local failure to other points where the local factor of safety is greater than 1. As long as the overall factor of safety is greater than 1, the slope will be stable.

c. Advantages and disadvantages. Where estimates of movements as well as factor of safety are required to achieve design objectives, the effort required to perform finite element analyses can be justified. However, finite element analyses require considerably more time and effort, beyond that required for limit equilibrium analyses and additional data related to stress-strain behavior of materials. Therefore, the use of finite element analyses is not justified for the sole purpose of calculating factors of safety.

Appendix D
Shear Strength Characterization

D-1. Introduction

Selection of shear strength for use in slope stability computations is covered in this chapter. Shear strengths are usually determined from laboratory tests performed on specimens prepared by compaction in the laboratory or undisturbed samples obtained from exploratory soil borings. The laboratory test data may be supplemented with in situ field tests and correlations between shear strength parameters and other soil properties such as grain size, plasticity, and Standard Penetration Resistance (N) values. This chapter focuses primarily on shear strength selection from laboratory test data.

D-2. Definition of Shear Strength

a. Shear strength for all of the slope stability analyses described in this manual is represented by a Mohr-Coulomb failure envelope that relates shear strength to either total or effective normal stress on the failure plane (Figure D-1). In the case of total stresses, the shear strength is expressed as:

$$s = c + \sigma \ \tan \ \phi \tag{D-1}$$

where

   c and ϕ = cohesion intercept and friction angle for the failure envelope

   σ = total normal stress on the failure plane

For effective stresses the shear strength is expresses as:

$$s = c' + (\sigma - u) \ \tan \ \phi' \tag{D-2}$$

where

   c' and ϕ' = intercept and slope angle for the failure envelope plotted in terms of effective stresses

   σ and u = total normal stress and pore water pressure, respectively, on the failure plane

The shear strength parameters, c and ϕ or c' and ϕ', are determined from laboratory shear test data. The stresses from each test representing failure are plotted and a suitable failure envelope is drawn. The specific way in which the data are plotted, selection of the point representing failure (failure criteria), and whether effective or total stresses are used to plot the data depend on the type of test, loading conditions, and several other factors which are covered in the following sections of this appendix.

b. Theoretically the failure envelope is tangent to all of the Mohr's circles representing the stresses at failure (Figure D-2a). However, in actual practice there will be variations among samples tested, such that the failure envelope represents a "best-fit" to the data from several tests (Figure D-2b). Also, when the failure envelope is derived from direct shear tests, the complete state of stress is not known -- only the stresses on the horizontal plane are known. The horizontal plane is assumed to be the failure plane, and the failure envelope is drawn through the series of points representing the values of τ and σ on the horizontal plane from each test.

a. Total stresses

b. Effective stresses
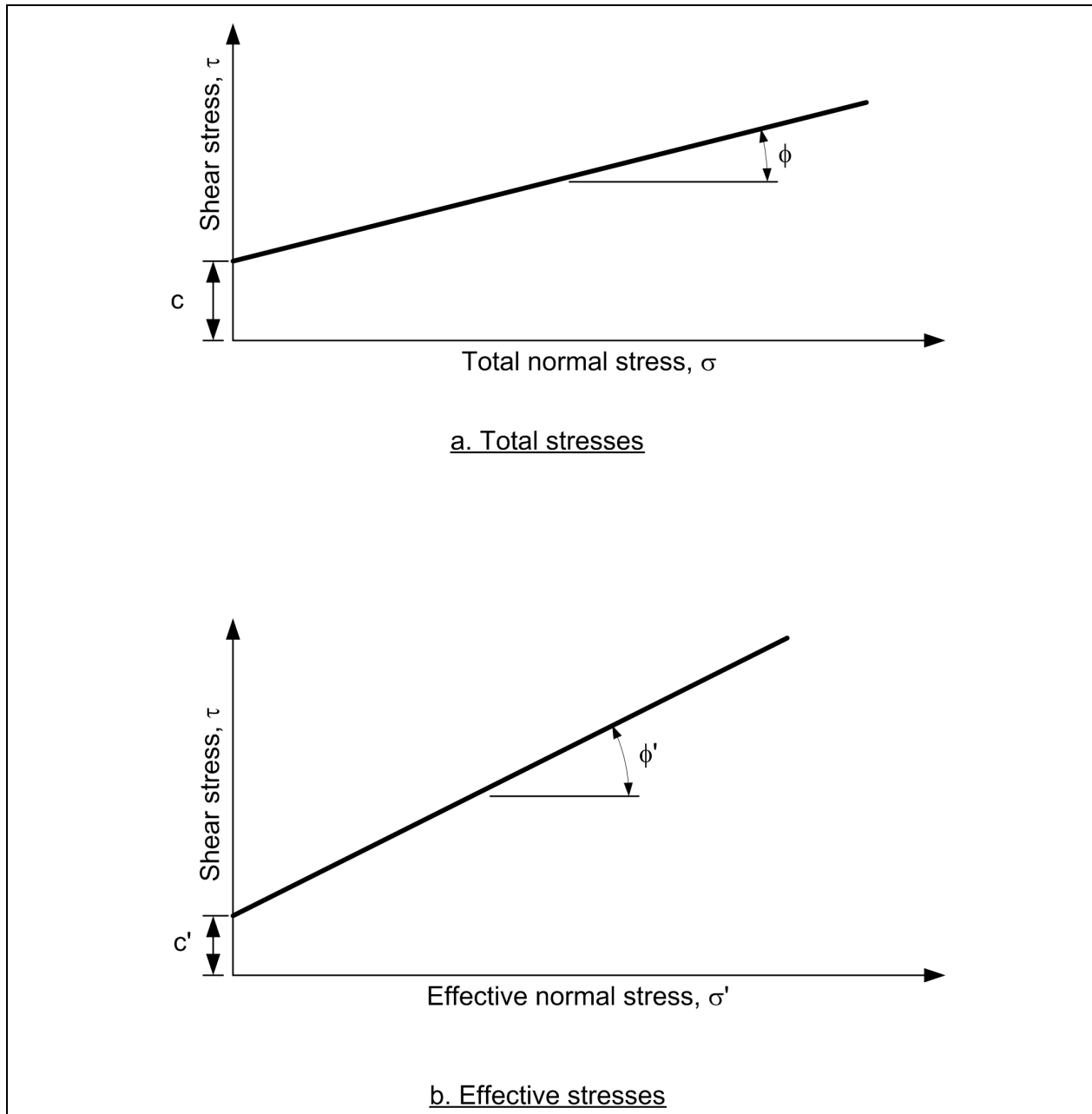
Figure D-1. Failure envelopes for total and effective stresses

 c. Sometimes failure envelopes are curved, as shown in Figure D-3. Examples include the failure envelope obtained from Unconsolidated-Undrained tests on compacted soils and the residual shear strength envelope determined from consolidated-drained shear tests. In these cases the appropriate curved envelope, as illustrated in Figure D-3, is determined and used in the stability analyses, rather than values of cohesion and friction angle.

a. Theoretical

b. Actual for most soils
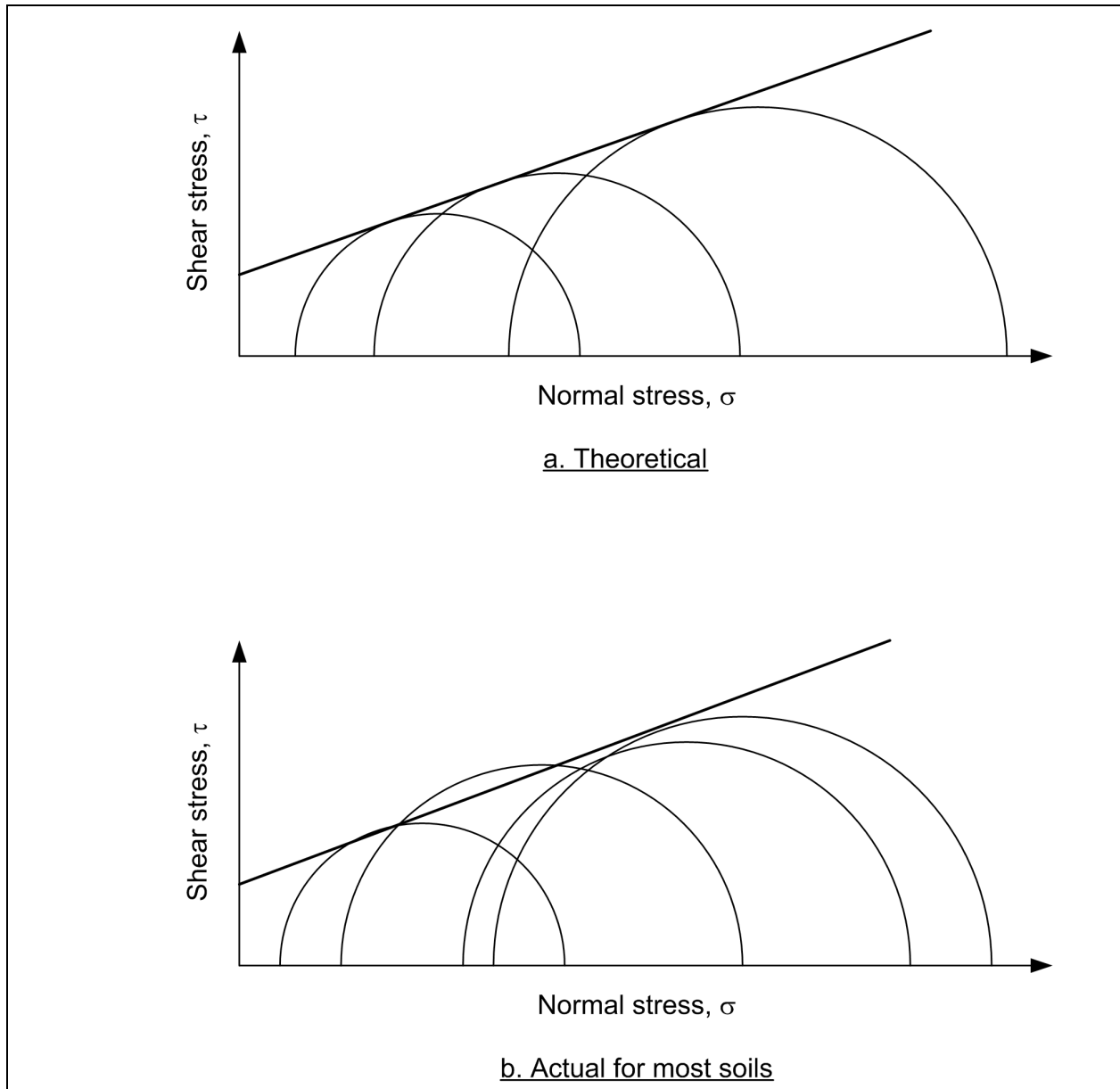
Figure D-2.   Mohr's circles and failure envelopes

D-3. Types of Laboratory Strength Test Procedures

a.   Most laboratory tests are performed using either triaxial compression or direct shear test equipment. A two-stage loading procedure is used in each of these tests. In the first stage, a confining stress is applied. In the triaxial test, the confining stress is applied by increasing the cell, or all-round pressure on the sample. In the direct shear test, the confining pressure is applied by applying a vertical load to the horizontal plane, which becomes the eventual failure plane. The normal stress on the vertical plane in the direct shear device increases when the stress is applied to the horizontal plane, but the stress on the vertical plan is not known.

(1) The second stage of a strength test involves shearing the specimen. In the triaxial test, the axial load is gradually increased (load control), or the specimen is deformed slowly in the axial direction and the axial load is measured (deformation control), to shear the specimen. In the direct shear test, the horizontal shear

a. Total stresses

b. Effective stresses
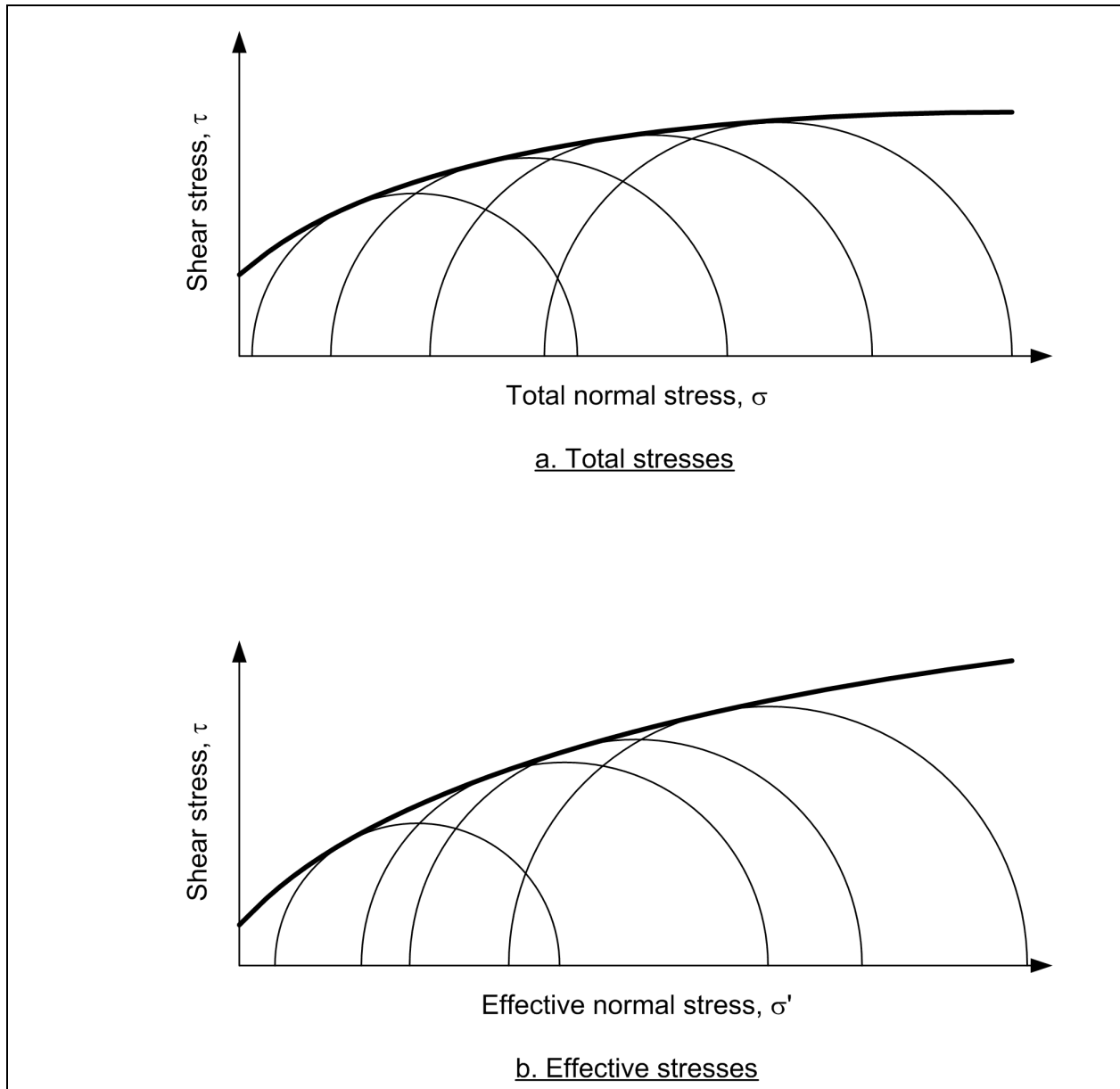
Figure D-3. Curved strength envelopes

load is gradually increased (load control) or the specimen is deformed horizontally by displacing the upper half of the shear box horizontally relative to the lower half and measuring the resulting load (deformation control).

     (2) In the triaxial test, drainage of water into or out of the specimen can be controlled during application of both the confining stress and the shear stress. Depending on the drainage allowed in these phases of the test, three different types of test are possible -- Unconsolidated-Undrained (UU or Q), Consolidated-Undrained (CU or R), and Consolidated-Drained (CD or S). The three loading procedures are illustrated in Figure D-4. The loading procedures are intended in part to simulate conditions of loading and drainage in the field. The loading condition used in the laboratory test depends on the stability condition that strengths are being measured for, e.g., end-of-construction, steady-state seepage, or rapid drawdown.

Stage 1: confinement — **Stage 2: shear**

UU - Q test

$\sigma_{1c} = \sigma_{3c}$

$\sigma_{3c} \, ; \, \sigma'_{3c} = ?$

$u_c = ?$

$\sigma_{1f} = \sigma_{3f} + \Delta\sigma_d$

$u_f = u_c + \Delta u = ?$

$\sigma_{3f} = \sigma_{3c}$

CU - R test

$\sigma_{1c} = \sigma_{3c} \, ; \, \sigma'_{1c} = \sigma'_{3c}$

$\sigma_{3c} \, ; \, \sigma'_{3c} = \sigma_{3c} - u_{bp}$

$u_c = u_{bp}$

$\sigma_{1f} = \sigma_{3f} + \Delta\sigma_d$

$u_f = u_c + \Delta u$

$\sigma_{3f} = \sigma_{3c}$

CD - S test

$\sigma_{1c} = \sigma_{3c} \, ; \, \sigma'_{1c} = \sigma'_{3c}$

$\sigma_{3c} \, ; \, \sigma'_{3c} = \sigma_{3c} - u_{bp}$

$u_c = u_{bp}$

$\sigma_{1f} = \sigma_{3f} + \Delta\sigma_d$

$u = u_c$

$\sigma_{3f} = \sigma_{3c} \, ; \, \sigma'_{3f} = \sigma'_{3c}$
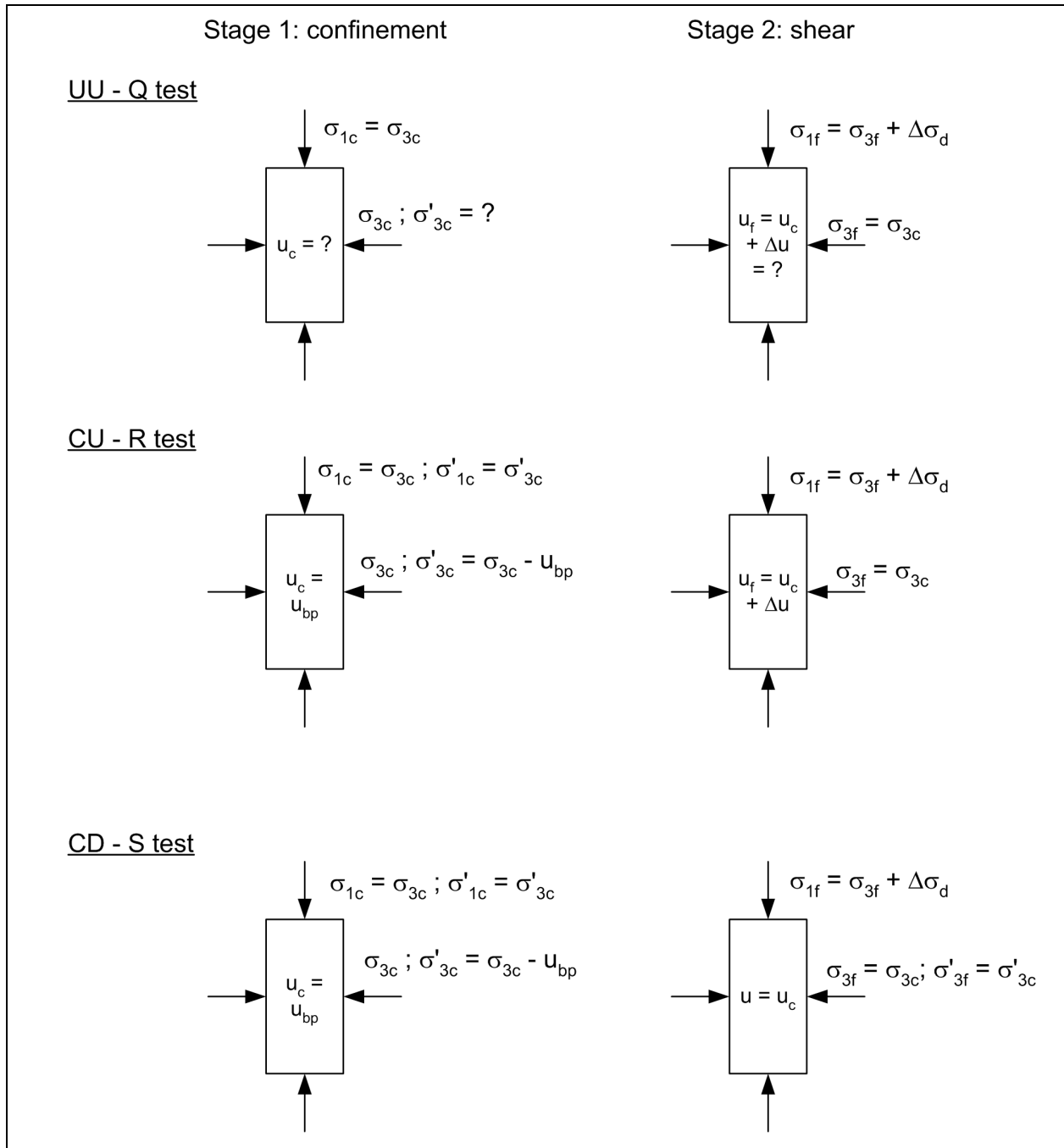
Figure D-4. Three types of triaxial shear tests

(3) In the direct shear test, drainage cannot be prevented. Thus, only the consolidated-drained (CD or S) loading procedure can be used. All three loading procedures (UU or Q, CU or R, and CD or S) are discussed in the following text.

b.   Unconsolidated-Undrained (UU or Q) test procedure. No drainage is allowed in a UU test during the application of either the confining pressure or shear stress. The confining pressure is applied and the specimen is sheared shortly afterward. Rates of loading are relatively fast, and need only be slow enough to

avoid inertial effects and allow adequate time for recording data. Typical rates of loading for shear produce failure of the specimen in 10 to 20 minutes.

(1) The Unconsolidated-Undrained test procedure is used to measure the shear strength where there will be no drainage (no change in water content) when the soil is loaded. The objective of this test procedure is to measure the shear strength of the soil at the same water content that the soil will have in the field. It is important that the specimens being tested have the proper water content, which represents the field condition. Specimens of natural soils must be at the field water content and not allowed to dry out or absorb water between the time they are sampled and the time they are tested. Compacted specimens should be prepared at moisture content representing expected field conditions. The shear strength of compacted clays decrease with decreasing dry density and increasing water content. Test specimens should be compacted to the lowest dry density and highest water content that will be permitted under the specification, to ensure that the strength in the field will not be lower than that measured in the laboratory tests.

(2) Results from tests performed using Unconsolidated-Undrained loading procedures are always plotted using total stresses. Thus, the shear strength is expressed in terms of total stress, using c and ϕ. Pore water pressures are not measured and are unknown.

c. Consolidated-Undrained (CU or R) test procedure. The Consolidated-Undrained test is used for several purposes and, depending on the purpose, pore water pressure may or may not be measured during shear. Each stage of the loading procedure is described further below, followed by discussion of how the test data are used.

(1) Consolidation stage. The first stage of Consolidated-Undrained loading is the consolidation stage, where the confining pressure is applied and the specimen is given time to consolidate fully. During this stage, the specimen is also saturated using back-pressure saturation techniques. Back-pressure saturation is done by increasing both the total confining stress and pore water pressure in equal increments until the specimen is saturated. Each increment of confining pressure is normally allowed to remain for some time to permit water to flow into the specimen and air to dissolve into the pore water. Increments should be small enough, and equilibration times long enough to avoid the specimen's being subjected to undesirably high effective stresses during back-pressure saturation. Until the specimen is saturated, increasing the confining pressure causes the effective stress to increase during the time required for the internal pore water pressures to equilibrate with the back pressure. It is desirable to back-pressure saturate specimens before consolidation to the final test confining pressures. In that way, reliable volume changes can be measured during consolidation by measuring the amount of water that flows into or out of the specimen as they consolidate. The volume changes should be recorded at suitable time intervals and plotted versus time to determine when consolidation is completed. The volume change-time data are also used to estimate the required times for shearing the specimen, as described in Section D-3.c(2) below.

(2) Shear stage. Once consolidation is complete, the drainage valve is closed to prevent further drainage as the axial load is increased to shear the specimen. In most Consolidated-Undrained shear tests, the pore water pressures developed during this stage of the test are measured. Pore water pressures are usually measured by measuring the water pressure in porous stones or disks at one or both ends of the specimen. Because of the end restraint at the two ends of the specimen, the strains in the specimen will not be uniform and, thus, the induced pore water pressures will not be entirely uniform over the height of the specimen. In order to measure representative values of the pore water pressures, the specimen should be sheared slowly enough for pore water pressures to equalize over the height of the specimen. To measure representative values of the pore water pressures, the specimen should be sheared slowly enough for pore water pressures to equalize over the height of the specimen. Suitable loading rates can be calculated from the time-volume change data recorded during the consolidation phase of the test. Axial load, axial deformation, and pore water pressure readings should be taken during shear. Specimens may be sheared using load control or deformation

control to increase the axial load on the specimens. Either method is adequate for measuring the peak load that the specimen can withstand. However, to measure the soil resistance beyond the point where the peak load is reached, it is necessary to control the deformation rate and measure the load. This is especially important for normally and slightly overconsolidated clays and some loose sands, where the peak effective stress shear strength parameters (c' and ϕ') may be developed at strains larger than the strains at which the peak load in undrained shear is reached.

(3) Use of data. Shear strength data from Consolidated-Undrained tests are used in four different ways for slope stability computations:

- To determine the effective stress shear strength parameters for long-term, steady-state seepage analyses.

- To determine the relationship between undrained shear strength and effective consolidation pressure (τ_{ff} vs. σ'_{fc}) for analyses of rapid drawdown.

- To estimate undrained-shear strengths and reduce effects of sample disturbance for end-of-construction stability analyses.

- To estimate undrained shear strength for analyses of staged construction of embankments.

These uses are each discussed separately below.

(a) By plotting the effective stresses at failure from Consolidated-Undrained tests, the Mohr-Coulomb failure envelope for effective stresses (c' and ϕ') can be determined. The failure envelope for effective stresses from Consolidated-Undrained tests is, for practical purposes, the same as the failure envelope from consolidated-drained (CD or S) tests. The failure envelope from either test can be used in slope stability computations for the long-term, steady-state seepage condition. Consolidated-Undrained (CU or R) tests are usually preferred over consolidated-drained (CD or S) tests for determining the effective stress failure envelope for clays, because Consolidated-Undrained tests can be performed more quickly. The time required for nonuniform pore water pressures to equalize in the specimen in a Consolidated-Undrained test is less than the time required for a specimen to fully drain during shear in a consolidated-drained test.

(b) Results of Consolidated-Undrained shear tests are also used to relate undrained shear strength to effective consolidation pressure for use in stability analyses for rapid drawdown. Further discussion of the plotting and use of the data for rapid drawdown analyses is presented in Appendix G.

(c) Data from Consolidated-Undrained shear tests can be used to estimate the undrained shear strength of <u>saturated</u> soils for use in analyses for end-of-construction stability. By reconsolidating specimens in the laboratory, it is possible to reduce some of the effects of sample disturbance. However, care must be used to avoid increasing the strength, and overestimating the undrained shear strength. When Consolidated-Undrained shear test procedures are used to estimate undrained shear strength the undrained shear strength is expressed as $S_u = (\sigma_1 - \sigma_3)/2$ and is related to the effective consolidation pressure. Two approaches may be used to do this. One approach is the SHANSEP approach suggested by Ladd and Foott (1974);[1] the other is the "recompression" technique suggested by Bjerrum (1973). These are explained more fully below. The SHANSEP procedure suggested by Ladd and Foott (1974) involves the following steps:

---

[1] Reference information is presented in Appendix A.

- Step 1: The variations of the present effective vertical stress and the maximum past pressure with depth are established. The present vertical effective stress is the current effective overburden pressure, calculated using unit weight and the groundwater level. The maximum past pressure is determined from consolidation tests on high-quality, undisturbed test specimens.

- Step 2: Consolidated-Undrained tests are performed using consolidation pressures that are higher than the maximum past pressure. If the clay is overconsolidated, the test specimens are allowed to swell after consolidation to achieve a suitable range of overconsolidation ratios, encompassing the range of values in the field. The test results are used to establish a relationship between the normalized shear strength $[S_u/\sigma'_{vc} = \frac{1}{2} (\sigma_1 - \sigma_3)/\sigma'_{vc}]$ and overconsolidation ratio.

- Step 3: Undrained shear strengths applicable to the field are estimated by multiplying the normalized strength, S_u/σ'_{vc}, determined in Step 2, by the effective vertical stress, σ'_{vc}, determined in Step 1.

Once undrained shear strengths are determined in the manner described, they are represented in the slope stability computations as cohesion values, c, with $\phi = 0$.

- The SHANSEP procedure removes some of the effects of sample disturbance but also alters the structure of the soil. Alteration of the structure can lead to values of shear strength that are not representative of those in the field. This approach is not recommended for heavily overconsolidated soils, or for soils that have distinct structure or cementation bonds.

- The "recompression" technique proposed by Bjerrum (1973) involves reconsolidating specimens to the same effective stress that the specimens currently experience in the field. Although this approach results in specimens that have somewhat lower water contents than in the field (and therefore higher shear strengths), it produces less change in the soil structure than the SHANSEP approach. The recompression technique is recommended over the SHANSEP approach for heavily overconsolidated soils, but the approach may overestimate the shear strength even for these soils and should be used cautiously.

- Further details of the SHANSEP and "recompression" procedures can be found in the cited references. The shear strength obtained from Consolidated-Undrained tests using either the SHANSEP or recompression technique is assigned as a cohesion value with ϕ = zero (these techniques apply only to saturated soils). The advantage of using Consolidated-Undrained tests, rather than Unconsolidated-Undrained tests to estimate the undrained shear strength is that some of the effects of sample disturbance can be reduced. However, care must be exercised to ensure that strengths are not overestimated. In addition, the offsetting effects of such factors as anisotropy and creep may need to be accounted for if the effects of sample disturbance are eliminated.

(d) The fourth use of Consolidated-Undrained shear tests is to measure shear strengths for use in analyses of staged construction of embankments. This is discussed in Section D-10.

d. Consolidated-Drained (CD or S). Complete drainage is allowed during the application of both the confining pressure and shear for consolidated-drained loading. Either the triaxial or direct shear apparatus may be used for testing. The two stages of loading (consolidation and shear) are described separately below, followed by a discussion of how the test data are used.

(1) Consolidation stage. The consolidation stage for consolidated-drained (CD or S) loading procedures is the same as the consolidation stage for Consolidation-Undrained (CU or R) test procedure. Back-pressure saturation is used to ensure complete saturation and to allow accurate measurements of volume change during

both consolidation and shear, by measuring the amount of water that flows into or out of the specimen. Volume change-time data from the consolidation phase of the test are used to estimate rates of loading and times to failure for the shear phase. Saturation is also important to eliminate effects of capillary stresses that would influence the strength measurements and their interpretation if the soil is partly saturated. The results of Consolidated-Drained shear tests are plotted using effective stresses that are equal to the total stresses minus the measured pore water pressures. One of the advantages of triaxial tests over direct shear test is that the specimen can be back-pressure saturated. Direct shear devices should only be used for testing soils which are either already saturated or will become saturated once placed in the direct shear apparatus and submerged.

(2) Shear stage. Specimens are sheared by slowly increasing either the axial load, in the case of triaxial tests, or the horizontal shear load, in the case of direct shear tests. It is very important to shear the specimen slowly enough that the soil can completely drain and no excess pore water pressures are developed. For some heavily overconsolidated clays and clay shales, the loading rates may need to be so slow that failure is reached only after several days or even weeks of shear. Suitable rates of loading to achieve complete drainage can be estimated from the volume change-time data recorded during the consolidation phase of the test. During triaxial shear the axial load, axial deformation, and volume changes of the specimen are recorded at various time intervals. The axial load-deformation data are used to determine the point where the specimen has failed, while the volume change information is used to make corrections for the change in cross-sectional area of the specimen that occurs during shear.

(3) Usage. Consolidated-Drained loading procedures are used to determine the effective stress shear strength parameters of freely draining soils. These soils will drain with relatively short testing times and the consolidated-drained loading procedure comes closest to representing the loading for long-term, drained conditions in the field. Consolidated-Drained tests procedures are also used to measure the residual shear strength of clays using direct shear or torsional shear equipment. The direct shear and torsional shear equipment allow for large strains, like those needed to measure residual shear strengths. When residual shear strengths are not needed and the soils are fine-grained, triaxial tests using Consolidated-Undrained (CU or R) procedures with pore water pressure measurements are preferred over Consolidated-Drained procedures because of the shorter testing times required for CU tests.

D-4. "Modified" Mohr-Coulomb Diagrams

Because the complete state of stress is known in the triaxial test, Mohr's circles of stress can be plotted on a Mohr diagram. However, it can be difficult to judge what is a "best-fit" line tangent to a number of circles. A more convenient techniques is to plot the data on a "modified" Mohr-Coulomb diagram where, rather than plotting circles, a point is plotted to represent the stresses at failure in each test. The diagrams used for this purpose are called "modified" Mohr-Coulomb diagrams. Several different forms of modified Mohr-Coulomb diagrams can be used. All modified Mohr-Coulomb diagrams are based on the fundamental relationship between the principal stresses and the Mohr-Coulomb shear strength parameters, c' and ϕ' or c and ϕ. Referring to Figure D-5 and the triangle formed by points, *def*, the following expression can be written:

$$\sin \ \phi = \frac{\dfrac{(\sigma_1 - \sigma_3)}{2}}{\dfrac{c}{\tan \ \phi} + \dfrac{(\sigma_1 + \sigma_3)}{2}} \tag{D-3}$$

Equation D-3 can be rearranged to obtain a number of different relationships between the principal stresses and the shear strength parameters, c and ϕ. Two of the most useful forms of Equation D-3 and the resulting modified Mohr-Coulomb diagrams are described in the following text.
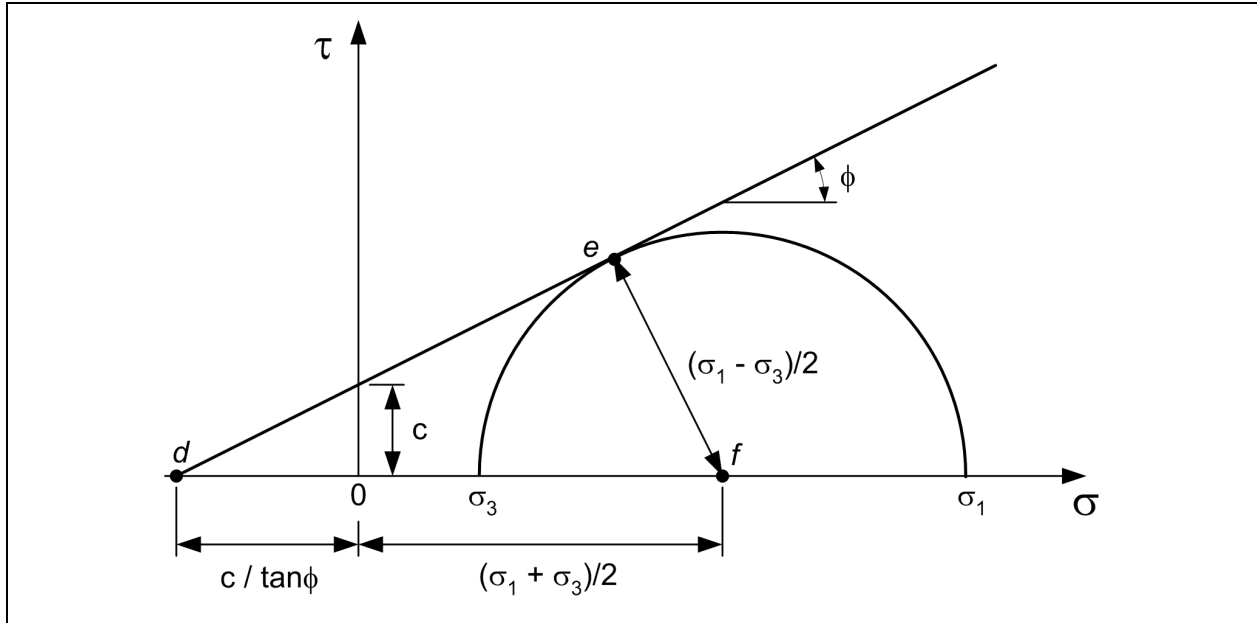
Figure D-5. Mohr's circle of stress used to derive equations for Modified Mohr-Coulomb diagram

a. "p-q" diagrams. One of the most commonly used modified Mohr-Coulomb diagrams is a "p-q" diagram. For this diagram, $q = (\sigma_1-\sigma_3)/2$ is plotted vs. $p = (\sigma_1+\sigma_3)/2$, as shown in Figure D-6a. The basis for such a plot can be seen by rewriting Equation D-3 in the form:

$$q = c \, \cos \, \phi + p \sin \phi \tag{D-4}$$

which can also be written as:

$$q = d + p \tan \psi \tag{D-5}$$

Equation D-5 expresses a linear relationship between the quantities q and p. The parameter d is the intercept and $\tan \Psi$ is the slope of the line on the modified Mohr-Coulomb diagram shown in Figure D-6a. The slope, $\tan \Psi$, is related to the friction angle, ϕ, by the expression:

$$\tan \, \psi = \sin \, \phi \tag{D-6}$$

or

$$\phi = \arcsin \, (\tan \, \psi) \tag{D-7}$$

Similarly, the cohesion on a Mohr-Coulomb diagram is related to the friction angle (ϕ) and the intercept (d) on a modified Mohr-Coulomb diagram by:

$$c = \frac{d}{\cos \, \phi} \tag{D-8}$$

$$q = \frac{\sigma_1 - \sigma_3}{2}$$

$$\phi = \arcsin(\tan\psi)$$

$$c = \frac{d}{\cos\phi}$$

$$p = \frac{\sigma_1 + \sigma_3}{2}$$

a. p-q diagram

$$\sigma_1 - \sigma_3$$

$$\phi = \arcsin\left(\frac{\tan\psi'}{2+\tan\psi'}\right)$$

$$c = \frac{d'(1-\sin\phi)}{2\cos\phi}$$

$$\sigma_3$$

b. Alternate modified Mohr-Coulomb diagram
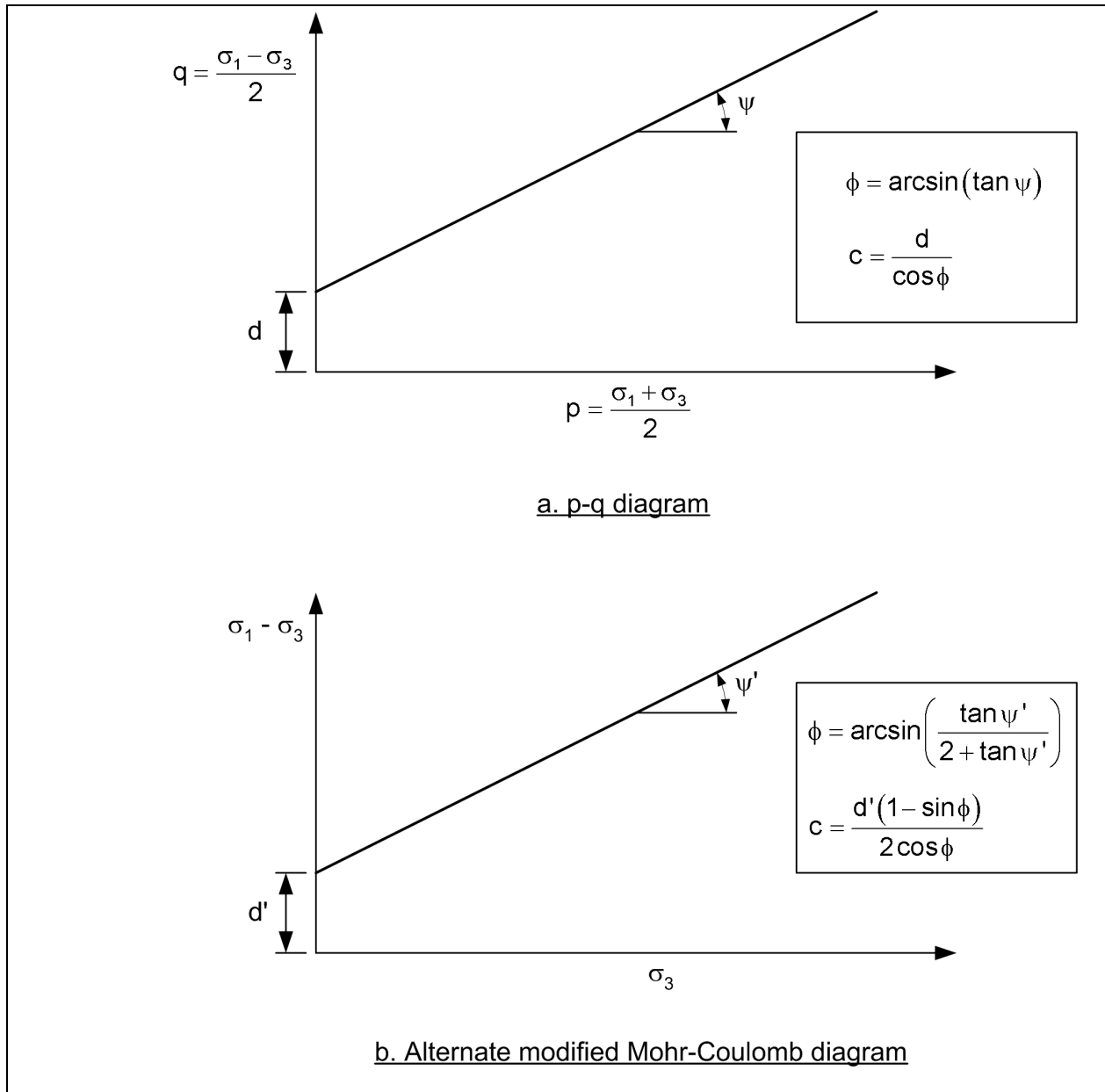
Figure D-6.   Modified Mohr-Coulomb diagrams

A p-q diagram can be used to plot the results of triaxial shear tests and determine the Mohr-Coulomb shear strength parameters. To do so, the values of $q = (\sigma_1 - \sigma_3)$ and $p = (\sigma_1 + \sigma_3)$ at failure are determined for each test and plotted on the diagram. A straight line is then drawn to fit the data and the slope ($\tan\Psi$) and intercept (d) are determined. Once the intercept and slope are found, Equations D-7 and D-8 are used to calculate the friction angle, ϕ, and cohesion, c. Care must be exercised in presenting "p-q" diagrams and reviewing such diagrams prepared by others, because an entirely different set of axes and quantities from the ones described above are sometimes used and referred to as "p-q" diagrams. The alternative nomenclature defines p and q for triaxial compression tests as follows:

$$p = \frac{1}{3}(\sigma_1 + 2\sigma_3) \tag{D-9}$$

and

$$q = (\sigma_1 - \sigma_3) \tag{D-10}$$

This notation was suggested by Roscoe, Schofield, and Wroth (1958) and has appeared in a number of texts and reference books, e.g., Head (1986), Budhu (2000). To avoid confusion, any "p-q" diagram should always have the axes labeled so that they show the relationship to the principal stresses, $q = (\sigma_1 - \sigma_3)/2$ and $p = (\sigma_1 + \sigma_3)/2$, instead of simply using the notation "p" and "q", which is subject to ambiguity.

   b.   Alternate modified Mohr-Coulomb diagram.   Another form of modified Mohr-Coulomb diagram that is useful is one in which the principal stress difference $(\sigma_1 - \sigma_3)$ is plotted vs. the confining pressure, σ_3, as shown in Figure D-6b. The basis for such a plot can be seen by rewriting Equation D-3 as:

$$(\sigma_1 - \sigma_3) = \frac{2c \, \cos \, \phi}{1 - \sin \, \phi} + \frac{2 \, \sin \, \phi}{1 - \sin \, \phi} \sigma_3 \tag{D-11}$$

This requires somewhat more algebraic manipulation than is required to write Equation D-4, but Equation D-11 can be shown to be a valid form of Equation D-3. Equation D-11 can be written as:

$$(\sigma_1 - \sigma_3) = d' + \sigma_3 \, \tan \, \psi' \tag{D-12}$$

where

$$d' = \frac{2c \, \cos \, \phi}{1 - \sin \, \phi} \tag{D-13}$$

and

$$\tan \, \psi' = \frac{2 \, \sin \, \phi}{1 - \sin \, \phi} \tag{D-14}$$

From Equation D-14, the following equation can be written:

$$\phi = \arcsin \left(\frac{\tan \, \psi'}{2 + \tan \, \psi'} \right) \tag{D-15}$$

and from Equation D-13, the following equation can be written.

$$c = \frac{d' \, (1 - \sin \, \phi)}{2 \, \cos \, \phi} \tag{D-16}$$

By plotting the results of triaxial tests in the form of $(\sigma_1 - \sigma_3)$ vs. σ_3 and fitting a straight line through the data points, the cohesion and friction angle can be determined from the slope and intercept of the line using Equations D-15 and D-16. A modified Mohr-Coulomb diagram like the one shown in Figure D-6b is particularly useful and instructive for plotting stress paths from triaxial tests (Section D-5). The horizontal axis represents the confining pressure in the test, σ_3, while the vertical axis is directly related to the applied

axial load used to shear the specimen, $(\sigma_1 - \sigma_3)$. Thus, the two axes correspond to the two independently controlled and measured stresses in the triaxial test.

D-5. Stress Paths

a.   Stress paths are plots representing the successive states of stress in a laboratory test. Although stress paths may be drawn to represent the stresses during both consolidation and shear, stress paths are most useful for the shearing stage of the test. Although a number of different diagrams can be used to plot stress paths; the two types of Modified Mohr-Coulomb diagrams described in Section D-4 are probably the most widely used and useful. While stress paths can be plotted for all three types of loading (UU, CU, and CD), only stress paths from Consolidated-Undrained (CU or R) shear tests are useful, and only they are covered in this section.

b.   Stress paths for Consolidated-Undrained shear tests can be plotted for either total or effective stresses. The stress paths for total stresses are shown in Figure D-7 on both p-q diagrams and the alternate $(\sigma_1 - \sigma_3)$ vs. σ'_3 diagram described earlier. On the p-q diagram, the total stress path is along a 45-degree line extending from the horizontal axis to the failure envelope. If the stresses decrease once failure is reached, the stress path will move back along the initial loading path. On the alternate modified Mohr-Coulomb diagram shown in Figure D-7, the total stress path rises vertically to the failure envelope because the total confining pressure does not change. If the strength drops off once failure is reached, the stress path will drop back vertically along the initial loading path.

c.   Effective stress paths during shear for Consolidated-Undrained loading are shown on a p-q diagram in Figure D-8 for a soil which tends to compress when sheared to failure (Figure D-8a) and for a soil which tends to dilate when sheared to failure (Figure D-8b). A broken 45-degree line extending from the initial stress point toward and across the failure envelope is also shown in each figure. The effective stress paths lie to the left of the 45-degree line when the pore water pressures increase during shear and to the right of the line when pore water pressures decrease during shear, i.e., when the soil tends to dilate. The horizontal distance between the 45-degree line and the stress path represents the change in pore water pressure Δu during shear.

d.   Effective stress paths plotted on an alternate, $(\sigma_1 - \sigma_3)$ vs. σ'_3, diagram are shown in Figure D-9. Stress paths are shown for a soil that compresses during shear and for a soil that dilates during shear. Broken lines are drawn on each diagram extending vertically from the initial stress point upward and across the failure envelope. Stress paths which lie to the left of these vertical lines represent stresses where the pore water pressure has increased during shear, while those to the right of the line represent decreases in pore water pressure. The horizontal distance between the vertical line and points on the stress paths represents the change in pore water pressure Δu during shear.

D-6. Failure Criteria

Mohr-Coulomb failure envelopes are determined by plotting stresses at failure and drawing a suitable line or curve either tangent to a series of circles or through a series of points. To define the stresses at failure, a suitable criterion that defines what is meant by "failure" must be established. The criterion chosen depends on the type of test, the type of soil, and the use that will be made of the failure envelope. Failure criteria are discussed for each type of test and loading condition in the sections below.

a. Unconsolidated-Undrained (UU or Q) test. For Unconsolidated-Undrained shear tests, failure is usually taken as the point of maximum axial stress, $(\sigma_1 - \sigma_3)_{max}$. However, if large strains are required to reach a peak axial stress, or if the test data show no peak, it is appropriate to use some value of strain as the failure criterion. The ASTM Standard for Unconsolidated-Undrained shear tests suggests that the stress at

$$q = \frac{\sigma_1 - \sigma_3}{2}$$

45°

$$p = \frac{\sigma_1 + \sigma_3}{2}$$

a. p-q Diagram

$\sigma_1 - \sigma_3$

σ'_3

b. Alternate modified Mohr-Coulomb diagram
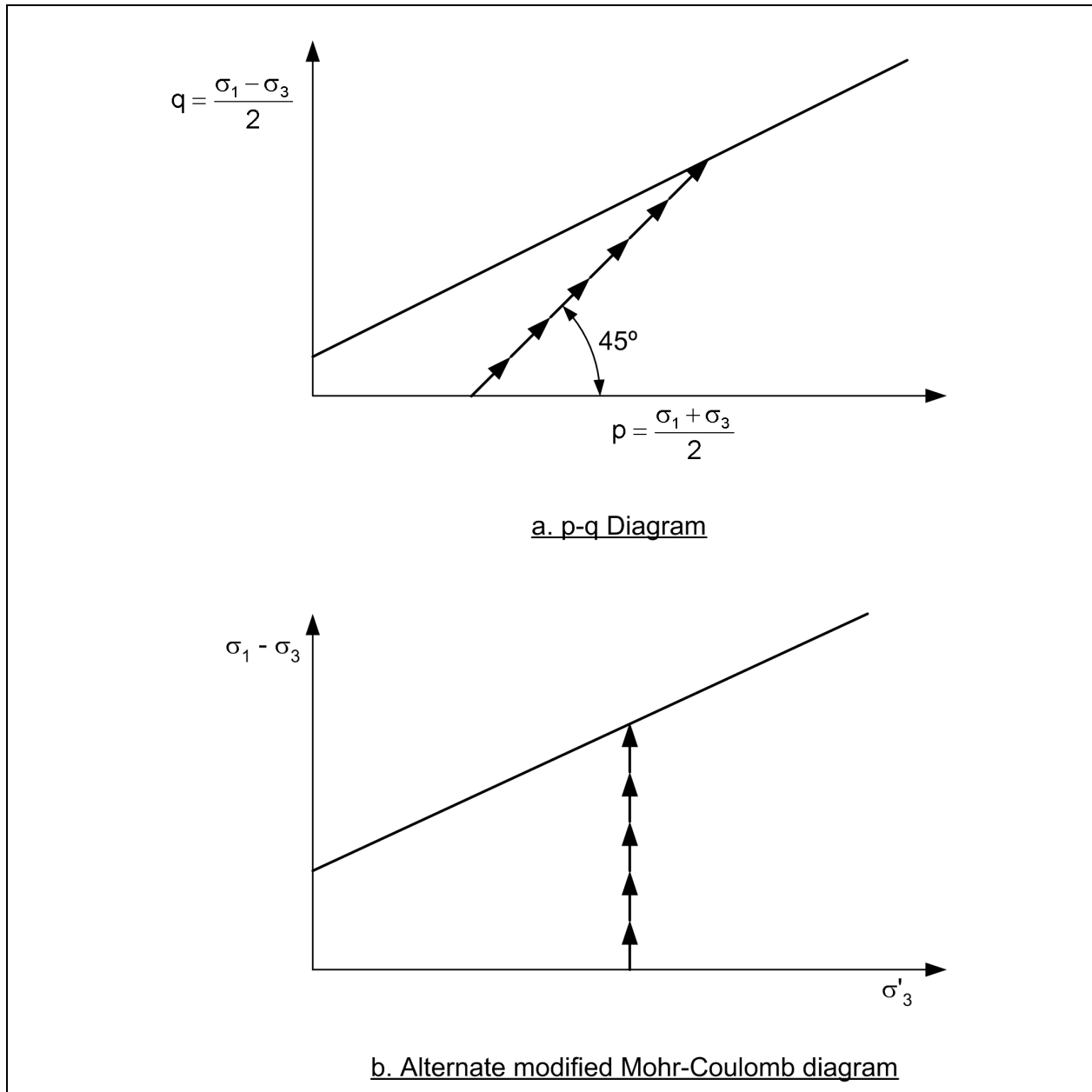
Figure D-7.   Total stress paths for shear plotted on modified Mohr-Coulomb diagrams

15 percent axial strain should be taken as the stress at failure if no peak is reached prior to that point (ASTM 1999). This recommendation is reasonable and should be followed unless the use of stresses at larger strains can be justified. Stresses less than the peak stress may also be used as the failure stresses when strain compatibility is of concern (Section D-9). Ordinarily it will not be possible to draw the failure envelope so that it is precisely tangent to the Mohr's circles on a conventional Mohr diagram or precisely through the points that are plotted on a modified diagram. Consequently, the envelope should be drawn to fit the data in a manner that seems reasonable. Prior Corps of Engineers' practice has been to draw the strength envelope in a position such that data from two-thirds of the tests lie above the failure envelope. This recommendation is reasonable.
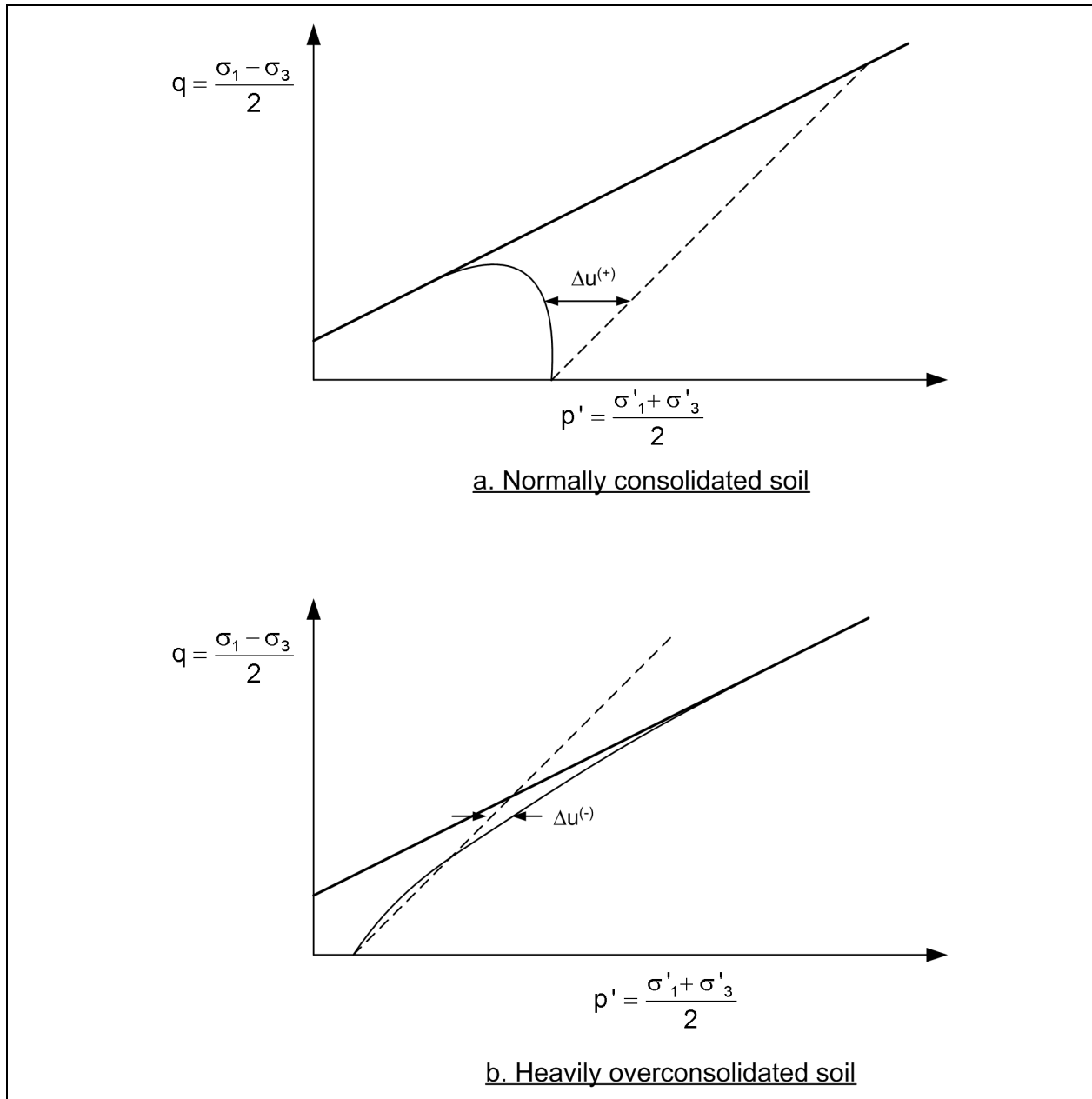
Figure D-8. Effective stress paths for shear plotted on p-q diagrams

   b.   Consolidated-Undrained (CU or R) test. How failure is defined for CU tests depends on the use that will be made of the results. Different criteria are appropriate depending on whether effective stress shear strength parameters or undrained shear strengths are being determined.

   (1) Effective stress shear strength parameters. The appropriate failure stresses for determining effective stress shear strength parameters, c' and ϕ', are best determined by plotting the effective stress paths for the shear phase of the tests. A typical series of effective stress paths is shown on a modified Mohr-Coulomb diagram in Figure D-10. The failure envelope should be drawn such that it is approximately tangent to the stress paths, as shown in this figure. This criterion is referred to as "stress path tangency." Although variations in soil and among the samples tested will probably make it impossible to draw a failure envelop

a. Normally consolidated soil

b. Heavily overconsolidated soil
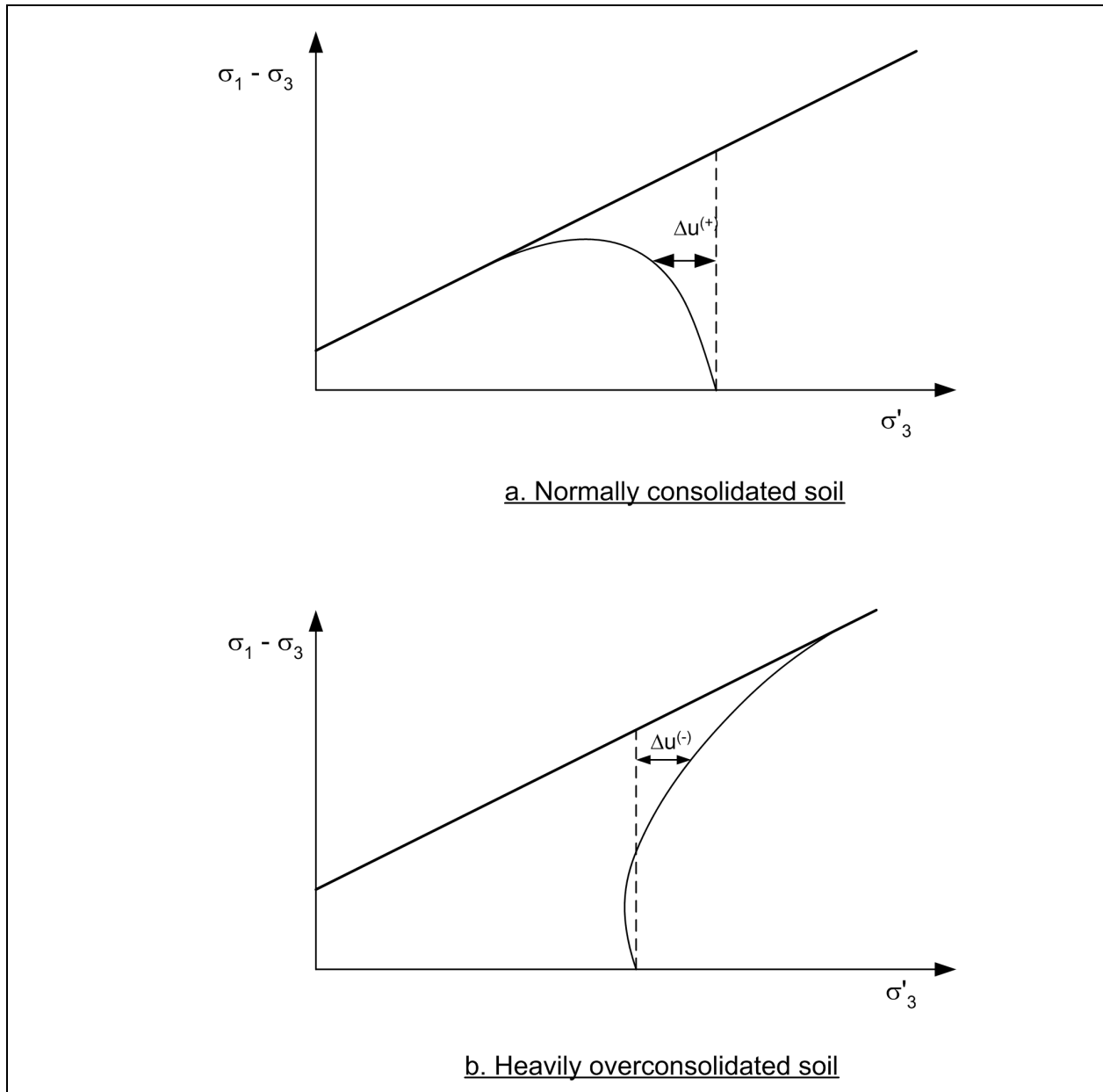
Figure D-9. Effective stress paths for shear plotted on alternate modified Mohr-Coulomb diagrams

that is precisely tangent to all stress paths, the envelope should be drawn as close to tangent as possible, with about two-thirds of the points of tangency above the line, and one-third below.

- The failure envelope may also be drawn by plotting the Mohr's circles of stress on a conventional Mohr-Coulomb diagram. In this case, it is much more difficult to determine when stress path tangency occurs; the particular set of stresses and Mohr's circle where stress path tangency occurs cannot be readily identified from the numerical test data. If several or all Mohr's circles representing the stresses at various stages of loading during each test are plotted, the number of circles becomes large and diagrams become complex and unclear.
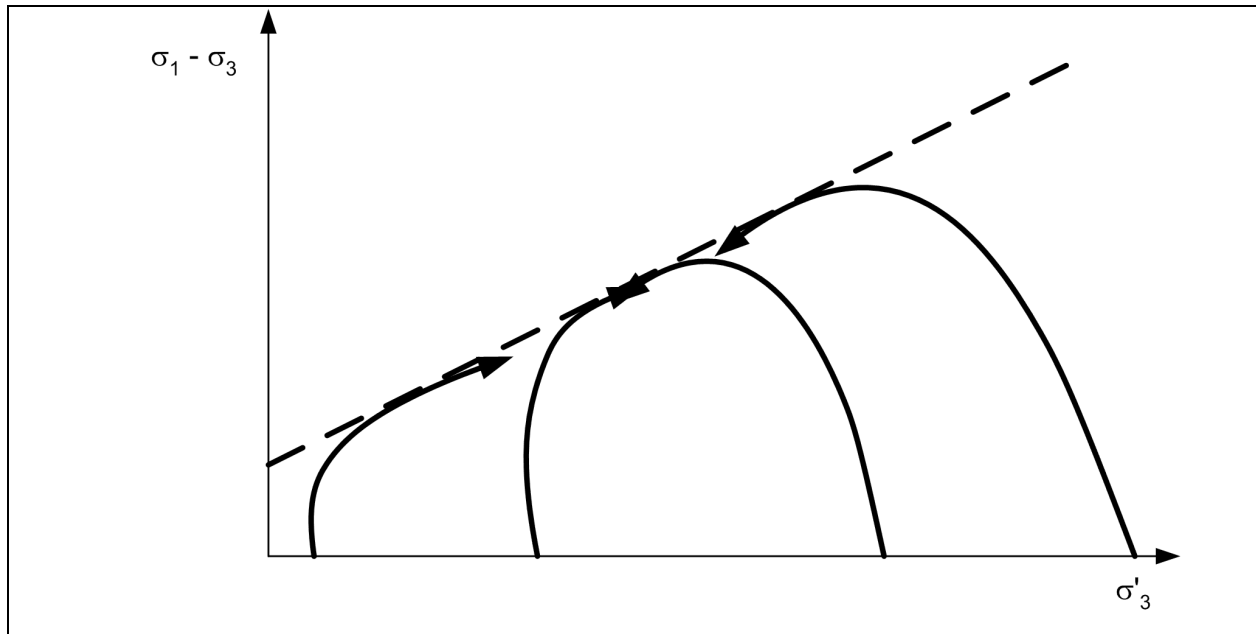
Figure D-10. Effective stress paths for Consolidated-Undrained shear tests plotted on a modified Mohr-Coulomb diagram

- One way of determining where the peak effective stress shear strength parameters are developed without plotting stress paths or Mohr circles for all the stresses during loading is to compute and examine the effective principal stress ratios, σ'_1/σ'_3, during shear for each data point recorded during the test. If the failure envelope passes through the origin of the Mohr-Coulomb diagram (c' = 0), the maximum value of the effective principal stress ratio, $(\sigma'_1/\sigma'_3)_{max}$, coincides with the point of stress path tangency. By calculating σ'_1/σ'_3 and determining where the maximum value occurs, the point of stress path tangency can be determined. The stresses at the point of tangency can then be used to plot the Mohr's circles on a Mohr-Coulomb diagram. However, this approach for determining the point of stress path tangency is only valid when the cohesion intercept, c', is zero.

- When the Mohr-Coulomb failure envelope is curved, test data must be plotted on a conventional Mohr-Coulomb diagram of τ vs. σ' in order to draw the failure envelope. This is necessary because no convenient means exists for transferring a curved envelope from a modified Mohr-Coulomb diagram back to the conventional diagram. However, even in instances where the failure envelope is curved, a modified Mohr-Coulomb diagram and stress paths may be drawn first to establish the point of stress-path tangency and failure. Once the point of stress path tangency is determined from stress-paths plotted on the modified Mohr-Coulomb diagram, the stresses can then be plotted on a conventional τ vs. σ' diagram and the curved Mohr-Coulomb failure envelope can be drawn.

- For many normally consolidated clays and loose sands, the point of stress-path tangency occurs after the maximum axial load is reached. In order to capture the point of stress-path tangency, it is necessary to continue to shear specimens past the point where the maximum load is developed. In order to do so, deformation-controlled loading, rather than load-controlled loading, must be used.

(2) Undrained shear strengths. When Consolidated-Undrained loading procedures are used to determine undrained shear strengths, the failure criterion for plotting the data are the same as those used for UU tests. The peak stress or the stress at a limiting value of strain, e.g., 15 percent axial strain, is used as the failure criterion.

   c. Consolidated-Drained (CD or S) tests. Failure in consolidated-drained tests is determined as the point of maximum principal stress difference, $(\sigma_1 - \sigma_3)_{max}$, or at some limiting, maximum value of axial strain. Fifteen percent axial strain is a reasonable value to use as a failure criterion. Heavily overconsolidated, stiff-fissured clays and dense sands sometimes exhibit significant reduction in shearing resistance with strain beyond the peak. In these materials it is not possible to develop the peak strength simultaneously at all points along the shear surface. Also, in slopes where prior sliding has resulted in development of slickensided slip surfaces, the shear resistance has already declined to its residual value. In these instances adequate stability can only be ensured by using residual shear strengths in stability analyses.

D-7 Generalized Stress-Strain-Strength Behavior

An understanding of the stress-strain response of soils is useful in interpreting the results of laboratory shear tests. The stress-strain response of soils in both drained and undrained shear tests is discussed below.

   a. Drained loading. Typical stress-strain curves from triaxial shear tests on dense and loose sands are shown in Figure D-11. The upper portion of this figure shows the axial stress-strain curves, while the lower portion shows volumetric strain vs. axial strain curves. Loose sands tend to compress (volume decreases) during shear. The axial stress may increase with increasing strain up to 20 or 25 percent axial strain or even more. Dense sands also tend to compress initially when sheared, but they then expand as they are sheared to larger strains. In dense sands, peak load is reached at much smaller strains than for loose sands, and the stress may then decrease significantly as strains are further increased. If loose and dense specimens of the same sand are sheared to large strains at the same confining pressure, the strengths will become similar at large strains, regardless of the initial density. At large strains, the soil is said to reach a "critical state" or "critical void ratio," and the shearing resistance at these large strains is largely independent of initial density. Normally and heavily overconsolidated clays tend to exhibit stress-strain response similar to those for loose and dense sands. Normally consolidated clays tend to compress throughout shear, developing a peak resistance at 10 to 20 percent axial strain. Heavily overconsolidated clays tend first to compress and then to dilate as they are sheared to large strains. Under drained loading, the peak resistance of heavily overconsolidated clays is usually developed at smaller strains than for normally consolidated clays.

   (1) The response to shear of both clays and sands with different stress histories or densities can be illustrated and explained with the concept of a "critical void ratio" or "critical state" first suggested by Casagrande (1936) and later promoted for clays by Roscoe, Schofield, and Wroth (1958). This is illustrated by the diagram of void ratio vs. confining pressure, σ_3, shown in Figure D-12. The curve labeled "critical state" in Figure D-12 represents the void ratios which soils eventually reach when they are sheared to large strains at various confining pressures. If a soil is loose, such that it starts shear at a point above the "critical state" line, the soil will compress (void ratio will decrease), as suggested by the path a-c in Figure D-12. In contrast, if a soil is dense, such that it starts shear at a point below the critical state line, the soil will tend to dilate as large strains are reached and the soil will dilate (void ratio will increase), as suggested by path b-c in Figure D-12). Regardless of the initial density, two specimens of the same soil tested at the same confining stress will tend to reach a similar void ratio and have very similar shear strengths at large strains. The dense soil will, however, have a higher peak strength.

   (2) For clays, a similar set of behavioral characteristics is observed. Normally consolidated clays tend to compress and reach a critical state when sheared, while heavily overconsolidated soils tend to expand as they reach the critical state at large strains.

   (3) Compacted soils can exhibit stress-strain responses varying from that for normally consolidated soil to that for heavily overconsolidated soils. At low confining pressures compacted clays tend to behave like overconsolidated clays, and at high confining pressures, where the effects of compaction no longer dominate their behavior, they behave more like normally consolidated soils.
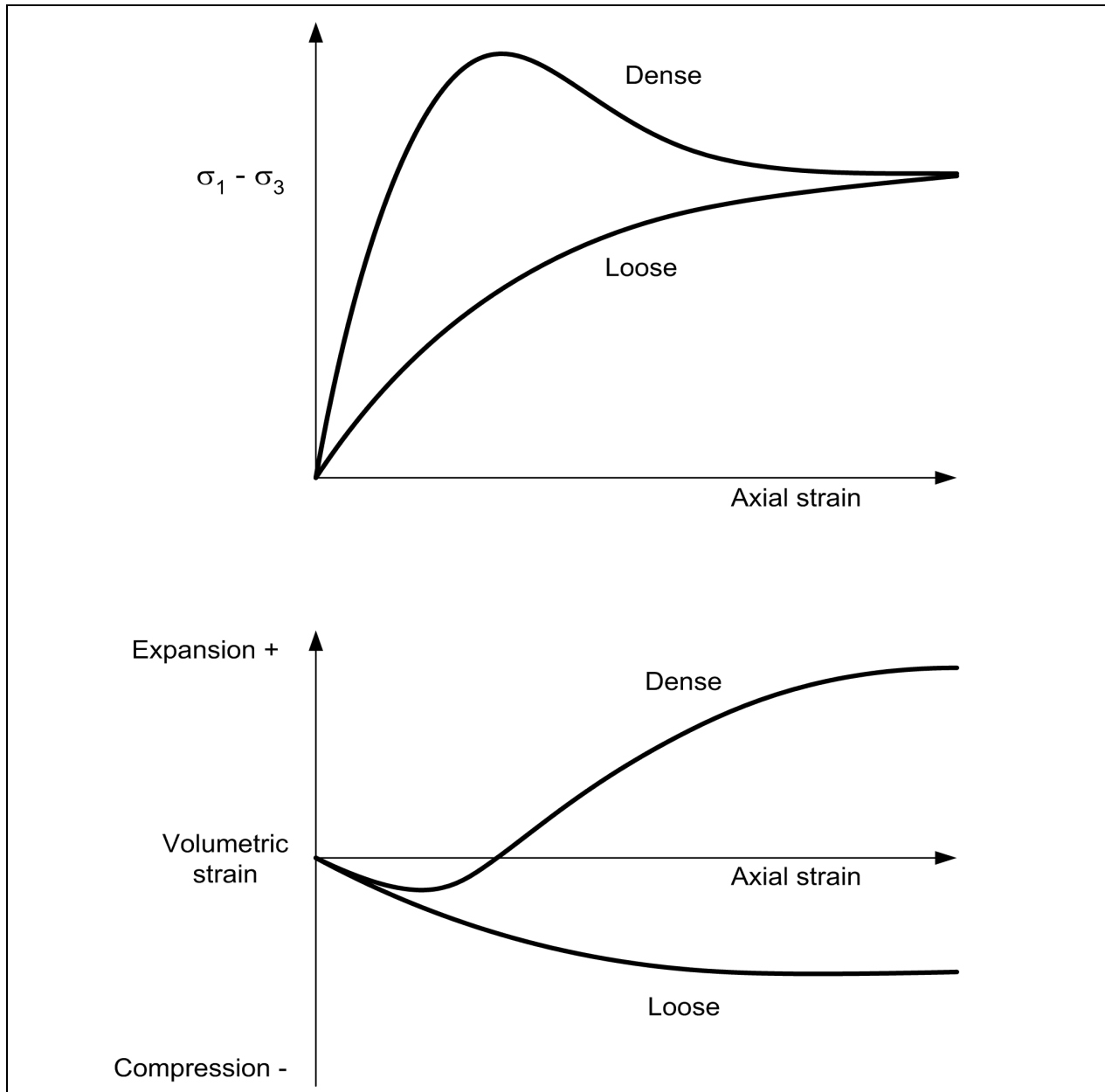
Figure D-11. Typical stress-strain curves from CD-S triaxial shear tests on dense and loose sands

b. Undrained loading. Typical effective stress paths for Consolidated-Undrained triaxial shear tests on normally consolidated and overconsolidated clays are illustrated in Figure D-13. Figure D-13a shows the stress paths on a p-q diagram, while Figure D-13b shows the stress paths on a modified Mohr-Coulomb diagram where $(\sigma_1 - \sigma_3)$ is plotted versus σ_3. Note how the stress paths for the normally consolidated clay reach a peak value of $(\sigma_1 - \sigma_3)$ prior to becoming tangent to the effective stress failure envelope. If the specimen were being sheared using controlled load, rather than controlled deformation, the postpeak behavior might either be lost or the sample might deform so rapidly as to make pore water pressure and effective stress measurements meaningless (result of unequalized pore water pressures in the specimen). This is the reason that deformation controlled, rather than load controlled loading is preferred for undrained tests on normally and lightly overconsolidated clays.
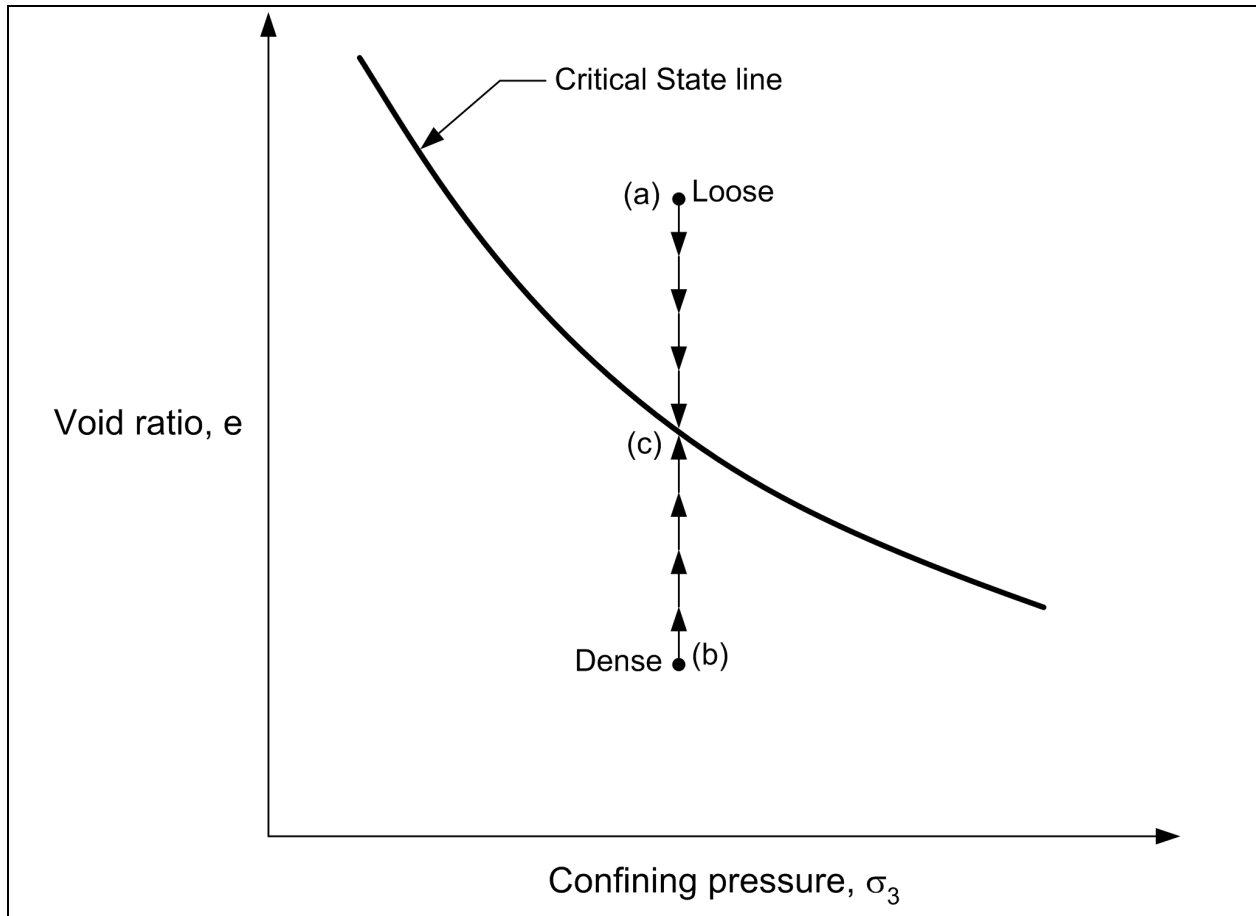
Figure D-12. Critical State line representing combinations of void ratio and confining pressure for soil that has been sheared to large strains – behavior in drained tests

(1) The concept of a "critical state" line presented earlier is applicable to undrained loading as well as drained loading. Figure D-14 shows a critical state line along with a line representing the line for virgin, isotropic consolidation. Specimens that are normally consolidated prior to undrained shear in the triaxial test have loading paths for shear that start along the virgin isotropic consolidation line. The line labeled a-b represents the loading path for a normally consolidated soil specimen that is sheared to large strains, and eventually reaches the critical state line. The pore water pressure in the specimen continually increases during shear, and the effective confining pressure, σ'_3, continually decreases. Similarly, the line labeled c-d represents a loading path for a heavily overconsolidated soil that is sheared to large strains at the same initial effective confining pressure. The pore water pressures at failure are less than they were at the start of shear and the effective stresses have increased. The lengths of the paths a-b and c-d represent the changes in pore pressure during the tests. Movement to the left indicates increase in pore pressure, and movement to the right indicates decrease in pore pressure.

(2) The line labeled e-b in Figure D-14 represents another overconsolidated specimen. However, in this case the specimen has the same void ratio as the normally consolidated specimen. Both specimens have the same void ratio, but prior to shear, the normally consolidated specimen is under a higher confining pressure than the overconsolidated specimen. During shear the pore water pressures in the normally consolidated specimen increase (line a-b) and the pore water pressures in the overconsolidated specimen decrease (line e-b). At large strains (at the critical state line), both specimens have the same void ratio and have reached a

$$\frac{\sigma_1 - \sigma_3}{2}$$

Normally consolidated

Heavily overconsolidated

$$\frac{\sigma'_1 + \sigma'_3}{2}$$

a. p - q diagram

$$\sigma_1 - \sigma_3$$

Heavily overconsolidated

Normally consolidated

$$\sigma'_3$$

b. Alternate modified Mohr-Coulomb diagram
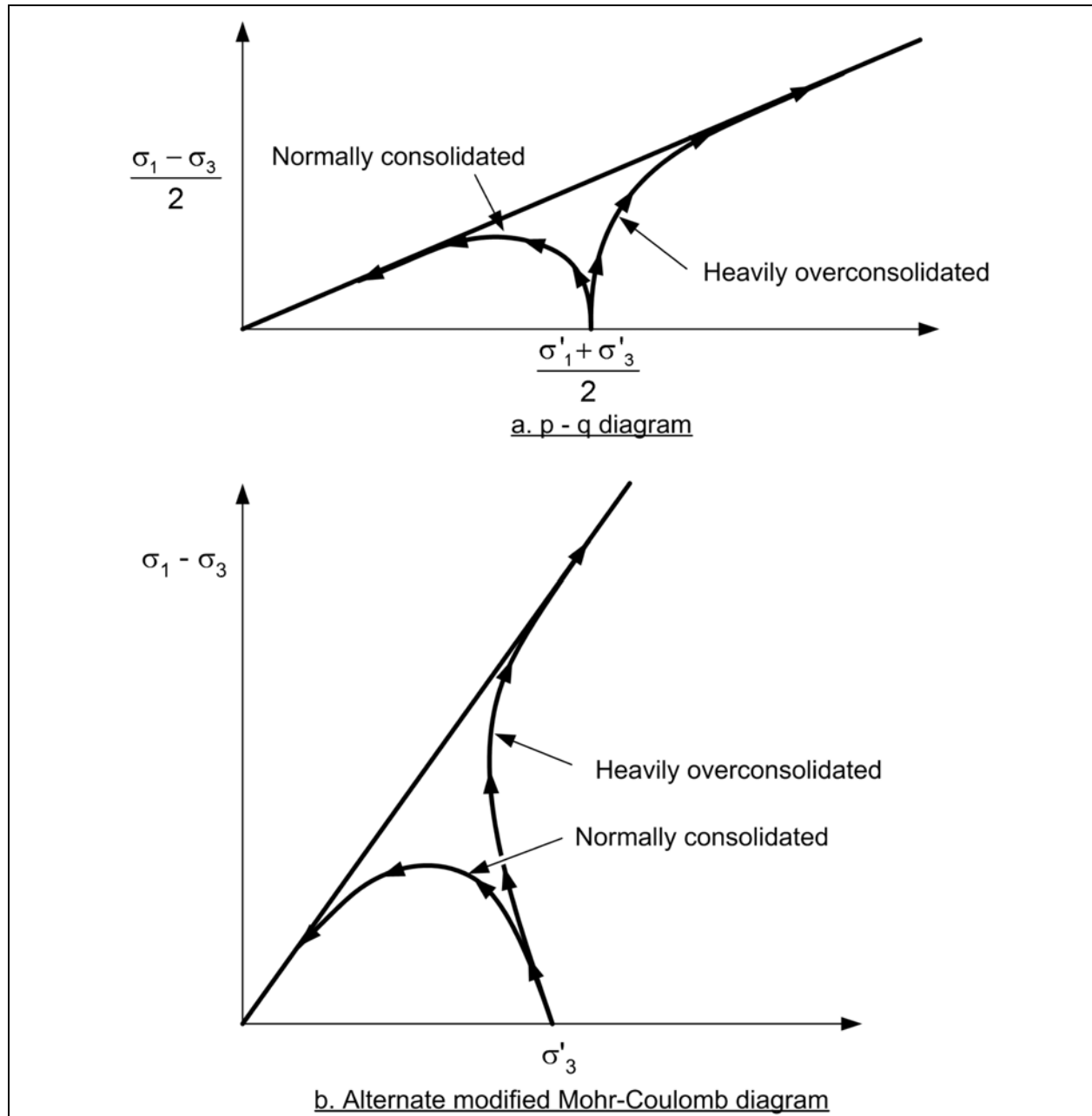
Figure D-13. Effective stress paths on two types of modified Mohr-Coulomb diagrams for normally consolidated and heavily overconsolidated clays

"critical confining pressure," $\sigma'_{3\text{-critical}}$. Both specimens also have the same shear strength at the large strains corresponding to the critical state line, although the <u>peak</u> shear strengths of the two specimens would be quite different.

   c. Sample disturbance. Disturbance of soil specimens caused by sampling and handling affects the stress-strain response of soils. Disturbance can sometimes be detected by simply examining the soil response during shear, especially when the soil is either loose sand or normally consolidated clay. Disturbance densifies loose sands and causes them to behave more like dense sands. Similarly, disturbance of normally
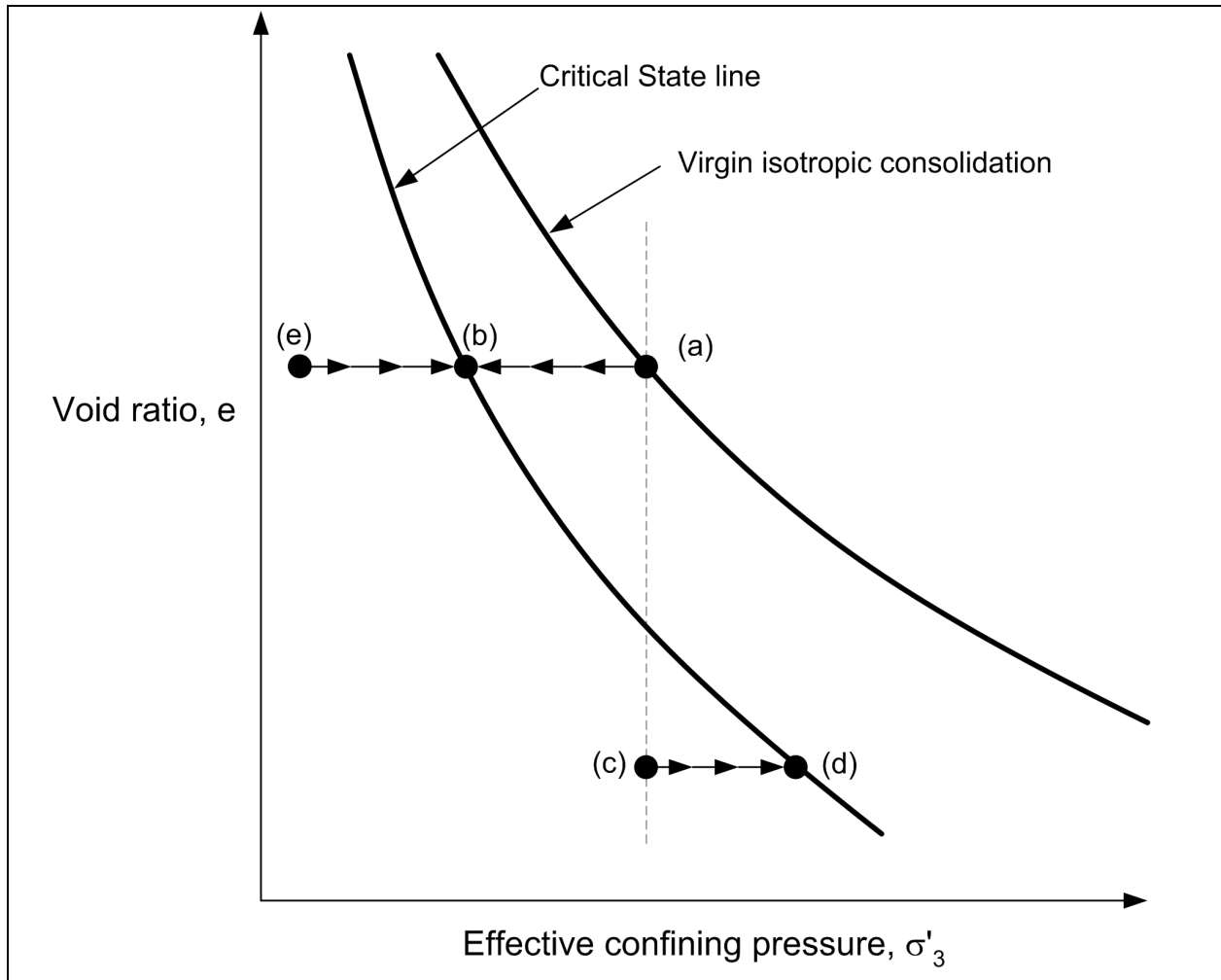
Figure D-14. Critical State line representing combinations of void ratio and confining pressure for soil that has been sheared to large strains – behavior in undrained tests

consolidated soil specimens makes them respond more like overconsolidated clays because disturbance causes the pore water pressure to increase and the effective stress to decrease. The axial strain at which the peak strength is developed in Unconsolidated-Undrained (UU or Q) tests may increase when specimens are disturbed, and instead of being in the typical range of 1 to 6 percent expected for normally consolidated clays, may increase to 10 percent or more if the specimens are disturbed. Pore water pressures generated during shear will also be lower if the specimens are disturbed. However, in the case of Unconsolidated-Undrained shear tests, the pore water pressures that exist prior to shear will be higher because of disturbance effects. The higher pore pressures at the start of shear will offset the lower pore water pressures developed during shear, such that sample disturbance will reduce the undrained shear strength measured in Unconsolidated-Undrained tests.

D-8. Curved Strength Envelopes

a. The strength envelopes for many soils are curved, rather than linear, as shown in Figure D-15. If the curvature is small and the range of stresses of interest is small, a curved failure envelope can be approximated by a straight line for purposes of analysis, as shown in Figure D-15b. However, if the envelope is distinctly curved over the range of stresses of interest, use of a straight line failure envelope may significantly

a. Curved strength envelope

b. Straight-line approximation of curved strength envelope
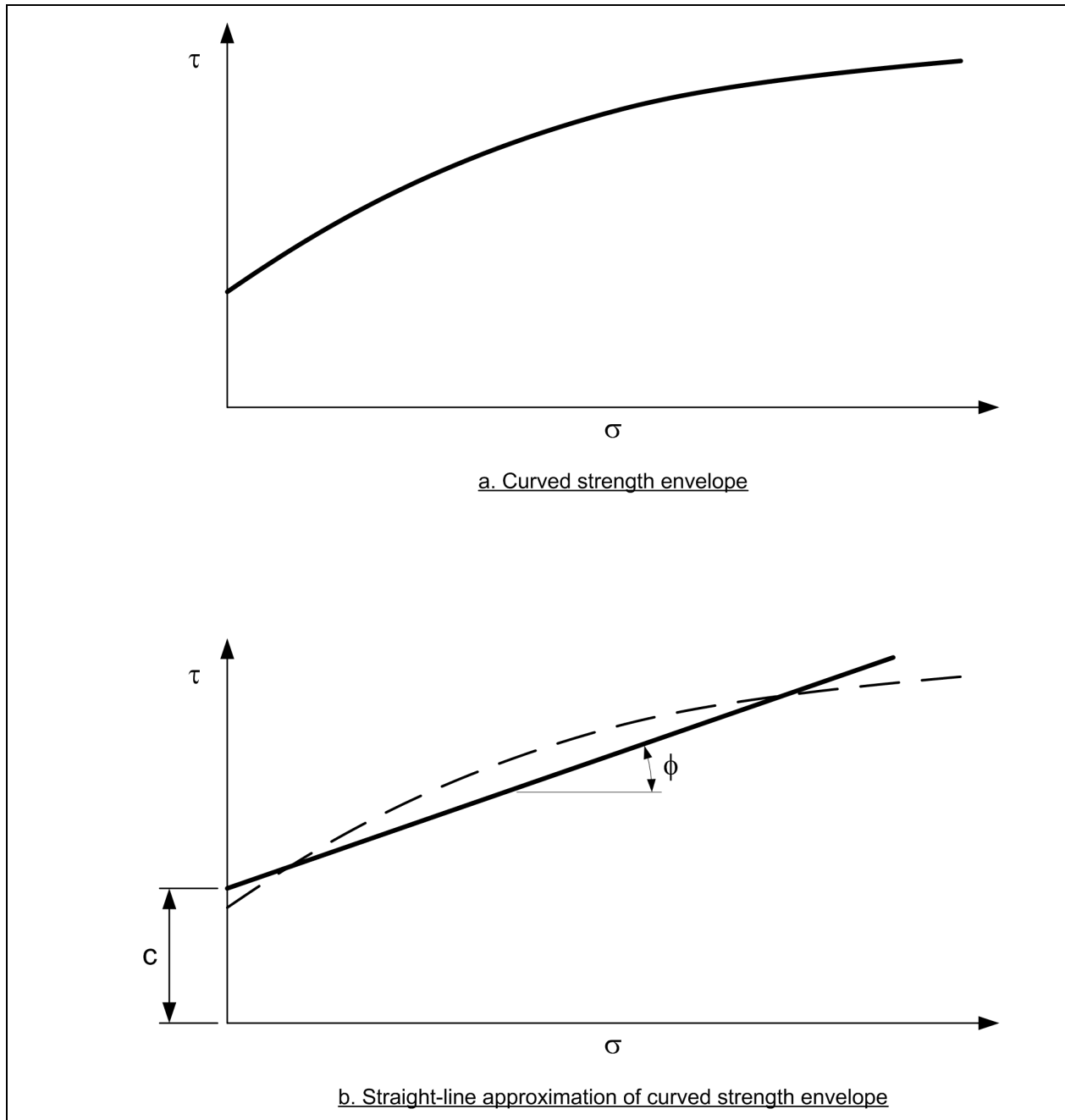
Figure D-15. Curved strength envelope and straight-line approximation

overestimate the shear strength at low and at high stresses. Extrapolation to higher or lower stresses can result in an overestimate of shear strength, and a factor of safety with regard to slope stability that is too high.

b. It is especially important that laboratory tests be conducted using a range in confining pressures that represents the range of stresses expected along potential sliding surfaces. Once tests have been conducted using a suitable range in stresses, an appropriate decision can be made regarding how the strength envelope will be represented. It is relatively easy to use curved strength envelopes in slope stability computations with software that is currently available, and there is little advantage to using a liner strength envelope when the data suggest otherwise.

   c.   Frequently, when the strength envelope is curved, the results of strength tests are reported in terms of a secant friction angle, ϕ_{secant} (Figure D-16). For example, Duncan, Horz, and Yang (1989) present useful correlations for the friction angle of a number of soils in terms of the secant friction angle at one atmosphere confining pressure, and the reduction in friction angle $\Delta\phi$, with each ten-fold increase in confining pressure. Stark and Eid (1994, 1997) present correlations for residual and fully softened shear strengths in terms of the secant friction angle at selected values of effective normal stress. Correlations such as those by Duncan, Horz, and Yang (1989) and Stark and Eid (1994, 1997), are useful for estimating shear strength values for preliminary stability analyses and to supplement data from laboratory tests. However, for slope stability computations it is usually preferable to express the strength envelope in terms of a continuous function of shear strength versus normal stress, rather that as a series of discrete values of secant friction angle. This can be done by selecting suitable values of normal stress, σ_j, and determining the corresponding friction angle, ϕ_{secant} for each value of σ_j. Values of the respective shear strength are then computed as:

$$s_j = \sigma_j \ \tan \ \phi_{secant\text{-}j} \tag{D-17}$$

where

$$\sigma_j = \text{one of a number of values of normal stress}$$

$$s_j \text{ and } \phi_{secant\text{-}j} = \text{corresponding values of secant friction angle and shear strength}$$

The values of shear strength s_j are plotted against the corresponding values of σ_j to develop a nonlinear strength envelope like the one shown in Figure D-17, which is then used in the slope stability computations.
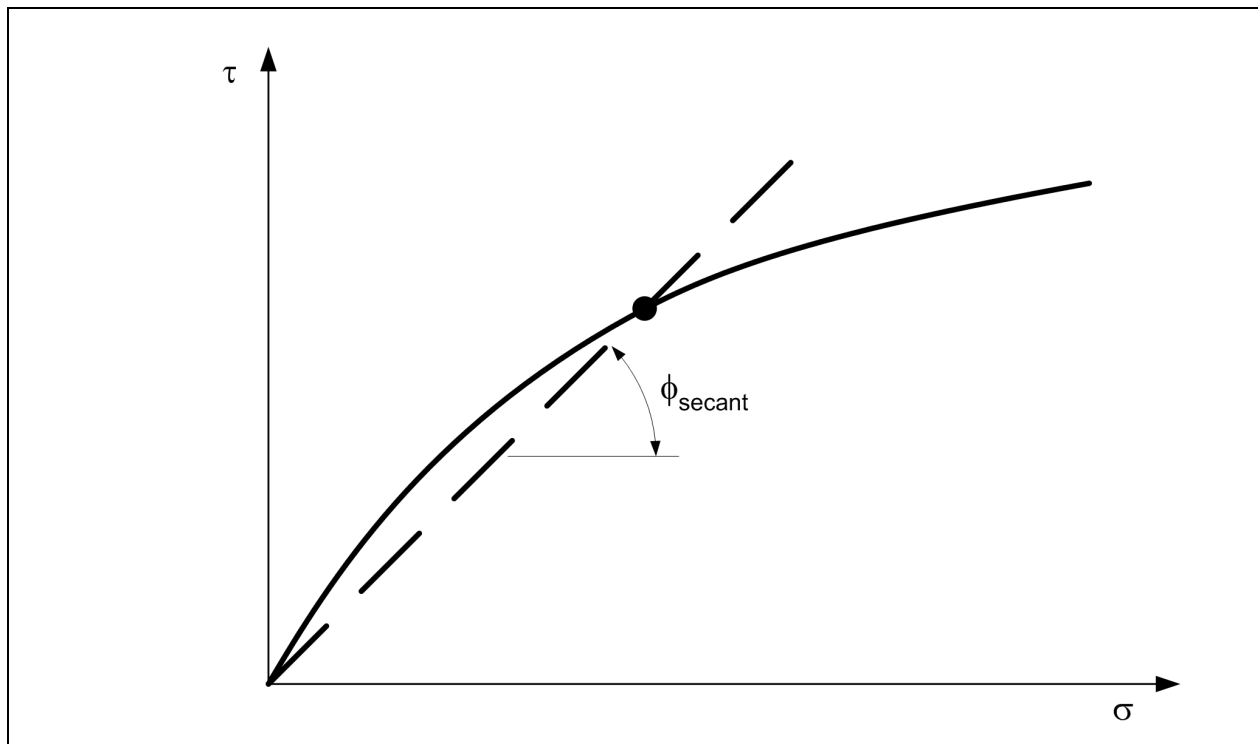
Figure D-16.   Curved strength envelope and equivalent secant friction angle
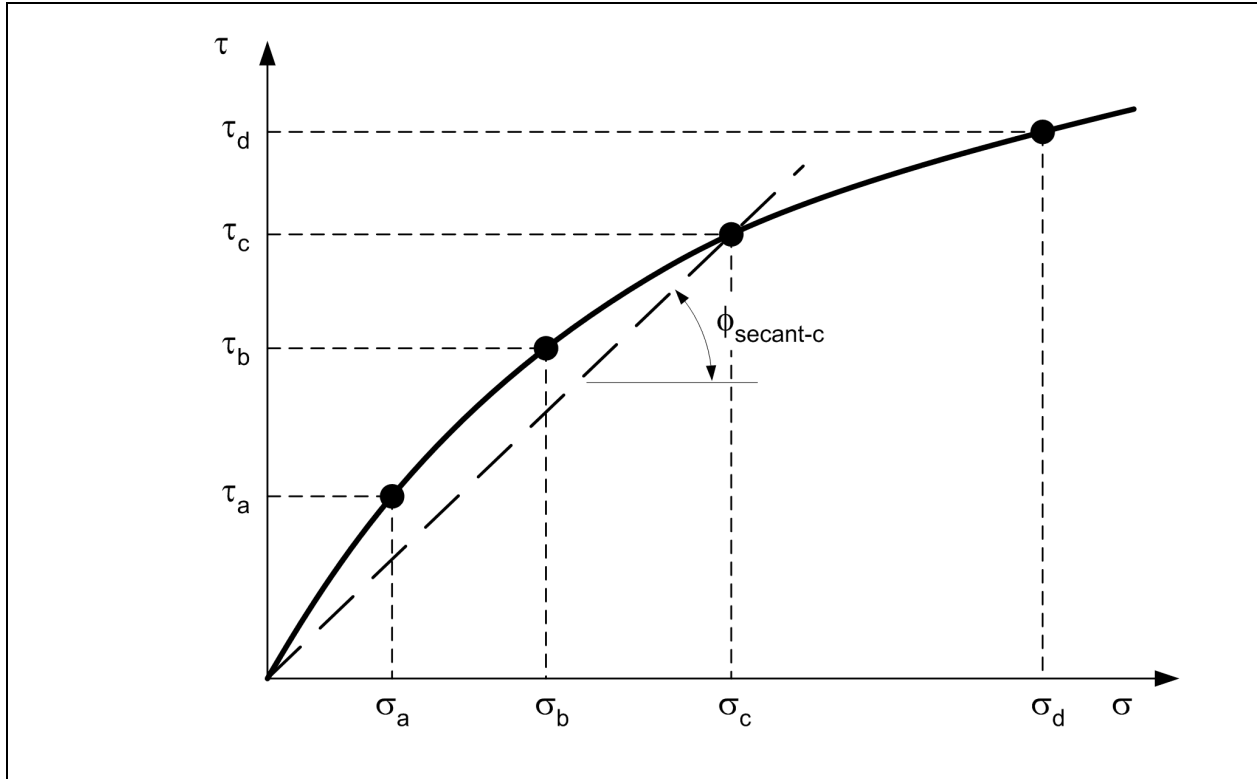
Figure D-17.   Construction of curved strength envelope using secant friction angles

D-9. Strain Compatibility

a.   "Strain Compatibility" is a term used to refer to the variation in the stress-strain properties of soils along a slip surface. In an actual slope, both the strains that are developed and the stress-strain properties will vary such that it is unlikely that the peak shear strength will be developed simultaneously along the full length of a slip surface. This is important if the soils within the slope exhibit significant strain softening. In such cases, it is appropriate to adopt lower shear strengths or to require higher factors of safety.

b.   Several approaches have been suggested for handling issues of strain incompatibility. Koutsoftas and Ladd (1985) have suggested a procedure for determining an "equivalent" strain that is used as the failure criterion for determining shear strengths from laboratory test data. Also, Chirapuntu and Duncan (1975) have developed procedures for reducing shear strengths when highly dissimilar soils exist along a potential slip surface. For many soils and slope conditions, no special provisions are necessary. For example, Wright, Kulhawy, and Duncan (1973) showed that for overall factors of safety of at least 1.5, the peak strength of the soil is not fully reached at any point along the potential slip surface, even though the strains and factor of safety may vary significantly. When the possibility of reduced strengths exists, it is helpful to compute the factor of safety using the ultimate (residual) shear strength. This represents a lower bound for shear strength and should indicate if there is any possibility of failure due to strain incompatibility problems. When such a conservative estimate for shear strengths is used, lower than conventional values of factor of safety are acceptable.

D-10. Staged Construction

a. In staged construction, an embankment is built in increments and the foundation soil is allowed to consolidate fully or partially under each stage so that the increased strength will increase stability during subsequent states. Staged construction is generally used when the foundation soils are so weak that the entire embankment cannot be built in a single increment. Analyses for stage construction require special consideration in developing shear strength parameters. One approach is to use Consolidated-Undrained tests to measure the strengths, taking into account increases in strength resulting from increases in effective consolidation pressure. This involves the following steps:

- Step 1: Initial effective stresses and maximum past pressures are determined. Initial stresses are computed from unit weights and the groundwater levels prior to embankment construction. Maximum past effective stresses are determined from oedometer tests on high quality, undisturbed samples.

- Step 2: Normalized shear strengths, S_u/σ'_{vc}, are determined for various overconsolidation ratios by performing Unconsolidated-Undrained shear tests using the SHANSEP procedure.

- Step 3: Pore water pressures and effective stresses in the field are estimated using an appropriate consolidation analysis. The consolidation analysis should take into account the initial stresses, the increase in stress because of added embankment loads, and the subsequent consolidation because of dissipation of excess pore water pressures.

- Step 4: Undrained shear strengths are estimated using the information from Steps 1, 2, and 3. Undrained shear strengths are calculated by multiplying the appropriate values of normalized shear strength by the effective vertical stress, thus accounting for consolidation.

- Step 5: Stability analyses are performed using undrained shear strengths. The undrained shear strengths are assigned as values of cohesion, c, and ϕ is equal to zero.

b. The above procedure requires assumptions about how the initial excess pore water pressures are generated by the embankment loads, especially regarding the pore water pressures beneath and beyond the toe of the slope. Also, a relatively complex analysis of consolidation is required to account for the variation in stresses and excess pore water pressures in the vertical and horizontal directions. Finally, the shear strength is usually related to the vertical effective stress in the field, which, unlike the stresses in the laboratory, is seldom the major principal stress during consolidation. More uncertainty exists in analyses of staged construction than for other cases, and this should be taken into consideration when selecting appropriate shear strength values and factors of safety for design.

c. An alternative approach to the undrained strength approach described above is to perform an effective stress analysis using effective stress shear strength parameters (c' and ϕ') and estimated pore water pressures. This approach requires the same relatively complex consolidation analysis used in the first approach and, thus, the second approach is also subject to the same errors. The effective stress approach will also give different values for the factor of safety as the result of fundamental differences between total and effective stress factors of safety: The effective stress approach is based on pore water pressures at working stress levels, rather than values at failure, while the undrained strength approach is based on pore water pressures generated at failure. Because there is no experience to guide selection of safety factors for the effective stress approach, it should not be used.

D-11. Partially Saturated Soils

a. Partially saturated soils present special problems when treated using effective stresses. Significant progress has been made in understanding how partially saturated soils behave and the role of effective stresses (Fredlund and Rahardjo 1993; Fredlund 2000). This work indicates that the simple expression for effective stress where the pore water pressure is subtracted from the total stress to evaluate the effective stress is not valid and that the Mohr-Coulomb shear strength equation for effective stresses in saturated soils is not valid for unsaturated soils. Rigorous treatment of effective stresses in partially saturated soils is beyond the scope of this manual.

b. Fortunately, consideration of effective stresses in unsaturated soils can be avoided for many practical slope stability problems. To evaluate strength and stability at the end of construction, Unconsolidated-Undrained shear tests are performed to measure the shear strength. In this case the shear strengths are expressed as a function of total stresses, and the approach is valid for both saturated and unsaturated soils. For long-term stability and stability during rapid drawdown, the soil may be fully or only partially saturated. However, if the soil is below the groundwater table or beneath the phreatic surface, the pore water pressures are positive and the soil is assumed to be saturated for design purposes. If the soil is above the water table or in a zone of capillarity and where pore pressures are negative, the beneficial effects of negative pore water pressures are conservatively neglected by assuming that the pore water pressures are zero. Conventional effective stress shear strength parameters are used for both the saturated (positive pressure) and partially saturated (zero pressure) zones. The effective stress shear strength parameters are measured on specimens that are fully saturated prior to laboratory testing, regardless of the saturation that may exist in the field.

c. For cases where substantial portions of the slope are partially saturated and long-term stability is being evaluated, neglecting negative pore water pressures can be very conservative. In such cases, some account of negative pore water pressures may be appropriate (Fredlund 1989, 1995). Beneficial effects of negative pore water pressure can easily be destroyed by rainfall and infiltration of surface water, as well as a rise in ground water table. Thus, negative pore water pressures should be included in stability computations with great caution. Use of negative pore water pressures is not recommended for design of dams and similar critical structures where the consequences of failure are great.

Appendix E
Chart Solutions for Embankment Slopes

E-1. General Use and Applicability of Slope Stability Charts

a. Slope stability charts provide a means for rapid analysis of slope stability. They can be used for preliminary analyses, for checking detailed analyses, or for complete analyses. They are especially useful for making comparisons between design alternatives, because they provide answers so quickly. The accuracy of slope stability charts is usually as good as the accuracy with which shear strengths can be evaluated.

b. In this appendix, chart solutions are presented for four types of slopes:

(1) Slopes in soils with $\phi = 0$ and uniform strength throughout the depth of the soil layer.

(2) Slopes in soils with $\phi > 0$ and $c > 0$ and uniform strength throughout the depth of the soil layer.

(3) Infinite slopes in soils with $\phi > 0$ and $c = 0$ and soils with and $\phi > 0$ and $c > 0$.

(4) Slopes in soils with $\phi = 0$ and strength increasing linearly with depth.

Using approximations in slope geometry and carefully selected soil properties, these chart solutions can be applied to a wide range of nonhomogenous slopes.

c. This appendix contains the following slope stability charts:

- Figure E-1: Slope stability charts for $\phi = 0$ soils (after Janbu 1968).[1]

- Figure E-2: Surcharge adjustment factors for $\phi = 0$ and $\phi > 0$ soils (after Janbu 1968).

- Figure E-3: Submergence and seepage adjustment factors for $\phi = 0$ and $\phi > 0$ soils (after Janbu 1968).

- Figure E-4: Tension crack adjustment factors for $\phi = 0$ and $\phi > 0$ soils (after Janbu 1968).

- Figure E-5: Slope stability charts for $\phi > 0$ soils (after Janbu 1968).

- Figure E-6: Steady seepage adjustment factor for $\phi > 0$ soils (after Duncan, Buchianani, and DeWet 1987).

- Figure E-7: Slope stability charts for infinite slopes (after Duncan, Buchianani, and DeWet 1987).

- Figure E-8: Slope stability charts for $\phi = 0$ soils, with strength increasing with depth (after Hunter and Schuster 1968).

E-2. Averaging Slope Inclinations, Unit Weights and Shear Strengths

a. For simplicity, charts are developed for simple homogenous soil conditions. To apply them to nonhomogeneous conditions, it is necessary to approximate the real conditions with an equivalent homogenous slope. The most effective method of developing a simple slope profile for chart analysis is to begin with a cross section of the slope drawn to scale. On this cross section, using judgment, draw a geometrically simple slope that approximates the real slope as closely as possible.

---

[1] Reference information is presented in Appendix A.

b. To average the shear strengths for chart analysis, it is useful to know the location of the critical slip surface. The charts contained in the following sections of this appendix provide a means of estimating the position of the critical circle. Average strength values are calculated by drawing the critical circle, determined from the charts, on the slope. Then the central angle of arc subtended within each layer or zone of soil is measured with a protractor. The central angles are used as weighting factors to calculate weighted average strength parameters, c_{avg} and ϕ_{avg} are as follows:

$$c_{avg} = \frac{\sum \delta_i c_i}{\sum \delta_i} \tag{E-1}$$

$$\phi_{avg} = \frac{\sum \delta_i \phi_i}{\sum \delta_i} \tag{E-2}$$

where

  c_{avg} = average cohesion (stress units)

  ϕ_{avg} = average angle of internal friction (degrees)

  δ_i = central angle of arc, measured around the center of the estimated critical circle, within zone i (degrees)

  c_i = cohesion in zone i (stress units)

  ϕ_i = angle of internal friction in zone i

c. One condition in which it is preferable not to use these averaging procedures is the case in which an embankment overlies a weak foundation of saturated clay, with $\phi = 0$. Using Equations E-1 and E-2 to develop average values of c and ϕ in such a case would lead to a small value of ϕ_{avg} (perhaps 2 to 5 degrees). With $\phi_{avg} > 0$, it would be necessary to use the chart shown in Figure E-5, which is based entirely on circles that pass through the toe of the slope. With $\phi = 0$ foundation soils, the critical circle usually goes below the toe into the foundation. In these cases, it is better to approximate the embankment as a $\phi = 0$ soil and to use the $\phi = 0$ slope stability charts shown in Figure E-1. The equivalent $\phi = 0$ strength of the embankment soil can be estimated by calculating the average normal stress on the part of the slip surface within the embankment (one-half the average vertical stress is usually a reasonable approximation of the normal stress on this part of the slip surface) and determining the corresponding shear strength at that point on the shear strength envelope for the embankment soil. This value of strength is treated as a value of S_u for the embankment, with $\phi = 0$. The average value of S_u is then calculated for both the embankment and the foundation using the same averaging procedure as described above.

$$(S_u)_{avg} = \frac{\sum \delta_i (S_u)_i}{\sum \delta_i} \tag{E-3}$$

The chart contains the following labels and annotations:

Factor of safety: $F = N_0 \dfrac{c}{P_d}$

$P_d = \dfrac{\gamma H + q - \gamma_w H_w}{\mu_q\ \mu_w\ \mu_t}$

Stability number - N_0

.... Slope circles
———— Toe circles
– – – – Deep circles

d = 0, 0.1, 0.2, 0.3, 0.5, 1.0, 1.5, 2, 3, d = ∞

Toe circles

b = cot β

0.25   0.50   0.75   1.0   1.5   2.0   3   4   6   10   ∞

Slope angle - β - degrees

Slope circle
Toe circle
Deep circle
d = D/H

Unit abcissa of center - x_0
d = 0
d = ∞
All circles
b = cot β
Slope angle - β - degrees

Center of Critical circle
X_0
Y_0
$X_0 = x_0 H$
$Y_0 = y_0 H$

Unit ordinate of center - y_0
d = 3
2
1
Toe circles
0
b = cot β
Slope angle - β - degrees

Figure E-1.   Slope stability charts for ϕ = 0 soils (after Janbu 1968)

where

$(S_u)_{avg}$ = average undrained shear strength (in stress units)

$(S_u)_i$ = S_u in layer i (in stress units)

δ_i = central angle of arc, measured around the center of the estimated critical circle, within zone i (degrees)

This average value of S_u is then used, with $\phi = 0$, for analysis of the slope.

d. To average unit weights for use in chart analysis, it is usually sufficient to use layer thickness as a weighting factor, as indicated by the following expression:

$$\gamma_{avg} = \frac{\sum \gamma_i h_i}{\sum h_i}$$ (E-4)

where

γ_{avg} = average unit weight (force per length cubed)

γ_i = unit weight of layer i (force per length cubed)

h_i = thickness of layer i (in length units)

e. Unit weights should be averaged only to the depth of the bottom of the critical circle. If the material below the toe of the slope is a $\phi = 0$ material, the unit weight should be averaged only down to the toe of the slope, since the unit weight of the material below the toe has no effect on stability in this case.

E-3. Soils with $\phi = 0$

The slope stability chart for $\phi = 0$ soils, developed by Janbu (1968), is shown in Figure E-1. Charts providing adjustment factors for surcharge loading at the top of the slope are shown in Figure E-2. Charts providing adjustment factors for submergence and seepage are shown in Figure E-3. Charts providing adjustment factors to account for tension cracks are shown in Figure E-4.

a. Steps for use of $\phi = 0$ charts:

(1) Using judgment, decide which cases should be investigated. For uniform soil conditions, the critical circle passes through the toe of the slope if the slope is steeper than about 1 (H) on 1 (V). For flatter slopes, the critical circle usually extends below the toe, and is tangent to some deep firm layer. The chart in Figure E-1 can be used to compute factors of safety for circles extending to any depth. Multiple possibilities should be analyzed, to be sure that the overall critical circle and overall minimum factor of safety have been found.

(2) The following criteria can be used to determine which possibilities should be examined:

(a) If there is water outside the slope, a circle passing above the water may be critical.

Figure E-2.   Surcharge adjustment factors φ = 0 and φ > 0 soils (after Janbu 1968)

(b) If a soil layer is weaker than the one above it, the critical circle may be tangent to the base of the lower (weaker) layer. This applies to layers both above and below the toe.

(c) If a soil layer is stronger than the one above it, the critical circle may be tangent to the base of either layer, and both possibilities should be examined. This applies to layers both above and below the toe.

(3) The following steps are performed for each circle:

(a) Calculate the depth factor, d, using the formula:

$$d = \frac{D}{H}$$

(E-5)

where

D = depth from the toe of the slope to the lowest point on the slip circle (L; length)

H = slope height above the toe of the slope (L)
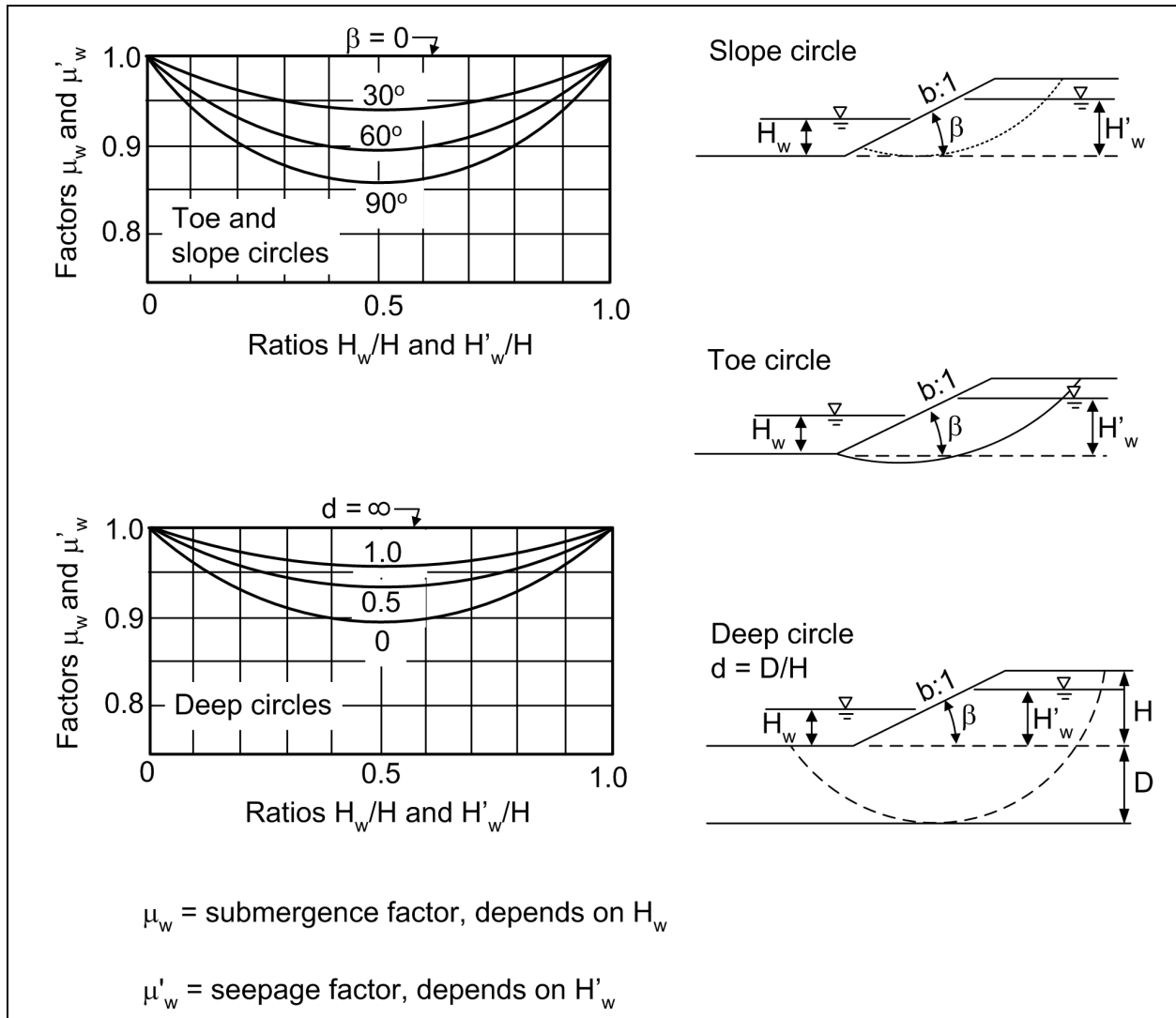
Figure E-3. Submergence and seepage adjustment factors $\phi = 0$ and $\phi > 0$ soils (after Janbu 1968)

The value of d is 0 if the circle does not pass below the toe of the slope. If the circle being analyzed is entirely above the toe, its point of interaction with the slope should be taken as an "adjusted toe," and all dimensions like D, H, and H_w must be adjusted accordingly in the calculations.

    (b) Find the center of the critical circle using the charts at the bottom of Figure E-1, and draw this circle to scale on a cross section of the slope.

    (c) Determine the average value of the strength, $c = S_u$, for the circle, using Equation E-3.

    (d) Calculate the quantity P_d using Equation E-6:

$$P_d = \frac{\gamma H + q - \gamma_w H_w}{\mu_q \mu_w \mu_t} \tag{E-6}$$

Figure E-4.   Tension crack adjustment factors φ = 0 and φ > 0 soils (after Janbu 1968)

where

γ = average unit weight of soil (F/L^3))

H = slope height above toe (L)

q = surcharge (F/L^2)

γ_w = unit weight of water (F/L^3)

H_w = height of external water level above toe (L)

μ_q = surcharge adjustment factor (Figure E-2)

μ_w = submergence adjustment factor (Figure E-3)

μ_t = tension crack adjustment factor (Figure E-4)

If there is no surcharge, $\mu_q = 1$.

If there is no external water above toe, $\mu_w = 1$; and if there are no tension cracks, $\mu_t = 1$.

(e) Using the chart at the top of Figure E-1, determine the value of the stability number, N_o, which depends on the slope angle, β, and the value of d.

(f) Calculate the factor of safety, F, using Equation E-7:

$$F = \frac{N_o c}{P_d} \tag{E-7}$$

where

N_o = stability number

c = average shear strength = $(S_u)_{avg}$ (F/L^2)

b. The example problems in Figures E-9 and E-10 illustrate the use of these methods. Note that both problems involve the same slope, and that the only difference between the two problems is the depth of the circle analyzed.

E-4. Soils with $\phi > 0$

a. The slope stability chart for $\phi > 0$ soils, developed by Janbu (1968), is shown in Figure E-5.

b. Adjustment factors for surcharge are shown in Figure E-2. Adjustment factors for submergence and seepage are shown in Figure E-3. Adjustment factors for tension cracks are shown in Figure E-4.

c. The stability chart in Figure E-5 can be used for analyses in terms of effective stresses. The chart may also be used for total stress analysis of unsaturated slopes with $\phi > 0$.

d. Steps for use of charts are:

$$F = N_{cf} \frac{c}{P_d} \qquad P_d = \frac{\gamma H + q - \gamma_w H_w}{\mu_q \mu_w \mu_t}$$

$$\lambda_{c\phi} = \frac{P_e \tan\phi}{c} \qquad P_e = \frac{\gamma H + q - \gamma_w H_w'}{\mu_q \mu_w'}$$

Stability numbers and center coordinates for circles passing through the toe of the slope.
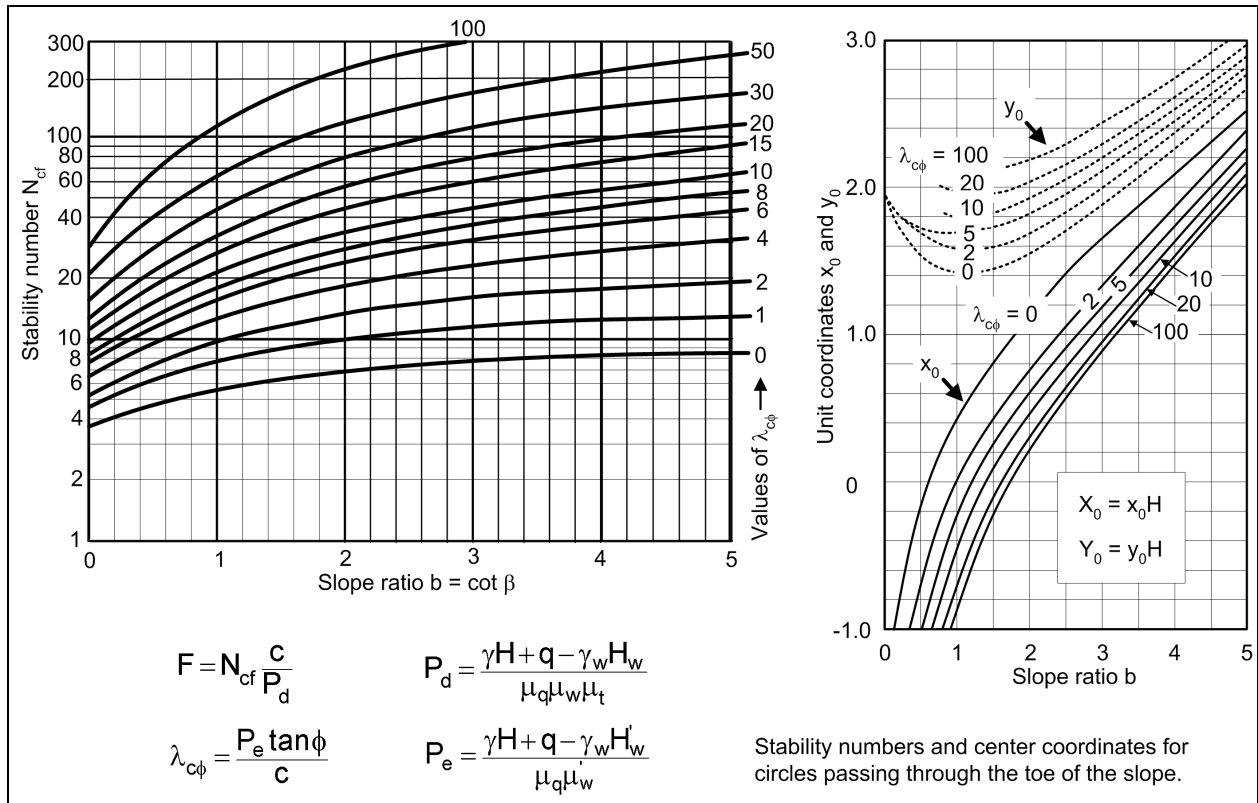
Figure E-5.   Slope stability charts for $\phi > 0$ soils (after Janbu 1968)

(1) Estimate the location of the critical circle. For most conditions of slopes in uniform soils with $\phi > 0$, the critical circle passes through the toe of the slope. The stability numbers given in Figure E-5 were developed by analyzing toe circles. In cases where $c = 0$, the critical mechanism is shallow sliding, which can be analyzed as the infinite slope failure mechanism. The stability chart shown in Figure E-7 can be used in this case. If there is water outside the slope, the critical circle may pass above the water. If conditions are not homogeneous, a circle passing above or below the toe may be more critical than the toe circle. The following criteria can be used to determine which possibilities should be examined:

(a) If there is water outside the slope, a circle passing above the water may be critical.

(b) If a soil layer is weaker than the one above it, the critical circle may be tangent to the base of the lower (weaker) layer. This applies to layers both above and below the toe.

(c) If a soil layer is stronger than the one above it, the critical circle may be tangent to the base of either layer, and both possibilities should be examined. This applies to layers both above and below the toe.

The charts in Figure E-5 can be used for nonuniform conditions provided the values of c and ϕ used in the calculation represent average values for the circle considered. The following steps are performed for each circle.

(2) Calculate P_d using the formula:

$$P_d = \frac{\gamma H + q - \gamma_w H_w}{\mu_q \mu_w \mu_t} \qquad \text{(E-8)}$$

where

γ = average unit weight of soil (F/L^3))

H = σλοπε height above toe (L)

q = συρχηαργε (F/L^2)

γ_w = unit weight of water (F/L^3)

H_w = height oφ external water level above toe (L)

μ_q = surcharge reduction factor (Figure E-2)

μ_w = submergence reduction factor (Figure E-3)

μ_t = tension crack reduction factor (Figure E-4)

μ_q = 1, if there is no surcharge

μ_w = 1, if there is no external water above toe

μ_t = 1, if there are no tension cracks

If the circle being studied passes above the toe of the slope, the point where the circle intersects the slope face should be taken as the toe of the slope for the calculation of H and H_w.

(3) Calculate P_e using the formula:

$$P_e = \frac{\gamma H + q - \gamma_w H_w{}'}{\mu_q \mu_w{}'}$$ (E-9)

where

H_w' = height of water within slope (L)

μ_w' = seepage correction factor (Figure E-3)

The other factors are as defined previously.

$H_w{}'$ is the average level of the piezometric surface within the slope. For steady seepage conditions this is related to the position of the phreatic surface beneath the crest of the slope as shown in Figure E-6 (after Duncan, Buchignani, and DeWet 1987). If the circle being studied passes above the toe of the slope, H_w' is measured relative to the adjusted toe.
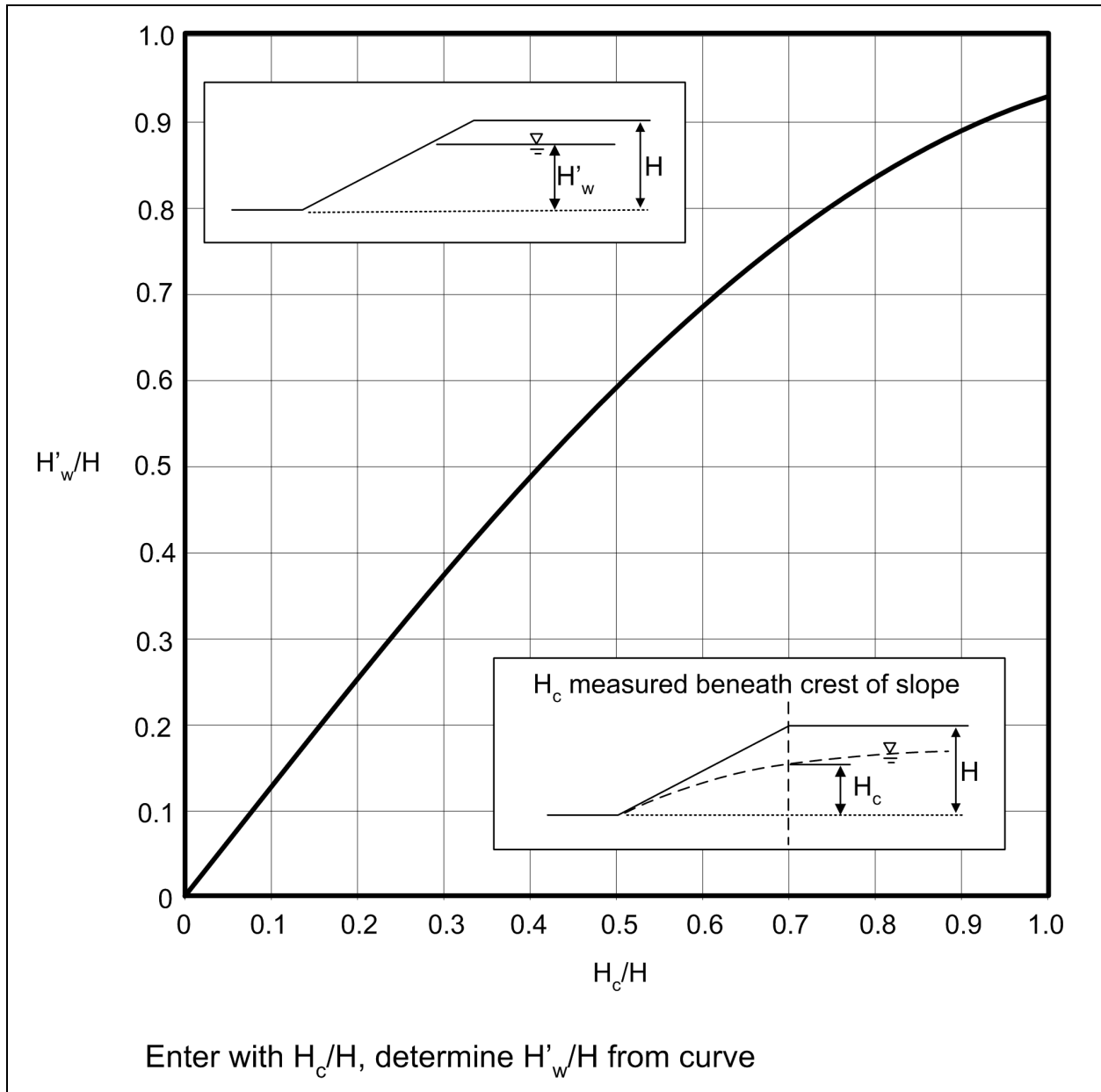
Figure E-6. Steady seepage adjustment factor $\phi > 0$ soils (after Duncan, Buchianani, and DeWet 1987)

$\mu_w' = 1$, if there is no seepage

$\mu_q = 1$, if there is no surcharge

In a total stress analysis, internal pore water pressure is not considered, so $H_w' = 0$ and $\mu_w' = 1$ in the formula for P_e.

(4) Calculate the dimensionless parameter $\lambda_{c\phi}$ using the formula:

$$\lambda_{c\phi} = \frac{P_e \tan \phi}{c}$$ (E-10)

where

ϕ = average value of ϕ

c = average value of c (F/L^2)

For c = 0, $\lambda_{c\phi}$ is infinite. Use the charts for infinite slopes in this case. Steps 4 and 5 are iterative steps. On the first iteration, average values of tan ϕ and c are estimated using judgment rather than averaging.

(5) Using the chart at the top of Figure E-5, determine the center coordinates of the circle being investigated.

(a) Plot the critical circle on a scaled cross section of the slope, and calculate the weighted average values of ϕ and c using Equations E-1 and E-2.

(b) Return to Step 4 with these average values of the shear strength parameters, and repeat this iterative process until the value of $\lambda_{c\phi}$ becomes constant. Usually one iteration is sufficient.

(6) Using the chart at the left side of Figure E-5, determine the value of the stability number N_{cf}, which depends on the slope angle, β, and the value of $\lambda_{c\phi}$.

(7) Calculate the factor of safety, F, using the formula:

$$F = N_{cf} \frac{c}{P_d} \tag{E-11}$$

The example problems in Figures E-11 and E-12 illustrate the use of these methods for total stress and effective stress analyses.

E-5. Infinite Slope Analyses

a. Two types of conditions can be analyzed using the charts shown in Figure E-7: These are:

(1) Slopes in cohesionless materials, where the critical failure mechanism is shallow sliding or surface raveling.

(2) Slopes in residual soils, where a relatively thin layer of soil overlies firmer soil or rock, and the critical failure mechanism is sliding along a plane parallel to the slope, at the top of the firm layer.

b. Steps for use of the charts for effective stress analyses:

(1) Determine the pore pressure ratio, r_u, which is defined by the formula:

$$r_u = \frac{u}{\gamma H} \tag{E-12}$$
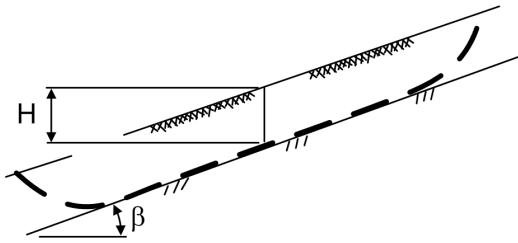
γ = total unit weight of soil

γ_w = unit weight of water

c' = cohesion intercept

ϕ' = friction angle

r_u = pore pressure ratio = $u/\gamma H$

u = pore pressure at depth H

Seepage parallel to slope

$$r_u = \frac{X}{T}\frac{\gamma_w}{\gamma}\cos^2\beta$$
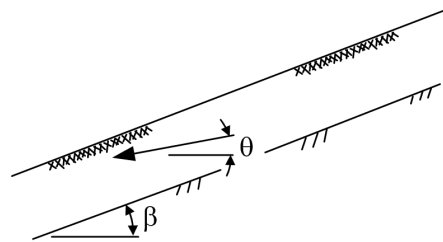
Seepage emerging from slope

$$r_u = \frac{\gamma_w}{\gamma}\frac{1}{1+\tan\beta\tan\theta}$$
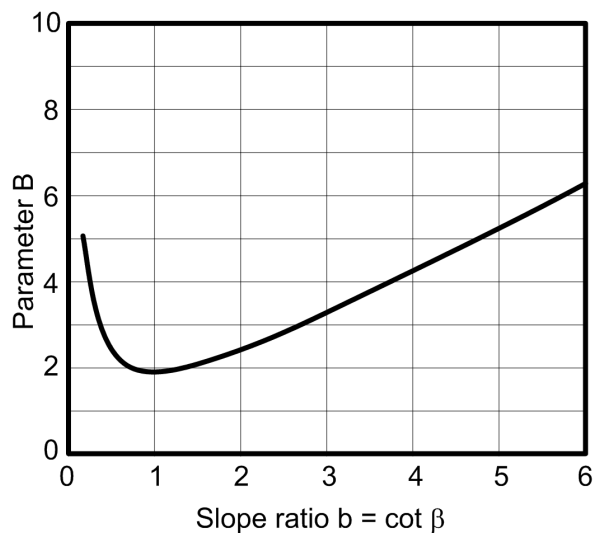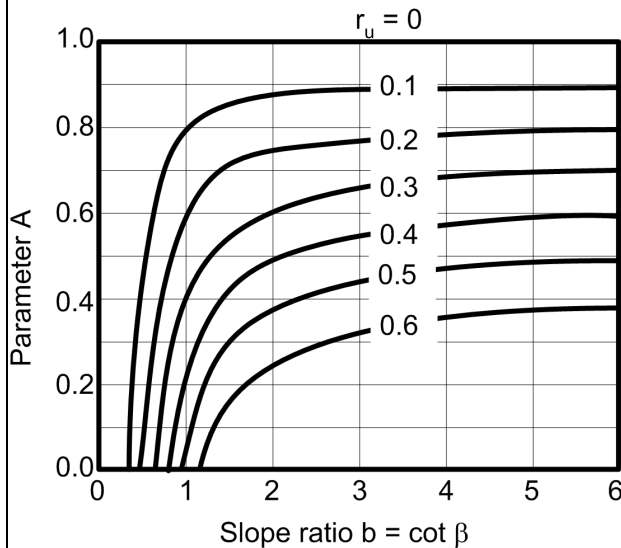
Steps:

1. Determine r_u from measured pore pressure or formulas at right.

2. Determine A and B from charts below.

3. Calculate $$F = A\frac{\tan\phi'}{\tan\beta} + B\frac{c'}{\gamma H}$$

Figure E-7.   Slope stability charts for infinite slopes (after Duncan, Buchianani, and DeWet 1987)

where

u = pore pressure (F/L^2)

γ = total unit weight of soil (F/L^3)

H = depth corresponding to pore pressure, u (L)

(a) For an existing slope, the pore pressure can be determined from field measurements, using piezometers installed at the depth of sliding, or estimated for the most adverse anticipated seepage condition.

(b) For seepage parallel to the slope, which is a condition frequently used for design, the value of r_u can be calculated using the following formula:

$$r_u = \frac{X}{T}\frac{\gamma_w}{\gamma}\cos^2\beta \tag{E-13}$$

where

X = distance from the depth of sliding to the surface of seepage, <u>measured normal to the surface of the slope</u> (L)

T = distance from the depth of sliding to the surface of the slope, <u>measured normal to the surface of the slope</u> (L)

γ_w = unit weight of water (F/L^3)

γ = total unit weight of soil (F/L^3)

β = slope angle

(c) For seepage emerging from the slope, which is more critical than seepage parallel to the slope, the value or r_u can be calculated using the following formula:

$$r_u = \frac{\gamma_w}{\gamma}\frac{1}{1 + \tan\beta\tan\theta} \tag{E-14}$$

where

θ = angle of seepage measured from the horizontal direction

The other factors are as defined previously.

(1) Submerged slopes with no excess pore pressures can be analyzed using $\gamma = \gamma_b$ (buoyant unit weight) and $r_u = 0$.

(2) Determine the values of the dimensionless parameters A and B from the charts at the bottom of Figure E-7.

(3) Calculate the factor of safety, F, using Equation E-15:

$$F = A\frac{\tan\phi'}{\tan\beta} + B\frac{c'}{\gamma H} \tag{E-15}$$

where

ϕ' = angle of internal friction in terms of effective stress

c' = cohesion intercept in terms of effective stress (F/L^2)

β = slope angle

H = depth of sliding mass <u>measured vertically</u> (L)

The other factors are as defined previously.

c. Steps for use of charts for total stress analyses:

(1) Determine the value of B from the chart in the lower right corner of Figure E-7.

(2) Calculate the factor of safety, F, using the formula:

$$F = \frac{\tan\phi}{\tan\beta} + B\frac{c}{\gamma H} \tag{E-16}$$

where

ϕ = angle of internal friction in terms of total stress

c = cohesion intercept in terms of total stress (F/L^2)

The other factors are as defined previously.

The example in Figure E-13 illustrates use of the infinite slope stability charts.

E-6. Soils with $\phi = 0$ and Strength Increasing with Depth

The chart for slopes in soils with $\phi = 0$ and strength increasing with depth is shown in Figure E-8. Steps for use of the chart are:

a. Select the linear variation of strength with depth that best fits the measured strength data. As shown in Figure E-8, extrapolate this straight line upward to determine H_o, the height at which the straight line intersects zero.

b. Calculate $M = H_o/H$, where H = slope height.

c. Determine the dimensionless stability number, N, from the chart in the lower right corner of Figure E-8.

d. Determine the value of c_b, the strength at the elevation of the bottom (the toe) of the slope.

Steps

1. Extrapolate strength profile upward to determine value of H_0, where strength profile intersects zero.

2. Calculate $M = H_0/H$.

3. Determine stability number from chart below.

4. Determine c_b = strength at elevation of toe of slope.

5. Calculate $$F = N\frac{c_b}{\gamma(H+H_0)}$$

Use $\gamma = \gamma_{buoyant}$ for submerged slope

Use $\gamma = \gamma_{total}$ for no water outside slope

Use average γ for partly submerged slope
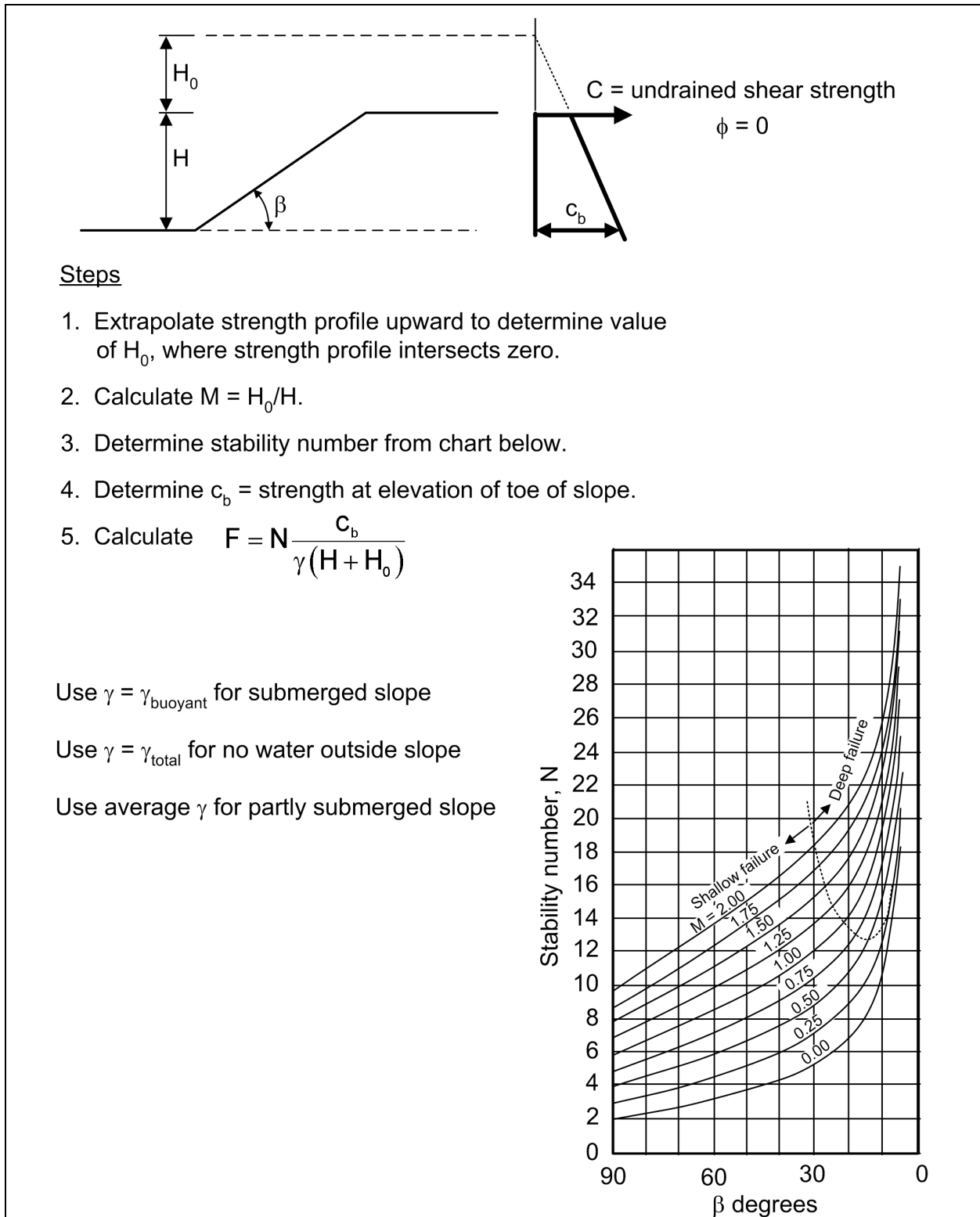
Figure E-8.   Slope stability chart for $\phi = 0$ soils, with strength increasing with depth (after Hunter and Schuster 1968)

e. Calculate the factor of safety, F, using the formula:

$$F = N \frac{c_b}{\gamma(H + H_o)} \tag{E-17}$$

where

γ = total unit weight of soil for slopes above water

γ = buoyant unit weight for submerged slopes

γ = weighted average unit weight for partly submerged slopes

The example shown in Figure E-14 illustrates use of the stability chart shown in Figure E-8.

Example Problem E-1

Figure E-9 shows a slope in $\phi = 0$ soil. There are three layers with different strengths. There is water outside the slope.
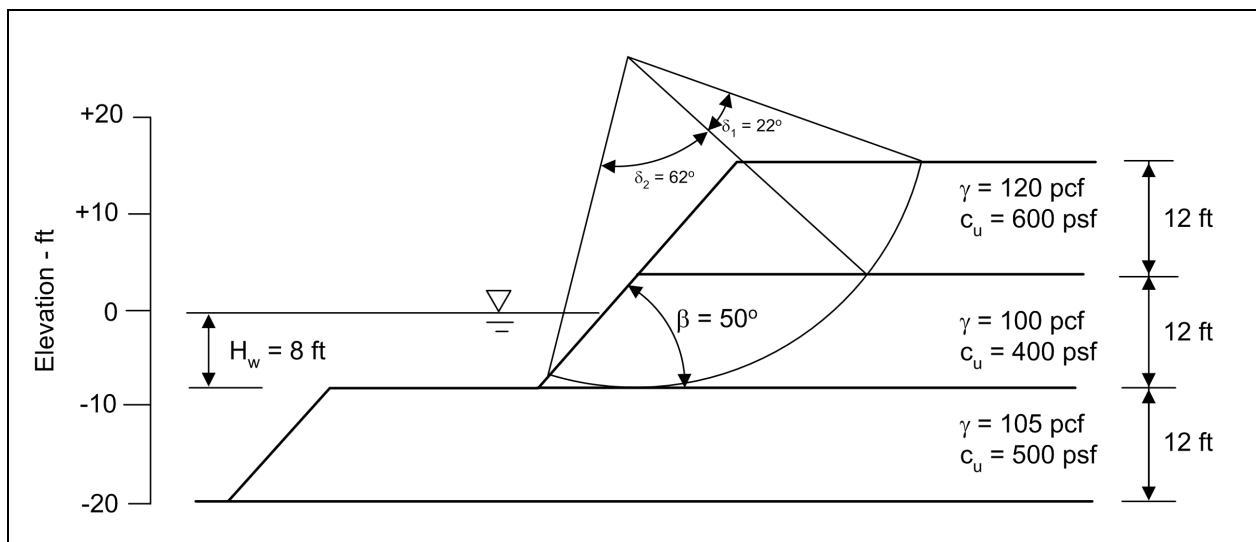
Figure E-9. Example for a circle tangent to elevation –8ft for cohesive soil with $\phi = 0$

Two circles were analyzed for this slope -- a shallow circle tangent to elevation -8 ft, and a deep circle tangent to elevation -20 ft.

The shallower circle, tangent to elevation –8 ft, is analyzed first.

For this circle:

$$d = \frac{D}{H} = \frac{0}{24} = 0$$

$$\frac{H_w}{H} = \frac{8}{24} = 0.33$$

Using the charts at the top of Figure E-1, with $\beta = 50°$ and $d = 0$:

$x_o = 0.35$ and $y_o = 1.4$

$X_o = (H)(x_o) = (24)(0.35) = 8.4$ ft

$Y_o = (H)(y_o) = (24)(1.4) = 33.6$ ft

Plot the critical circle on the slope. The circle is shown in Figure E-9.

Measure the central angles of arc in each layer using a protractor. Calculate the weighted average strength parameter c_{avg} using Equation E-1.

$$c_{avg} = \frac{\sum \delta_i c_i}{\sum \delta_i} = \frac{(22)(600) + (62)(400)}{22 + 62} = 452 \text{ psf}$$

From Figure E-3, with $\beta = 50°$ and $\frac{H_w}{H} = 0.33$, find $\mu_w = 0.93$.

Use layer thickness to average the unit weights. Unit weights are averaged only to the bottom of the critical circle.

$$\gamma_{avg} = \frac{\sum \gamma_i h_i}{\sum h_i} = \frac{(120)(10) + (100)(10)}{10 + 10} = 110$$

Calculate the driving force term P_d as follows:

$$P_d = \frac{\gamma H + q - \gamma_w H_w}{\mu_q \mu_w \mu_t} = \frac{(110)(24) + 0 - (62.4)(8)}{(1)(0.93)(1)} = 2302$$

From Figure E-1, with $d = 0$ and $\beta = 50°$, find $N_o = 5.8$:

Calculate the factor of safety using Equation E-7:

$$F = \frac{N_o c}{P_d} = \frac{(5.8)(452)}{2302} = 1.14$$

Example Problem E-2

Figure E-10 shows the same slope as in Figure E-9.

The deeper circle, tangent to elevation –20 ft, is analyzed as follows:
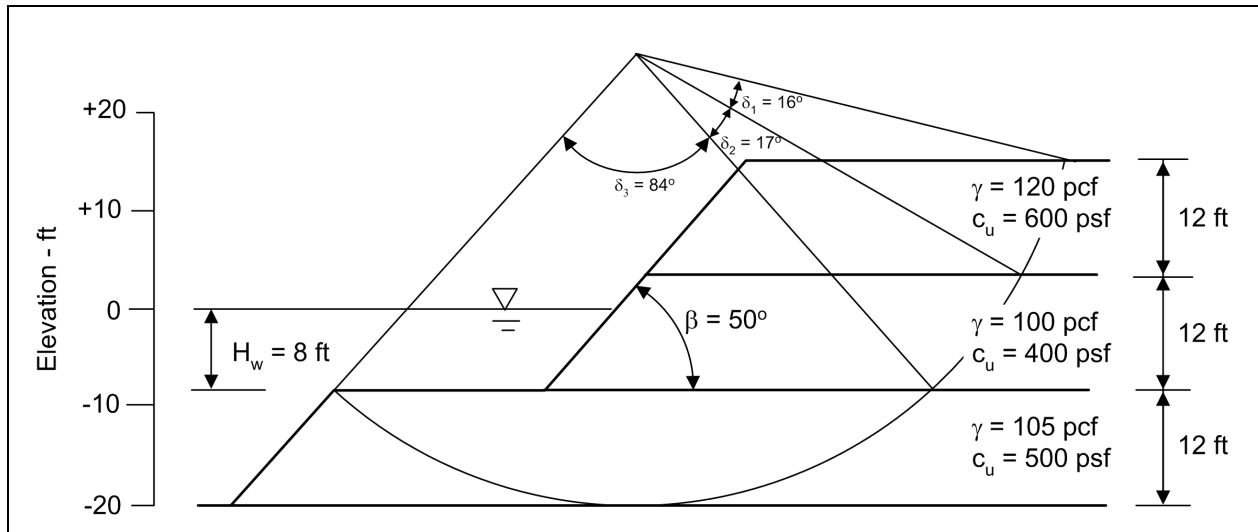
Figure E-10. Example for a circle tangent to elevation –20 ft for cohesive soil with $\phi = 0$

For this circle:

$$d = \frac{D}{H} = \frac{12}{24} = 0.5$$

$$\frac{H_w}{H} = \frac{8}{24} = 0.33$$

Using the charts at the bottom of Figure E-1, with $\beta = 50°$ and d = 0.5:

$x_o = 0.35$ and $y_o = 1.5$

$X_o = (H)(x_o) = (24)(0.35) = 8.4$ ft

$Y_o = (H)(y_o) = (24)(1.5) = 36$ ft

Plot the critical circle on the slope as shown in Figure E-10.

Measure the central angles of arc in each layer using a protractor. Calculate the weighted average strength parameter c_{avg}: using Equation E-1.

$$c_{avg} = \frac{\sum \delta_i c_i}{\sum \delta_i} = \frac{(16)(600) + (17)(400) + (84)(500)}{16 + 17 + 84} = 499 \text{ psf}$$

From Figure E-3, with d = 0.5 and $\frac{H_w}{H} = 0.33$:

$\mu_w = 0.95$

Use layer thickness to average the unit weights. Since the material below the toe of the slope is a $\phi = 0$ material, the unit weight is averaged only down to the toe of the slope. The unit weight below the toe has no influence on stability if $\phi = 0$.

$$\gamma_{avg} = \frac{\sum \gamma_i h_i}{\sum h_i} = \frac{(120)(10) + (100)(10)}{10 + 10} = 110$$

Calculate the driving force term P_d as follows:

$$P_d = \frac{\gamma H + q - \gamma_w H_w}{\mu_q \mu_w \mu_t} = \frac{(110)(24) + 0 - (62.4)(8)}{(1)(0.95)(1)} = 2253$$

From Figure E-1, with d = 0.5 and $\beta = 50°$, $N_o = 5.6$:

Calculate the factor of safety using Equation E-7:

$$F = \frac{N_o c}{P_d} = \frac{(5.6)(499)}{2253} = 1.24$$

This circle is less critical than the circle tangent to elevation –8 ft, analyzed previously.

Example Problem E-3

Figure E-11 shows a slope in soils with both c and ϕ. There are three layers with different strengths. There is no water outside the slope.
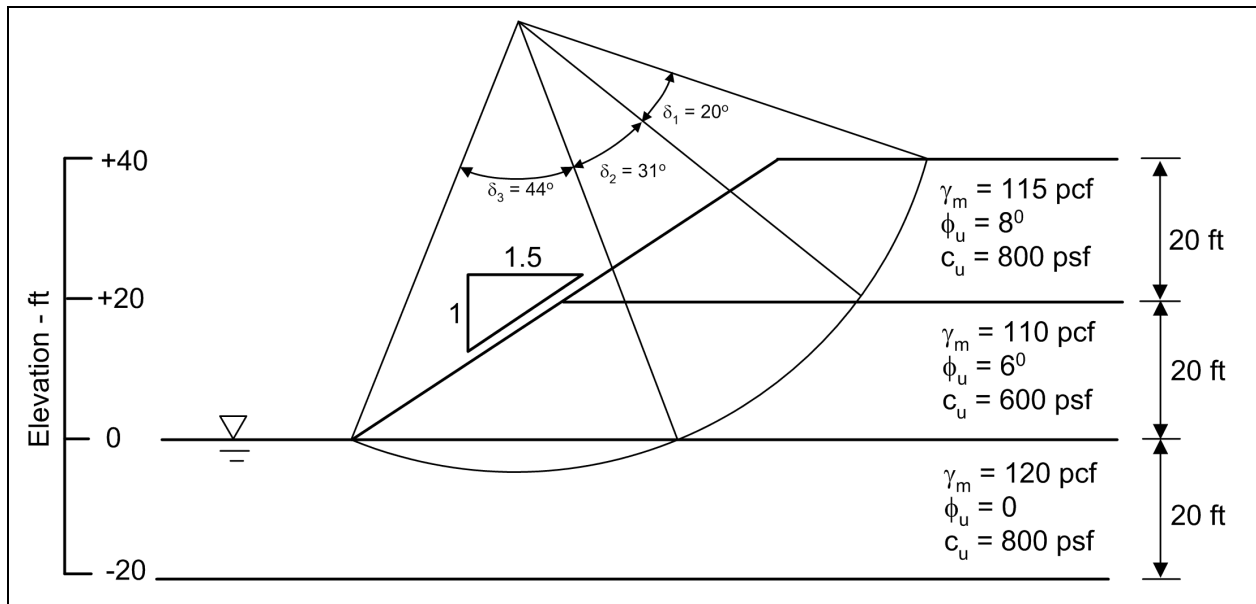
Figure E-11. Example for a total stress analysis of a toe circle in soils with both c and ϕ

The factor of safety for a toe circle is calculated as follows:

Use layer thickness to average the unit weights. Unit weights are averaged down to the toe of the slope, since the unit weight of the material below the toe has no effect on stability in this case.

$$\gamma_{avg} = \frac{\sum \gamma_i h_i}{\sum h_i} = \frac{(115)(10) + (110)(10)}{10 + 10} = 112.5$$

Since there is no surcharge, $\mu_q = 1$

Since there is no external water above toe, $\mu_w = 1$

Since there is no seepage, $\mu_w' = 1$

Since there are no tension cracks, $\mu_t = 1$

Calculate the driving force term P_d as follows:

$$P_d = \frac{\gamma H + q - \gamma_w H_w}{\mu_q \mu_w \mu_t} = \frac{(112.5)(40)}{(1)(1)(1)} = 4500 \text{ psf}$$

Calculate P_e as follows:

$$P_e = \frac{\gamma H + q - \gamma_w H_w'}{\mu_q \mu_w'} = \frac{(112.5)(40)}{(1)(1)} = 4500 \text{ psf}$$

Estimate $c_{avg} = 700$ psf and $\phi_{avg} = 7°$, and calculate $\lambda_{c\phi}$ as follows:

$$\lambda_{c\phi} = \frac{P_e \tan \phi}{c} = \frac{(4500)(0.122)}{700} = 0.8$$

From Figure E-5, with b = 1.5 and $\lambda_{c\phi} = 0.8$:

$x_o = 0.6$ and $y_o = 1.5$

$X_o = (H)(x_o) = (40)(0.6) = 24$ ft

$Y_o = (H)(y_o) = (40)(1.5) = 60$ ft

Plot the critical circle on the given slope, as shown in Figure E-11.

Calculate c_{avg}, $\tan \phi_{avg}$, and $\lambda_{c\phi}$ as follows:

$$c_{avg} = \frac{\sum \delta_i c_i}{\sum \delta_i} = \frac{(20)(800) + (31)(600) + (44)(800)}{20 + 31 + 44} = 735 \text{ psf}$$

$$\tan\phi_{avg} = \frac{\sum \delta_i \tan\phi_i}{\sum \delta_i} = \frac{(20)(\tan 8°) + (31)(\tan 6°) + (44)(\tan 0°)}{20 + 31 + 44} = 0.064$$

$$\lambda_{c\phi} = \frac{P_e \tan\phi}{c} = \frac{(4500)(0.064)}{735} = 0.4$$

From Figure E-5, with b = 1.5 and $\lambda_{c\phi}$ = 0.4:

x_o = 0.65 and y_o = 1.45

X_o = (H)(x_o) = (40)(0.65) = 26 ft

Y_o = (H)(y_o) = (40)(1.45) = 58 ft

This circle is close to the previous iteration, so keep $\lambda_{c\phi}$ = 0.4 and c_{avg} = 735 psf

From Figure E-5, with b = 1.5 and $\lambda_{c\phi}$ = 0.4

N_{cf} = 6

Calculate the factor of safety as follows:

$$F = N_{cf}\frac{c}{P_d} = 6.0\frac{735}{4500} = 1.0$$

Example Problem E-4

Figure E-12 shows the same slope as shown in Figure E-11. Effective stress strength parameters are shown in the figure, and the analysis is performed using effective stresses. There is water outside the slope, and seepage within the slope.

Use layer thickness to average the unit weights. Unit weights are averaged only down to the toe of the slope.

$$\gamma_{avg} = \frac{\sum \gamma_i h_i}{\sum h_i} = \frac{(115)(10) + (115)(10)}{10 + 10} = 115$$

For this slope:

$$\frac{H_w}{H} = \frac{10}{40} = 0.25$$

$$\frac{H_w{'}}{H} = \frac{30}{40} = 0.75$$

Since there is no surcharge, μ_q = 1
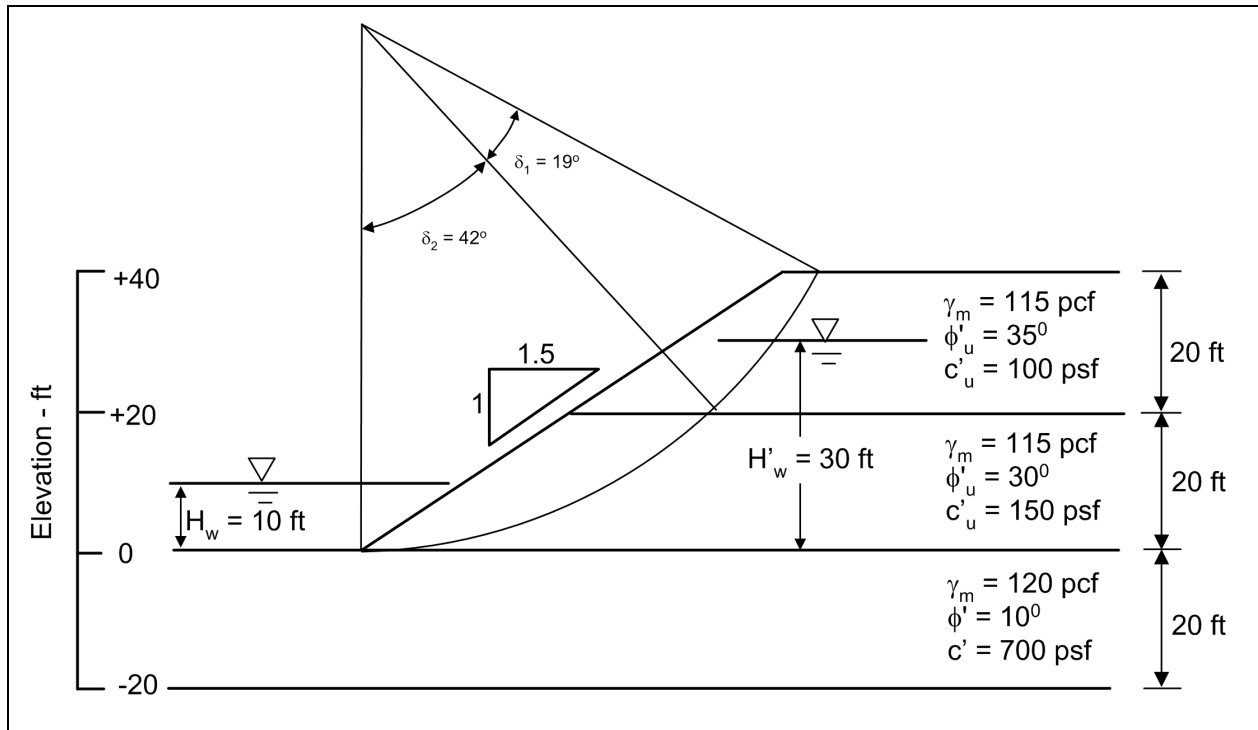
Figure E-12.   Example for an effective stress analysis of a toe circle in soils with both c′ and ϕ′

Using Figure E-3 for toe circles, with $H_w/H = 0.25$ and $\beta = 33.7°$, find $\mu_w = 0.96$

Using Figure E-3 for toe circles, with $H_w'/H = 0.75$ and $\beta = 33.7°$, find $\mu_w' = 0.95$

Since there are no tension cracks, $\mu_t = 1$

Calculate the driving force term P_d as follows:

$$P_d = \frac{\gamma H + q - \gamma_w H_w}{\mu_q \mu_w \mu_t} = \frac{(115)(40) + 0 - (62.4)(10)}{(1)(0.96)(1)} = 4141 \text{ psf}$$

Calculate P_e as follows:

$$P_e = \frac{\gamma H + q - \gamma_w H_w{}'}{\mu_q \mu_w{}'} = \frac{(115)(40) + 0 - (62.4)(30)}{(1)(0.95)} = 2870 \text{ psf}$$

Estimate $c_{avg} = 120$ psf and $\phi_{avg} = 33°$

$$\lambda_{c\phi} = \frac{P_e \tan \phi}{c} = \frac{(2870)(0.64)}{120} = 15.3$$

From Figure E-5, with b = 1.5 and $\lambda_{c\phi} = 15.3$:

$x_o = 0$ and $y_o = 1.9$

$X_o = (H)(x_o) = (40)(0) = 0$ ft

$Y_o = (H)(y_o) = (40)(1.9) = 76$ ft

Plot the critical circle on the given slope as shown in Figure E-12.

Calculate c_{avg}, $\tan \phi_{avg}$, and $\lambda_{c\phi}$ as follows:

$$c_{avg} = \frac{\sum \delta_i c_i}{\sum \delta_i} = \frac{(19)(100) + (42)(150)}{19 + 42} = 134 \text{ psf}$$

$$\tan \phi_{avg} = \frac{\sum \delta_i \tan \phi_i}{\sum \delta_i} = \frac{(19)(\tan 35°) + (42)(\tan 30°)}{19 + 42} = 0.62$$

$$\lambda_{c\phi} = \frac{(2870)(0.62)}{134} = 13.3$$

From Figure E-5, with b = 1.5 and $\lambda_{c\phi}$ = 13.3:

$x_o = 0.02$ and $y_o = 1.85$

$X_o = (H)(x_o) = (40)(0.02) = 0.8$ ft

$Y_o = (H)(y_o) = (40)(1.85) = 74$ ft

This circle is close to the previous iteration, so keep $\lambda_{c\phi}$ = 13.3 and c_{avg} = 134 psf

From Figure E-5, with b = 1.5 and $\lambda_{c\phi}$ = 13.3:

$N_{cf} = 35$

Calculate the factor of safety as follows:

$$F = N_{cf} \frac{c}{P_d} = 35 \frac{134}{4141} = 1.13$$

Example Problem E-5

Figure E-13 shows a slope where a relatively thin layer of soil overlies firm soil. The critical failure mechanism for this example is sliding along a plane parallel to the slope, at the top of the firm layer. This slope can be analyzed using the infinite slope stability chart shown in Figure E-7.

Calculate the factor of safety for seepage parallel to the slope and for horizontal seepage emerging from the slope.
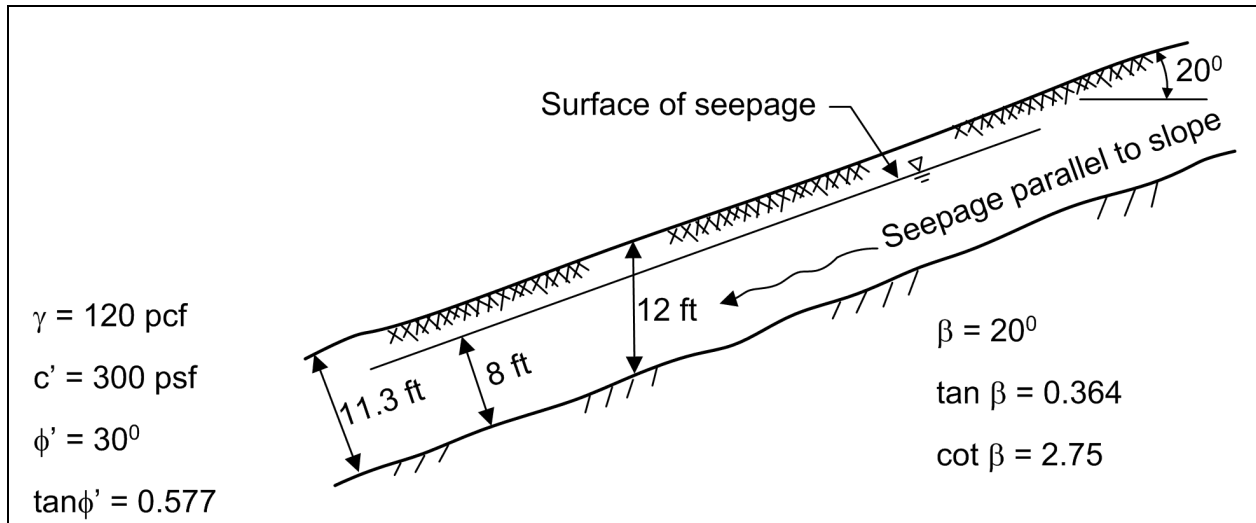
Figure E-13. Example of an infinite slope analysis

For seepage parallel to slope:

X = 8 ft and T = 11.3 ft

$$r_u = \frac{X}{T}\frac{\gamma_w}{\gamma}\cos^2\beta = \frac{8}{11.3}\frac{62.4}{120}(0.94)^2 = 0.325$$

From Figure E-7, with $r_u = 0.325$ and cot $\beta = 2.75$:

A = 0.62 and B = 3.1

Calculate the factor of safety, as follows:

$$F = A\frac{\tan\phi'}{\tan\beta} + B\frac{c'}{\gamma H} = 0.62\frac{0.577}{0.364} + 3.1\frac{300}{(120)(12)} = 0.98 + 0.65 = 1.63$$

For horizontal seepage emerging from slope, $\theta = 0º$

$$r_u = \frac{\gamma_w}{\gamma}\frac{1}{1+\tan\beta\tan\theta} = \frac{62.4}{120}\frac{1}{1+(0.364)(0)} = 0.52$$

From Figure E-7, with $r_u = 0.52$ and cot $\beta = 2.75$:

A = 0.41 and B = 3.1

Calculate the factor of safety, as follows:

$$F = A\frac{\tan\phi'}{\tan\beta} + B\frac{c'}{\gamma H} = 0.41\frac{0.577}{0.364} + 3.1\frac{300}{(120)(12)} = 0.65 + 0.65 = 1.30$$

Note that the factor of safety for seepage emerging from the slope is smaller than the factor of safety for seepage parallel to the slope.

Example Problem E-6

Figure E-14 shows a submerged clay slope with $\phi = 0$ and strength is increasing linearly with depth.
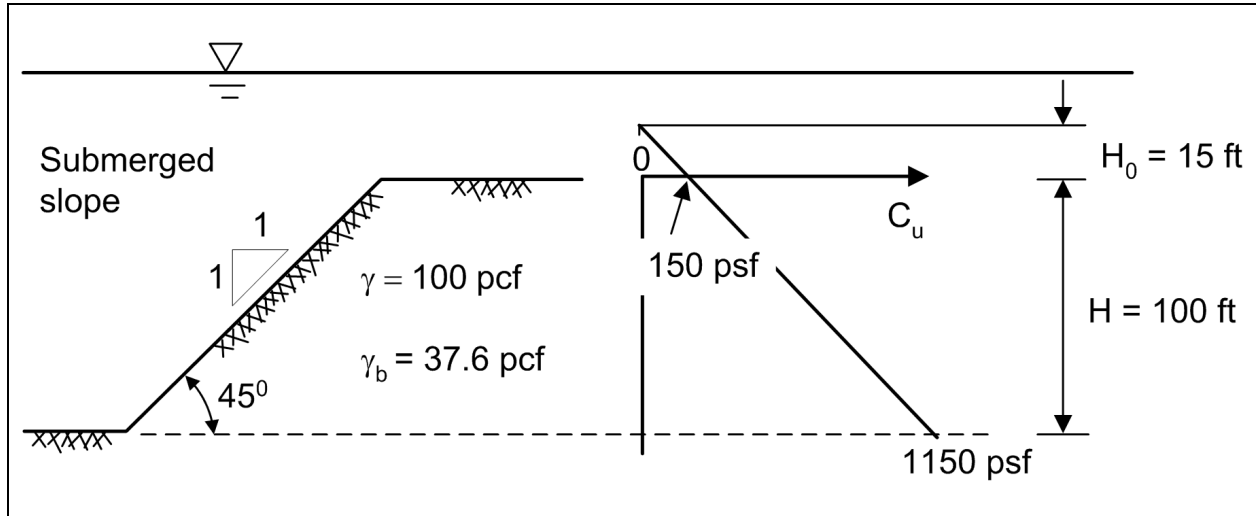
Figure E-14.   Example of $\phi = 0$, and strength increasing with depth

The factor of safety is calculated using the slope stability chart shown in Figure E-8.

Extrapolating the strength profile up to zero gives $H_o = 15$ ft

Calculate M as follows:

$$M = \frac{H_o}{H} = \frac{15}{100} = 0.15$$

From Figure E-8, with $M = 0.15$ and $\beta = 45°$:

$N = 5.1$

From the soil strength profile, $c_b = 1150$ psf:

Calculate the factor of safety as follows:

$$F = N \frac{c_b}{\gamma(H + H_o)} = (5.1)\frac{1150}{(37.6)(115)} = 1.36$$

Appendix F
Example Problems and Calculations

F-1. General

This appendix presents a series of example problems and calculations. The examples illustrate the procedures used in the Simplified Bishop and Modified Swedish methods of slope stability analysis and provide guidance for checking and verifying the results of slope stability analyses. Examples for end-of-construction and steady seepage conditions are presented in this appendix. Examples for rapid drawdown are presented in Appendix G.

a. Manual and spreadsheet calculations of the type described here are performed to check the results of computer analyses of slope stability. These analyses are performed to check the factors of safety calculated for the critical slip surface, and for other slip surfaces considered significant. The slip surfaces used for these examples were selected to illustrate the computational procedures and are not the most critical slip surfaces for the slopes.

b. As discussed elsewhere in this manual, the soil mass above the slip surface is subdivided into vertical slices. Computer programs use more slices than are needed for hand calculations. Six to twelve slices are sufficient for hand calculations. Fewer than 6 slices do not provide sufficient accuracy, and more than 12 slices makes the computations unwieldy, especially for computations using graphical methods.

c. In the following examples, computations are performed beginning with the uppermost slice near the top of the slope and proceeding to the toe area, regardless of the direction that the slope faces. Thus, in some cases the computations are performed for slices from left-to-right and in other cases for slices from right-to-left, depending on the direction that the slope faces.

d. All of the computations for the procedures of slices were initially performed using a computer spreadsheet program and then summarized in tabular form. The spreadsheet calculations were performed with the number of significant figures used by the spreadsheet program, with no arithmetic rounding. Values were rounded as appropriate for the tables presented in this appendix. Accordingly, some of the values may differ slightly from what might be calculated by hand. For example the value shown for the term $W \sin \alpha$ may not be exactly equal to the values that would be computed using the values of the slice weight (W) and the slope of the base of the slice (α) shown in the tables. Any such discrepancies caused by rounding off are insignificant.

F-2. Simplified Bishop Method

The Simplified Bishop Method is only applicable to analyses with circular slip surfaces. The computations shown here have been performed using computer spreadsheet software. Detailed steps are presented below for a total stress analysis of a slope with no water and for an effective stress analysis of a slope with water, internal seepage, and external water loads.

a. Slope without seepage or external water loads – total stress analyses. Computations for the Simplified Bishop Method for slopes, where the shear strength is expressed in terms of total stresses and where there are no external water loads, are illustrated in Figure F-1. As for all of the examples presented, slices are numbered beginning with the uppermost slice and proceeding toward the toe of the slope. Once a trial slip surface has been selected, and the soil mass is subdivided into slices, the following steps are used to compute a factor of safety:

a. Slope and trial slip surface with slices

1	2	3	4	5	6	7	8	9	10	11	12	13	14	15	16
Slice	Horizontal Width (b)	Average Height (h_{avg})	Area (A)	Weight (W)	Base Inclination (α)	W sin α	Cohesion (c)	Friction Angle (ϕ)	$cb + W\tan\phi$	m_α (Trial F_1)	Numerator (Col. 10 ÷ Col. 11)	m_α (Trial F_2)	Numerator (Col. 11 ÷ Col. 13)	m_α (Trial F_3)	Numerator (Col. 11 ÷ Col. 15)
1	. . .	. . .	. . .	. . .	. . .	. . .	. . .	. . .	. . .	. . .	. . .	. . .	. . .	. . .	. . .
2	. . .	. . .	. . .	. . .	. . .	. . .	. . .	. . .	. . .	. . .	. . .	. . .	. . .	. . .	. . .
3	. . .	. . .	. . .	. . .	. . .	. . .	. . .	. . .	. . .	. . .	. . .	. . .	. . .	. . .	. . .
4	. . .	. . .	. . .	. . .	. . .	. . .	. . .	. . .	. . .	. . .	. . .	. . .	. . .	. . .	. . .
5	. . .	. . .	. . .	. . .	. . .	. . .	. . .	. . .	. . .	. . .	. . .	. . .	. . .	. . .	. . .
6	. . .	. . .	. . .	. . .	. . .	. . .	. . .	. . .	. . .	. . .	. . .	. . .	. . .	. . .	. . .
7	. . .	. . .	. . .	. . .	. . .	. . .	. . .	. . .	. . .	. . .	. . .	. . .	. . .	. . .	. . .
8	. . .	. . .	. . .	. . .	. . .	. . .	. . .	. . .	. . .	. . .	. . .	. . .	. . .	. . .	. . .
9	. . .	. . .	. . .	. . .	. . .	. . .	. . .	. . .	. . .	. . .	. . .	. . .	. . .	. . .	. . .

Σ W sinα = ⎣ . . . ⎦ Σ_1 = ⎣ . . . ⎦ Σ_2 = ⎣ . . . ⎦ Σ_3 = ⎣ . . . ⎦

b. Table used to compute factor of safety

c. Assumed and calculated trial values for factor of safety

Figure F-1.   Simplified Bishop Method with no water - total stress analyses

(1) The width, b, average height, h_{avg}, and inclination, α, of the bottom of each slice are determined (Columns 2, 3, and 6 in Figure F-1b). The sign convention used throughout this appendix for the inclination, α, is illustrated in Figure F-2. The inclination is positive when the base of the slice is inclined in the same direction as the slope.

(2) The area, A, of each slice is calculated by multiplying the width of the slice by the average height, i.e., $A = b\,h_{avg}$ (Column 4 in Figure F-1b).

(3) The weight of each slice is calculated by multiplying the total unit weight of soil by the area of the slice, i.e., $W = \gamma A$. If the slice crosses zones having different unit weights, the slice is subdivided vertically into subareas, and the weights of the subareas are summed to compute the total slice weight (Column 5 in Figure F-1b).

(4) The quantity, $W \sin \alpha$, is computed for each slice, and these values are summed to obtain the term in the denominator of the equation for the factor of safety (Column 7 in Figure F-1b).

a. Left-facing slope

b. Right-facing slope
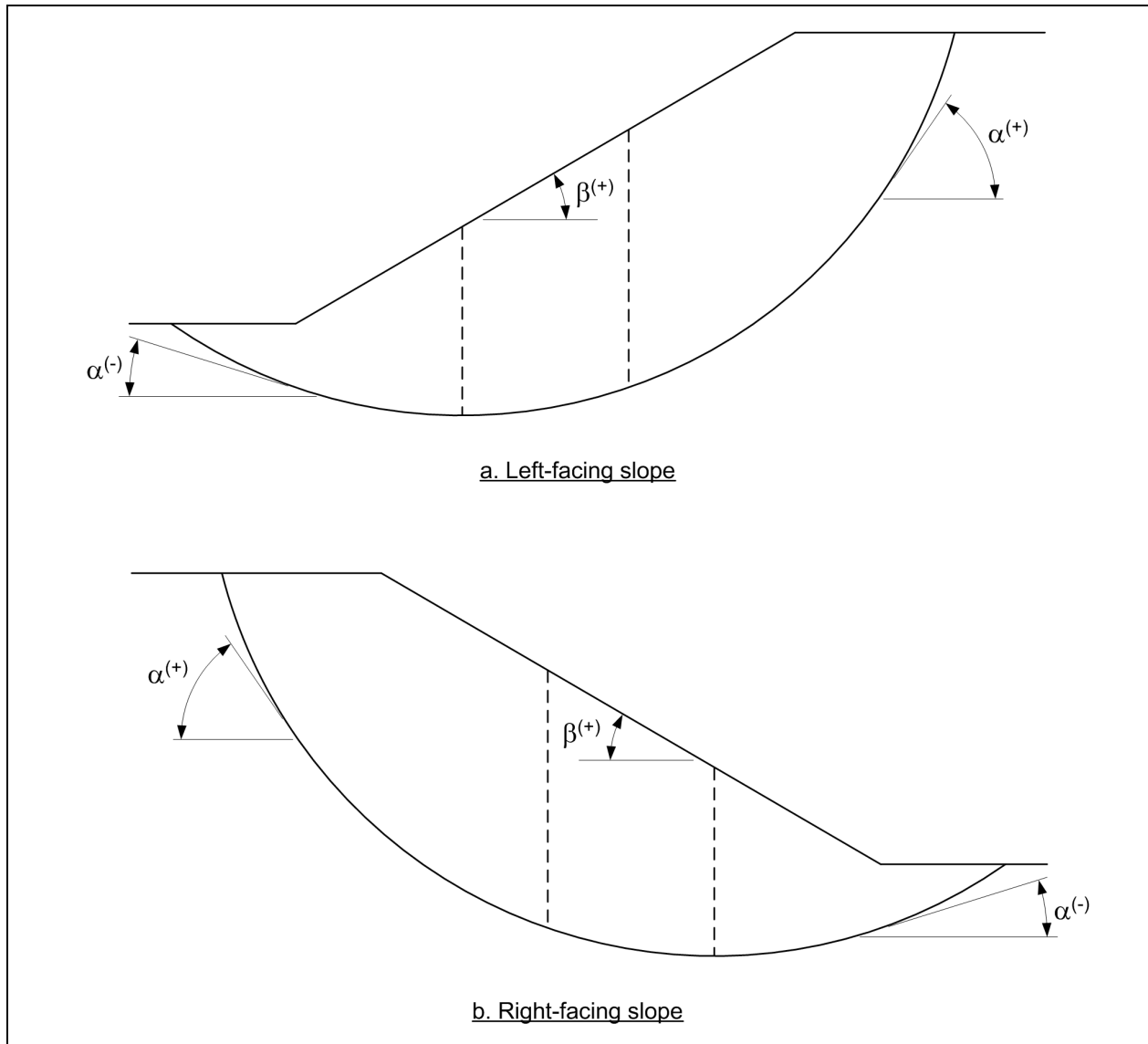
Figure F-2.   Sign convention used for angles α and β

(5) The cohesion, c, and friction angle, ϕ, for each slice are entered in Columns 8 and 9 in Figure F-1b. The shear strength parameters are those for the soil at the bottom of the slice; they do not depend on the soils in the upper portions of the slice.

(6) The quantity $c \cdot b + W \tan(\phi)$ is computed for each slice (Column 10 in Figure F-1b).

(7) A trial value is assumed for the factor of safety and the quantity, m_α, is computed from the equation shown below (Column 11 in Figure F-1b):

$$m_\alpha = \cos\alpha + \frac{\sin\alpha \tan\phi'}{F}$$

(F-1)

(8) The numerator in the expression for the factor of safety is computed by dividing the term cb + W tan(ϕ) by m_α for each slice and then summing the values for all slices (Column 12 in Figure F-1b).

(9) A new factor of safety is computed from the equation:

$$F = \frac{\sum \left[\dfrac{c \cdot b + W \cdot \tan \phi}{m_\alpha} \right]}{\sum W \sin \alpha}$$

(F-2)

This corresponds to dividing the summation of Column 12 by the summation of Column 7 in Figure F-1b.

(10) Additional trial values are assumed for the factor of safety and Steps 7 through 9 are repeated (Columns 13 through 16 in Figure F-1b). For each trial value assumed for the factor of safety, the assumed value and the value computed for the factor of safety using Equation F-2 are plotted as shown in Figure F-1c. The chart in Figure F-1c serves as a guide for selecting additional trial values. Values are assumed and new values are calculated until the assumed and calculated values for the factor of safety are essentially the same, i.e., until the assumed and calculated values fall close to the broken 45-degree line shown in Figure F-1c.

b. Slope with seepage or external water loads – effective stress analyses. Computations for slopes where the shear strength is expressed in terms of effective stresses, and where there are pore water pressures and external water loads, are illustrated in Figure F-3. In this case, the pore water pressures on the base of each slice must be determined. Loads from external water are included in all analyses, whether they are performed using total stress or effective stress. External water may be represented either as another soil, as described in Appendix C, or as an external force. In the description which follows, water is represented as an external load rather than as soil. Accordingly, a force on the top of the slice and the moment the force produces about the center of the circle must be computed. For a given trial circle, the following steps are required:

(1) For each slice the width, b, bottom inclination, α, and average height, $h_{avg.}$, are determined (Columns 2, 3, and 6 in Figure F-3c). The sign convention used for the angle, α, is illustrated in Figure F-2.

(2) The area of the slice, A, is computed by multiplying the width of the slice by the average height, $h_{avg.}$ (Column 4 in Figure F-3c).

(3) The weight, W, of the slice is computed by multiplying the area of the slice by the total unit weight of soil: $W = \gamma A$ (Column 5 in Figure F-3c). If the slice crosses zones having different unit weights, the slice is subdivided vertically into subareas, and the weights of the subareas are summed to compute the total slice weight

(4) The term $W \sin \alpha$ is computed for each slice and then summed for all slices to compute $\sum W \sin \alpha$ (Column 7 in Figure F-3c).

(5) The height, h_s, of water above the slice at the midpoint of the top of the slice is determined (Column 8 in Figure F-3c).

(6) The average water pressure on the top of the slice, $p_{surface.}$, is calculated by multiplying the average height of water, h_s, by the unit weight of water (Column 9 in Figure F-3c).

(7) The inclination of the top of the slice, β, is determined (Column 10 in Figure F-3c). The sign convention for this angle is shown in Figure F-2. β is positive, except when the inclination of the top of the slice is opposite to the inclination of the slope. Negative values of β will exist when the inclination of the slope is reversed over some distance, such as a "bench" that is inclined inward toward the slope.

P

d_h

d_v

8

b. Surface load and
moment arms for slice

Solution

Trial F

Calculated F

d. Assumed and calculated trial
values for factor of safety

a. Slope and trial slip
surface with slices

c. Table used to compute factor of safety

Surface Loads

1	2	3	4	5	6	7	8	9	10	11	12	13	14	15	16	17	18	19	20	21	22	23	24	25
Slice	Horizontal Width (β)	Average Height (h_avg.)	Area (A)	Weight (W)	Base Inclination (α)	W sin α	Height of surface water (h_s)	Avg. Surface Press. (p_surface)	Surface Inclination (β)	Surface Load (P)	Horizontal moment arm (d_h)	Vertical moment arm (d_v)	Moment (M_p)	Piezometric height (h_p)	Pore water pressure (u)	Cohesion c'	Friction angle φ'	c'b + (W + P cosβ - ub) tanφ'	m_α (Trial F_1)	Numerator (Col. 19 ÷ Col. 20)	m_α (Trial F_2)	Numerator (Col. 17 ÷ Col. 20)	m_α (Trial F_3)	Numerator (Col. 17 ÷ Col. 22)
1																								
2																								
3																								
4																								
5																								
6																								
7																								
8																								
9																								
						ΣW sinα =							ΣM_P =							Σ_1 =		Σ_2 =		Σ_3 =

Figure F-3. Simplified Bishop Method with water - effective stress analyses

(8) The length of the top of the slice is multiplied by the average surface pressure, $p_{surface}$, to compute the external water force, P, on the top of the slice (Column 11 in Figure F-3c). The force P is equal to $p_{surface} \cdot b / \cos(\beta)$.

(9) The horizontal and vertical distances, d_h and d_v, respectively, between the center of the circle and the points on the top center of each slice are determined (Columns 12 and 13 in Figure F-3c). Positive values for these distances are illustrated in Figure F-3b. Loads acting at points located upslope of the center of the circle (to the left of the center in the case of the right-facing slope shown in Figure F-3) represent negative values for the distance, d_h.

(10) The moment, M_P, the result of external water loads is computed from the following (Column 14 in Figure F-3c):

$$M_P = P\cos\beta d_h + P\sin\beta d_v \tag{F-3}$$

The moment is considered positive when it acts opposite to the direction of the driving moment produced by the weight of the slide mass, i.e., positive moments tend to make the slope more stable. Positive moments are clockwise for a right-facing slope like the one shown in Figure F-3.

(11) The piezometric height, h_p, at the center of the base of each slice is determined (Column 15 in Figure F-3c). The piezometric height represents the pressure head for pore water pressures on the base of the slice.

(12) The piezometric height is multiplied by the unit weight of water to compute the pore water pressure, u (Column 16 in Figure F-3c). For complex seepage conditions, or where a seepage analysis has been conducted using numerical methods, it may be more convenient to determine the pore water pressure directly, rather than evaluating the piezometric head and converting to pore pressure. In such cases Step 11 is omitted, and the pore water pressures are entered in Column 16.

(13) The cohesion, c', and friction angle, ϕ', for each slice are entered in Columns 17 and 18 in Figure F-3c. The shear strength parameters are those for the soil at the bottom of the slice; they do not depend on the soils in the upper portions of the slice.

(14) The following quantity is computed for each slice (Column 19 in Figure F-3c):

$$c'b + \left(W + P\cos\beta - ub\right)\tan\phi' \tag{F-4}$$

(15) A trial factor of safety, F_1, is assumed and the quantity, m_α, is computed from the equation shown below (Column 20 in Figure F-3c):

$$m_\alpha = \cos\alpha + \frac{\tan\phi'\sin\alpha}{F_1} \tag{F-5}$$

(16) The numerator in the equation used to compute the factor of safety is calculated by dividing the term $c'b + \left(W + P\cos\beta - ub\right)\tan\phi'$ by m_α for each slice and then summing the values for all slices (Column 21 in Figure F-3c).

(17) A new value is computed for the factor of safety using the following equation:

$$F = \frac{\sum\left[\dfrac{c'b + (W + P\cos\beta - ub)\tan\phi'}{m_\alpha}\right]}{\sum W\sin\alpha - \dfrac{1}{R}\sum M_P}$$

(F-6)

where R is the radius of the circle.

The summations computed in Columns 7, 14, and 21 of the table in Figure F-3c are used to compute the new value for the factor of safety.

(18) Additional trial values are assumed for the factor of safety and steps 14 through 16 are repeated (Columns 22 through 25 in Figure F-3c). For each trial value assumed for the factor of safety, the assumed and calculated values of the factor of safety are plotted as shown in Figure F-3d, to provide a guide for selecting additional trial values. Values are assumed and new values are calculated until the assumed and calculated values for the factor of safety are essentially equal, i.e., until the assumed and calculated values fall close enough to the broken 45-degree line shown in Figure F-3d.

F-3. Modified Swedish Method – Numerical Solution

The factor of safety can be calculated by the Modified Swedish Method using either numerical or graphical procedures. The numerical procedure is presented in this section and the graphical procedure is presented in Section F-4. Detailed steps are presented below for a total stress analysis of a slope with no water outside the slope and for an effective stress analysis of a slope with internal seepage and external water loads.

   a. Slope without seepage or external water loads – total stress analyses. Computations for the Modified Swedish Method with total stresses and no external water loads are illustrated in Figure F-4. The Modified Swedish Method may be used with slip surfaces of any shape, and the procedure is the same regardless of the shape of the slip surface. For simplicity, a circle has been used for the example illustrated in Figure F-4. Once a trial slip surface has been selected and the soil mass has been subdivided into slices, the steps listed below are used to compute a factor of safety. Slices are numbered beginning with the uppermost slice and proceeding toward the toe of the slope.

   (1) The width, b, average height, $h_{avg.}$, and base inclination, α, are determined (Columns 2, 3 and 6 in Figure F-4b).

   (2) The area of the slice, A, is computed by multiplying the width, b, of the slice by the average height, $h_{avg.}$ (Column 4 in Figure F-4b).

   (3) The weight, W, of the slice is computed by multiplying the area of the slice by the total unit weight of soil: $W = \gamma A$ (Column 5 in Figure F-4b). If the slice crosses zones having different unit weights, the slice is subdivided vertically into subareas, and the weights of the subareas are summed to compute the total slice weight.

   (4) The length of the bottom of the slice, $\Delta\ell$, is determined; the length can be computed from the width, b, and base inclination, α: $\Delta\ell = b / \cos\alpha$ (Column 7 in Figure F-4b).

   (5) The cohesion value, c, and friction angle, ϕ, are determined for the base of each slice (Columns 8 and 9 in Figure F-4b). The shear strength parameters are those for the soil at the bottom of the slice; they do not depend on the soils in the upper portions of the slice.

c. Variation of force imbalance with trial factor of safety

a. Slope and trial slip surface with slices

b. Table used to compute factor of safety
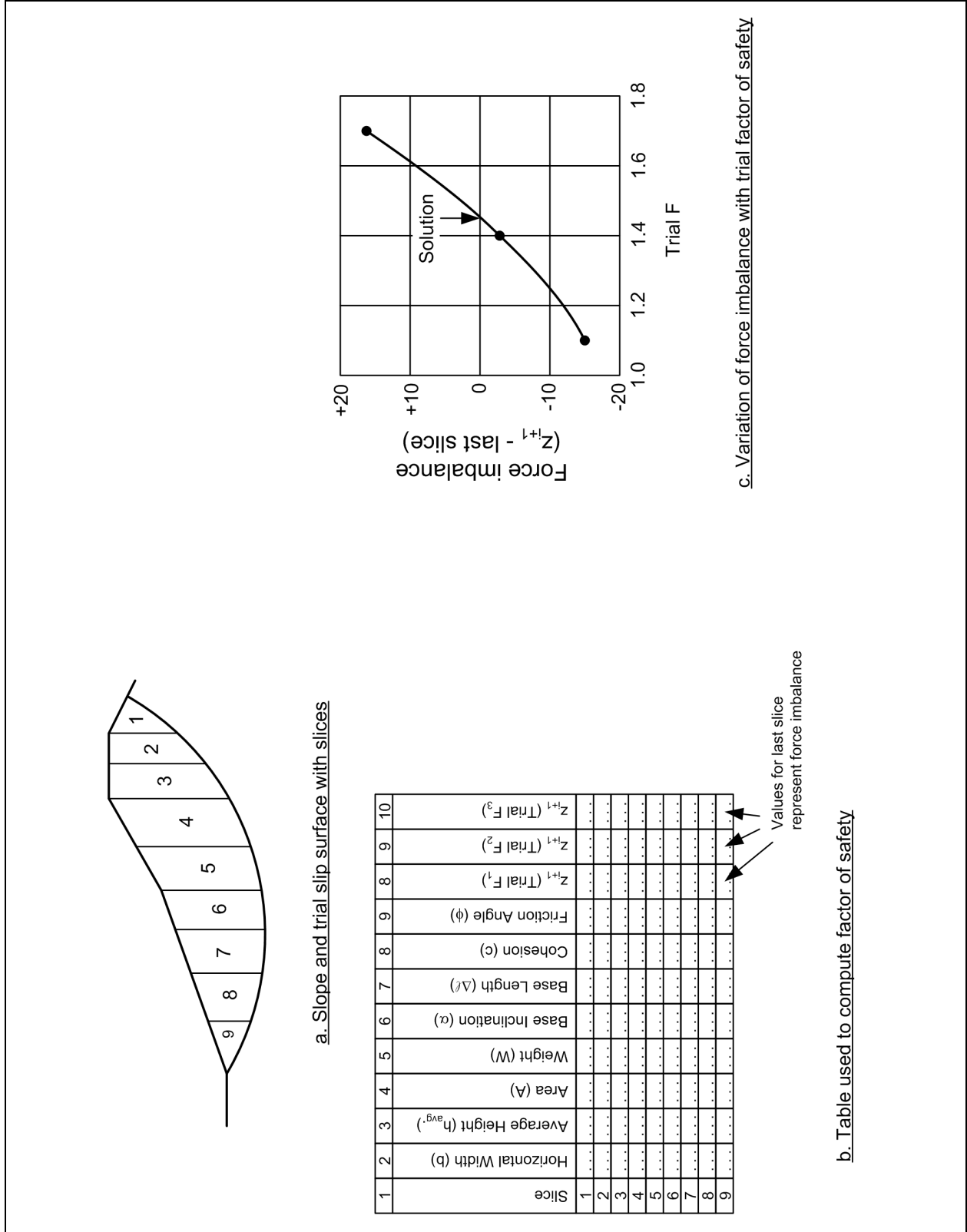
Figure F-4.   Modified Swedish Method - numerical solution with no water - total stress analysis

(6) The inclination, θ, of the interslice forces is determined. If the computations are being performed to check an analysis performed using Spencer's Method, the interslice force inclination determined from Spencer's Method should be used. Otherwise, the interslice force inclination should be assumed in accordance with the guidelines and discussion presented in Appendix C.

(7) A trial factor of safety, F_1, is assumed.

(8) Beginning with the first slice the side force, Z_{i+1}, on the "downslope" side (left side for the slope illustrated in Figure F-4) of each slice is computed from the equation:

$$Z_{i+1} = Z_i + \frac{W\left[\sin\alpha - \dfrac{\tan\phi\cos\alpha}{F}\right] - \dfrac{c\cdot\Delta\ell}{F}}{\cos(\alpha-\theta) + \dfrac{\tan\phi\sin(\alpha-\theta)}{F}} \tag{F-7}$$

(9) If the force computed for the last slice, Z_{i+1}, is not sufficiently close to zero, a new trial value is assumed for the factor of safety and the process is repeated. By plotting the force imbalance, Z_{i+1}, for the last slice versus the factor of safety, the value of the factor of safety that satisfies equilibrium can usually be found to an acceptable degree of accuracy in about three trials (Figure F-4c).

b.   Slope with seepage or external water loads – effective stress analyses. Computations for slopes where the shear strength is expressed in terms of effective stresses and where there are pore water pressures and external water loads are illustrated in Figure F-5. In addition to the quantities required when there is no water, the pore water pressures on the base of each slice, along with the forces from water on the top of the slice, must be determined. For a given trial slip surface, the following steps are required:

(1) For each slice, the width, b, average height, $h_{avg.}$, and base inclination, α, are determined (Columns 2, 3, and 6 in Figure F-5b).

(2) The area of the slice, A, is computed by multiplying the width, b, of the slice by the average height, $h_{avg.}$ (Column 4 in Figure F-5b).

(3) The weight, W, of the slice is computed by multiplying the area of the slice by the total unit weight of soil: $W = \gamma A$ (Column 5 in Figure F-5b). If the slice crosses zones having different unit weights, the slice is subdivided vertically into subareas, and the weights of the subareas are summed to compute the total slice weight

(4) The piezometric height is determined at the upslope boundary, center and downslope boundary of each slice (Columns 7, 8, and 9 in Figure F-5b). The piezometric height at the upslope and downslope boundaries of the slice, h_i and h_{i+1}, respectively, are used to compute the forces from water pressures on the sides of the slice. Here, a triangular hydrostatic distribution of pressures is assumed on the sides of the slice. If the distribution of water pressures is more complex, it may be necessary to compute the water forces differently from what is illustrated in Figure F-5. Assuming triangular distributions of water pressures provides sufficient accuracy for most analyses. The piezometric height at the center of the slice, h_p, represents the pressure head for pore water pressures at the base of the slice (Column 8 in Figure F-5b).

(5) Hydrostatic forces from water pressures on the sides of the slice are computed from the equations shown below (Columns 10 and 11 in Figure F-5b):

c. Trial F versus side force imbalance

Trial F

Force imbalance $(z_{i+1}$ - last slice)

+20 +10 0 -10 -20

Solution

1.0 1.2 1.4 1.6 1.8

a. Slope and trial slip surface with slices

1 2 3 4 5 6 7 8 9

Values for last slice represent force imbalance

b. Table used to compute factor of safety

1	2	3	4	5	6	7	8	9	10	11	12	13	14	15	16	17	18	19	20	21	22	23	24
Slice	Horizontal Width (b)	Average Slice Height (h_{avg}')	Area (A)	Weight (W)	Base Inclination (α)	Upslope Side (h_i)	Center (h_p)	Downslope Side (h_{i+1})	Water Upslope Side Force (U_i)	Water Downslope Side Force (U_{i+1})	Ht. of Water Above Slice (h_s)	Pressure at Top of Slice (p_{avg})	Slope at Top of Slice (β)	Length of Top of Slice (ℓ_{top})	Surface Load (P)	Base Inclination (α)	Slice Base Length ($\Delta\ell$)	Pore water pressure (u)	Cohesion (c')	Friction Angle (ϕ')	z_{i+1} (Trial F_1)	z_{i+1} (Trial F_2)	z_{i+1} (Trial F_3)

(Columns 7–9 grouped under "Piezometric Height"; columns 13–16 grouped under "Surface Load")

Slices: 1, 2, 3, 4, 5, 6, 7, 8, 9

Figure F-5.   Modified Swedish Method - numerical solution with water - effective stress analysis

$$U_i = \frac{1}{2}\gamma_w h_i^2 \tag{F-8}$$

and

$$U_{i+1} = \frac{1}{2}\gamma_w h_{i+1}^2 \tag{F-9}$$

where h_i and h_{i+1} are the heights determined in Step 4.

(6) The average height of water, h_s, above the top of the slice is determined (Column 12 in Figure F-5b). The height is used to compute the average water pressure and eventually the total force on the top of the slice (See Columns 13 and 16 in Figure F-5b). It is best to select the interslice boundaries so that a boundary is located at the point where the surface of the water outside the slope meets the slope. If this is done, the water pressures will vary linearly across each slice, and the average height of water is equal to the height of water above the midpoint of the slice.

(7) The average water pressure on the top of the slice, p_{avg}, is computed by multiplying the height of water, h_s, by the unit weight of water (Column 13 in Figure F-5b).

(8) The inclination of the top of the slice, β, is determined (Column 14 in Figure F-5b). This is the same as the inclination of the slope above the slice.

(9) The length of the top of the slice, ℓ_{top}, is determined (Column 15 in Figure F-5b). The length can be computed from the relationship, $\ell_{top} = b/\cos\beta$.

(10) The water load on the top of the slice, P, is computed by multiplying the average water pressure, p_{avg}, by the length of the top of the slice, ℓ_{top} (Column 16 in Figure F-5b).

(11) The length of the base of the slice, $\Delta\ell$, is computed from the relationship, $\Delta\ell = b/\cos\alpha$ (Column 18 in Figure F-5b).

(12) The pore water pressure is computed by multiplying the piezometric head at the center of the base of the slice by the unit weight of water: $u = \gamma_w h_p$ (Column 19 in Figure F-5b). For complex seepage conditions, or where a seepage analysis has been conducted using numerical methods, it may be more convenient to determine the pore water pressure directly, rather than evaluating the piezometric head and converting to pore pressure. In such cases, the pore water pressures are entered in Column 19.

(13) The cohesion and friction angle are determined for each slice depending on the soil at the bottom of the slice (Columns 20 and 21 in Figure F-5b). The shear strength parameters, c' and ϕ', are those for the soil at the bottom of the slice and do not depend on the soils located in the upper portions of the slice.

(14) The inclination, θ, of the interslice forces is determined. If the computations are being performed to check an analysis performed using Spencer's Method, the interslice force inclination determined from Spencer's Method should be used. Otherwise, the interslice force inclination should be assumed in accordance with the guidelines and discussion presented in Appendix C.

(15) A trial value is assumed for the factor of safety, and interslice forces are calculated, slice-by-slice, to determine the force imbalance or "error of closure." The steps for this portion of the computations are the

same as those described for analyses with no water pressures, except the following equation for interslice forces is used:

$$Z_{i+1} = Z_i + \frac{W\left[\sin\alpha - \frac{\tan\phi'\cos\alpha}{F}\right] + (U_i - U_{i+1})\left[\cos\alpha + \frac{\tan\phi'\sin\alpha}{F}\right] + P\left[\sin(\alpha-\beta) - \frac{\tan\phi'}{F}\cos(\alpha-\beta)\right] - (c' - u\tan\phi')\frac{\Delta\ell}{F}}{\cos(\alpha-\theta) + \frac{\tan\phi'\sin(\alpha-\theta)}{F}} \quad \text{(F-10)}$$

(16) If the force computed for the last slice, Z_{i+1}, is not sufficiently close to zero, a new trial value is assumed for the factor of safety and the process is repeated. By plotting the force imbalance, Z_{i+1}, for the last slice versus the factor of safety, the value of the factor of safety that satisfies equilibrium can usually be found to an acceptable degree of accuracy in about three trials (Figure F-5c).

F-4. Modified Swedish Method – Graphical Solution

Graphical solution for the factor of safety by the Modified Swedish Method requires a trial and error process of assuming values for the factor of safety and constructing force equilibrium polygons until "closure" (force equilibrium) is established. Detailed steps are presented below for a total stress analysis of a slope with no water and for an effective stress analysis of a slope with water internal seepage and external water loads.

   a. Slope without seepage or external water loads – total stress analyses. The graphical solution procedure using total stresses and no water pressures is illustrated in Figures F-6 and F-7. The calculations required to determine the magnitudes of the forces in the force polygons are shown in tabular form in Figure F-6; and the force polygons are shown in Figure F-7. The steps for determining the factor of safety once a trial shear surface is selected are as follows:

   (1) For each slice the width, b, and the average height, $h_{avg.}$, are determined (Columns 2 and 3 in Figure F-6b).

   (2) The area of the slice, A, is computed by multiplying the width, b, by the average height, $h_{avg.}$, of each slice (Column 4 in Figure F-6b).

   (3) The slice weight, W, is computed by multiplying the area of the slice, A, by the total unit weight of soil, γ: $W = \gamma A$ (Column 5 in Figure F-6b). If the slice crosses zones having different unit weights, the slice is subdivided vertically into subareas, and the weights of the subareas are summed to compute the total slice weight.

   (4) The base length, $\Delta\ell$, for each slice is determined (Column 7 in Figure F-6). The base length may either be measured from a scaled drawing of the slope or computed by dividing the slice width, b, by the cosine of the inclination angle, α, of the base of the slice, i.e., $\Delta\ell = b/\cos\alpha$.

   (5) The cohesion value, c, and friction angle, ϕ, are determined for the base of each slice (Columns 8 and 9 in Figure F-6b). The shear strength parameters are those for the soil at the bottom of the slice; they do not depend on the soils in the upper portions of the slice.

   (6) The available force resulting from cohesion is calculated by multiplying the cohesion value, c, by the length of the base of the slice, $\Delta\ell$ (Column 10 in Figure F-6b).

   (7) A trial value, F_1, is assumed for the factor of safety.

a. Slope and trial slip surface with slices

b. Table used to compute numerical
   values for graphical solution

c. Trial F versus side force imbalance
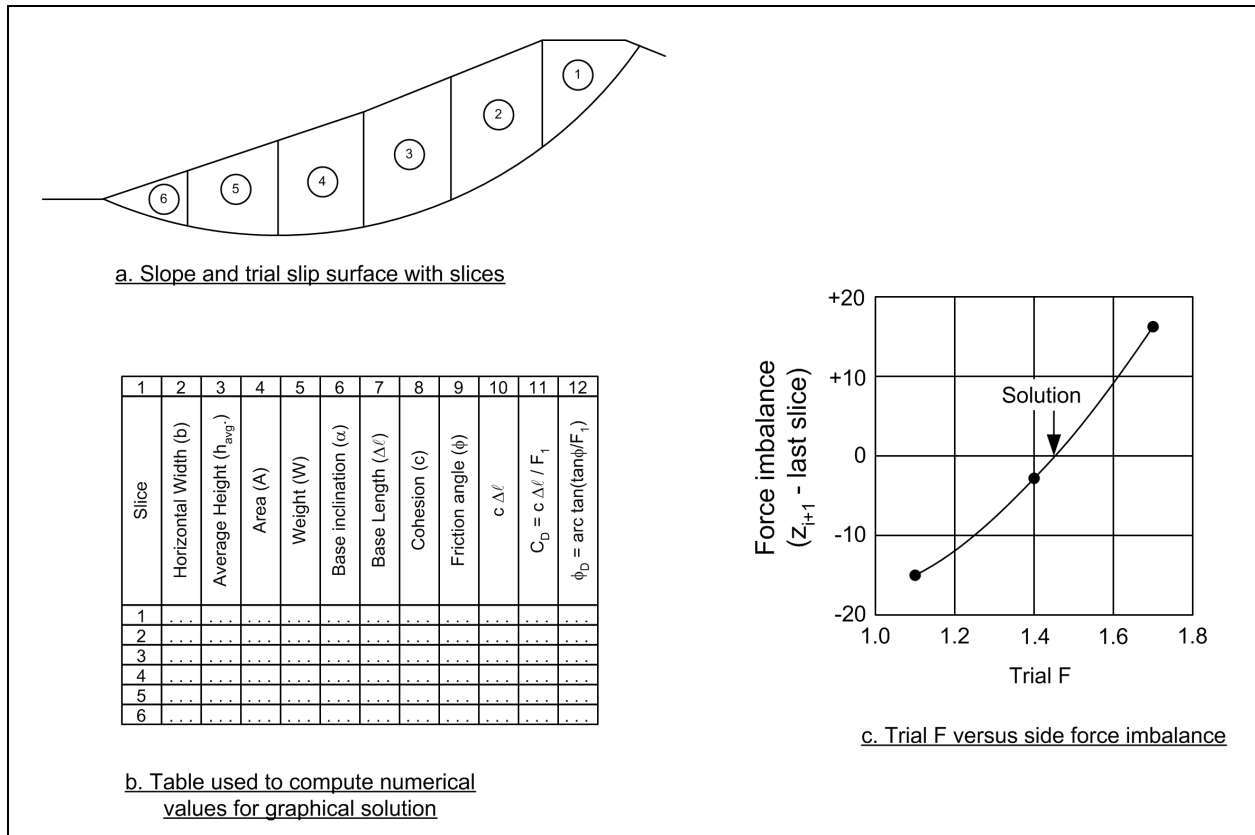
Figure F-6. Modified Swedish Method - graphical solution with no water - slope and numerical table

(8) The "developed" force from cohesion, C_D, is calculated by dividing the available force computed in Step 6 by the assumed value for the factor of safety: $C_D = \dfrac{c\Delta\ell}{F_1}$ (Column 11 in Figure F-6b).

(9) The "developed" friction angle, ϕ_D, is calculated from the relationship, $\phi_D = \arctan\left(\dfrac{\tan\phi}{F_1}\right)$ (Column 12 in Figure F-6b).

(10) A suitable scale for force is selected and a vector representing the weight of the slice, W_1, is drawn vertically downward to start the equilibrium force polygons. The force polygons are illustrated in Figure F-7. Steps 11 through 17, which follow, are used to complete the forces in the force polygons, and to check for equilibrium. All vectors are drawn using the same force scale.

(11) A vector representing the developed cohesion force on the first slice, C_{D1}, is drawn in a direction parallel to the base of the first slice, extending from the tip of the weight vector drawn in Step 10.

(12) A line is drawn from the start (tail) of the weight vector in a direction perpendicular to the base of the slice. This line is shown as a broken line labeled N_1 in Figure F-7b.

(13) A second line is drawn from the start (tail) of the weight vector so that the angle between the new line and line representing the normal vector (N_1) is equal to the developed friction angle, ϕ_D. The new line should be drawn such that the component of the vector parallel to the bottom of the slice acts in the direction of the resisting shear force, i.e., clockwise from the normal vector in the case of a left-facing slope. This

a. Slope and trial slip surface with slices

b. Force polygon for slice 1

Numbers in parentheses - (1) through (5) represent sequences of steps involved in drawing polygon.

d. Completed set of force polygons

Error of closure
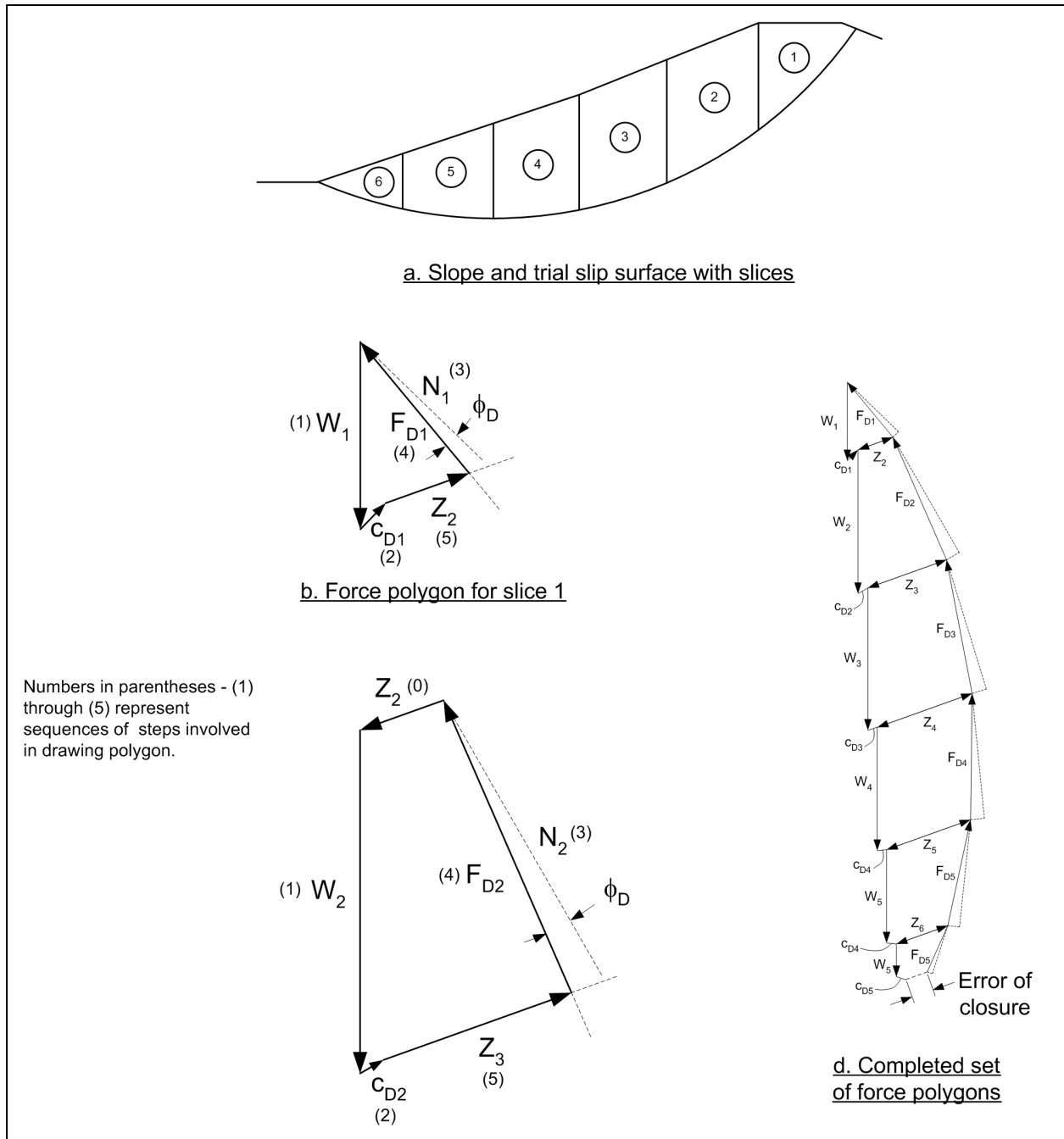
Figure F-7. Modified Swedish method - graphical solution with no water - force polygons

vector is labeled F_{D1} in Figure F-7b. If the soil at the bottom of the slice has $\phi = 0$, the lines drawn in Steps 11 and 12 are the same, i.e., the vectors N_1 and F_{D1} are the same.

(14) A line is drawn from the tip (end) of the developed cohesion vector, in the direction assumed for the interslice forces. This line is labeled Z_2 in Figure F-7b. If the computations are being performed to check computations that were performed using Spencer's Method, the interslice force inclination should be the one calculated in Spencer's Method. Otherwise, the interslice force inclination should be assumed in accordance with the guidelines and discussion presented in Appendix C.

(15) The intersection between the line directions drawn in Step 13 (F_D) and Step 14 (Z_2) is found. This defines the magnitudes of the forces F_{D1} and Z_2.

(16) The process continues by drawing the equilibrium force polygon for the next slice. A vector representing the weight of the slice is drawn vertically downward from the point where the cohesion and interslice force vectors, C_{D1} and Z_2, intersect. The force polygon for the second slice is shown in Figure F-7c. Closure of the force polygon is used to determine the magnitude of the forces F_{D2} and Z_3 for the second slice.

(17) Force polygons are drawn consecutively, slice-by-slice, for all of the remaining slices. If the trial value of factor of safety is not the correct value, the force polygon for the last slice will not close. The error of closure is a measure of the inaccuracy in the assumed factor of safety. Additional trial values for the factor of safety are assumed until the force polygons close with an acceptable degree of accuracy. By plotting the error of closure versus the assumed values of factor of safety as shown in Figure F-6c, the correct value of factor of safety can usually be determined within a few trials.

b.   Slope with seepage or external water loads – effective stress analyses. The graphical solution procedure for slopes where the shear strength is expressed in terms of effective stresses and where there are pore water pressures and external water loads are illustrated in Figures F-8 and F-9. The calculations required to determine the magnitudes of the forces in the force polygons are shown in tabular form in Figure F-8; and the force polygons are shown in Figure F-9. The steps for determining the factor of safety once a trial shear surface is selected are as follows:

(1) The width, b, average height, $h_{avg.}$, and length of the slice base, $\Delta\ell$, are determined for each slice (Columns 2, 3, and 17 in Figure F-8b).

(2) The area of the slice is computed by multiplying the width, b, by the average height, $h_{avg.}$ (Column 4 in Figure F-8b).

(3) The weight, W, of the slice is computed by multiplying the area by the total unit weight of soil: $W = \gamma A$ (Column 5 in Figure F-8b). If the slice crosses zones having different unit weights, the slice is subdivided vertically into subareas, and the weights of the subareas are summed to compute the total slice weight.

(4) The water loads on the sides and top of the slice are computed (Columns 7 thorough 16 in Figure 7b). The water loads are computed as described in Steps (4) through (10) in Section F-3b.

(5) The pore water pressure is computed by multiplying the piezometric head at the center of the base of the slice by the unit weight of water: $u = \gamma_w h_p$ (Column 18 in Figure F-8b). For complex seepage conditions, or where a seepage analysis has been conducted using numerical methods, it may be more convenient to determine the pore water pressure directly, rather than evaluating the piezometric head and converting to pore pressure. In such cases the pore water pressures determined directly are entered in Column 18.

(6) The force, U_b, produced by the water pressure on the bottom of the slice is computed by multiplying the length of the base of the slice, $\Delta\ell$, by the pore water pressure, u (Column 19 in Figure F-8b).

(7) The "available" force resulting from cohesion is computed by multiplying the cohesion., c', by the length of the base of the slice, $\Delta\ell$, (Column 22 in Figure F-8b).

(8) A trial value for the factor of safety, F, is assumed, and the developed cohesion force, C_D, is computed by dividing the available cohesion force by the factor of safety: $C_D = c' \Delta\ell / F$ (Column 23 in

a. Slope and trial slip surface with slices

1	2	3	4	5	6	7	8	9	10	11	12	13	14	15	16	17	18	19	20	21	22	23	24
						Piezometric Height					Surface Load												
Slice	Horizontal Width (b)	Average Slice Height ($h_{avg.}$)	Area (A)	Weight (W)	Base inclination (α)	Upslope Side (h_i)	Center (h_p)	Downslope Side (h_{i+1})	Water Upslope Side Force (U_i)	Water Downslope Side Force (U_{i+1})	Ht. of Water Above Slice (h_s)	Pressure at Top of Slice (p_{avg})	Slope at Top of Slice (β)	Length of Top of Slice (ℓ_{top})	Surface Load (P)	Slice Base Length ($\Delta\ell$)	Pore water pressure (u)	$U_b = u\,\Delta\ell$	Cohesion (c')	Friction angle (ϕ')	c' $\Delta\ell$	$C_D = c'\,\Delta\ell$ / F	ϕ_D = arc tan(tanϕ' / F)
1	...	...	...	...	...	...	...	...	...	...	...	...	...	...	...	...	...	...	...	...	...	...	...
2	...	...	...	...	...	...	...	...	...	...	...	...	...	...	...	...	...	...	...	...	...	...	...
3	...	...	...	...	...	...	...	...	...	...	...	...	...	...	...	...	...	...	...	...	...	...	...
4	...	...	...	...	...	...	...	...	...	...	...	...	...	...	...	...	...	...	...	...	...	...	...
5	...	...	...	...	...	...	...	...	...	...	...	...	...	...	...	...	...	...	...	...	...	...	...
6	...	...	...	...	...	...	...	...	...	...	...	...	...	...	...	...	...	...	...	...	...	...	...

b. Table used to compute numerical values for graphical solution

Figure F-8.   Modified Swedish Method – graphical solution with water – slope and table of numerical values

a. Slope and trial slip surface with slices

b. Slice with forces

c. Resultant of weight and water forces for slice 1

d. Resultant of weight and water forces for slice 6

e. Complete equilibrium force polygons

Numbers in parentheses - (1) through (4), (5) represent steps in construction.
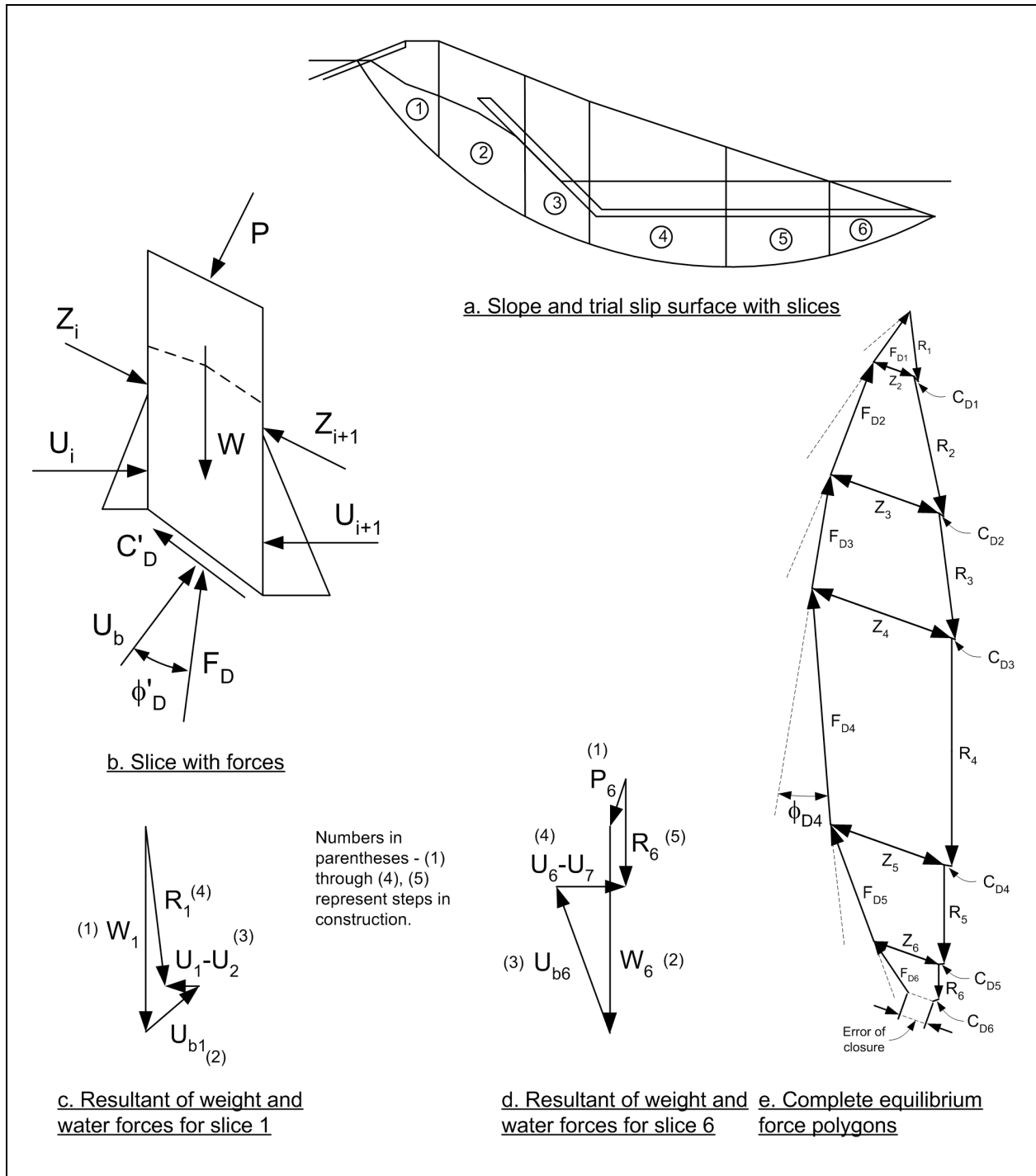
Figure F-9. Modified Swedish Method – graphical solution with water – force polygons

Figure F-8b). The developed friction angle, ϕ_D, is computed from the relationship, $\phi_D = \arctan\left(\dfrac{\tan \phi'}{F_1}\right)$

(Column 24 in Figure 8b). The trial force equilibrium polygons can now be constructed as described in the following steps.

(9) The resultant force from the weight of the slice and any water pressures on the top, sides, and bottom of the slice are determined for each slice separately. The first step in determining this resultant involves drawing a vector representing the water load on the top of the slice, as shown for the last slice in Figure F-9d. This water force vector, and all subsequent vectors, are drawn to the same scale.

(10) The second step in determining the resultant is to draw a vector representing the weight of the slice vertically downward from the tip of the vector representing the water loads on the top of the slice drawn in Step 9. See Figures F-9c and F-9d, for the first and last slices. If there are no external water loads, the weight vector is drawn from any convenient starting point, as in Figure F-9c.

(11) A vector representing the force, U_b, resulting from water pressures on the bottom of the slice is drawn extending from the tip of the weight vector in a direction perpendicular to the base of the slice (See U_{b1} and U_{b6} in Figures F-9c and F-9d).

(12) A vector representing the difference between the forces from water pressures on the upslope and downslope sides of the slice, $U_i - U_{i+1}$, is drawn horizontally, starting at the tip of the vector drawn in Step 11 (See U_1-U_2 and U_6-U_7 in Figures F-9c and F-9d).

(13) A vector, R, is drawn from the start of the vector representing the water loads, P, on the top of the slice, to the tip of the vector that was drawn in Step 12 to represent the water loads on the sides of the slice (See vector R_6 in Figure F-9d). If there is no water load on the top of the slice, the vector is drawn starting at the point where the weight vector, W, was started (Figure F-9c). The R-vector closes the force polygon for the known water and gravity forces (Figures F-9c and F-9d). The R-vector represents the resultant force produced by the slice weight and water pressures on the top, sides, and bottom of the slice. Steps 9 through 13 are carried out for each slice individually.

(14) The set of force polygons for the entire slope are begun by drawing a vector representing the force, R_1, for the first slice, beginning at a convenient starting point, as shown in Figure F-9e.

(15) A vector representing the developed cohesion force, C_{D1}, is drawn in a direction parallel to the base of the first slice, extending from the tip of the resultant force vector, R_1, drawn in Step 14.

(16) A line is drawn from the start (tail) of the resultant force vector (R_1) in a direction perpendicular to the base of the slice. This line is shown as a broken line in Figure F-9e.

(17) A second line is drawn from the start (tail) of the resultant force vector (R_1) such that the new line makes an angle equal to the developed friction angle, ϕ_D, with the vector drawn in Step 16. The new line should be drawn so that the component of the vector parallel to the bottom of the slice (the shear component) acts in the direction of the resisting shear force, i.e., counter-clockwise from the normal vector in the case of a right-facing slope like the one shown in Figure F-9. This vector is labeled F_{D1} in Figure F-9e.

(18) A line is drawn from the tip (end) of the developed cohesion vector, in the direction assumed for the interslice forces. This line is labeled Z_2 in Figure F-9e. If hand calculations are being performed to check computations that were performed with Spencer's Method, the side force inclination should be the one found with Spencer's Method. Otherwise, the side force inclination should be assumed in accordance with the guidelines and discussion presented in Appendix C.

(19) The intersection between the two line directions drawn in Steps 17 and 18 is found. This determines the magnitude of the forces F_{D1} and Z_2.

(20) The process described above in Steps 14 through 19 is continued for the next slice, where a vector representing the resultant force, R_2, for the second slice is drawn from the point where the developed cohesion vector, C_{D1}, and interslice vector, Z_2, intersect. The force polygon for the second slice is shown in Figure F-9e. Closure of the force polygon is used to determine the magnitude of the forces F_{D2} and Z_3 for the second slice.

(21) Force polygons are drawn slice-by-slice for the remaining slices. If the trial value of factor of safety is not the correct value, the force polygon for the last slice will not close. This error of closure is a measure of the inaccuracy in the assumed value for the factor of safety. Additional trial values are assumed for the factor of safety until the equilibrium force polygons close with an acceptable degree of accuracy. By plotting the error of closure versus the assumed values of factor of safety as shown in Figure F-6c, the correct value of factor of safety can usually be determined within a few trials.

F-5. End-of-Construction (Short-Term Stability) Example

Example calculations are presented for stability at the end of construction of the embankment shown in Figure F-10. The embankment cross section contains two materials -- the embankment soil and the foundation soil. Both soils are fine-grained and undrained during construction.

a.   Shear Strengths. Because the soils in this case are do not drain during construction, undrained shear strengths are used for both. For the embankment, samples would be prepared by compacting representative samples of the fill material at appropriate densities and moisture contents. For the natural foundation soil, undisturbed samples would be obtained for testing. The shear strengths would be determined using Unconsolidated-Undrained (UU or Q) triaxial compression tests. If the natural soil was saturated, Consolidated-Undrained (CU or R) or field vane shear tests could also be used to estimate undrained shear strengths, as described in Appendix D.

(1) Compacted, fined-grained fills are always partly saturated at the end of construction. The foundation soil in this example is also assumed to be partly saturated. Thus, the shear strengths of both soils are characterized by total stress friction angles greater than zero. If the foundation soil was saturated, its total stress friction angle, ϕ, would be equal to zero.

(2) If the embankment contained zones of free-draining soils, their strengths would be characterized using effective stress shear strength parameters.

b.   Water pressures. For the example problem illustrated in Figure F-10, all water pressures are zero, because there is no external water. If external water exists, the external water loads would be computed and included in the analysis in the same way they are included in the example described previously where there was water outside the slope. External water loads must always be included, regardless of whether the shear strength is represented using total or effective stresses. Because the strengths are characterized in terms of total stresses, pore water pressures within the slope are not included. However, if the embankment contained free-draining soils being characterized in terms of effective stress, pore water pressures would be included in the analysis for these materials.

c.   Unit weights. Total unit weights are used for all soils. Total unit weights should always be used, regardless of whether the shear strength is represented using total or effective stresses. The total unit weights for the example problem are shown in Figure F-10b.

d.   Simplified Bishop Method. Calculations using the Simplified Bishop Method for the example are illustrated in Figure F-11. Slices 6 through 10 contain both embankment and foundation soils, and these slices were divided into two portions for calculating the slice weights. The average height in each soil was

Center of circle

101 ft.

259 ft.

R = 278 ft.

EL. 91 ft.

EL. 58 ft.

2.5:1

3:1

EL. 0

① ② ③ ④ ⑤ ⑥ ⑦ ⑧ ⑨ ⑩

a. Slope cross section

Material	Total unit weight, γ (pcf)	c (psf)	ϕ (degrees)
Embankment	135	1780	5
Foundation	127	1600	2

b. Material properties
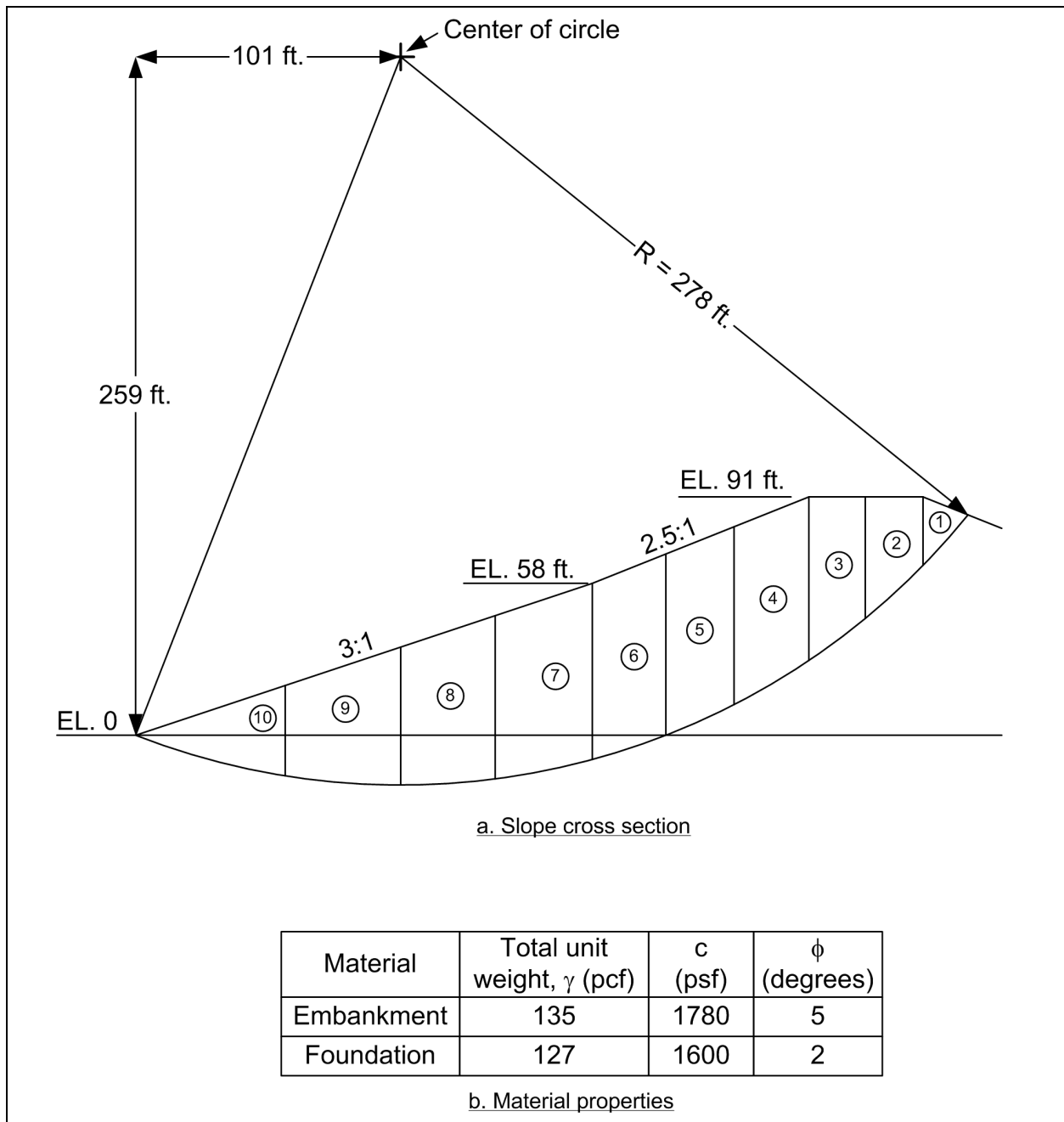
Figure F-10.   Slope used for example calculations for end-of-construction stability condition

determined and used to compute the area and weight for that portion of the slice. The weights of two parts of the slices were then added to compute the total slice weight. The bottoms of slices 1 through 5 are located in the embankment soil and were assigned the shear strength properties of the embankment. The bottoms of slices 6 though 10 are located in the foundation, and these slices were assigned the shear strength properties of the foundation soil. Computations for the final value of the factor of safety (F = 1.33) are shown in Columns 14 and 15 of the table in Figure F-11. Computations were also performed for three trial values for the factor of safety: 1.0, 1.5, and 2.0. The computed values for each trial value are plotted versus the assumed values in Figure F-11d. As can be seen in this figure, the computed value of F varied only slightly with changes in the assumed value.

a. Cross section

b. Material properties

Material	Total Unit Weight, γ (pcf)	c (psf)	φ (degrees)
Embankment	135	1780	5
Foundation	127	1600	2

1	2	3	4	5	Weight, kips		8	9	10	11	12	13	14	15
Sliding Surface in	Slice	Horizontal Width (b) ft	Average Slice Height	Slice Area, sq. ft.	Embank./Found.	Total Weight	Slope of Slip Surface (α) degrees	Base Length of Slice (Δℓ) ft.	$W \sin(\alpha)$	c, ksf	φ, degrees	$c\Delta x + W \tan(\phi)$	m_α (Assumed F = 1.33)	$[c\Delta x + W \tan(\phi)] \div m_\alpha$
Embankment	1	57	13	224	30	30	48	59.1	23	1.78	5	33	0.71	46
	2	44	36	797	108	108	43	44.1	73	1.78	5	49	0.78	62
	3	36	54	1170	158	158	37	36.1	95	1.78	5	52	0.84	62
	4	37	65	1857	251	251	31	37.7	128	1.78	5	73	0.89	81
	5	28	69	1782	241	241	24	29.5	99	1.78	5	67	0.94	72
Foundation	6 6'	26	64 5	1781 129	241 16	257	18	28.5	80	1.60	2	54	0.96	56
	7 7'	29	52 13	1918 479	259 61	320	11	33.1	63	1.60	2	70	0.99	71
	8 8'	22	40 18	1428 642	193 82	275	4	26.8	18	1.60	2	67	1.00	67
	9 9'	22	26 17	1159 759	156 97	253	-5	29.9	-20	1.60	2	79	0.99	80
	10 10'	17	10 8	542 442	73 56	129	-15	25.8	-34	1.60	2	96	0.96	100
								Sum for all slices:	524					698

d. Trial vs computed factors of safety

c. Computation table

Figure F-11.   End-of-construction example – Simplified Bishop Method

e.   Modified Swedish Method – numerical solution. Calculations using numerical calculations for the Modified Swedish Method for the same slope are summarized in Figure F-12. For this example the interslice force inclination was assumed to be equal to the average embankment slope. The average embankment slope is 2.8 (horizontal) to 1 (vertical). The side force inclination used in the calculations was θ = arctan(1/2.8) = 19.7 degrees.

1	2	3	4	5	6	7	8	9	10	11	12	13
Sliding Surface in	Slice	Horizontal Width (b) ft	Average Slice Height	Slice Area, sq. ft.	Weight, kips — Embank./Found.	Total Weight	Slope of Slip Surface (α) degrees	Base Length of Slice (Δℓ) ft.	c, ksf	φ, degrees	Z_i - Trial F = 1.6	Z_{i+1} - Trial F = 1.6
Embankment	1	57	13	224	30	30	48	59.1	1.78	5	0	-8
	2	44	36	797	108	108	43	44.1	1.78	5	0	37
	3	36	54	1170	158	158	37	36.1	1.78	5	37	97
	4	37	65	1857	251	251	31	37.7	1.78	5	97	177
	5	28	69	1782	241	241	24	29.5	1.78	5	177	232
Foundation	6 / 6'	26	64 / 5	1781 / 129	241 / 16	257	18	28.5	1.60	2	232	277
	7 / 7'	29	52 / 13	1918 / 479	259 / 61	320	11	33.1	1.60	2	277	296
	8 / 8'	22	40 / 18	1428 / 642	193 / 82	275	4	26.8	1.60	2	296	270
	9 / 9'	22	26 / 17	1159 / 759	156 / 97	253	-5	29.9	1.60	2	270	193
	10 / 10'	17	10 / 8	542 / 442	73 / 56	129	-15	25.8	1.60	2	193	75

(Note at row 1, col 13: "Negative interslice force set to zero for next slice.")

a. Table used to compute factor of safety
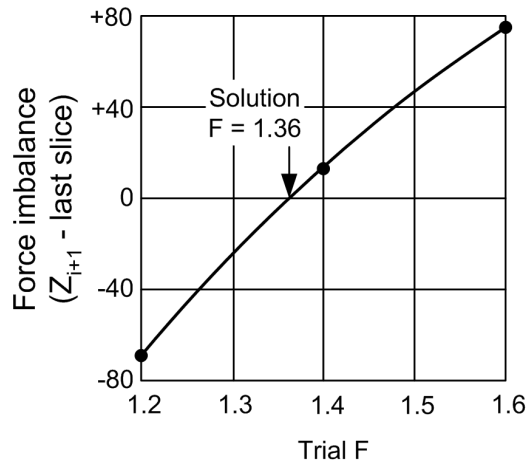
b. Variation in force imbalance with trial factor of safety

Figure F-12. Example calculations for end-of-construction stability condition – Modified Swedish Method – numerical solution

   (1) Many of the quantities shown in the table in Figure F-12a are the same as those for the Simplified Bishop Method in Figure F-11c. Only the interslice forces Z_i and Z_{i+1}, in Columns 12 and 13 in Figure F-12a, are different from the Simplified Bishop Method. The interslice forces were calculated by first assuming a trial value for the factor of safety, and setting Z_1 for the first slice to zero. The value of Z_2 was then calculated from Equation F-7. Values of the interslice forces were calculated successively for the remaining slices using

Equation F-7. Calculations are shown in the table in Figure F-12a for an assumed value of factor of safety equal to 1.6. The value of Z_{i+1} on the last slice is 75 kips, which represents the force imbalance, or error of closure, for this assumed factor of safety.

(2) Calculations were performed for three assumed values of factor of safety: F = 1.20, 1.40, and 1.60. The force imbalances for these three factors of safety are plotted versus factor of safety in Figure F-12b. It can be seen from this figure that the correct value satisfying force equilibrium with essentially zero imbalance is approximately 1.36.

f.   Modified Swedish Method – graphical solution. Calculations for the end-of-construction example using the graphical solution for the Modified Swedish Method are illustrated in Figures F-13 and F-14. The necessary numerical computations are shown in Figure F-13a. Most of the calculations and values shown in this table are the same as those shown previously for the numerical solution in Figure F-12. In addition, values for the force because of the developed cohesion, C_D, and the developed friction angle, ϕ_D, are shown in Columns 12 and 13 of Figure F-13a. These values are shown for only one of the assumed values for the factor of safety (F = 1.6). Three trial values (1.2, 1.4 and 1.6) were assumed for the factor of safety, and similar computations were made for each assumed value. The error of closure (Z_{i+1} for the last slice) is plotted versus the assumed value of factor of safety in Figure F-13b. The equilibrium force polygons are shown in Figure F-14 for a trial value for the factor of safety of 1.6. For this assumed value the error of closure is 75 kips. Note that the force polygons for the first three slices are shown twice in Figure F-14 to the same force scale as for the other slices, and to an expanded scale for clearer illustration.

F-6. Steady Seepage (Long-Term Stability) Example

Figure F-15 shows an embankment with steady seepage. The cross section contains two principal zones -- the embankment fill and the foundation. There are also three smaller zones of material in the embankment: an upstream layer of rip-rap, an internal chimney drain and a horizontal drainage blanket. For these example stability calculations, all of these smaller zones were treated as being the same as the embankment. The trial slip surface used for the computations does not intersect any of the smaller zones, and their strength properties therefore do not influence the results of the analyses.

a.   Shear strengths. For steady-state seepage conditions, drained shear strengths characterized by c' and ϕ' are appropriate for all soils. The effective stress shear strength parameters are determined using consolidated-drained (CD or S) test procedures for testing coarse-grained soils, and consolidated-undrained (CU or R) test procedures with pore water measurements for fine-grained soils. The shear strength parameters used in this example are shown in the table at the top of Figure F-15. Samples of the embankment materials would be prepared by compacting samples at appropriate densities and moisture contents. For the natural foundation soils, test specimens would be obtained by undisturbed sampling.

b.   Water pressures. The pore water pressures for the steady seepage condition were characterized by the piezometric line shown in Figure F-15. The piezometric line begins at the reservoir surface at the point where the reservoir intersects the fine-grained embankment soil (beneath the rip-rap), slopes downward to intersect the inclined chimney drain, then follows along the bottom side of the chimney drain until it reaches the elevation of the tailwater (el 22.5) and, finally, extends horizontally to the downstream face of the slope at the tailwater level. Pore water pressures are calculated for each slice by multiplying the vertical distance between the center of the base of the slice and the piezometric line by the unit weight of water. Alternatively, a more rigorous seepage analysis could have been performed and the pore water pressure from this analysis used in the computations. For the slip surface and slices illustrated in Figure F-16 there is only water on the external surface of the slope above the last slice, Slice 9. The external water load on the last slice is calculated and included in the computations for the factor of safety.

1	2	3	4	5	6	7	8	9	10	11	12	13
					Weight, kips						Trial F = 1.6	
Sliding Surface in	Slice	Horizontal Width (b) ft	Average Slice Height	Slice Area, sq. ft.	Embank./Found.	Total Weight	Base Length of Slice (Δℓ) ft	c, ksf	cΔℓ, kips	φ, degrees	$C_D = c\Delta\ell/F$, kips	$\phi_D = \arctan(\tan\phi/F)$, degs.
Embankment	1	57	13	224	30	30	59.1	1.78	46	5	29	3.1
	2	44	36	797	108	108	44.1	1.78	53	5	33	3.1
	3	36	54	1170	158	158	36.1	1.78	48	5	30	3.1
	4	37	65	1857	251	251	37.7	1.78	59	5	37	3.1
	5	28	69	1782	241	241	29.5	1.78	51	5	32	3.1
Foundation	6 / 6'	26	64 / 5	1781 / 129	241 / 16	257	28.5	1.60	47	2	29	1.3
	7 / 7'	29	52 / 13	1918 / 479	259 / 61	320	33.1	1.60	60	2	38	1.3
	8 / 8'	22	40 / 18	1428 / 642	193 / 82	275	26.8	1.60	58	2	36	1.3
	9 / 9'	22	26 / 17	1159 / 759	156 / 97	253	29.9	1.60	71	2	44	1.3
	10 / 10'	17	10 / 8	542 / 442	73 / 56	129	25.8	1.60	95	2	59	1.3

a. Table of numerical values computed for graphical solution

b. Error of closure of force polygons vs. trial factor of safety

Figure F-13. Example calculations for end of construction stability condition – Modified Swedish Method – numerical computations for graphical solution

c.   Unit weights. Total unit weights are used for all soils. Total unit weights should always be used regardless of whether the shear strength is represented using total or effective stresses. The total unit weights for the example problem are shown in the table at the top of Figure F-15.

d.   Slip surface and slices. The circular slip surface shown in Figure F-16 was used for the example stability calculations. This surface is not the most critical slip surface. The factor of safety for an infinite slope failure in the upper part of the slope (F = 1.68) is lower than the factor of safety (F = 2.01) for the slip surface shown in Figure F-16. The infinite slope slip surface is very shallow, however, and the factor of safety for that failure mechanism is of less significance with respect to the safety of the embankment than the slip surface shown in Figure F-16. The soil above the slip surface is divided into the nine slices shown in Figure F-16. The same circle and slices are used for both the Simplified Bishop and the Modified Swedish Method analyses.

e.   Simplified Bishop Method. Calculations performed using the Simplified Bishop Method are shown in Figure F-17. Slices 4 through 9 contain both embankment and foundation soil and were divided into two sections to calculate the slice weight. The average height in each soil was determined and used to compute the area and weight for that portion of the slice. The weights of two parts of the slices were then added to

b. Slices 1, 2 & 3

a. All Slices

Error of closure = 75 kips

Z_2 (negative - set to zero for slice 2)
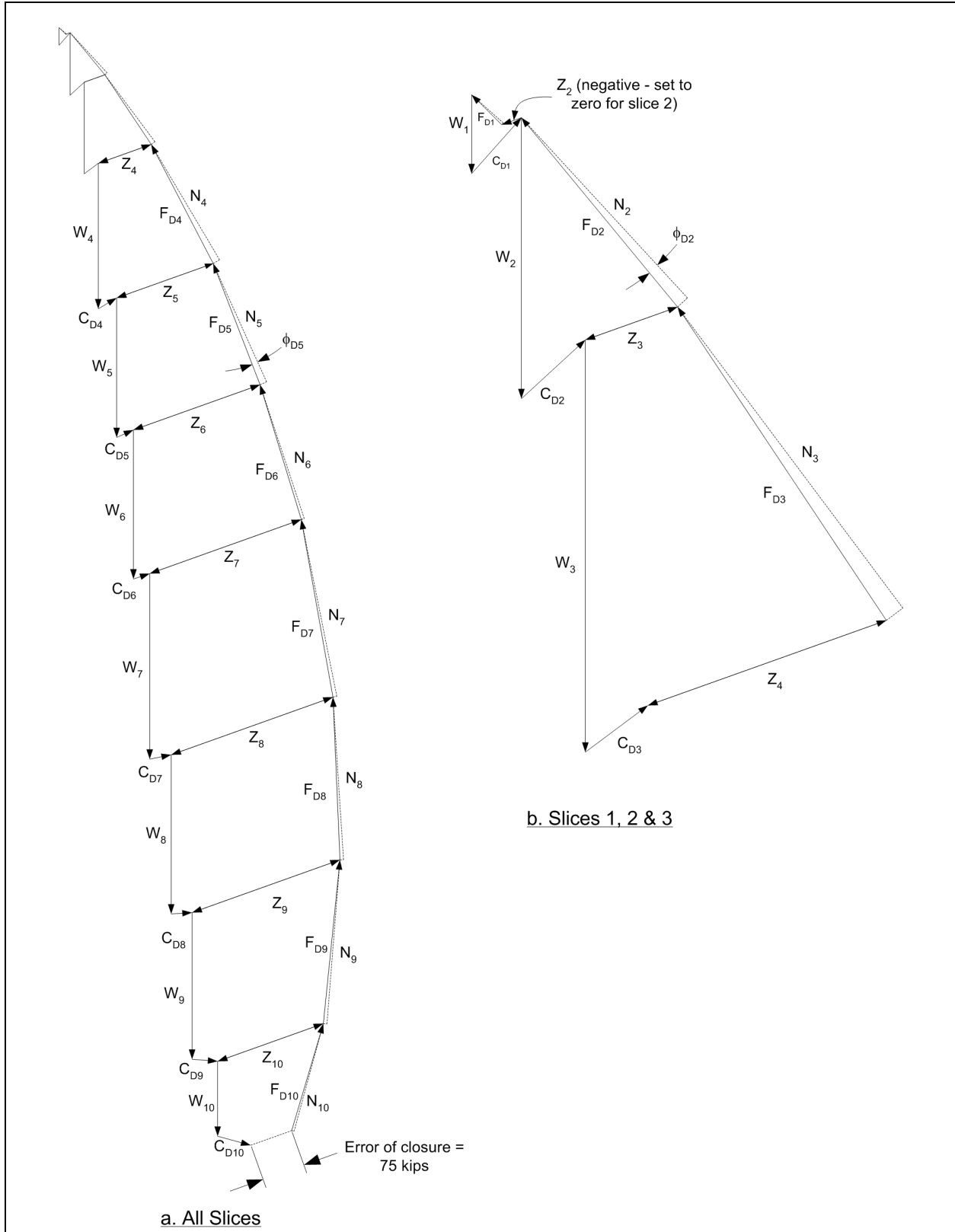
Figure F-14. Example calculations for end of construction stability condition – Modified Swedish Method – force polygons for graphical solution

	Total unit weight (γ), lbs./cu.ft.	Cohesion (c'), psf	Friction angle (φ'), degrees
Embankment	130	0	34
Foundation	125	0	35
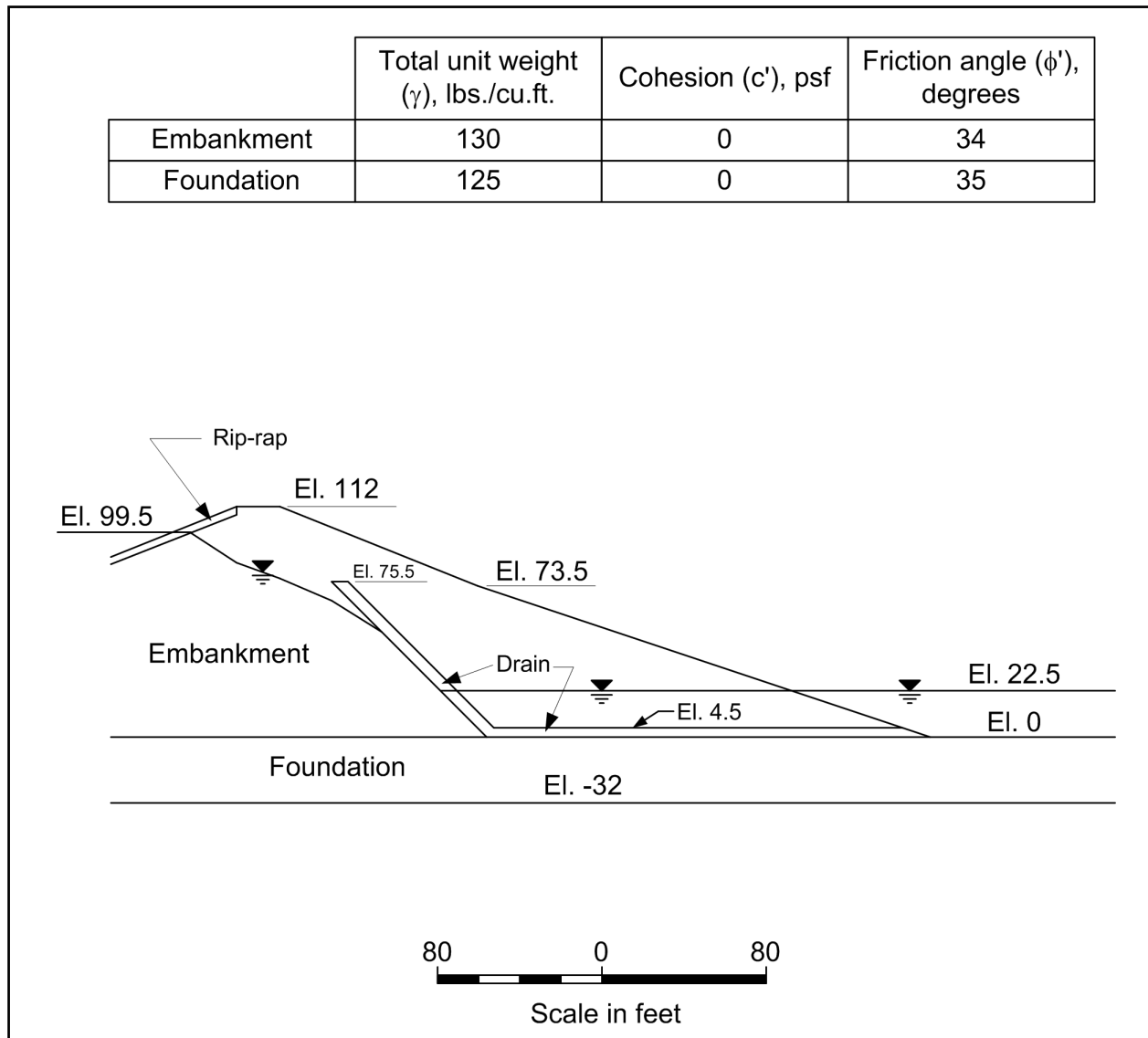
Figure F-15.   Slope for example steady seepage computations

compute the total slice weight. The bottoms of Slices 1 through 3 are located in the embankment and these slices were assigned the shear strength properties of the embankment soil (c' = 0, φ' = 34 degrees). The bottoms of slices 4 through 9 are located in the foundation soil and these slices were assigned the shear strength properties of the foundation (c' = 0, φ' = 35 degrees). Computations are shown in Columns 22 and 23 of the table in Figure F-17a for the final value of the factor of safety (F = 2.01). Computations were also performed for trial values of the factor of safety of 1.5, 2.0, and 2.5. The computed values are plotted versus the assumed values in Figure F-17b. The calculated values varied only slightly with the assumed value, as shown in Figure F-17b.

f.   Modified Swedish Method – numerical solution. Calculations using the numerical solution for the Modified Swedish Method are summarized in Figure F-18. For this example the interslice force inclination was assumed to be equal to the average embankment slope. The average embankment slope is 2.8 (horizontal) to 1 (vertical). The side force inclination used in the calculations was θ = arctan (1/2.8) = 19.7 degrees. Except for the forces from water pressures, most of the calculations and quantities shown in
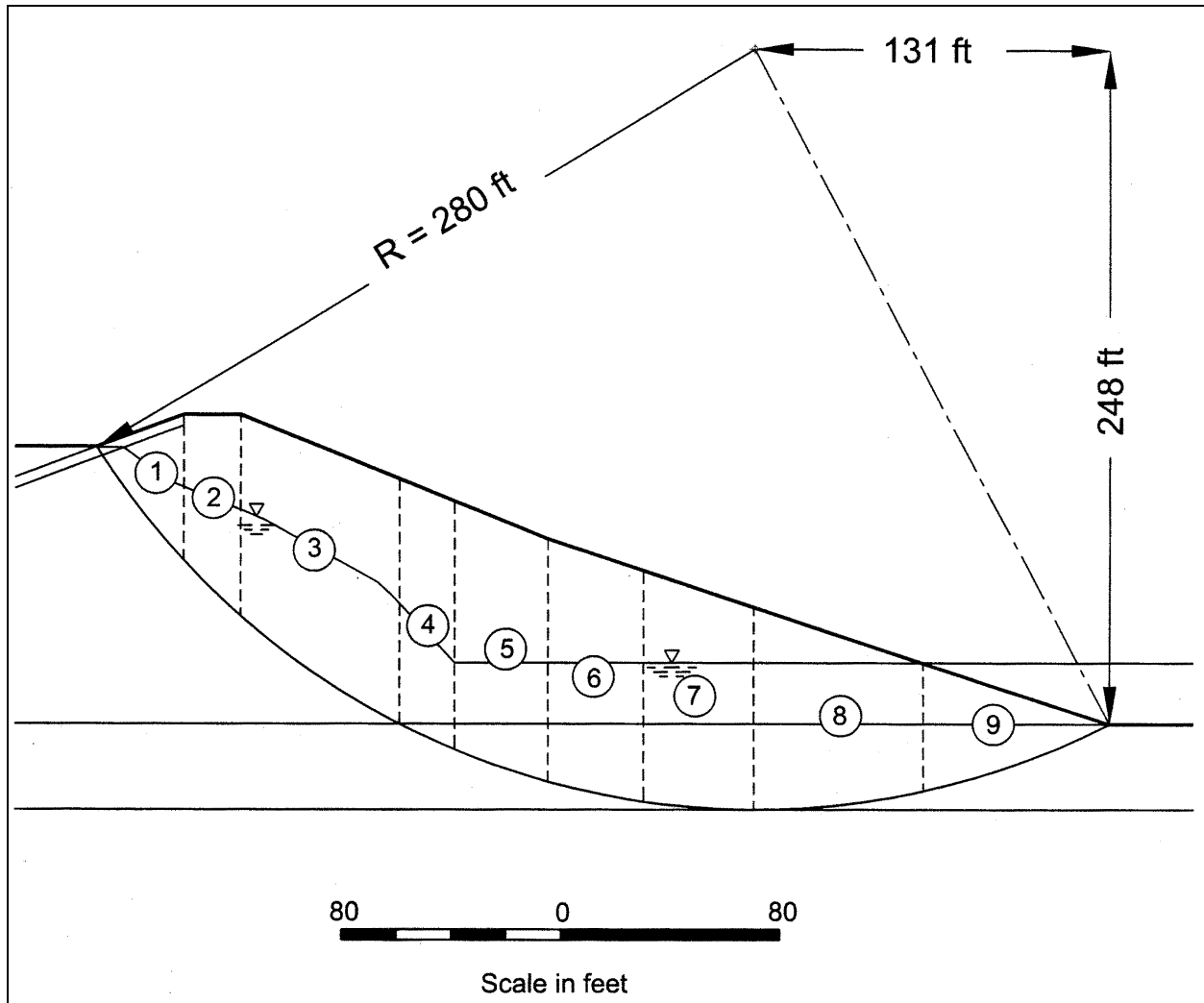
Figure F-16.   Circular slip surface and slices used for example computations for steady-state seepage

the table in Figure F-18 are the same as the ones used previously for the Simplified Bishop Method. The interslice forces, Z, are considered to be the effective forces and the water pressures on the sides of the slices are calculated independently. The calculations for the water pressures on the sides and top of the slices are shown in Columns 8 through 17 in the table in Figure F-18a. Calculation of the interslice forces is summarized in Column 23 in Figure F-18a for the final value of the factor of safety (F = 2.07), which satisfies force equilibrium. Calculations were also performed for three trial values of factor of safety F = 1.75, 2.00, and 2.25. The force imbalance for each assumed value of factor of safety is plotted versus the factor of safety in Figure F-18b. It can be seen that a value of F of 2.07 results in zero force imbalance.

   g.   Modified Swedish Method – graphical solution. Calculations using the graphical solution for the Modified Swedish Method are shown in Figures F-19, F-20, and F-21. The necessary numerical computations and the variation in error of closure with the assumed factor of safety are shown in Figure F-19. The force vector diagrams for the resultants of the forces due to water pressures and the weight of the slice (R_1, R_2, etc) are shown in Figure F-20. Finally, the equilibrium force polygons are shown in Figure F-21 for the final solution (F = 2.07), where the force polygons close without significant force imbalance.

1 Sliding Surface in	2 Slice Number	3 Horizontal Width (b), ft.	4 Average Slice Height, ft.	5 Slice Area, sq. ft	6 Embankment/Foundation	7 Total Weight	8 Base Inclination (α), degs.	9 W sin (α)	10 Height of Surface Water (h_s), ft	11 Avg. Surface Press. (P_surface), ksf	12 Surface Inclination (β), degs.	13 Surface Load (P), kips	14 Horiz. Moment arm (d_h), ft.	15 Vert. Moment arm (d_v), ft.	16 Moment (M_p), kip-ft.	17 Piezometric height (h_p), ft.	18 Pore Water Pressure (u), ksf	19 Cohesion (c), ksf	20 Friction Angle (φ'), degs.	21 c'b + (W + P cos β - ub) tan φ'	22 m_α (Assumed F = 2.01)	23 [c'b + (W + P cos β - ub) tan φ] ÷ m_α
Embankment	1	31	27	833	108	108	53	86	-	-	-	-	-	-	-	16	1.00	0	34	52	0.87	59
Foundation	2	21	64	1335	174	174	44	121	-	-	-	-	-	-	-	32	2.03	0	34	88	0.95	93
Foundation	3	56	82	4543	591	591	34	334	-	-	-	-	-	-	-	46	2.84	0	34	292	1.01	288
Foundation	4 4'	23	85 5	1938 121	252 15	267	25	113	-	-	-	-	-	-	-	39	2.44	0	35	148	1.05	141
Foundation	5 5'	35	74 16	2565 569	333 71	405	19	130	-	-	-	-	-	-	-	39	2.43	0	35	225	1.06	212
Foundation	6 6'	35	62 26	2176 906	283 113	396	11	78	-	-	-	-	-	-	-	48	3.02	0	35	203	1.05	194
Foundation	7 7'	38	50 31	1900 1167	247 146	393	4	27	-	-	-	-	-	-	-	53	3.32	0	35	187	1.02	183
Foundation	8 8'	64	33 28	2101 1801	273 225	498	-7	-57	-	-	-	-	-	-	-	51	3.17	0	35	208	0.95	218
Foundation	9 9'	68	11 12	759 835	99 104	203	-20	-70	11	0.70	18	50	97	238	8363	35	2.18	0	35	73	0.82	89
						764									8363							1476

$$F = \frac{1476}{764 - \dfrac{8363}{281}} = 2.01$$

a. Computation table (values shown for F = 2.01)

b. Trial vs calculated factor of safety

Figure F-17. Sample calculations for steady-state seepage – Simplified Bishop Method

b. Force imbalance vs. trial factor of safety

#	Parameter		1	2	3	4 / 4'	5 / 5'	6 / 6'	7 / 7'	8 / 8'	9 / 9'
1	Sliding Surface in		Embankment	Embankment	Embankment	Foundation	Foundation	Foundation	Foundation	Foundation	Foundation
2	Slice Number		1	2	3	4 / 4'	5 / 5'	6 / 6'	7 / 7'	8 / 8'	9 / 9'
3	Horizontal Width (b), ft.		31	21	56	23	35	35	38	64	68
4	Average Slice Height, ft.		27	64	82	85 / 5	74 / 16	62 / 26	50 / 31	33 / 28	11 / 12
5	Slice Area, sq. ft		833	1335	4543	1938 / 121	2565 / 569	2176 / 906	1900 / 1167	2101 / 1801	759 / 835
6	Weight kips	Embankment / Foundation	108	174	591	252 / 15	333 / 71	283 / 113	247 / 146	273 / 225	99 / 104
7		Total Weight	0	174	591	267	405	396	393	498	203
8	Piezometric Height	Upslope Side (h$_i$), ft.	27	53	74	90	91	90	86	76	47
9		Center (h$_{center}$), ft.	53	64	82	91	91	88	81	61	24
10		Downslope Side (h$_{i+1}$), ft.	0	74	90	91	90	86	76	47	0
11	Water Upslope Side Force (U$_i$), kips/ft		0	21	47	63	34	63	84	93	70
12	Water Downslope Side Force (U$_{i+1}$), kips/ft		21	47	63	34	63	84	93	70	0
13	Surface Loads	Height of Surface Water (h$_s$), ft	-	-	-	-	-	-	-	-	11
14		Press. At Top of Slice (P$_{surface}$), ksf	-	-	-	-	-	-	-	-	0.70
15		Slope at Top of Slice (β), degs	-	-	-	-	-	-	-	-	18
16		Length of Top of Slice (ℓ$_{top}$), ft	-	-	-	-	-	-	-	-	71
17		Surface Load (P), kips/ft	-	-	-	-	-	-	-	-	50
18	Base Inclination (α), degs.		53	44	34	25	19	11	4	-7	-20
19	Slice Base Length (Δℓ), ft.		51	29	67	25	36	36	38	64	72
20	Pore Water Pressure (u), ksf		1.00	2.03	2.84	2.44	2.43	3.02	3.32	3.17	2.18
21	Cohesion (c), ksf		0	0	0	0	0	0	0	0	0
22	Friction Angle (φ), degs.		34	34	34	35	35	35	35	35	35
23	Interstice Force on Downslope Side (Z$_{i+1}$), kips (Assumed F = 2.07)		62	134	346	426	426	385	302	124	0

a. Computation table for factor of safety (values shown for trial F = 2.07)

Figure F-18. Sample calculations for steady-state seepage – Modified Swedish Method – numerical solution

b. Error of closure of force
Equilibrium polygons vs. trial
factor of safety

a. Table of numerical values computed for graphical solution

1 Sliding Surface in	2 Slice Number	3 Horizontal Width (b), ft.	4 Average Slice Height, ft.	5 Slice Area, sq. ft	6 Weight kips Embankment / Foundation	7 Weight kips Total Weight	8 Piezometric Height Upslope Side (h_i), ft.	9 Piezometric Height Center (h_center), ft.	10 Piezometric Height Downslope Side (h_{i+1}), ft.	11 Water Upslope Side Force (U_i), kips/ft	12 Water Downslope Side Force (U_{i+1}), kips/ft	13 Height of surface water (h_s), ft	14 Press. At Top of Slice (P_surface), ksf	15 Slope at Top of Slice (β), degs	16 Length of Top of Slice (ℓ_top), ft	17 Surface Load (P), kips/ft	18 Slice Base Length (ℓ), ft.	19 Pore Water Pressure (u), ksf	20 U_b = u Δℓ, kips/ft	21 c'Δℓ, kips/ft	22 C_D = c'Δℓ/F, kips/ft	23 φ_D = arctan(tan φ/F), degs
Embankment	1	31	27	833	108	0	27	53	0	0	21	-	-	-	-	-	51	1.00	51	0	-	18.1
Embankment	2	21	64	1335	174	174	53	64	74	21	47	-	-	-	-	-	29	2.03	60	0	-	18.1
Embankment	3	56	82	4543	591	591	74	82	90	47	63	-	-	-	-	-	67	2.84	192	0	-	18.1
Foundation	4 / 4'	23	85 / 5	1938 / 121	252 / 15	267	90	91	91	63	34	-	-	-	-	-	25	2.44	61	0	-	18.7
Foundation	5 / 5'	35	74 / 16	2565 / 569	333 / 71	405	91	91	90	34	63	-	-	-	-	-	36	2.43	89	0	-	18.7
Foundation	6 / 6'	35	62 / 26	2176 / 906	283 / 113	396	90	88	86	63	84	-	-	-	-	-	36	3.02	108	0	-	18.7
Foundation	7 / 7'	38	50 / 31	1900 / 1167	247 / 146	393	86	81	76	84	93	-	-	-	-	-	38	3.32	126	0	-	18.7
Foundation	8 / 8'	64	33 / 28	2101 / 1801	273 / 225	498	76	61	47	93	70	-	-	-	-	-	64	3.17	203	0	-	18.7
Foundation	9 / 9'	68	11 / 12	759 / 835	99 / 104	203	47	24	0	70	0	11	0.70	18	71	50	72	2.18	156	0	-	18.7

Figure F-19. Sample calculations for steady-state seepage – Modified Swedish Method – graphical solution - numerical values

Figure F-20. Sample calculations for steady-state seepage – Modified Swedish Method – graphical solution – resultant force (R) diagrams
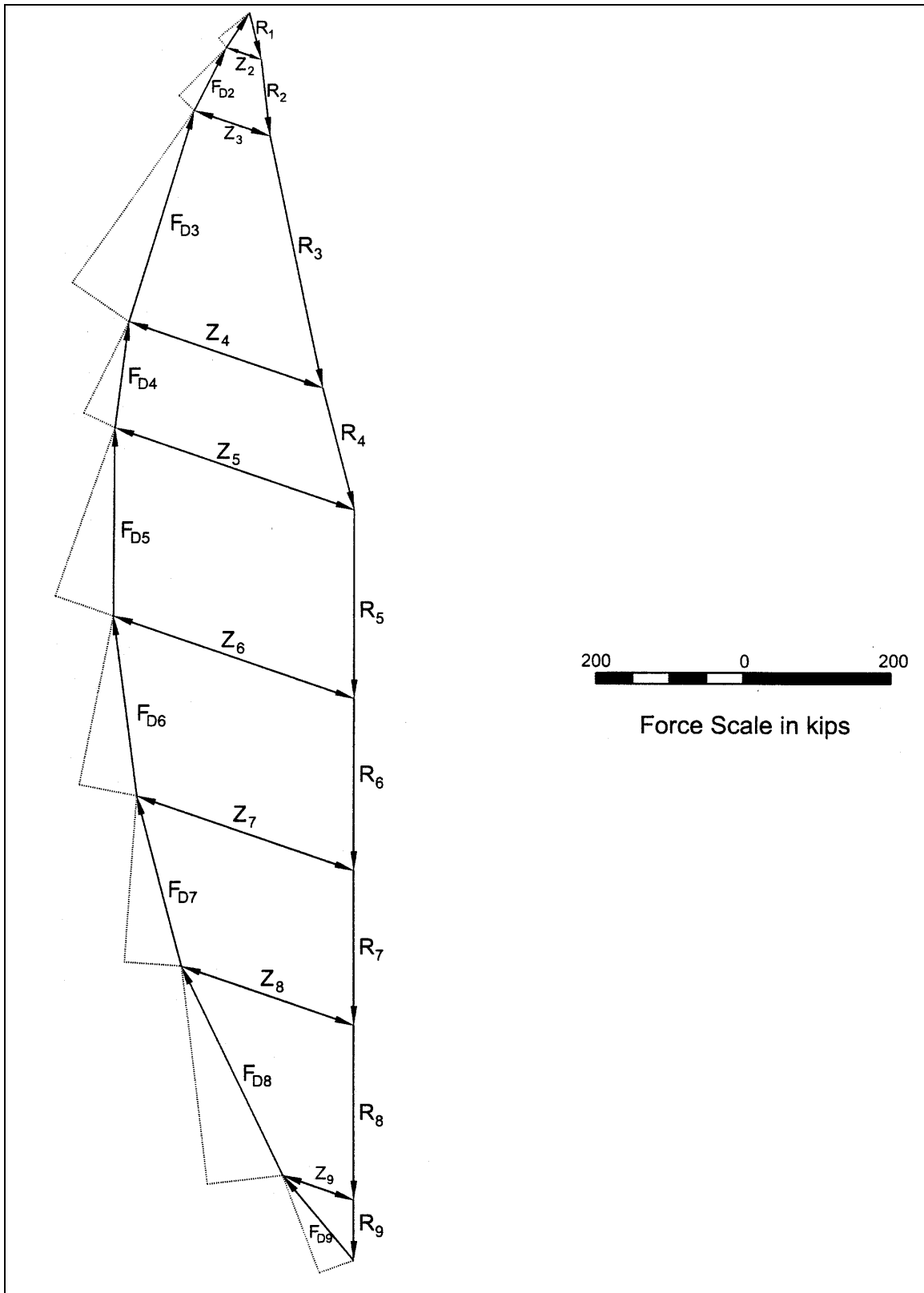
Figure F-21.   Sample calculations for steady-state seepage – Modified Swedish Method – graphical solution – force equilibrium polygons

Appendix G
Procedures and Examples for Rapid Drawdown

G-1. General

Embankments may become saturated by seepage during a prolonged high reservoir stage. If subsequently the reservoir pool is drawn down faster than the pore water can escape, excess pore water pressures and reduced stability will result. For analysis purposes it is assumed that drawdown is very fast, and no drainage occurs in materials with low permeability. Two separate procedures for computing slope stability for rapid drawdown are presented in this appendix.

   a. The first method is the one described in the 1970 version of this manual. It will be referred to here as the "Corps of Engineers' 1970 procedure."

   b. The second method is the one developed by Lowe and Karafiath (1960),[1] and modified by Wright and Duncan (1987), and by Duncan, Wright, and Wong (1990). The objectives of the modifications were (1) to simplify the method, and (2) to account more accurately for shear strength in zones where drained strength is lower than undrained strength. The second method is more rational than the first, and is recommended. The first method may be unrealistically conservative for soils that dilate during shear, and may lead to uneconomical designs.

G-2. U.S. Army Corps of Engineers' 1970 Procedure - Background

This method was presented in the previous (1970) version of this manual (USACE 1970). It involves two complete sets of stability calculations for each trial shear surface. The first set of calculations is performed for the conditions before drawdown, and is used to estimate the effective stresses to which the soil is consolidated before drawdown. Although a factor of safety is computed in the first set of calculations, the purpose of the first set of calculations is to compute the consolidation stresses. The effective stresses before drawdown are used to estimate the undrained shear strengths that would exist during rapid drawdown. These shear strengths are then used to perform a second set of stability calculations for conditions immediately after drawdown. The factor of safety from the second set of calculations is the factor of safety for the rapid drawdown condition.

   a. First-stage computations. The first-stage computations are performed to calculate the effective stresses to which the soil is consolidated prior to drawdown. The soil strengths and pore water pressures used in the analysis are the same as those used for the long-term analysis of the steady seepage condition. Effective stress shear strength parameters derived from Consolidated-Undrained (CU or R) tests with pore water pressure measurements, or from Consolidated-Drained (CD or S) tests should be used. Pore water pressures are computed from hydrostatic conditions or an appropriate seepage analysis. External water pressures from the reservoir or other adjacent water are applied as loads to the face of the slope. The objective of the computations is to evaluate the effective stresses on the base of each slice along the assumed slip surface. The effective stresses are obtained by dividing the total normal force (N) on the base of each slice by the length of the base, and subtracting the pore water pressure, i.e.,

$$\sigma'_c = \frac{N}{\Delta \ell} - u \tag{G-1}$$

---

[1] Reference information is presented in Appendix A.

The stress σ'_c is the effective normal stress, or consolidation stress, on the slip surface before drawdown.

b. Second-stage shear strengths. Once the effective consolidation stresses have been calculated from the first-stage computations, shear strengths are estimated for the second stage. The shear strengths are estimated from a "composite," bilinear shear strength envelope. The envelope represents the lower bound of the R and S strength envelopes.

(1) The R envelope is determined by plotting a circle using the effective minor principal stress during consolidation, σ'_{3c}, and the principal stress difference at failure, $(\sigma_1 - \sigma_3)_f$, as shown in Figure G-1, together with the corresponding R envelope. Figure G-1a shows the envelope using conventional axes $(\sigma - \tau)$; while Figure G-1b shows the envelope on a modified diagram of $(\sigma_1 - \sigma_3)_f$ versus σ_3. Neither envelope is a valid Mohr-Coulomb envelope, because they are plotted using one stress that existed during consolidation, σ'_{3c}, and another stress that existed at failure, $(\sigma_1 - \sigma_3)_f$. Accordingly, this envelope is not consistent with the fundamental principles of soil mechanics. It is empirical and should only be used in empirical procedures like the 1970 procedure for rapid drawdown.

(2) The composite envelope used to determine the shear strengths for the second-stage computations is shown in Figure G-2. The envelope represents the lower bound of the empirical R envelope described above, and the effective stress S envelope. Shear strengths are determined for the second-stage computations using the effective normal stress calculated for the first stage (from Equation G-1) and the composite envelope shown in Figure G-2. Shear strengths are determined in this manner for each slice whose base lies in material that does not drain freely.

c. Second-stage computations. The second-stage computations are performed to calculate the stability immediately after drawdown. For materials that do not drain freely the shear strengths are determined in the manner described in G-2b. These strengths are assigned as values of cohesion, c, with ϕ equal to zero. For materials that drain freely, effective stress shear strength parameters, c' and ϕ', are used, and appropriate pore water pressures are prescribed. The pore water pressures for free-draining materials should represent the values after drawdown has occurred and steady-state seepage has been established at the new lower water level. The pore water pressures for materials which do not drain freely are set equal to zero. If a portion of the slope remains submerged after drawdown, the external water pressures acting on the submerged part of the slope are calculated and applied as external loads to the surface of the slope.

G-3. Improved Method for Rapid Drawdown – Background

This method was developed by Lowe and Karafiath (1960), and modified by Wright and Duncan (1987) and Duncan, Wright, and Wong (1990). The method involves either two or three separate slope stability calculations for each trial slip surface. The first computation is the same as that for the Corps of Engineers' 1970 procedure and is used to calculate the effective stresses to which the soil is consolidated before drawdown. The second set of computations is performed using undrained shear strengths corresponding to the effective consolidation stresses calculated in the first stage. If the drained shear strength is less than the undrained shear strength for any slices, a third set of calculations is performed, using drained shear strengths for those slices. The factor of safety from the last stage (the second or third stage) is the factor of safety after rapid drawdown.

a. First-stage computations. The first-stage computations are the same as those for the Corps of Engineers' 1970 method. However, in addition to computing the consolidation normal stress on the base of each slice, σ'_c, the shear stress at consolidation, τ_c, is also calculated for each slice. The shear stress at consolidation is calculated by dividing the shear force (S) on the base of the slice by the length of the base, i.e.,

a. Mohr-Coulomb diagram

b. Modified Mohr-Coulomb diagram

$$\phi_R = \arcsin\left(\frac{\tan\Psi_R}{2 + \tan\Psi_R}\right)$$

$$C_R = \frac{d_R(1-\sin\phi_R)}{2\cos\phi_R}$$
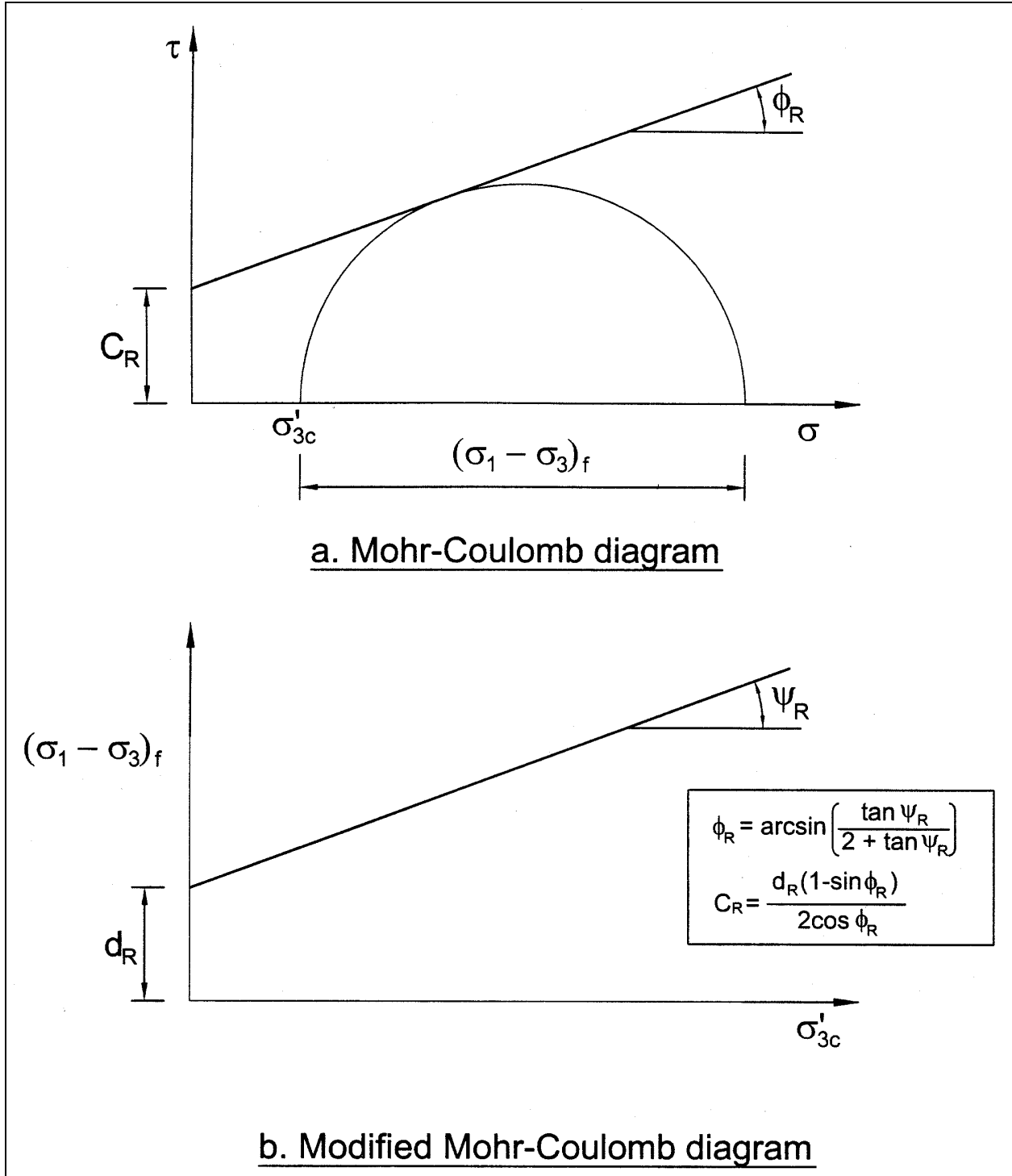
Figure G-1.   R Shear strength envelope used in Corps of Engineers' (1970) method for rapid drawdown
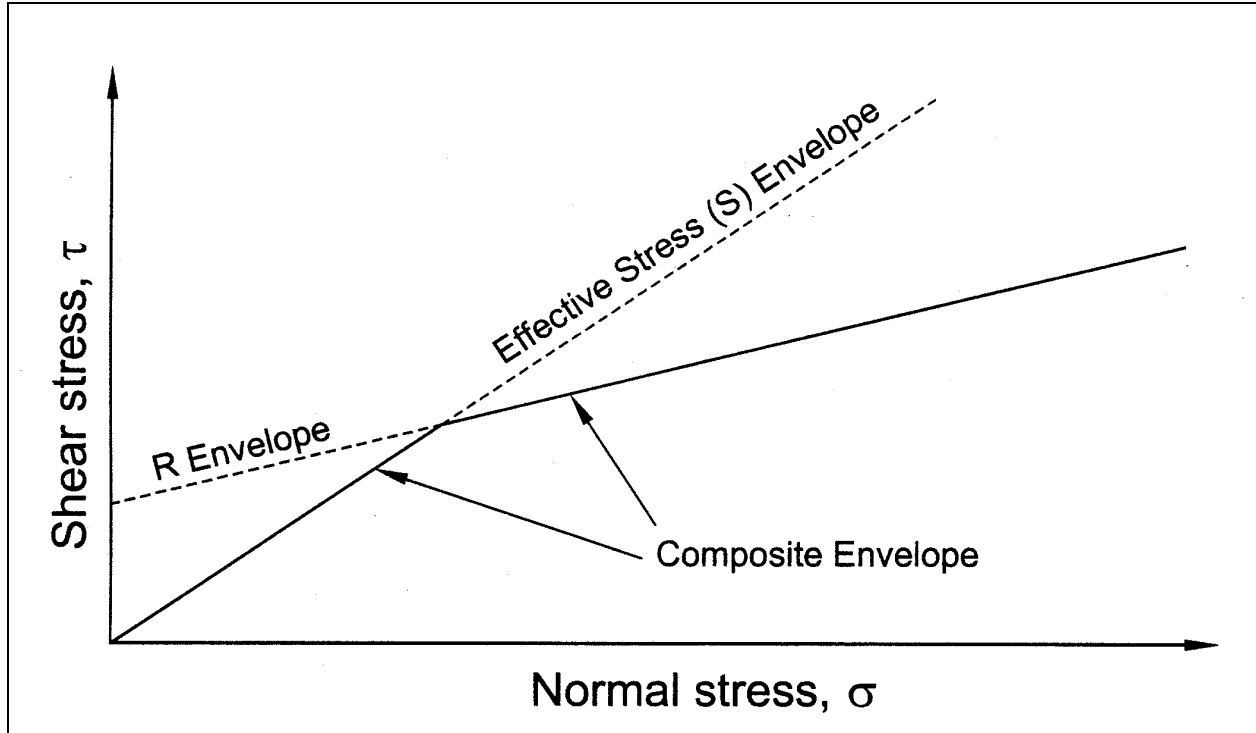
Figure G-2. Composite shear strength envelope used in Corps of Engineers' (1970) method for rapid drawdown

$$\tau_c = \frac{S}{\Delta \ell} \tag{G-2}$$

b. Second-stage shear strengths. Two shear strength relationships are used to evaluate shear strengths for the second-stage computations.

(1) The first is the relationship between undrained shear strength (shear stress on the failure plane at failure), τ_{ff}, and effective normal stress on the failure plane during consolidation, σ'_{fc}. This relationship can be determined directly from the results of isotropically consolidated-undrained (CU or R) tests, or it can be calculated from the strength parameters, c_R and ϕ_R, that are determined from the R envelope shown in Figure G-1.

(a) To determine the relationship between τ_{ff} and σ'_{fc} directly from the results of isotropically consolidated-undrained triaxial compression tests, the shear stress on the failure plane at failure, τ_{ff}, is plotted versus the effective stress on the failure plane at consolidation, σ'_{fc}. The values of τ_{ff} and σ'_{fc} are calculated using the following equations:

$$\tau_{ff} = \frac{(\sigma_1 - \sigma_3)_f}{2} \; \cos \; \phi' \tag{G-3}$$

and

$$\sigma'_{fc} = \sigma'_{3c} \tag{G-4}$$

where

$(\sigma_1 - \sigma_3)_f$ = principal stress difference at failure

ϕ' = effective stress angle of internal friction

σ'_{3c} = CU test consolidation pressure

σ'_{fc} is equal to σ'_{3c} because the consolidation pressure is the same on all planes in an isotropic consolidated undrained triaxial test.

(b) An example relationship of τ_{ff} vs. σ'_{fc} is shown in Figure G-3. The intercept and slope of this envelope are designated, $d_{K_c=1}$ and $\psi_{K_c=1}$. If values of τ_{ff} and σ'_{fc} are determined directly from the CU test results, the values of $d_{K_c=1}$ and $\psi_{K_c=1}$ are determined by drawing a line through the data and measuring the intercept and the slope as indicated in Figure G-3.

$$\tau_{ff} = \frac{(\sigma_1 - \sigma_3)_f}{2} \cos \phi'$$
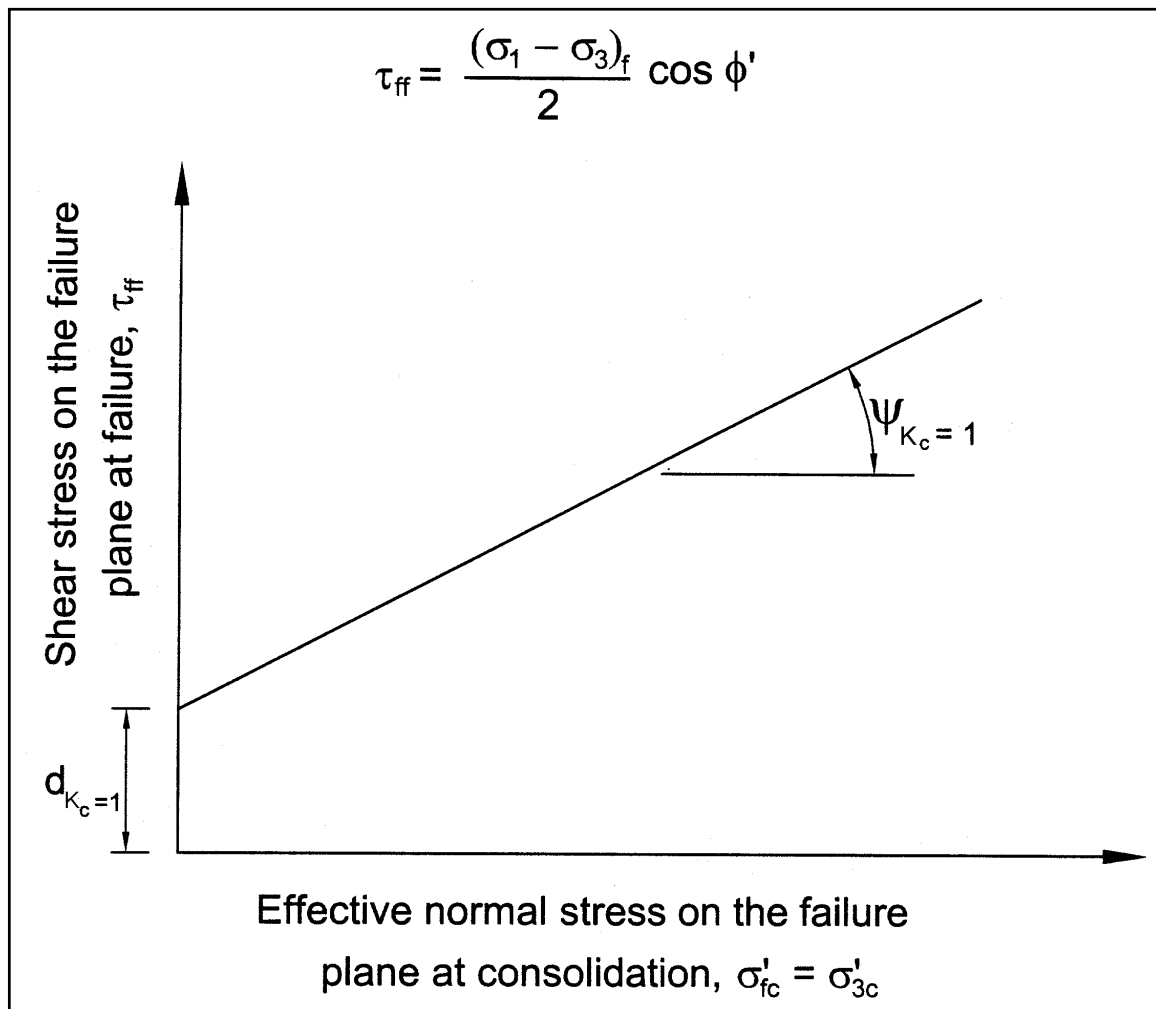
Figure G-3. τ_{ff} **vs** σ'_{fc} **Shear strength envelope from isotropically consolidated undrained (CU or R) triaxial compression tests**

(c) The values of $d_{K_c=1}$ and $\psi_{K_c=1}$ are related to the intercept and slope (c_R and ϕ_R) of the R-envelope shown in Figure G-1 and can be computed if c_R and ϕ_R have been evaluated. The relationships between the parameters $d_{K_c=1}$ and $\psi_{K_c=1}$ and the parameters c_R and ϕ_R are follows:

$$d_{K_c=1} = c_R \left(\frac{\cos \phi_R \; \cos \phi'}{1 - \sin \phi_R} \right) \tag{G-5}$$

$$\psi_{K_c=1} = \tan^{-1} \left(\frac{\sin \phi_R \; \cos \phi'}{1 - \sin \phi_R} \right) \tag{G-6}$$

(2) The other shear strength relationship needed for the second-stage computations is the effective stress envelope. Although this envelope is for drained strengths, it may also be viewed as an envelope representing the undrained shear strength of soil that is consolidated to stresses that bring the soil to failure before any undrained loading is applied. In this case, no additional load can be applied in undrained shear before the soil fails. In such a test, the stresses at failure are the same as those at consolidation.

(a) The two shear strength envelopes that are used to determine undrained shear strengths for the second-stage stability computations are shown in Figure G-4. Both envelopes represent relationships between undrained shear strength, τ_{ff}, and effective consolidation pressure on the failure plane, σ'_{fc}.
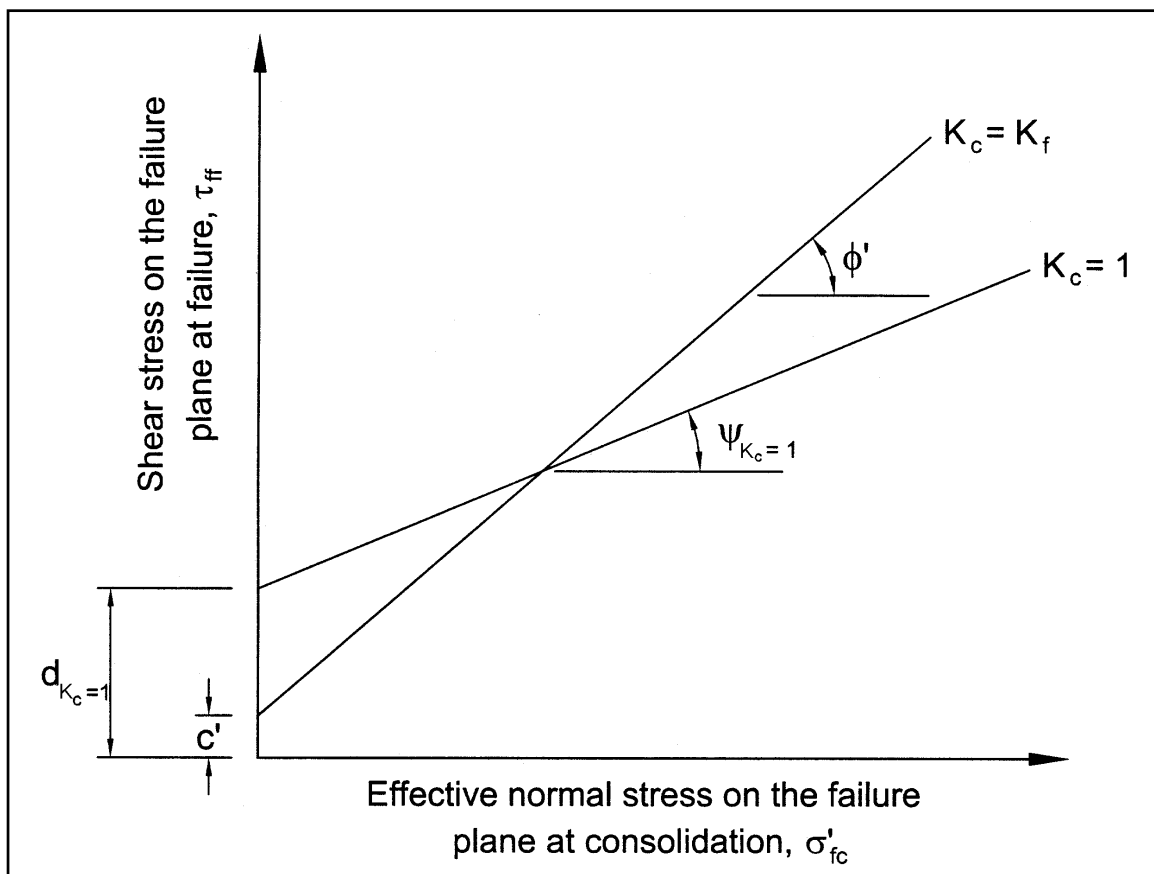
Figure G-4. τ_{ff} **vs** σ'_{fc} **Shear strength envelope used for improved procedure for rapid drawdown analysis**

(b) The two envelopes shown in Figure G-4 correspond to the extreme possible values of the ratio of $\sigma'_{1c}/\sigma'_{3c} = K_c$. As discussed above, one of the envelopes corresponds to isotropic consolidation, or $K_c = 1$, and the other corresponds to the maximum possible ratio, or $K_c = \sigma'_{1f}/\sigma'_{3f} = K_f$. The undrained shear strengths needed for the second-stage stability analyses are interpolated between these envelopes, using the value of K_c for each slice determined from the first stage computations as the basis for interpolating between the envelopes.

(c) As noted above, the values of K_c ranges from 1.0 to K_f. If $c' = 0$, the value of K_f is given by the following equation:

$$K_f = \frac{1 + \sin\ \phi'}{1 - \sin\ \phi'} \tag{G-7}$$

If c' is not equal to zero, the value of K_f varies with the effective consolidation pressure σ'_{fc}, as shown by the following equation:

$$K_f = \frac{(\sigma'_{fc} + c'\ \cos\ \phi')(1 + \sin\ \phi')}{(\sigma'_{fc} - c'\ \cos\ \phi')(1 - \sin\ \phi')} \tag{G-8}$$

(3) The following steps are used to compute undrained shear strength values for each slice using the stresses σ'_c and τ_c from the first-stage computations:

(a) Compute undrained shear strengths from the two shear strength envelopes shown in Figure G-3. The shear strengths are computed using the effective consolidation stress, σ'_c, as follows:

$$\tau_{(ff - K_c = 1)} = d_{(K_c = 1)} + \sigma'_c\ \tan(\psi_{K_c = 1}) \tag{G-9}$$

$$\tau_{(ff - K_c = K_f)} = c' + \sigma'_c\ \tan(\phi') \tag{G-10}$$

(b) Compute the effective principal consolidation stress ratio at failure, K_f, from Equation G-7 or G-8.

(c) Calculate the principal stress ratio at consolidation, K_c, for the stresses on the base of the slice,

$$K_c = \frac{\sigma'_c + \tau_c\ \dfrac{\sin\ \phi' + 1}{\cos\ \phi'}}{\sigma'_c + \tau_c\ \dfrac{\sin\ \phi' - 1}{\cos\ \phi'}} \tag{G-11}$$

where the stresses σ'_c and τ_c are those from the first-stage computations.

Equation G-11 is derived by assuming that the orientation of the principal stresses during consolidation is the same as at failure, as suggested by Lowe and Karafiath (1960).

(d) Calculate, by linear interpolation between the two values of shear strength determined in Step a, the undrained shear strength, τ_{ff}, for the slice. The undrained shear strength is calculated using the following equation:

$$\tau_{ff} = \frac{(K_f - K_c)\tau_{ff-K_c=1} + (K_c - 1)\tau_{ff-K_c=K_f}}{K_f - 1} \tag{G-12}$$

c. Second-stage computations. The second-stage computations are performed to calculate stability immediately after drawdown, assuming that all low-permeability materials are undrained. The low-permeability materials are assigned undrained shear strength values calculated from Equation G-12, with ϕ set equal to zero. Effective stress shear strength parameters are used for materials that drain freely, and appropriate pore water pressures are prescribed. The pore water pressures for free-draining materials are those after drawdown has occurred and steady-state seepage has been reestablished. The pore water pressures in the low-permeability materials are set equal to zero. If a portion of the slope remains submerged after drawdown, the external water pressures acting on the submerged part of the slope are calculated and applied as external loads to the surface of the slope.

d. Strengths for third-stage computations. Once the second-stage computations have been completed, each slice is examined to determine if the drained strength would be less than the undrained strength determined from Equation G-12. The drained shear strength is estimated as follows:

(1) The total normal stress on the base of each slice is calculated by dividing the normal force, N, calculated in the second-stage computations by the length of the base, i.e.,

$$\sigma = \frac{N}{\Delta\ell} \tag{G-13}$$

(2) An approximate value of the drained effective stress, σ'_d, after steady-state seepage is reestablished is computed by subtracting the pore water pressure from the total stress, i.e.,

$$\sigma'_d = \sigma - u \tag{G-14}$$

where σ is the total normal stress calculated in Equation G-13.

Because the total normal stress is based on the second-stage computations, it is not necessarily the same as the total normal stress that would exist after drainage has occurred. However, it should not be much different, and it is reasonable to assume that it is the same for the purpose of these analyses. The pore water pressure, u, in Equation G-14 should be the pore water pressure after steady-state seepage is reestablished following drawdown. The pore water pressure is not the same as the pore water pressure used in the first-stage computations.

(3) The drained shear strength is estimated using the effective stress calculated in Equation G-14 and the effective stress shear strength parameters, c' and ϕ', which are the same as those used in the first-stage computations. The drained shear strength, s_d, is calculated from:

$$s_d = c' + \sigma'_d \tan(\phi') \tag{G-15}$$

(4) The drained shear strength calculated in Equation G-15 is compared to the value of undrained shear strength for this slice that was used in the second-stage computations. If the drained shear strength is greater than the undrained shear strength for all slices where the undrained shear strength was used previously, then no further computations are required. In that case, the factor of safety after rapid drawdown is equal to the factor of safety calculated for the second stage. If for any slice the drained shear strength is less than the undrained shear strength used for the second-stage computations, a third-stage computation is performed. For

those slices where the drained shear strength is less than the undrained shear strength, the effective stress drained shear strength parameters, c' and ϕ', are assigned to those slices for the third-stage computations. Pore water pressures are assigned based on the reestablished steady-state seepage conditions. For those slices where the undrained shear strength is less than the estimated drained shear strength, the same undrained shear strengths used for the second-stage computations are used for the third stage.

e. Third-stage computations. The third-stage stability computations are performed using the same conditions as for the second-stage computations, except for those materials where drained strengths are lower than undrained strengths. For those slices the drained strength parameters and appropriate pore water pressures are used, as noted above. The factor of safety after rapid drawdown is equal to the factor of safety calculated for the third stage. If the third-stage computations are not required, the factor of safety after rapid drawdown is equal to the factor of safety calculated for the second stage.

G-4. Example Problems

Three examples of rapid drawdown stability analyses of the slope shown in Figure G-5 are presented in the following sections. The slope is homogeneous, with the shear strength properties indicated in the table shown in Figure G-5. The unit weight of soil is 135 pcf. The unit weight is assumed to be the same above and below the water levels and does not change as a result of drawdown. Drawdown is from a maximum pool level of 103 feet to a minimum pool of 24 feet.

a. All computations are performed for the circular slip surface shown in Figure G-6. The soil mass above the trial slip surface is subdivided into 12 slices. The slip surface is not the critical slip surface.

b. For simplicity in the example calculations, it was assumed that the piezometric line was horizontal at the elevation of the maximum pool. Similarly, after drawdown and reestablishment of steady-state seepage, the piezometric line was assumed to be horizontal at the reservoir level after drawdown. In many slopes it would be appropriate to perform seepage analyses to determine the pore water pressures before and after drawdown.

c. In the following sections, three analyses are presented. The first uses the Corps of Engineers' 1970 procedure (USACE 1970) for rapid drawdown, and the Modified Swedish Method for the stability calculations. The second uses the improved (and recommended) procedure for rapid drawdown and the Simplified Bishop Method for the stability calculations. The third uses the improved procedure for rapid drawdown, and the Modified Swedish Method for stability calculations, with side force inclinations determined using Spencer's Method.

G-5. U.S. Army Corps of Engineers' 1970 Procedure - Example

The first analysis uses the U.S. Army Corps of Engineers' 1970 procedure (USACE 1970) for rapid drawdown analyses. Although the improved method described in Section G-3 is recommended, the 1970 method has been used for design of many dams, and it may be necessary to use this method to check those older designs. Stability calculations for the 1970 method were performed using the Modified Swedish Method and the 1970 recommendations regarding the inclination of interslice forces. This was done for consistency with the original procedure as described in the earlier manual, although Spencer's Method is currently recommended. The interslice forces are assumed to be parallel to the average embankment slope. The average embankment slope is 2.84 (horizontal) to 1 (vertical), yielding an interslice force inclination of 19.4 degrees measured from the horizontal.

Effective stress (CD or S) envelope		R-envelope		τ_{ff} vs. σ'_{fc} envelope	
Intercept, c'	Slope, ϕ	Intercept, c_R	Slope, ϕ_R	Intercept, $d_{kc=1}$	Slope, $\psi_{kc=1}$
0	30°	1200 psf	16°	1379 psf	18.2°

Max. Pool: El. 103
El. 110
2.5:1
El. 74
Unit weight, γ = 135 pcf
3:1
Min. Pool: El. 24
El. 0
Note: All elevations in feet
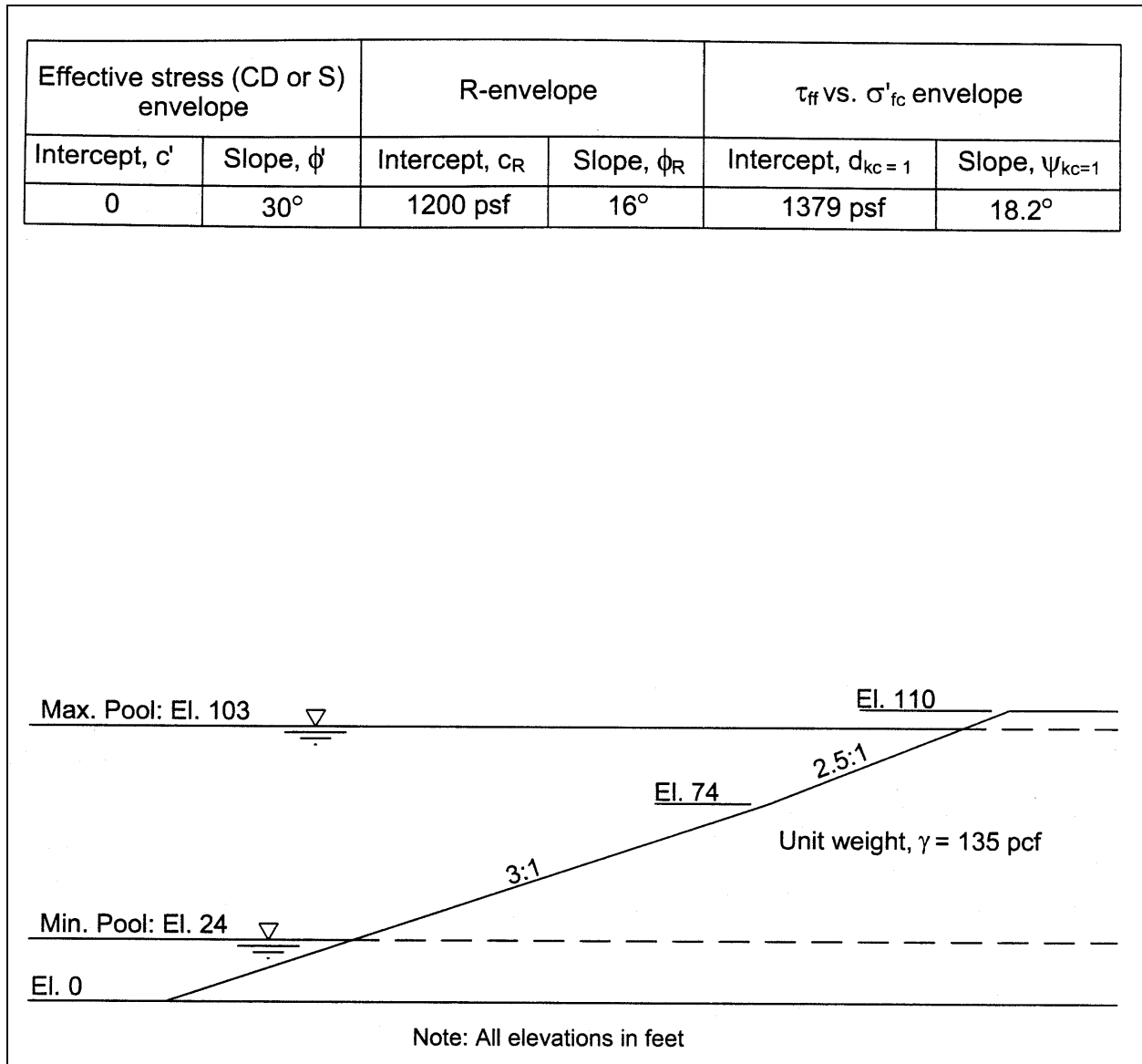
Figure G-5. Slope and soil properties for example problem

a.   The interslice forces are total forces and thus include the water pressures on the sides of the slices. This approach is necessary for the second stage where undrained shear strengths are used and pore water pressures are therefore unknown. For consistency, the same approach was used for both stages. The use of total, rather than effective, interslice forces is also consistent with most computer software. The stability calculations are performed using the numerical Modified Swedish Method. Because undrained shear strengths must be computed from the results of the first-stage analysis, the numerical solution procedures is more suitable than the graphical procedure. Calculations for the numerical procedure are easily performed using spreadsheet software, making the calculations relatively easy as compared with the graphical procedure.

(1) *Step 1 – First-stage computations* Calculations for the first-stage computations are summarized in the table presented in Figure G-7a. Effective stress shear strength parameters (c' = 0, ϕ' = 30 degrees) are used for all slices. Slice weights are computed using total unit weight. The pore water pressures are calculated from the horizontal piezometric surface assumed for this example, as explained above.
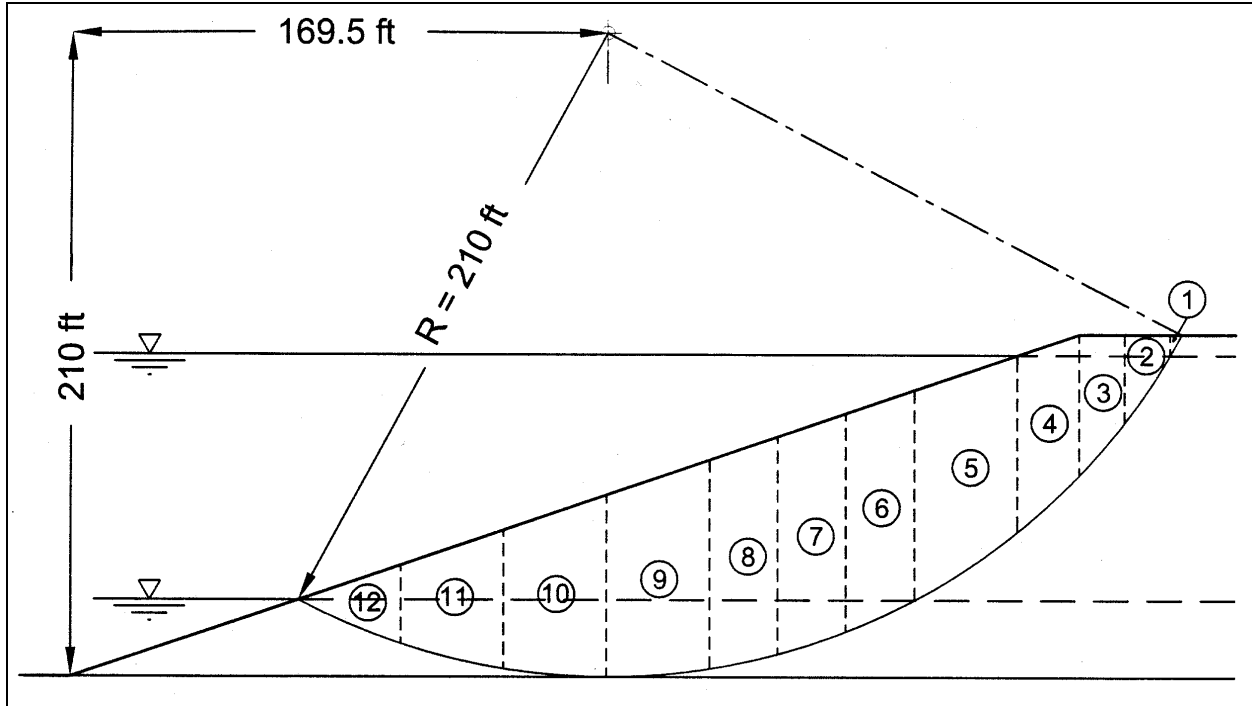
Figure G-6. Circular slip surface and slices used for computations

Calculations are shown in Figure G-7a for the final trial value for factor of safety (F = 3.49), which satisfies equilibrium. The factor of safety for the first stage is of little interest. The purpose of the calculations is to determine the stresses on the slip surface for use in computing undrained shear strengths for the second-stage analysis.

(2) *Step 2 – Computation of shear strengths for second-stage analysis*. Calculation of the effective consolidation stress and the shear strengths for the second-stage computations are illustrated in the table shown in Figure G-7b. The steps involved in the computations are as follows:

(a) The total normal force on the base of each slice is calculated using the equation,

$$N = \frac{W + P\cos\beta - (Z_i - Z_{i-1})\sin\theta - (c' - u\,\tan\phi')\dfrac{\Delta\ell}{F}\sin\alpha}{\cos\alpha + \dfrac{\tan\phi'\sin\alpha}{F}} \tag{G-16}$$

The terms in this equation are as defined in Appendix C.

(b) The effective normal stress, σ'_{fc}, is calculated by dividing the total normal force (N) by the length of the base of the slice, $\Delta\ell$ and subtracting the pore water pressure, i.e.,

$$\sigma'_{fc} = \frac{N}{\Delta\ell} - u \tag{G-17}$$

a. First-stage stability computations

1	2	3	4	5	6	7	8	9	10	11	12	13	14	15	16	17
					Surface loads											
Slice Number	Horizontal Width (b), ft.	Average Slice Height, ft.	Slice Area, sq. ft	Total Weight (W), kips	Height of Surface Water (h_s), ft	Press. At Top of Slice ($P_{surface}$), ksf	Slope at Top of Slice (β), degs	Length of Top of Slice (ℓ_{top}), ft	Surface Load (P), kips	Base Inclination (α), degs.	Slice Base Length (ℓ), ft.	Piezometric height (h_p), ft.	Pore Water Pressure (u), ksf	Cohesion (c), ksf	Friction Angle (φ), degs.	Interstice Force on Downslope Side (Z_{i+1}), kips (Assumed F = 3.49)
1	4	4	14	2	0	0	18	4	0	61	8	0	0.00	0	30	2
2	20	21	428	58	0	0	18	20	0	55	35	14	0.89	0	30	53
3	18	45	807	109	0	0	18	18	0	46	26	38	2.36	0	30	132
4	18	58	1015	137	0	0	18	19	0	40	23	55	3.40	0	30	215
5	28	65	1785	241	6	0.34	18	30	10	32	32	70	4.39	0	30	332
6	22	69	1508	204	15	0.96	18	24	23	24	24	84	5.24	0	30	403
7	23	68	1570	212	24	1.52	18	25	38	18	24	93	5.78	0	30	448
8	22	66	1449	196	33	2.04	18	23	47	11	22	99	6.15	0	30	465
9	31	60	1644	249	41	2.58	18	32	83	4	31	102	6.36	0	30	439
10	35	49	1702	230	52	3.26	18	36	119	-5	35	102	6.34	0	30	338
11	30	34	1005	136	63	3.93	18	32	124	-14	31	97	6.02	0	30	195
12	33	12	410	55	73	4.59	18	35	159	-23	35	86	5.36	0	30	10

b. Strength computations for second stage

1	2	3	4	5	6
Total Normal Force (N), kips	Pore Water Pressure (u), ksf	Effective Normal Stress (σ'_{fc}), ksf	Cohesion (c), ksf	Friction Angle (φ), degrees	2nd Stage Shear Strength (s_2), ksf
20	0	0.25	0	30	1.47
63	0.89	0.92	0	30	0.53
111	2.36	1.9	0	30	1.1
134	3.4	2.51	0	30	1.45
240	4.39	2.99	0	30	1.73
214	5.24	3.64	0	30	2.1
238	5.78	4.08	0	30	2.35
236	6.15	4.38	1.2	16	2.46
336	6.36	4.62	1.2	16	2.53
379	6.34	4.61	1.2	16	2.52
315	6.02	4.18	1.2	16	2.4
302	5.36	3.08	0	30	1.78

Figure G-7. Computations with Corps of Engineers' (1970) method – first stage

(c) The shear strength, s_2, for the second-stage computations is calculated using the composite shear strength envelope shown in Figure G-8. This envelope is the lower bound envelope derived from the R and S envelopes. The shear strength, s_2, is calculated using the composite envelope and the effective consolidation pressure, σ'_c, determined in Step 2. For the example calculations shown in Figure G-7b, the effective normal stress, σ'_{fc}, shown in Column 3 was first compared with the effective stress, τ_{ff} and σ_i, corresponding to the point where the R and S envelopes intersect. The stress where the two envelopes intersect is given by:
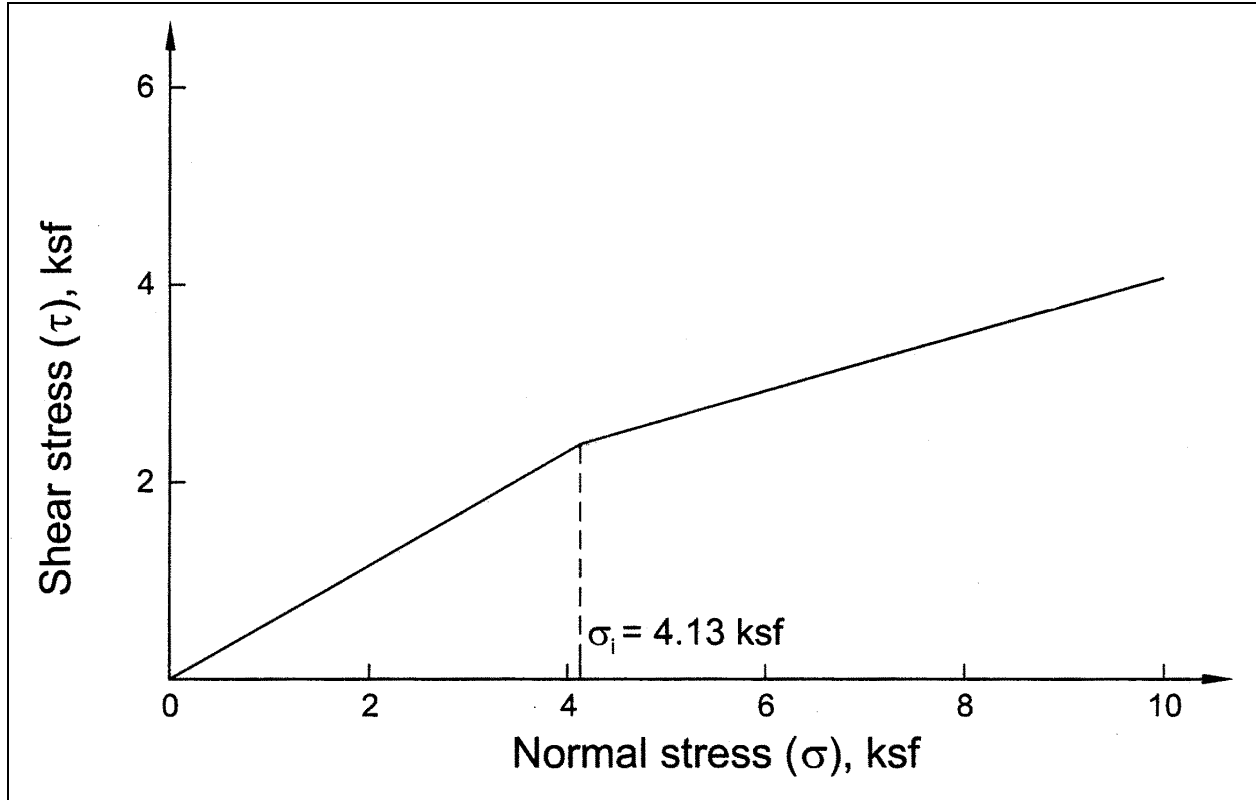
Figure G-8. Composite shear strength envelope for example problem – Corps of Engineers' (1970) method

$$\sigma_i = \frac{c_R - c_S}{\tan \phi_S - \tan \phi_R} \tag{G-18}$$

(d) For the example problem, the two envelopes intersect at $\sigma_i = 4.13$ ksf. If the effective stress, σ'_c, is less than σ_i, the effective stress shear strength parameters (c' and ϕ') are used to compute the strength, s_2. Otherwise, the R envelope parameters (c_R and ϕ_R) are used (Columns 4 and 5 of table in Figure G-7b). The shear strength was computed from the relationship:

$$s_2 = c + \sigma'_c \tan(\phi) \tag{G-19}$$

where c and ϕ are the appropriate values shown in Columns 4 and 5 in Figure G-7b.

The shear strengths are shown in Column 6 of the table in Figure G-7b.

(3) *Step 3 – Second-stage computations*. Calculations for the second stage are shown in the table presented in Figure G-9. The specific details of the computations shown in Figure G-9 are as follows:

(a) The slice weight is calculated using the total unit weights after drawdown. In this example, the soil is assumed to be saturated before and after drawdown. Thus the total unit weights and the weights of the slices are the same as for the first stage. This will not always be the case.

(b) Because the reservoir is below the top of the lowest slice after drawdown, the surface loads (P) are zero. In other cases the surface loads may not be zero.

1	2	3	4	5	6	7	8	9	10	11	12	13	14	15
				Surface Loads										
Slice Number.	Slice Area, sq. ft.	Total Weight (W), kips.	Height of Surface Water (h_s), ft.	Press. At Top of Slice ($P_{surface}$), ksf	Slope at Top of Slice (β), degs	Length of Top of Slice (ℓ_{top}), ft	Surface Load (P), kips	Base Inclination (α), degs.	Slice Base Length (ℓ), ft.	Piezometric height (h_p), ft.	Pore Water Pressure (u), ksf	Cohesion (c), ksf	Friction Angle (ϕ'), degs.	Interstice Force on Downslope Side (Z_{i+1}), kips (Assumed F = 1.35)
1	14	2	0	0	18	4	0	61	8	0	0	0.15	0	1
2	428	58	0	0	18	20	0	55	35	0	0	0.53	0	42
3	807	109	0	0	18	18	0	46	26	0	0	1.1	0	106
4	1015	137	0	0	18	19	0	40	23	0	0	1.45	0	174
5	1785	241	0	0	18	30	0	32	32	0	0	1.73	0	262
6	1508	204	0	0	18	24	0	24	24	0	0	2.1	0	309
7	1570	212	0	0	18	25	0	18	24	0	0	2.35	0	331
8	1449	196	0	0	18	23	0	11	22	0	0	2.46	0	329
9	1844	249	0	0	18	32	0	4	31	0	0	2.53	0	288
10	1702	230	0	0	18	36	0	-5	35	0	0	2.52	0	197
11	1005	136	0	0	18	32	0	-14	31	0	0	2.4	0	93
12	410	55	0	0	18	35	0	-23	35	0	0	1.78	0	0

Figure G-9. Computations with Corps of Engineers' (1970) method – second stage

(c) The shear strengths (s_2) calculated in Step 2 are assigned as values of cohesion (c) and ϕ is set equal to zero. Pore water pressures are not relevant because ϕ is equal to zero. If the bases of some slices had been located in soils that drain freely, effective stress shear strength parameters (c' and ϕ') and appropriate pore water pressures would have been assigned to those slices for the second-stage computations. The pore water pressures in the freely draining soils would be those following drawdown.

(d) The side forces, Z_{i+1}, shown in Figure G-9 are the final values calculated using the value of the factor of safety that satisfies force equilibrium. Equilibrium is confirmed by the negligible force on the right side of the last slice (slice 12). The factor of safety computed for the second-stage analyses is 1.35. This value is the factor of safety after rapid drawdown for the assumed slip surfaces. It would be necessary to analyze additional slip surfaces to determine the critical surface and the lowest factor of safety.

G-6. Improved Method for Rapid Drawdown – Example Calculations with Simplified Bishop Method

a. First-stage computations. Calculations for the first stage of the computations are summarized in the table presented in Figure G-10a. The calculations follow the same steps and procedure described in section F.2.b for steady seepage analyses. Effective stress shear strength parameters (c' = 0, ϕ' = 30 degrees) are used for all slices. Slice weights are computed using total unit weights. The pore water pressures and external water loads are calculated from the maximum pool piezometric surface shown in Figure G-5. Calculations are shown in Figure G-10 for the final trial value of the factor of safety (F = 2.20).

b. Calculation of shear strengths for second-stage computations. Calculations of the consolidation stresses and undrained shear strengths for the second stage of the computations are presented in the table in Figure G-10b. The specific steps involved are as follows:

(1) The total normal force on the base of each slice is calculated using the equation:

$$N = \frac{W + P\cos\ \beta - \frac{1}{F}\left[(c' - u\ \tan\ \phi')\ b\ \tan\alpha\right]}{\left(\cos\ \alpha + \frac{\sin\alpha\tan\phi'}{F}\right)} \tag{G-20}$$

where the terms are as defined previously. The values for all quantities are from the first-stage computations.

(2) Pore water pressures, u, are determined from the initial condition with the piezometric level at elevation 103 ft (Column 2 in Figure G-7b). These pore water pressures are the same as the ones used for the first-stage computations (Column 16 in Figure G-7a).

(3) The effective normal stress, σ'_c, is calculated by dividing the total normal force (N) by the length of the base of the slice, $\Delta\ell$, and subtracting the pore water pressure:

$$\sigma'_c = \frac{N}{\Delta\ell} - u \tag{G-21}$$

(4) The shear force (S) on the base of the slice is calculated from the equation:

a. First-stage stability computations

1	2	3	4	5	6	7	8	9	10	11	12	13	14	15	16	17	18	19	20	21
Slice Number	Horizontal Width (b), ft.	Average Slice Height, ft.	Slice Area, sq. ft	Total Weight (W), kips	Base Inclination (α), degs.	W sin (α), kips	Height of Surface water (h_s), ft.	Avg. Surface Press. (P_Surface), ksf	Surface Inclination (β), degs.	Surface Load (P), kips.	Horiz. Moment arm (d_h), ft.	Vert. Moment arm (d_v), ft.	Moment (M_p), kip-ft.	Piezometric Height (h_p), ft.	Pore Water Pressure (u), ksf	Cohesion (c), ksf	Friction Angle (φ'), degs.	c'b + (W + P cosβ - ub) tanφ'	m_α (Assumed F = 2.20)	[c'b + (W + P cosβ - ub) tanφ'] ÷ m_α
1	4	4	14	2	61	2	0	0	0	0	-	-	-	0	0	0	30	1	0.72	1
2	20	21	428	58	55	47	0	0	0	0	-	-	-	14	0.89	0	30	23	0.79	29
3	18	45	807	109	46	79	0	0	0	0	-	-	-	38	2.36	0	30	38	0.88	44
4	18	58	1015	137	40	87	0	0	21.8	0	-	-	-	55	3.4	0	30	45	0.94	48
5	28	65	1785	241	32	128	6	0.34	21.8	10	-111	113	-626	70	4.39	0	30	75	0.99	76
6	22	69	1508	204	24	84	15	0.96	21.8	23	-86	122	-793	84	5.24	0	30	63	1.02	62
7	23	68	1570	212	18	65	24	1.52	21.8	38	-64	131	-401	93	5.78	0	30	66	1.03	64
8	22	66	1449	196	11	39	33	2.04	18.4	47	-42	140	227	99	6.15	0	30	61	1.03	59
9	31	60	1844	249	4	18	41	2.58	18.4	83	-15	148	2698	102	6.36	0	30	77	1.02	76
10	35	49	1702	230	-5	-19	52	3.26	18.4	119	17	159	7911	102	6.34	0	30	71	0.98	73
11	30	34	1005	136	-14	-32	63	3.93	18.4	124	50	170	12521	97	6.02	0	30	42	0.91	46
12	33	12	410	55	-23	-21	73	4.59	18.4	159	81	180	21358	86	5.36	0	30	17	0.82	21
						476							**42895**							**599**

Surface loads: columns 8–14

$$F = \frac{599}{476 - \dfrac{42895}{210}} = 2.20$$

b. Strength computations for second stage

1	2	3	4	5	6	7	8	9	10
Total Normal Force (N), kips	Pore Water Pressure (u), ksf	Effective Normal Stress (σ'_c), ksf	Shear Force (S), kips	Shear Stress (τ_c), ksf	Consolidation Stress Ratio (K_c)	τ_ff (K_c = 1), ksf	τ_ff (K_c = K_f), ksf	Effective Prin. Stress Ratio at Failure, K_f	Interpolated Strength (τ_ff), ksf
3	0	0.32	1	0.08	1.71	1.49	0.19	3.00	1.02
81	0.89	1.44	13	0.38	1.71	1.85	0.83	3.00	1.49
137	2.36	2.9	20	0.76	1.71	2.33	1.67	3.00	2.1
160	3.4	3.64	22	0.95	1.71	2.58	2.1	3.00	2.41
274	4.39	4.05	34	1.06	1.71	2.71	2.34	3.00	2.58
234	5.24	4.45	28	1.17	1.71	2.84	2.57	3.00	2.75
250	5.78	4.57	29	1.2	1.71	2.88	2.64	3.00	2.8
240	6.15	4.54	27	1.19	1.71	2.87	2.62	3.00	2.78
326	6.36	4.31	35	1.13	1.71	2.8	2.49	3.00	2.69
346	6.34	3.66	33	0.96	1.71	2.58	2.11	3.00	2.42
266	6.02	2.6	21	0.68	1.71	2.23	1.5	3.00	1.97
228	5.36	1.01	10	0.27	1.71	1.71	0.59	3.00	1.31

Figure G-10. Computations with improved drawdown procedure – Simplified Bishop Method – first stage

$$S = \frac{1}{F}\left[\frac{c'b + (W + P\ \cos\ \beta - ub)\ \tan\ \phi'}{\cos\alpha + \frac{\sin\alpha\ \tan\phi'}{F}} \right] \tag{G-22}$$

where the values for all quantities are from the first stage analysis.

(5) The shear stress, τ_c, during consolidation is calculated by dividing the shear force (S) by the length of the base of the slice, $\Delta\ell$:

$$\tau_c = \frac{S}{\Delta\ell} \tag{G-23}$$

(6) The effective principal stress ratio for consolidation, K_c, is calculated for each slice using the equation:

$$K_c = \frac{\sigma'_c + \tau_c\ \dfrac{\sin\phi' + 1}{\cos\phi'}}{\sigma'_c + \tau_c\ \dfrac{\sin\phi' - 1}{\cos\phi'}} \tag{G-24}$$

where σ'_c and τ_c are the values calculated in Steps 3 and 5 above, and ϕ' is the effective stress friction angle.

(7) Undrained shear strengths, expressed as the shear stresses on the failure plane at failure, $\tau_{ff\text{-}K_c=1}$ and $\tau_{ff\text{-}K_c=K_f}$, are calculated from the τ_{ff} vs. σ'_{fc} shear strength envelopes for $K_c = 1$ and $K_c = K_f$, respectively (Columns 7 and 8 in Figure G-10b).

(8) The effective principal stress ratio at failure, K_f, is calculated from:

$$K_f = \frac{(\sigma'_c + c'\ \cos\ \phi')(1 + \sin\phi')}{(\sigma'_c - c'\ \cos\phi')(1 - \sin\phi')} \tag{G-25}$$

or, when c' = 0:

$$K_f = \frac{1 + \sin\phi'}{1 - \sin\phi'} = \tan^2\left(45° + \frac{\phi'}{2} \right) \tag{G-26}$$

(9) Undrained shear strengths, τ_{ff}, are computed by linear interpolation between the values of shear strength from the $K_c = 1$ envelope and the $K_c = K_f$ envelopes:

$$\tau_{ff} = \frac{(K_f - K_c)\tau_{ff-K_c=1} + (K_c - 1)\tau_{ff-K_c=K_f}}{K_f - 1} \tag{G-27}$$

These undrained shear strengths are used for the second-stage computations.

c. Second-stage computations. Calculations for the second stage are shown in the table in Figure G-11a. The specific details of the computations shown in Figure G-11a are as follows:

(1) The slice weight is calculated using the total unit weights after drawdown.

(2) Because the reservoir is below the top of the lowest slice after drawdown, the surface loads (P) are zero. In other cases, the surface loads may not be zero.

(3) The shear strengths computed in Step 2 are assigned as values of cohesion (c), and ϕ is set equal to zero. Pore water pressures are not relevant because ϕ is zero. If the base of some slices had been located in soils that drain freely, effective stress, shear strength parameters (c' and ϕ'), and appropriate pore water pressures would be assigned to those slices for the second-stage computations. The pore water pressures in the freely draining soils would be those following drawdown.

(4) The stability calculations in Figure G-11a for the second-stage are shown for the final value of the factor of safety (F = 1.52), where the assumed and calculated values are equal.

d. Evaluation of strengths for third-stage analyses. The drained strengths of the soil are calculated as shown in Figure G-11b. The specific steps are as follows:

(1) The total normal force on the base of each slice is calculated from Equation G-16. The values of the quantities in this equation are from the second-stage computations. For slices that were considered to be freely draining, effective stress, shear strength parameters and second-stage pore water pressures are used. For slices that were assumed to be undrained, the value of c in Equation G-19 is the undrained shear strength and ϕ is set equal to zero.

(2) The pore water pressures, u, after drawdown are calculated from the final reservoir level.

(3) The effective normal stress, σ'_d, is calculated using the normal forces and pore water pressures calculated in Steps 1 and 2, and the following equation:

$$\sigma'_d = \frac{N}{\Delta\ell} - u \tag{G-28}$$

(4) The drained shear strength is estimated from:

$$s_d = c' + \sigma'_d \tan(\phi') \tag{G-29}$$

where c' and ϕ' are the effective stress shear strength parameters.

(5) The drained shear strengths calculated in Step 4 are compared with the undrained shear strengths, τ_{ff}, used in the second-stage computations to determine which is lower. If the drained shear strength (s_d) is lower for any slice, a third-stage of computations is required. In this case, effective stress shear strength parameters, c' and ϕ', are used for slices where the drained shear strengths are lower, and undrained shear strengths are used for the slices where the undrained strengths are lower. The undrained shear strengths used are the same as for the second-stage computations. If the undrained shear strengths are lower than the drained strengths for all slices, the undrained shear strengths are more critical and the third-stage computations are not required. In this case, the factor of safety for rapid drawdown is the factor of safety calculated for the second stage.

a. Second-stage stability computations

	1	2	3	4	5	6	7	8	9	10	11	12	13	14	15	16	17	18	19
	Slice Number.	Slice Area, sq. ft.	Total Weight (W), kips.	Base Inclination (α), degs.	W sin (α), kips.	Height of Surface Water (h_s), ft.	Avg. Surface Press. (P_surface), ksf	Surface Inclination (β), degs.	Surface Load (P), kips.	Horiz. Moment arm (d_h), ft.	Vert. Moment arm (d_v), ft.	Moment (M_p), kip-ft.	Piezometric Height (h_p), ft.	Pore Water Pressure (u), ksf	Cohesion (c), ksf	Friction Angle (φ), degs.	c'b + (W + P cos β - ub) tan φ	m_α (Assumed F = 1.52)	[c'b + (W + P cos β - ub) tan φ] ÷ m_α
	1	14	2	61	2	0	0	0	0	-	-	0	-	0	1.02	0	4	0.49	8
	2	428	58	55	47	0	0	0	0	-	-	0	-	0	1.49	0	30	0.58	52
	3	807	109	46	79	0	0	0	0	-	-	0	-	0	2.10	0	38	0.69	55
	4	1015	137	40	87	0	0	21.8	0	-	-	0	-	0	2.41	0	42	0.77	55
	5	1785	241	32	128	0	0	21.8	0	-	-	0	-	0	2.58	0	71	0.85	84
	6	1508	204	24	84	0	0	21.8	0	-	-	0	-	0	2.75	0	60	0.91	66
	7	1570	212	18	65	0	0	21.8	0	-	-	0	-	0	2.80	0	64	0.95	68
	8	1449	196	11	39	0	0	18.4	0	-	-	0	-	0	2.78	0	61	0.98	62
	9	1844	249	4	18	0	0	18.4	0	-	-	0	-	0	2.69	0	82	1.00	82
	10	1702	230	-5	-19	0	0	18.4	0	-	-	0	-	0	2.42	0	83	1.00	84
	11	1005	136	-14	-32	0	0	18.4	0	-	-	0	-	0	1.97	0	59	0.97	61
	12	410	55	-23	-21	0	0	18.4	0	-	-	0	-	0	1.31	0	43	0.92	47
					476							0							723

$$F = \frac{723}{476} - \frac{0}{210} = 1.52$$

b. Strength computations for third stage

	1	2	3	4	5	6	7
	Total Normal Force (N), kips	Piezometric Height (h_p), ft.	"Drained" Pore Pressure (u), ft	Drained Effective Stress (σ_drained), ksf	Undrained Shear Strength (τ_ff), ksf	Drained Shear Strength (S_drained), ksf	Strength for Third Stage*
	-6	0	0	-0.72	1.02	0	D
	52	0	0	1.48	1.49	0.86	D
	120	0	0	4.61	2.1	2.66	U
	148	0	0	6.52	2.41	3.76	U
	250	0	0	7.69	2.58	4.44	U
	204	5	0.31	8.13	2.75	4.69	U
	208	14	0.85	7.77	2.8	4.49	U
	191	20	1.22	7.3	2.78	4.22	U
	246	23	1.43	6.61	2.69	3.81	U
	235	23	1.41	5.38	2.42	3.11	U
	149	18	1.09	3.75	1.97	2.16	U
	73	7	0.43	1.61	1.31	0.93	D

c. Third-stage stability computations

	1	2	3	4	5	6
	Pore Water Pressure (u), ksf	Cohesion (c), ksf	Friction Angle (φ), degs.	c'b + (W + P cos β - ub) tan φ'	m_α (Assumed F = 1.44)	[c'b + (W + P cos β - ub) tan φ] ÷ m_α
	0	0	30	1	0.84	1
	0	0	30	33	0.91	37
	0	2.1	0	38	0.69	55
	0	2.41	0	42	0.77	55
	0	2.58	0	71	0.85	84
	0	2.75	0	60	0.91	66
	0	2.8	0	64	0.95	68
	0	2.78	0	61	0.98	62
	0	2.69	0	82	1.00	82
	0	2.42	0	83	1.00	84
	0	1.97	0	59	0.97	61
	0.43	0	30	24	0.77	31
						685

$$F = \frac{685}{476} - \frac{0}{210} = 1.44$$

Figure G-11. Computations with improved drawdown procedure – Simplified Bishop Method – second and third stages

e. Third-stage computations. For the example problem, the drained strengths are lower than the undrained strengths for slices 1, 2, and 12. Therefore, third-stage computations are required. The third-stage computations are shown in the table in Figure G-11c. For the third-stage computations, the conditions are the same as those for the second stage except for the shear strength parameters and the pore water pressures assigned to slices 1, 2, and 12, where the drained shear strengths were determined to be lower. For these slices the pore water pressures are calculated from the piezometric surface at el 24 feet. For all other slices, the undrained shear strengths used for the second-stage computations are also used for the third-stage computations. Pore water pressures were set equal to zero for slices where undrained shear strengths are used. There were no external water loads for the second- or third-stage computations, because the water level was below the top of the last slice after drawdown.

The third-stage computations are summarized in Figure G-11c for the final trial value of the factor of safety, F = 1.44. This value is the factor of safety after rapid drawdown for this method.

G-7. Improved Procedure for Rapid Drawdown – Example Calculations with Modified Swedish/Spencer Procedure

This example uses the improved procedure for rapid drawdown analysis and the Modified Swedish Method. In these calculations, the inclination of the interslice forces was determined by first computing the factor of safety using Spencer's Method. Thus, the factors of safety computed are identical to those calculated by Spencer's Method. These calculations are the type of calculations that would be performed to check the results of an analysis performed using Spencer's Method. When this procedure is used for analysis, the recommended procedure for checking the calculations is to use the Modified Swedish Method with the interslice force inclination computed in the analysis with Spencer's Method.

The interslice force inclinations determined for Spencer's Method are different for each of the three stages. The interslice force inclinations from Spencer's analysis are summarized in the tabulation below:

Stage	Interslice Force Inclination (degrees)
1	6.0
2	12.2
3	13.7

a. First-stage computations. Calculations for the first stage of the computations are summarized in the table in Figure G-12a. Except for differences resulting from the assumed interslice force inclination, the quantities shown in Figure G-12a are the same as those shown previously for the first-stage computations with the Corps of Engineers' (1970a) method, described in Section G-5a. Refer to Section G-5 for discussion of shear strength parameters, pore water pressures, slice weights and external loads. Figure G-12a shows the calculations for the final value of factor of safety (F = 2.23).

b. Calculation of shear strengths for second-stage computations. Calculations of the consolidation stresses and undrained shear strengths for the second-stage computations are shown in the table in Figure G-12b. Except for the formula used to compute the total normal force (N) on the bottom of the slices, the calculations are identical to those described in Section G-6b, where the Simplified Bishop Method was used. For the Modified Swedish Method, the total normal force is calculated using Equation G-16.

c. Second-stage computations. Except for the procedure used to calculate the factor of safety, the quantities and calculations are the same as those used with the Simplified Bishop Method described in Section G-6c. The second-stage stability calculations in Figure G-13a are for the final value of the factor of safety (F = 1.52).

b. Strength computations for second stage

1	2	3	4	5	6	7	8	9	10
Total Normal Force (N), kips	Pore Water Pressure (u), ksf	Effective Normal Stress (σ'_c), ksf	Shear Force (S), kips	Shear Stress (τ_{fc}), ksf	Consolidation Stress Ratio (K_c)	τ_{ff} (K_c = 1), ksf	τ_{ff} ($K_c = K_f$), ksf	Effective Prin. Stress ratio at failure, K_f	Interpolated strength (τ_{ff}), ksf
2	0	0.29	1	0.08	1.70	1.47	0.17	3.00	1.01
74	0.89	1.24	11	0.32	1.70	1.79	0.72	3.00	1.41
127	2.36	2.53	17	0.66	1.70	2.21	1.46	3.00	1.95
151	3.4	3.24	19	0.84	1.70	2.44	1.87	3.00	2.24
262	4.39	3.69	31	0.96	1.70	2.59	2.13	3.00	2.43
228	5.24	4.19	26	1.09	1.70	2.76	2.42	3.00	2.64
247	5.78	4.43	28	1.15	1.70	2.83	2.56	3.00	2.74
239	6.15	4.51	26	1.17	1.70	2.86	2.61	3.00	2.77
330	6.36	4.44	35	1.15	1.70	2.84	2.56	3.00	2.74
357	6.34	3.98	36	1.03	1.70	2.69	2.3	3.00	2.55
281	6.02	3.09	25	0.8	1.70	2.39	1.78	3.00	2.18
249	5.36	1.59	15	0.41	1.70	1.9	0.92	3.00	1.56

a. First-stage stability computations

1	2	3	4	5	6 (Surface loads)	7	8	9	10	11	12	13	14	15	16	17
Slice Number	Horizontal Width (b), ft.	Average Slice Height, ft.	Slice Area, sq. ft	Total Weight (W), kips	Height of surface water (h_s), ft	Press. At Top of Slice ($P_{surface}$), ksf	Slope at Top of Slice (β), degs	Length of Top of Slice (ℓ_{top}), ft	Surface Load (P), kips	Base Inclination (α), degs.	Slice Base Length (ℓ), ft.	Piezometric height (h_p), ft.	Pore Water Pressure (u), ksf	Cohesion (c), ksf	Friction Angle (ϕ), degs.	Interstice Force on Downslope Side (Z_{i+1}), kips (Assumed F = 2.23)
1	4	4	14	2	0	0	18	4	0	61	8	0	0	0	30	2
2	20	21	428	58	0	0	18	20	0	55	35	14	0.89	0	30	56
3	18	45	807	109	0	0	18	18	0	46	26	38	2.36	0	30	137
4	18	58	1015	137	0	0	18	19	0	40	23	55	3.4	0	30	219
5	28	65	1785	241	6	0.34	18	30	10	32	32	70	4.39	0	30	329
6	22	69	1508	204	15	0.96	18	24	23	24	24	84	5.24	0	30	391
7	23	68	1570	212	24	1.52	18	25	38	18	24	93	5.78	0	30	426
8	22	66	1449	196	33	2.04	18	23	47	11	22	99	6.15	0	30	432
9	31	60	1844	249	41	2.58	18	32	83	4	31	102	6.36	0	30	395
10	35	49	1702	230	52	3.26	18	36	119	-5	35	102	6.34	0	30	292
11	30	34	1005	136	63	3.93	18	32	124	-14	31	97	6.02	0	30	161
12	33	12	410	55	73	4.59	18	35	159	-23	35	86	5.36	0	30	0

Figure G-12. Computations with improved drawdown procedure – Modified Swedish/Spencer's Method – first stage

a. Second-stage stability computations

1 Slice Number	2 Slice Area, sq. ft	3 Total Weight (W), kips	4 Height of surface water (h_s), ft	Surface Loads 5 Press. At Top of Slice ($P_{surface}$), ksf	6 Slope at Top of Slice (β), degs	7 Length of Top of Slice (ℓ_{top}), ft	8 Surface Load (P), kips	9 Base Inclination (α), degs	10 Slice Base Length (ℓ), ft	11 Piezometric height (h_p), ft	12 Pore Water Pressure (u), ksf	13 Cohesion (c), ksf	14 Friction Angle (φ), degs	15 Interstice Force on Downslope Side (Z_{i+1}), kips (Assumed F = 1.52)
1	14	2	0	0	18	4	0	61	8	0	0	1.01	0	-6
2	428	58	0	0	18	20	0	55	35	0	0	1.41	0	14
3	807	109	0	0	18	18	0	46	26	0	0	1.95	0	69
4	1015	137	0	0	18	19	0	40	23	0	0	2.24	0	130
5	1785	241	0	0	18	30	0	32	32	0	0	2.43	0	211
6	1508	204	0	0	18	24	0	24	24	0	0	2.64	0	254
7	1570	212	0	0	18	25	0	18	24	0	0	2.74	0	275
8	1449	196	0	0	18	23	0	11	22	0	0	2.77	0	273
9	1844	249	0	0	18	32	0	4	31	0	0	2.74	0	236
10	1702	230	0	0	18	36	0	-5	35	0	0	2.55	0	156
11	1005	136	0	0	18	32	0	-14	31	0	0	2.18	0	71
12	410	55	0	0	18	35	0	-23	35	0	0	1.56	0	0

b. Strength computations for third stage

1 Total Normal Force (N), kips	2 Piezometric height (h_p), ft	3 "Drained" Pore Pressure (u), ksf	4 Drained Effective Stress ($\sigma_{drained}$), ksf	5 Undrained Shear Strength (τ_{ff}), ksf	6 Drained Shear Strength ($S_{drained}$), ksf	7 Lowest Shear Strength - Use for Third Stage
-3	0	0	-0.41	1.01	0.00	Drained
47	0	0	1.35	1.41	0.78	Undrained
106	0	0	4.07	1.95	2.35	Undrained
133	0	0	5.87	2.24	3.39	Undrained
232	0	0	7.13	2.43	4.12	Undrained
195	5	0.31	7.75	2.64	4.47	Undrained
204	14	0.85	7.59	2.74	4.38	Undrained
192	20	1.22	7.33	2.77	4.23	Undrained
254	23	1.43	6.86	2.74	3.96	Undrained
252	23	1.41	5.88	2.55	3.40	Undrained
169	18	1.09	4.38	2.18	2.53	Drained
92	7	0.43	2.13	1.56	1.23	Drained

c. Third-stage stability computations

1 Pore Water Pressure (u), ksf	2 Cohesion (c), ksf	3 Friction Angle (φ), degs	4 Interstice Force on Downslope Side (Z_{i+1}), kips (Assumed F = 1.44)
0	0	30	1
0	0	30	34
0	1.95	0	86
0	2.24	0	144
0	2.43	0	221
0	2.64	0	262
0	2.74	0	281
0	2.77	0	276
0	2.74	0	236
0	2.55	0	152
0	2.18	0	63
0.43	0	30	0

Figure G-13. Computations with improved drawdown procedure – Modified Swedish/Spencer's Method – second and third stages

d. Evaluation of shear strengths for third-stage computations. Once the computations for the second stage are completed, drained strengths are computed as shown in Figure G-13b. Except for the equation used to compute the total normal force on the bottom of the slices, the computations are the same as those for the Simplified Bishop Method in Section G-6d.

e. Third-stage computations. The quantities for the third-stage computations are summarized in Figure G-13c. As with any analysis using the Modified Swedish Method, a trial value is assumed for the factor of safety, and interslice forces are computed using Equation C-19. The process is repeated with other trial values of factor of safety until the force on the downslope side of the last slice is essentially zero. The interslice force computations in Figure G-13c are shown for the final value of the factor of safety (F = 1.44). This value is the factor of safety after rapid drawdown for this method. This value is the same as the value computed using the Simplified Bishop Method. This is not surprising because the two methods (Spencer and Simplified Bishop) usually give values for the factor of safety that are the same or very nearly the same.

G-8. Summary of Examples

The results of the three examples discussed above are as follows:

Example	Method	Factor of Safety
1	Corps of Engineers' (1970) rapid drawdown and stability calculations performed using the Modified Swedish Method, with total side forces inclined at the average slope of the embankment, θ = 19.4 degrees.	1.35
2	Improved rapid drawdown procedure and stability calculations performed using the Simplified Bishop Method.	1.44
3	Improved rapid drawdown procedure and stability calculations performed using the Modified Swedish Method, with side force inclinations determined using Spencer's Method, θ = 12.2 degrees for stage 2, and θ = 13.7 degrees for stage 3. This is the same as Spencer's Method.	1.44

The methods used in Examples 2 and 3 – the improved rapid drawdown procedure, with stability calculations performed using the Simplified Bishop or Spencer's Method – give factors of safety that are slightly higher than the factor of safety computed for example 1. It might seem tempting to conclude that, since the differences in factor of safety shown here are small, the choice between these methods can be made on the basis of which is simpler, or more familiar. However, this would not be a valid conclusion, and should not be used as a justification for continued use of the less accurate Corps of Engineers' (1970) rapid drawdown procedure.

The Corps of Engineers' (1970) rapid drawdown procedure is inherently conservative, because it under-estimates undrained shear strength. Counteracting this conservatism is the fact that the Modified Swedish Method, with total side forces inclined at the average slope of the embankment, overestimates factor of safety as compared with more accurate methods (Simplified Bishop or the Spencer Method). Although these effects nearly balance out for this particular embankment, and the difference in factors of safety is fairly small in this example, there is no reason to believe that this will always be the case. Because the improved procedure for rapid drawdown analysis is based on sound soil mechanics principles and because it employs realistic representations of soil strengths, it provides more meaningful and reliable factors of safety. It should be used, in combination with accurate stability analysis methods (Simplified Bishop or the Spencer Method), on future Corps of Engineers' projects. The minimum required factors of safety to be used with the improved procedure (given in Chapter 3) are 8 to 10 percent higher than those required in the 1970 manual. This consistent with the fact that factors of safety computed using the improved procedure are somewhat higher than those computed using the Corps' drawdown procedure (1970), as noted above.